Microalgal co-cultures for biomanufacturing applications.

Gloria Padmaperuma

Department of Chemical and Biological Engineering

Thesis submitted for the degree of Doctor of Philosophy

To the University of Sheffield, Sheffield, UK

20th December 2017

Declaration

This is a declaration to state that this thesis is an account of the author's work, which was conducted at The University of Sheffield, United Kingdom. This work has not been submitted for any other degree of qualification.

Acknowledgments

“If life's journey be endless, where is its goal? The answer is, it is everywhere.”

- R. Tagore

The PhD, in itself, has been a roller coaster of self-discovery and dwelling deeper into the unknown… or at least that is how it felt like.
The main pillars of my life, Ammi and Thathi; I have, and always will dedicate all my achievements.

My two supervisors, Raman and Jim, have been sources of guidance and reference. I would like to thank you both, for your time, valuable contributions and support. Your experience and inputs have indeed shaped my research and taken me into discovering knowledge pools to me previously hidden. I am grateful to the EPSRC for funding me.

Thank you to Rahul, Esther, Joy, Tamas, James and the Workshop guys, for taking time out their busy working hours to help me and encourage.

My PhD has not just been an academic journey. My friends have been with me through good and bad times. In the time of need, I did not feel alone. I thank you all for seeing me through this and for never doubting that I could make it.

To my Sister and Efi… I am very lucky to know that you will always have my back.

Publications

Microbial consortia: a critical look at microalgae co-cultures for enhanced biomanufacturing

Gloria Padmaperuma[a], Rahul Vijay Kapoore[a], Daniel James Gilmour[b] and Seetharaman Vaidyanathan[a]

[a]ChELSI Institute, Advanced Biomanufacturing Centre, Department of Chemical and Biological Engineering, The University of Sheffield, Sheffield, UK; [b]Department of Molecular Biology and Biotechnology, The University of Sheffield, Sheffield, UK

CRITICAL REVIEWS IN BIOTECHNOLOGY, 2017
https://doi.org/10.1080/07388551.2017.1390728

List of Abbreviations

AHLs	N-acylhomoserine lactones
BBM	Bold's Basal Medium
BBM+	Bold's Basal Modified Medium
BSA	Bovine Serum Albumin
Ca, Chl a	Chlorophyll a
Cb, Chl b	Chlorophyll b
CBE	Chemical and Biological Engineering
CCAP	Culture Collection of Algae and Protozoa
CFU	Colony formation unit
CHO	Chinese Hamster Ovary
CTC	Copper Tartarate
Cx+c	Carotenoids
D. salina	*Dunaliella Salina*
DCW	Dry Cell Weight
DHAP	Dihydroxyacetone phosphate
DIC	Dissolved Inorganic Carbon
DIN	Dissolved Inorganic Nitrogen
EPS	Extracellular Polymeric Substances
ETC	Electron Transport Chain
FACS	Fluorescence-Activated Cell Sorting
FAME	Fatty Acid Methyl Esthers
GDPH	Glyceraldehyde 3-phosphate dehydrogenase
GHGs	Greenhouse Gases
H. salinarum	*Halobacterium salinarum*
HEPES	Hepes Medium
HEPES+	Hepes Modified medium
MBB	Molecular Biology and Biotechnology
MSTFA	N-methyl-N-trimethylsilyltrifluoroacetamide
NCIMB	National Collection of Industrial, Food and Marine Bacteria

NCYC	National Collection of Yeast Cultures
OD	Optical Density
PC1	Principle Component 1
PCA	Principle Component Analysis
QSI	Quorum Sensing Inhibiting
R. toruloides	*Rhodosporidium toruloides*
RIs	Retention Indices
RuBisCO	ribulose-1, 5-busphate carboxylase/oxygenase
S. obliquus	*Scenedesmus obliquus*
TAGs	Triglycerides
THF	Tetrahydrofuran
UNFCCC	United Nations Framework Convention on Climate Change
VOSCs	Volatile Organic Sulphur Compounds
YM	Yeast Mold Media

Abstract

High demands in consumer goods and pressures from governments to meet environmental regulations have pushed industries to find innovative, carbon-neutral solutions. Sustainable methods in biotechnology are sought to increase productivity whilst keeping at bay one of the major problems in monoculture production routes: contamination. The use of engineered consortia is seen as a viable option. In nature, microorganisms exist as part of complicated networks known as consortia. Within the consortia, each member plays a role in facilitating communication, tasks distribution, nutrients acquisition and protection. This emerging field uses the conundrums that govern natural microbial assemblages to create artificial co-culture within the laboratory. Purpose fit, co-cultures have been created, to enhance productivity yields of desired products, for bioremediation and to circumvent contamination.

The use of microalgae in co-cultures is the focus of this study. Microalgae have application in many fields and are ideal candidates for bioproduction and carbon sequestration. The results of two different systems are presented, which aim to increase the productivity of microalgae biomass and of β-carotene or lipids. The natural consortium of *Dunaliella salina*, *Halomonas* and *Halobacterium salinarum* showed both an increase in microalgae cell concentration by 79% and higher β-carotene productivity compared to the monoculture. This association also showed that *Halomonas* is able to aid *D. salina* when subjected to abiotic stress. The artificial co-culture of *Scenedesmus obliquus* and *Rhodosporidium toruloides* showed an increase in microalgae biomass by 20%; however, the FAME levels of 26% dw were not a significant increase, compared to monocultures. Both systems demonstrated that if one member of the assemblage is in dire stress, this stress will translate to the entire community. Characterisation of exopolymeric substances and metabolites provided a fuller picture on how these microorganisms co-exist. Additionally, a novel method, duo-plates, was developed and successfully tested to trap metabolites within co-cultures.

Table of Contents

List of Tables

List of Graphs

List of Figures

Introduction

The field of co-culture and its application in biotechnology is at the forefront of research. After the challenges encountered using monocultures for biomanufacturing, co-cultures are possible solution to tackle contamination and improving production titres. Amongst the various microorganisms used in biomanufacturing, microalgae have been deemed as suitable candidates for mixed culture production. In nature, these organisms live in symbiosis with other microorganisms by exchanging biomolecules [1,2]. These biomolecules facilitate communication, division of labour and nutrient acquisition.

Microalgae have applications in the field of bioremediation, biomanufacturing and bioenergy. Their ability to produce an array of molecules within a given process makes them more desirable from an industrial perspective. Constructing a consortium within the laboratory will come with many challenges. Selecting microorganisms will be a key factor affecting the outcome of the study. Additionally, by keeping the primary partner as the focus, trade-off between optimal and sustainable growth conditions of the aiding partners needs to be considered: with trade-offs being beneficial to the end-goal [3]. Other challenges are encountered when monitoring the population, preventing contamination, avoiding competition, which may result in over-/under-yielding effects [4,5]. Amongst the other factors to be considered are priority effects and consortium behaviour to abiotic stresses [6].

Two co-culture research systems are presented in this thesis and studies of these co-culture research systems will attempt to overcome these challenges and address rationales to be adopted when constructing co-cultures. Some of the key points are whether microalgae based co-cultures are suitable for biotechnological application. Co-culturing microalgae with bacteria, archaea or yeast improve microalgae biomass accumulation alongside desired product yields. Evaluation of whether the trade-off of the co-culture brings benefit to the assemblage. The impact of abiotic stress on the co-culture is also to be considered as during large scale processing, non-uniformity in growth systems can create imbalances in the assemblage.

Keeping these points in mind, two different co-culture systems were chosen. The first co-culture looked at the interaction of *Dunaliella salina*, microalga used for the production of β-carotene, with *Halomonas* (bacterium) and the haloarchaeon *Halobacterium salinarum* (Chapter 3). As these microorganisms associate in nature; therefore, strong interactions were expected. The second study focused on an artificial co-culture involving *Scenedesmus obliquus* (microalga) and *Rhodosporidium toruloides* (yeast) for increased biomass and lipid production (Chapter 4). The methods of evaluation of each set-up were similar in terms of microalgae monoculture

assessment, however divergent in experimental design. The experimental approaches taken are fully described in each chapter.

The final objective of increasing microalgae growth rate and productivity were reached using the co-culture method. The co-cultures were assessed in terms of microalgae growth rate, changes in population density, product of interest yields, gaseous exchange and behaviours during abiotic stress. Exopolymeric substances, quorum sensing molecules and metabolites were investigated in Chapter 5 to provide more information on how these microorganisms communicated. The results highlighted the differences in the two-systems and brought to light new lines of thinking, such as UV-Vis absorption data for monitoring co-cultures, as seen in Chapter 6.

The investigation carried out revealed the potential hidden behind microalgal co-culture as possible biomanufacturing tools.

References

[1] Santos CA, Reis A. Microalgal symbiosis in biotechnology. Appl. Microbiol. Biotechnol. 2014;98:5839–5846.

[2] Delaux P-M, Radhakrishnan G V., Jayaraman D, et al. Algal ancestor of land plants was preadapted for symbiosis. Proc. Natl. Acad. Sci. 2015;112:13390–13395.

[3] Padmaperuma G, Kapoore RV, Gilmour DJ, et al. Microbial consortia: a critical look at microalgae co-cultures for enhanced biomanufacturing. Crit. Rev. Biotechnol. 2017;0:1–14.

[4] Goers L, Freemont P, Polizzi KM. Co-culture systems and technologies: taking synthetic biology to the next level. J. R. Soc. Interface. 2014;11:65.

[5] Danger M, Oumarou C, Benest D, et al. Bacteria can control stoichiometry and nutrient limitation of phytoplankton. Funct. Ecol. 2007;21:202–210.

[6] Fukami T. Historical contingency in community assembly : integrating niches, species pools, and priority effects. Annu. Rev. Ecol. Evol. Syst. 2015;46:1–23.

Chapter 1: Literature Review

1.1. Introduction

Axenic monocultures are predominantly used in biomanufacturing, due to ease of monitoring and to meet stringent safety regulations [1]. However, such monocultures are at high risk of contamination resulting in capital and product loss during manufacturing [2,3]. Controlled, symbiotic co-cultures possess features that provide solutions to surmount these bottlenecks. Though not universally applicable to all cell systems, co-cultures have shown improvements in yields of biomass, lipids [4] and high value products [5].

Symbiotic microbial communities have existed from the beginning of time, within benthic mats and fossil remains [6–8]. The first human civilizations used combinations of various microbes, for the production of fermented food and alcoholic beverages [9,10]. Nowadays, industry has harnessed microorganisms as means of production, due to their innate abilities to synthesise complex compounds and ease of scale-up. Cells derived from mammals, such as Chinese Hamster Ovary (CHO) cells [11,12], HeLA cells and mouse cells are workhorses of the biopharmaceutical industry, alongside yeast [13,14] and bacteria [9] which are used predominantly in the food industry, due to their quick turn-around times. The need for sustainable production routes has seen microorganisms deployed for bioremediation of water and soils and as carbon capture and storage options to minimise greenhouse gas emissions. Microbial communities are increasingly being investigated for the production of valuable accessory pigments [15–17] and in microbial fuel cells for electricity generation [18,19].

Maintaining axenic cultures has proved to be expensive and labour intensive, given the recurrent problem of contamination by bacteria, viruses, protozoa, yeast, fungi and mycoplasma [20] . Parasites or grazers can out-compete the working cell culture and influence cell health and production outputs. The 5th Annual Report and Survey of Biopharmaceutical Manufacturing Capacity and Production by Langer [20] reported that a failure rate of 7%, would amount to US$1-2 billion in expenses. Across 434 biomanufacturing companies, contamination was the main reason for batch spoilage.

Biomanufacturing with the help of defined artificial co-cultures and consortia may hold a key to increase production rates and tackle contamination [21–23].

In recent years, researchers have started to question whether an axenic culture is strictly the best way forward, as in the natural environment microorganisms thrive alongside other organisms. As thinking processes have evolved, research into harnessing consortia into biotechnological applications has increased [21] and thanks to synthetic biology and 'omics' analysis, the knowledge pool on microbial communication is expanding.

This review aims to examine critically the utility and characteristics of controlled co-cultures in biomanufacturing. An insight into natural consortia and the characteristics that are relevant and transferrable to the industrial world is presented followed by a case study scenario of the application of this principle in developing processes that employ microalgae.

1.2. Microbial Consortia

1.2.1. Consortia in Nature

Microbial consortia are encountered within various natural habitats, such as mammalian guts [24], foods [25], soils [26–28], water bodies, and wastes [29]. A question that arises is why do naturally occurring microorganisms prefer to live as part of a community. As with human communities, in which a group of individuals play a role in the advancement of society, so do microorganisms. Microbial associations may be symbiotic [6,30,31], which include mutualism and commensalism [32], parasitic, or predator-prey type [33–35].

Compared to a single taxon, microbial assemblages have been proven to be resilient when faced with adverse conditions [36] and resist invasion from other species [37]. A consortium can overcome challenges through communication [38–41] and division of labour [22,23,36,37], evolving into a stable assemblage of community [42,43]. Biofilms are good examples of community assemblages [44–46]. Work conducted by Brenner [39] elucidates the bi-directional patterns present within complex systems, which shape and govern the mode in which the populations within the matrix grow, evolve and assert their roles [47].

Communication through metabolites [6,48–50] plays a key-role in defining relationships, protection, evolution, selection of partners and division of labour [40], as shown in Figure 1.2.1. Primary metabolites shape growth, development, and reproduction, as seen in quorum sensing. During quorum sensing, bacterial populations release regulatory metabolites, such as N-acylhomoserine lactones (AHLs) [51–53], as the population density grows [54]. The same applies to interactions in the rhizosphere, where sugars, polysaccharides, amino acids, and sterols are chemical cues [55]. Secondary metabolites facilitate external interactions [10,56]; toxins, pigments, antibiotics, alkaloids and carotenoids, are accumulated by cells as responses to abiotic and/or biotic factors [49,57,58], and can be extracted and marketed. A balanced competition within the consortium does not allow other microorganisms to be able to "readily plunder" nutrients. Division of labour has applications in bioremediation [59,60], with microorganisms working together to counteract the effect of toxins [61–63]. Thanks to these overarching characteristics, consortia are robust and readily adaptable [64], and better at outcompeting microbial contaminants and predators.

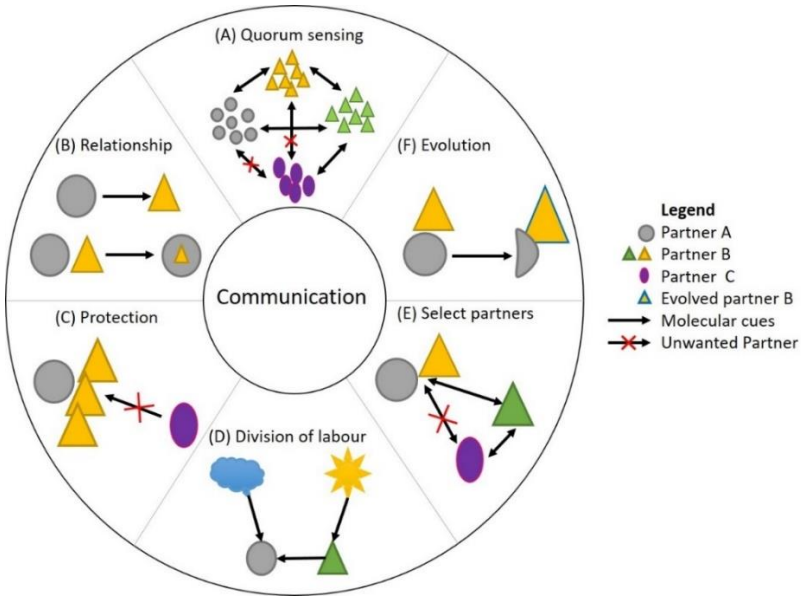

Figure 1.2.1: Communication within microbial communities.

Metabolite exchanges (arrows) facilitate various modes in which microorganisms (geometrical shapes) exhibit intra- or inter-species interactions. Communication is used for (A) quorum sensing and defining the abundance of each species and (B) type of symbiosis and roles played by partners, such as in (C) protection and (D) nutrient acquisition and division of labour. Further to this, as the community evolves, so does the communication, with the effect of causing changes to the microbial communities that are part of it, for example by recruiting new partners (E) or by evolving existing members (F).

Microbial communities have successfully evolved in nature, from macro- to micro-sphere natural scenarios. This widespread natural occurrence gives reason to believe that synthetic consortia have the potential to drive production and improve industrial biotechnology.

1.3. Artificial Co-cultures: learning from Nature

The argument for moving towards co-cultures stems from the following: (1) current technology such as transcriptomics, metagenomics, metabolomics coupled to computer modelling allow for better understanding of microbial interactions [65,66].; (2) contamination issues can be minimised or completely eliminated [22,23,67]; (3) growth profiles of primary producers can be improved [9,68]; (4) the release of new molecules could be triggered [69]; (5) bioremediation and production can be coupled [70]. From a biotechnological perspective, a good consortium would be scalable, robust, self-sustainable, reproducible, versatile in terms of feedstock and/or production [38,71–73] and profitable [3,74].

When constructing an artificial consortium, factors to consider include priority effects, community backgrounds, and competitiveness for resources. Overyielding or underyielding effects [75] may arise, with overpowering microorganisms monopolising the nutrients or with competition inhibiting growth of all members [76,77]. Nevertheless, artificial co-cultures have outperformed monocultures, when used for the production of antioxidants, pigments and aromatic compounds, as shown in Table 1.3.1.

Table 1.3.1: Microbial co-cultures in bio-production

Product	Reported organisms	Mode	Reported Product yield/concentration			Ref.
			Monoculture		Co-culture	
Acetate	*Weissella confusa 11GU1 P.freudenreichii JS15*	Fermentation at 1:1 culture ratios	0.08g/kg	0.09g/kg	0.5g/kg	[78]
Astaxanthin	*Haematococcus pluvialis, Phaffia rhodozyma AS2-1557*	Gas Exchange: CO_2 and O_2 3g/L of glucose	3.68mg/L	1.09mg/L	12.95mg/L	[5]
Biomass	*Haematococcus pluvialis, Phaffia rhodozyma AS2-1557*	Gas Exchange: CO_2 and O_2 25g/L of glucose	0.62g/L	5.02g/L	5.70g/L	[5]
	Scenedesmus obliquus	Direct mixing, 3:1 ratio	3.5g/L	n.d.	4.38g/L	[79]
	Isochrysis galbana 8701 Ambrosiozyma cicatricosa	Direct mixing, 1:1 ratio	1.17g/L	0.31g/L	1.32g/L	[80]
	Spirulina platensis UTEX 1926 Rhodotorula glutinis 2.541	Direct mixing, 2:1 ratio	0.20g/L	1.7g/L	3.6g/L	[81]
	Chlorella vulgaris TISTR 8261 Trichosporonoides spathulata	Direct mixing	0.75g/L	10.23g/L	12.2g/L	[77]
	Chlorella sp. KKUS2 Toluraspore YU5/2	Direct mixing	1.933g/L	8.333g/L	8.010g/L	[82]
	Chlorella sp. KKUS2 Toluraspore Y30	Direct mixing	1.933g/L	8.267g/L	8.733g/L	[82]
Carotenoids	*Rhodutola glutinis DBVPG 3853, Debaryomyces castellii DBVPG 3503*	Fed-batch system with co-culture 1:1 ratio	5.3mg/L, batch co-culture		8.2mg/L	[83]
EPS	*Weissella confusa 11GU1 P. freudenreichii JS15*	Fermentation at 1:1 , with 15% w/w added flour	n.d.	1g/kg	1.52g/kg	[78]
	Agaricus blazei LPB03, Chlorella vulgaris LEB106	Direct mixing, 1:1 ratio	4g/L	0.95g/L	5.17g/L	[69]
2-keto-L-gulonic acid	*Gluconobacter oxydans, Ketogulonicigenium vulgare*	Fermentation with gene manipulation	n.d.	n.d.	76.6g/L (89.7%)	[84]
Propionate	*Weissella confusa 11GU1 P.freudenreichii JS15*	Fermentation at 1:1 culture ratios	1.15g/kg	0g/kg	0.59g/kg	[78]
Lipids	*Chlorella pyrenoidosa FACHB-9 Rhodospiridium toruloides AS2.1389*	Wastewater, co-culture 1:1 ratio	3g/L	3.4g/L	4-4.6g/L	[85]
	Spirulina platensis UTEX 1926 Rhodotorula glutinis 2.541	Direct mixing, 2:1 ratio	0.013g/L	0.135g/L	0.467g/L	[81]
	Chlorella vulgaris TISTR 8261 Trichosporonoides spathulata JU4-57	Direct mixing	4.14g/L	n.d.	5.74g/L	[77]
	Chlorella sp. KKUS2 Toluraspore YU5/2	Direct mixing	0.052g/L	1.141g/L	2.424g/L	[82]
	Chlorella sp. KKUS2 Toluraspore Y30	Direct mixing	0.052g/L	0.920g/L	1.564g/L	[82]

Co-cultures employed for specific products are listed, along with the organisms employed, cultivation mode and reported product yields/productivity/concentrations in mono and co-cultures. The monoculture data provided lists the yield/concentration of the primary partner (A) followed by the secondary partner, if both organisms produce the desired product (n.d. – not determined).

1.4. Co-culture design

A bottom-up pipeline is proposed in Figure 1.4.1 to design and set-up co-cultures. This involves starting with the end-product to then shortlisting a handful of suitable primary partners (A). The primary partner will then dictate the nature of the secondary partner (B), usually an aider, ideally with bioproduction capabilities. A two-way 'trigger and response' system would be ideal, such as mutualism or a commensal symbiosis [32]. It is important to realize that growth increments do not always translate into more product, as productivity can be additionally dependent on the activity of co-culture partners. This is true for microalgae, where co-culture of partner A with B may increase biomass of A, but appropriate stress inducers may be needed to increase specific product yields [86,87].

1.4.1. Shortlisting suitable candidates

The secondary partner (B) should possess some of the following characteristics: (a) be non-toxic, (b) be capable of co-habiting [59], (c) match in growth rates, (d) provide nutrients and/or stimulators to enhance A [88], (e) not cause underyielding effects [75] (f) enhance the capability of A to utilise multiple feedstocks [89], (g) remove inhibitory molecules (h) use A's waste as feed [90], (i) maintain genetic integrity over prolonged periods of culture, and (j) be a bioproducer.

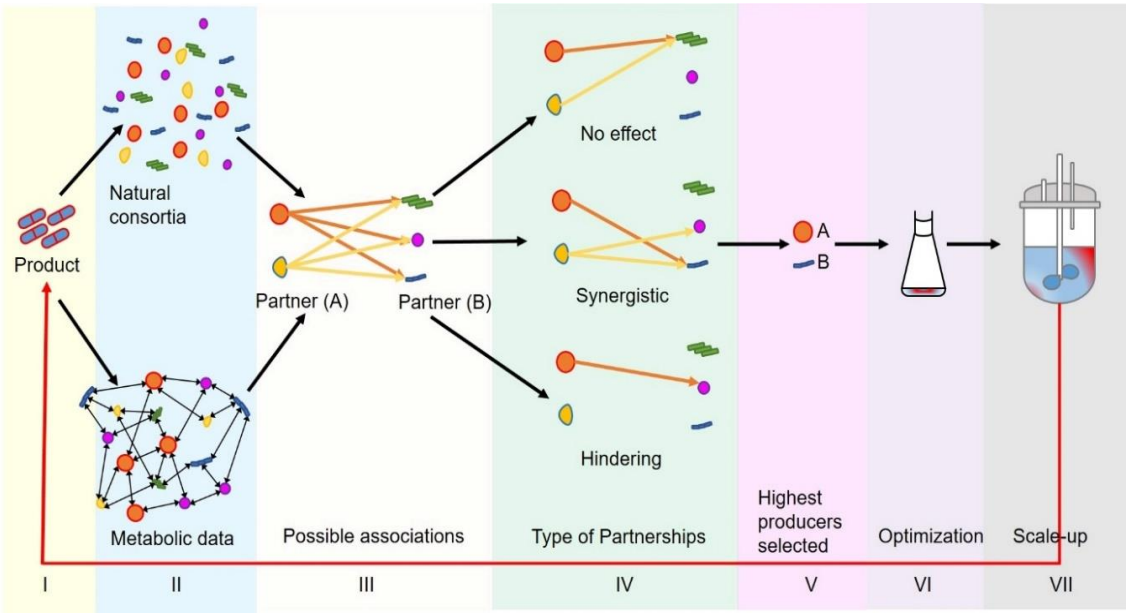

Figure 1.4.1: Steps involved in constructing an artificial co-culture.

A bottom-up approach is shown. The desired product is defined first (I), the microbial producers are short-listed next. This can be based on metabolite profiling or on natural associations (II). From selected candidates (III) co-cultures need to be investigated to elucidate the type of partnership (IV). The highest yielding co-culture is to be selected (V), optimized (VI) and upscaled (VII).

1.5. Selecting co-culture partners

Co-culture partners are selected according to (1) communication (metabolite/peptide/protein) profiling and/or (2) from existing natural associations. Screening based on communication profiling involves surveying the literature for secondary partners that release compounds to enhance the primary partner (A). Whilst, the second method consists in picking partners from a natural symbiotic consortium. Angelis et al. [69] tested combinations between 8 Basidiomycetes and 4 strains of microalgae, to evaluate the best co-culture partners. The candidates were selected

according to exopolysaccharide (EPS) production, on the basis that co-culturing fungi with algae would increase overall EPS production. An increased yield with a diverse composition of EPS was recovered, and the co-culture of *Agaricus blazei* (Basidiomycete) and *Chlorella vulgaris* (microalgae) was chosen for further studies [69]. Similarly, *Weissella confusa* 11GU-1 (a yeast) and *Propionibacterium freudenreichi* JS15 (a bacterium) were deemed to be a working co-culture in bread-making, as the molecules released through their association served to be better antifungal, texture-building and anti-stalling agents [78].

1.5.1. Co-culture media

A communal growth medium is required for co-culturing. Microorganisms isolated from symbiotic consortia will thrive in their original media. However, for artificial co-cultures, a new recipe has to be developed and tested. Conventionally, growth medium of the primary partner, A [4], or a mixed medium of A and B [91] in which both partners can grow are used. In a mutualistic symbiosis, co-culturing in growth medium A, should be sufficient. In commensal symbiosis a supplement to help partner B may be needed. For example, glucose, yeast extract [4] and/or corn syrup [83] were added to the algal media to assist the yeast strains.

1.5.2. Inoculation: ratio and timing

The inoculum density of each partner will affect the final co-culture outcome. This can be determined by analysing the growth rate of the organisms in co-culture media. Buzzini [83] demonstrated that when the inoculation ratio of *R. glutinis* (yeast) and *D. castellii* (starch accumulating bacteria) was 1:1, it resulted in a 150% increase in β-carotene production (by the yeast). This is not always the case, as seen in the *C. vulgaris* and *R. glutinis* (algae-yeast) co-culture where higher yields of lipids and biomass were achieved compared to monoculture, irrespective of the starting inoculum [76]. The timing, order and growth phase at which the inoculums are introduced into the culture vessel will influence the general structure of the co-culture and its performance. This phenomenon has been termed priority effect [92,93], and can be an integral factor in bioreactor systems, as shown by Zhang et al. [91]. The co-culturing of *C. vulgaris* and *R. glutinis*, achieved higher levels of biomass and lipids, reaching 17.3% and 70.9%

respectively, when each culture was inoculated in their respective log-phase, at a ratio of 1:1. Similarly, the co-culture of *Dinoroseobacter shibae* (a bacterium) and *Thalassiosira pseudonana* (a diatom), required *T. pseudonana* to be in exponential growth phase before the bacterial inoculation [94].

1.6. Reactor design and available technologies for co-culture

Bioreactors (photo, airlift, pulsed, stirred, packed, fixed-bed, fluidised, etc.) that can be run in continuous, semi-batch/fed-batch and batch modes have been devised for the culturing of axenic cultures, where monitoring and nutritional requirements are relatively simpler when compared to co-cultures. The challenges rest in finding suitable methods to maximise the growth of co-cultures.

Non-compartmentalised approaches, such as co-inoculation, pelletisation [95], biofilms, and encapsulation [77], allow for close contact of the organisms facilitating metabolite exchange. However, this approach has problems with respect to monitoring population dynamics, third party contamination, and meeting nutritional requirements of the primary partner to ensure it is not outcompeted. In compartmentalised approaches the physical contact of the interacting organisms is limited [70]. However, it offers the advantage of independent harvesting and easier monitoring of the bioreactor environment. Each culture is treated as a monoculture, whilst exploiting co-culture characteristics. Approaches here include membrane segregation [94] including dialysis/hydrogel system [96], transwell systems [70,97] and adhesion matrix, bead entrapment [77], agar plate growth [98], growth in microfluidic channels, gaseous separation [99], cell droplets [100], and matrix immobilisation [101].

1.7. Critical considerations

Setting up a co-culture for biotechnological application will involve compromising on certain species characteristics. Trade-off between optimal conditions and the growth conditions, in the two or more species selected need to be taken into account. Trade-off may involve slower growth rate of the organisms, compared to optimal growth levels, but with higher product yields. This has an impact on processing times. However, the higher titres may outweigh the disadvantage. Viabilities of the co-culture can then be pre-determined with an overall system mass balance. Monitoring the population

dynamics to prevent competition, over-/under-yielding effects [102], contamination, toxicity, priority effects [43,92] and abiotic factors have to be addressed for system reproducibility and to prevent production failures or diminishing yields

1.8. Case study: microalgae co-cultures for biotechnological application

Microalgae can be prokaryotic (cyanobacteria) and eukaryotic photosynthetic microorganisms. They play a major role in the function of both aqueous and non-aqueous ecosystems due to their ability to grow photo-autotrophically, hence converting inorganic to organic matter that may serve as a source of nutrition for other microorganisms [103]. The simplicity of microalgae, in terms of nutrient requirements and manipulation, makes them ideal candidates for biofuel production [104–109], with some strains of *Schizochytrium sp.* reportedly accumulating oil up to 77 % dry wt. [110].

The multitude of high value biomolecules, such as astaxanthin, β-carotene, omega-3 fatty acids, phycocyanin, EPS, organic acids, and allelopathic chemicals [10,111–114] that can be produced by these organisms, makes them of commercial interest to the pharmaceutical and nutraceutical industries. However, their performance is affected by various factors, such as contamination, pH, temperature, nutrient limitations, and light availability [115–119]. Lipid accumulation[120–124], and accumulation of other bio-active compounds is usually a response to stress caused by nutrient starvation, high light, temperature, pH and salinity [125–129]. Usually, the biomolecules are chemically extracted, however in the case of algae belonging to the genera *Chlorella* and *Dunaliella*, they are also secreted into the growth medium [130].

Current established industrial productions include, β-carotene using *Dunaliella salina* [131] , astaxanthin *using Haematococcus pluvialis* [132], proteins from *Spirulina platensis* [133], fatty acids from *Chlorella sp.* [134] and pigments using *Nostoc sp.* [135]. Other products also include lutein, xanthophylls, antimicrobials, anticoagulants in addition to carbohydrates (starch and other polysaccharides) [71,136–140]. Table 1.1 lists examples of high value products from microalgae species, which have been commercially successful. The market value for lutein for example was estimated to be US $187 million in 2009 [141] with astaxanthin products being worth about US $200M

per year [142]. Though some of these compounds can be synthesized artificially, manufacturers are steering towards natural products, due to limitations in biological functions and implications in food safety [143].

Table 1.8.1: A selection of high value products derived from microalgae species as monocultures.

Bioproduct	Reported Species	Reported Product yield/concentration	Ref.
Astaxanthin	*Chlorella zofingiensis* ATCC 30412	10.3 mg/L	[144]
	C. zofingiensis CCAP 211/14	0.1 pg/cell	[145]
	Haematococcus pluvialis LB 16	91.7 pg/cell	[146]
	H. pluvialis 26	40.25 - 51.06 mg/L	[147]
	H. pluvialis 34/7	2.7% dry wt	[148]
β- carotene	*D. salina* Sambhar Salt Lake	4.21 pg/cell	[128]
	D. salina 19.3	7.05 - 8.26 pg/cell	[149]
	D. salina SAG 42.88	3.99 pg/cell	[129]
	D. salina CONC-007	72.7 pg/cell	[150]
	D. salina CCAP 19/18	31.6 pg/cell	[150]
	D. salina Urmia Lake isolate	8.94 - 11.4 pg/cell	[151]
	D. salina KU01	56.25 pg/cell	[152]
	Dunaliella bardawii - KU01	52.91 pg/cell	[152]
	D. salina CCAP 19/18	70 pg/cell	[153]
Glycerol	*Dunaliella sp* Sambhar Salt Lake	94.26 pg/cell	[128]
Lipids	*Botryococcus braunii* UTEX 572	5.51 -21 mg/L/d	[154]
	Chlorella vulgaris KCTC AC10032	6.91 mg/L/d	[154]
	Scenedesmus sp. KCTC AG20831	20.65 – 39 mg/L/d	[154]
Lutein	*Chlamydomonas acidophila*	20 mg/L	[155]
	Muriellopsis sp. Empordámarsh	1.4 - 0.8 mg/L/d	[141]
	C. zofingiensis CCAP 211/14	4 mg/g dry wt	[145]
Phycobilin	*Nostoc muscorum* *Gloeotrichia* Nat*ans*	0.0229% p/v 0.21 g/L	[140] [135]
Phycocyanin	*Galdieria sulphuraria* 074G *Spurilina platensis* *S. pluriformis* *Nostoc sp.*	8-28 mg/g dry wt 46% w/w 9.6% w/w 20% dry wt	[156] [71] [71] [135]

The species involved and reported product yields/productivity/concentration are provided in different units as reported in the references.

1.9. Microalgae co-cultures: current status

Microalgae are good candidates for co-culture, and research in this field is yet to harness its full potential. There is a considerable body of work on consortia and co-cultures in the wastewater treatment and anaerobic digestion, where microalgae are increasingly being investigated as co-culture partners. Here, we focus primarily on microalgae co-cultures that can be used in biomanufacturing. Work at bench scale and small pilot scale trials have been carried out on the interaction between microalgae and other

microorganisms. Popularly, bacteria have been the focus of the investigation, as many bacterial species are endogenous in most non-axenic microalgal cultures. The tight-knit relationship that exists between bacteria and algae comes down to the fact that many microalgae rely on exogenous sources of cobalamin (vitamin B_{12}), thiamine (vitamin B_1) and/or biotin (vitamin B_7) to grow [157–159]. These compounds are widely synthesised by a vast array of bacterial species [68,158,160] and available for consumption.

Investigations have shown that co-culture of the bacterium *Mesorhizobium loti* with the green alga *Lobomonas rostrate* [157,158] and the bacterium *Sinorhizobium meliloti 1021* (*Ensifer meliloti*) with the green alga *Chlamydomonas reinhardtii* [159] are based on vitamin association. Furthermore, cobalamin producing bacteria, such as *Mesorhizobium sp., Mesorhizobium plurifurium, Roseomonas mucosa, S. meliloti Mn04-gfp, S. meliloti* 1021*, Alcaligenes faecalis,* and *Pseudomonas putida* mt2, have also been shown to live in successful symbiotic associations with microalgae *C. reinhardtii*, *L. rostrate* and *C. nivalis* [157]. The studies concluded that the consortium established a defined algal morphology development, nutrient acquisition as well as bacterial growth [159].

Another potentially important relationship is between microalgae and yeast*,* where the microalgae provided O_2 for yeast to assimilate and the yeast release CO_2 to aid algal photosynthesis. Work conducted in the co-culturing of yeast and algae has shown increases in overall biomass with impacts on lipid profiles. The coupling of microalgal species with a symbiotic organism led to an increase in biomass and desired products, and has gained popularity in bioremediation and biodiesel production, as shown in Table 1.1. When using microalgae assemblages for bioremediation, the waste streams are high in nutrients, which may cause the bacterial strains to outgrow the algal ones. This would affect the lipid profile for biodiesel production, as bacterial strains are low lipid producers. Similarly, with no nutrient starvation, lipid synthesis may not occur within the algal strain. Thus, other forms of energy recovery such as anaerobic digestion and hydrothermal liquefaction are more suitable.

1.9.1. Factors Affecting Microalgae Co-Cultures

As in monocultures, pH, nutrients, N/P ratio, availability of carbon source, light intensity and salinity will affect the growth kinetics of the co-culture. Likewise, the priority effects and history of the community, as discussed in section 3.3, will influence the co-culture. A limiting step would be co-culturing an organism with higher growth rate compared to algae (bacteria/yeast), which may result in the algae population being outcompeted, light limitation due to shading, and competition, all factors affecting final product yields [37,158,161].

Work carried out by Cai et al. [80] investigated the growth and biochemical composition of alga *I. galbana* and the yeast *A. cicatricosa* co-cultures for aquaculture food. The co-culture inoculum of 1:1 was used yielding higher biomass of 1.32g/L compared to maximum obtained from *I. galbana* 8701 (1.17g/L) and *A. cicatricosa* (0.31g/L) monocultures, with enhancements in C14 and C18 fatty acid contents, 18.85% and 9.03% of total fatty acids. At the end of the experimental period, the co-culture population was 96.64% algae cells. Zhang et al. [91] demonstrated that inoculating *C. vulgaris* and *R. glutinis* co-culture at log-phase improved biomass and lipid yields by 17.3% and 70.9%, with seeding ratios of 1:1 and 1:2 (yeast:algae).

Shu et al. [162] investigated *Chlorella sp.* and *Saccharomyces cerevisiae*, at the following seeding ratios, 1:2, 1:1, 2:1, the best ratio was 2:1. (algae: yeast), with higher lipid and biomass produced. In the case of *S. obliquus* with *Candida tropicalis* and *S. cerevisiae*, a ratio of 3:1 (algae: yeast) increased the algal biomass yield by 30% [79].

1.9.2. Microalgae Co-Culture: Future Potential

In the case of eukaryotic microalgae, the partnership with other organisms such as bacteria, yeast or cyanobacteria may be beneficial in production outputs. Selecting symbiotic/synergistic/mutualistic organisms for artificial co-cultures, that themselves produce marketable products, allows for a biorefinery mode of production [71,72]. Extrapolating this concept to symbiotic poly-cultures, thus mimicking natural consortia in the laboratory, would fully exploit the system. A possible future multi-production scheme, for an algae photobioreactor, is represented in Figure 1.9.1.

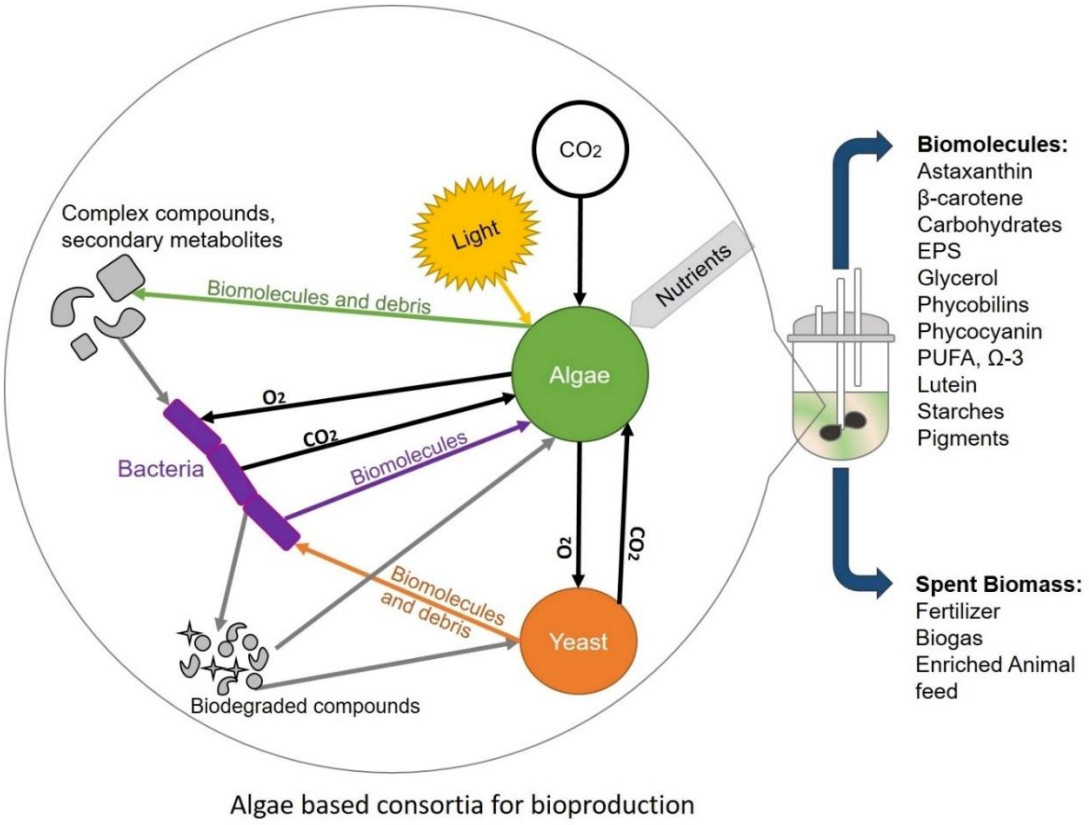

Figure 1.9.1: Representation of a microalgae-based consortium for biotechnological applications.

A photo-illuminated bioreactor for culturing an artificially created synergistic consortium between algae, yeast and bacteria within a small-scale reactor is represented. The microalgae take up carbon dioxide and produce oxygen (through photosynthesis) that is, consumed by the aerobic bacteria and yeast, which in turn supply carbon dioxide (through respiration) to be consumed by the algae. Cell secretions and degradation will release biomolecules (vitamins, proteins, carbohydrates, nucleic acids and secondary metabolites) into the growth media. The bacteria will break these down into simpler compounds to be consumed by all members of the consortium.

1.10. Work presented in the thesis

The work undertaken in this investigation will aim at creating two co-cultures for bioproduction. By putting the suggestions in this literature review to test, the co-cultures developed for this investigation aimed at improving biomass and productivity of the main partner (microalgae). Co-culture design, selection of partners, priority effects, and trade-offs encountered shaped the decisions on how to conduct the experimental design. The association between *D. salina*, *Halomonas sp.* and *Halobacterium salinarum*, a natural based halophilic co-culture, will be assessed in terms of microalgae growth rate, biomass yield and β-carotene productivity. Similarly, artificial

co-culture the artificial co-culture of *S. obliquus* and *Rhodosporidium toruloides* will be used maximise biomass and lipid production.

Various analytical techniques (detailed in Materials and Methods, Chapter 2) were implemented to understand the modus *operandi* of the two co-cultures. Population dynamics were evaluated using cell counts and dry weight analysis. Intracellular compounds (β-carotene, lipids and pigments) and extracellular compounds (glycerol, carbon, and nitrates) were quantified using biochemical assays coupled to analytical instruments. The exopolymeric substances from liquid culture systems was analysed for total proteins, carbohydrates and quorum molecules. Additionally, an agar system was developed to identify extracellular metabolites that governed the freshwater interactions.

1.11. Co-cultures and consortia: challenges and future possibilities

The literature presented in this review shows the benefits of co-culture, with the design of co-cultures on trigger-response mechanisms to increase outputs [49,58]. However, slight variations in the culturing system could alter the behaviour of the consortium and destabilise the synergistic balance, leading to loss of product. Potential reactor design based on the actual metabolic fluxes, as proposed by Stenuit and Agathos [64], is a tool to be used to monitor and predict culture behaviour, and from which to build upon for further optimization.

Understanding the underlying communication and population dynamics is necessary to engineer a successful industrial consortium. Identifying the extracellular chemical cues (metabolites/peptides/proteins) released by species within a co-culture/consortium would provide a canvas from which to develop the consortium production [34,57]. Various methods have been used to track molecular exchanges between microorganisms, outlined by Narihiro et al. [163] and Beale et al. [164]. These include extraction using organic solvents, cation exchange [165] combined with chromatography techniques and Mass Spectrometry [166] in combination with intracellular metabolic profiling [167,168]. Challenges exist with respect to trapping and concentrating the molecules of interest [97,164], sample processing, and separation of intra- and extra-cellular metabolites. In addition, the interference from matrix

components, such as salts found in growth media of marine algae need to be considered [168,169].

1.11.1. Co-culture database

Natural consortia have evolved over very long periods and the associations constructed by the microorganisms themselves have gone through selection phenomena to produce the extant scenarios. In the biotechnological world however, it would be unworkable to screen all positive associations. A valuable tool would be to have an open access database, detailing successful and failed, co-culture trials, with proper documentation of extracellular compound yields and relevant metadata. This would be beneficial for academic research and facilitate the transition from bench-scale to industrial applications.

Databases have found their role in engineering and more recently in synthetic biology. The compilation of databases, such as the Synthetic Biology Open Language database allows the user to search and find the right combinations to meet research requirements. The standardisation of key aspects that govern biological phenomenon has propelled research in synthetic biology. In a similar fashion, databases have been created for the metabolites and metabolic pathways, for pathogens and drugs, as outlined by the Metabolomics Society [170]; these databases are viewed by millions of users on a daily basis, who consult, update and contribute data. The identification of communication systems would benefit structuring future artificial co-cultures. Some quorum sensing, allelopathic chemical and signalling molecules from various extracellular polymeric subclasses have been identified [171,172]. It is important to preserve the bio-molecular interactions within a database that is easily accessible. Many extracellular substances are of great interest to the industry. A compendium incorporating such information also improves on the understanding and provides a better framework in which co-culturing can be exploited.

A useful co-culture database would provide standardised culturing-conditions or at least valuable metadata. This database should contain information of the microorganisms, relating to their growth dynamics, biomolecules released in axenic and in co-cultures, in addition to bioreactor conditions. The addition of an online simulator,

such as HYSIS and UniSim in Chemical Engineering, would facilitate analysis, simulation and design of co-cultures and consortia in biomanufacturing.

1.12. Conclusions

Research for the creation of artificial co-cultures in biomanufacturing has merits. As shown in this review, benefits include minimisation of contamination and enhanced co-production of similar products. Assembling and implementing co-cultures, derived naturally or artificially, is not straightforward. The ability to create very stable lichen like systems in the laboratory may not be feasible for another decade. However, the first steps to take should be in the direction of understanding the trigger-response mechanisms in co-cultures to build a versatile engineering framework. With the right tools and systematic approaches, such as the proposed database, the use of co-cultures can be developed and steered towards more complex and dynamic consortia that can be used in biomanufacturing. In this regard, microalgae based co-cultures offer promise, given their natural associations, versatility and ability to thrive with dissimilar species. The advantage of using them as the core on which to build the consortia rests on the fact that they are widely available, produce an array of products with significant importance in the welfare of humans and animals, alike, and offer environmentally sustainable biomanufacturing routes to be developed, given their ability to fix atmospheric carbon dioxide. In future, systematic construction of consortia with appropriate documentation and development should enable co-cultures to be put to effective use in biomanufacturing.

1.13. References

[1] Mcneil B, Giavasis I, Archer D, et al. Microbial production of food ingredients, enzymes and nutraceuticals. 1st ed. Mcneil B, Giavasis I, Archer D, et al., editors. Woodhead Publishing; 2013.

[2] Suvarna K, Lolas A, Hughes P, et al. Case Studies of Microbial Contamination in Biologic Product Manufacturing. Am. Pharm. Rev. 2011;50–57.

[3] Ryan J. Understanding and managing cell culture contamination. Corning Tech. Bull. 2008;1–24.

[4] Yen H-W, Chen P-W, Chen L-J. The synergistic effects for the co-cultivation of

oleaginous yeast-Rhodotorula glutinis and microalgae-Scenedesmus obliquus on the biomass and total lipids accumulation. Bioresour. Technol. 2014;184:148–152.

[5] Dong Q, Zhao X. In situ carbon dioxide fixation in the process of natural astaxanthin production by a mixed culture of Haematococcus pluvialis and Phaffia rhodozyma. Catal. Today. 2004;98:537–544.

[6] Delaux P-M, Radhakrishnan G V., Jayaraman D, et al. Algal ancestor of land plants was preadapted for symbiosis. Proc. Natl. Acad. Sci. 2015;112:13390–13395.

[7] Taylor MW, Radax R, Steger D, et al. Sponge-Associated Microorganisms: Evolution, Ecology, and Biotechnological Potential. Microbiol. Mol. Biol. Rev. 2007;71:295–347.

[8] Thiel V, Peckmann J, Richnow HH, et al. Molecular signals for anaerobic methane oxidation in Black Sea seep carbonates and a microbial mat. Mar. Chem. 2001;73:97–112.

[9] Santos CCA do A, Libeck B da S, Schwan RF. Co-culture fermentation of peanut-soy milk for the development of a novel functional beverage. Int. J. Food Microbiol. 2014;186:32–41.

[10] Kouzuma a, Watanabe K. Microbial Ecology Pushes Frontiers in Biotechnology. Microbes Environ. 2014;29:1–3.

[11] Kim JY, Kim Y-G, Lee GM. CHO cells in biotechnology for production of recombinant proteins: current state and further potential. Appl. Microbiol. Biotechnol. 2012;93:917–930.

[12] Yang Z, Wang S, Halim A, et al. Engineered CHO cells for production of diverse, homogeneous glycoproteins. Nat. Biotechnol. 2015;33:2014–2017.

[13] Johnson I. Human insulin from recombinant DNA technology. Science (80-.). 1983;219:632–637.

[14] Williams DC, Frank R M V, Muth WL, et al. Cytoplasmic Inclusion Bodies in Escherichia coli Producing Biosynthetic Human Insulin Production. Science (80-.). 1982;215:687–688.

[15] Chen T, Wang Y. Optimized Astaxanthin Production in Chlorella zofingiensis under Dark Condition by Response Surface Methodology. Food Sci. Biotechnol. 2013;22:1343–1350.

[16] Graverholt OS, Eriksen NT. Heterotrophic high-cell-density fed-batch and continuous-flow cultures of Galdieria sulphuraria and production of phycocyanin. Appl. Microbiol. Biotechnol. 2007;77:69–75.

[17] Prieto A, Canavate JP, Garcia-Gonzalez M. Assessment of carotenoid production by Dunaliella salina in different culture systems and operation regimes. J. Biotechnol. 2011;151:180–185.

[18] Malvankar NS, Lovley DR. Microbial nanowires for bioenergy applications. Curr. Opin. Biotechnol. 2014;27:88–95.

[19] Lovley DR. Microbial fuel cells: novel microbial physiologies and engineering approaches. Curr. Opin. Biotechnol. 2006;17:327–332.

[20] Langer ES. Batch Failure Rates in Biomanufacturing Good Training and Investing in the Right Equipment Upfront Are Among Solutions. Genertic Eng. Biotechnol. news. 2008;28.

[21] Kazamia E, Riseley AS, Howe CJ, et al. An Engineered Community Approach for Industrial Cultivation of Microalgae. Ind. Biotechnol. 2014;10:184–190.

[22] Brenner K, You L, Arnold FH. Engineering microbial consortia: a new frontier in synthetic biology. Trends Biotechnol. 2008;26:483–489.

[23] Williams P. Quorum sensing, communication and cross-kingdom signalling in the bacterial world. Microbiology. 2007;153:3923–3938.

[24] Koenig JE, Spor A, Scalfone N, et al. Succession of microbial consortia in the developing infant gut microbiome. Proc. Natl. Acad. Sci. U. S. A. 2011;108:4578–4585.

[25] Cocolin L, Ercolini D. Zooming into food-associated microbial consortia: a 'cultural' evolution. Curr. Opin. Food Sci. 2015;2:43–50.

[26] Singh BK, Millard P, Whiteley AS, et al. Unravelling rhizosphere–microbial interactions: opportunities and limitations. Trends Microbiol. 2004;12:386–393.

[27] Johansson JF, Paul LR, Finlay RD. Microbial interactions in the mycorrhizosphere and their significance for sustainable agriculture. FEMS Microbiol. Ecol. 2004;48:1–13.

[28] Kent AD, Triplett EW. Microbial Communities and Their Interactions in Soil and Rhizosphere Ecosystems. Annu. Rev. Microbiol. 2002;56:211–236.

[29] Bayer E a, Lamed R, Himmel ME. The potential of cellulases and cellulosomes for cellulosic waste management. Curr. Opin. Biotechnol. 2007;18:237–245.

[30] Visick KL, Ruby EG. Vibrio fischeri and its host: it takes two to tango. Curr. Opin. Microbiol. 2006;9:632–638.

[31] Moissl-Eichinger C, Huber H. Archaeal symbionts and parasites. Curr. Opin. Microbiol. 2011;14:364–370.

[32] Santos CA, Reis A. Microalgal symbiosis in biotechnology. Appl. Microbiol. Biotechnol. 2014;98:5839–5846.

[33] Gebuhr C, Pohlon E, Schmidt AR, et al. Development of microalgae communities in the phytotelmata of allochthonous populations of Sarracenia purpurea (Sarraceniaceae). Plant Biol. 2006;8:849–860.

[34] Mendes B, Brantes L, Vermelho AB. Allelopathy as a potential strategy to improve microalgae cultivation. Biotechnol. Biofuels. 2013;6:152.

[35] Benavente-Valdes JR, Aguilar C, Contreras-Esquivel JC, et al. Strategies to enhance the production of photosynthetic pigments and lipids in chlorophycae species. Biotechnol. Reports. 2016;10:117–125.

[36] Natrah FMI, Bossier P, Sorgeloos P, et al. Significance of microalgal-bacterial interactions for aquaculture. Rev. Aquac. 2014;6:48–61.

[37] Subashchandrabose SR, Ramakrishnan B, Megharaj M, et al. Consortia of cyanobacteria/microalgae and bacteria: biotechnological potential. Biotechnol. Adv. 2011;29:896–907.

[38] Bernstein HC, Carlson RP. Microbial Consortia Engineering for Cellular Factories: in Vitro To in Silico Systems. Comput. Struct. Biotechnol. J. 2012;3:1–8.

[39] Brenner K, Karig DK, Weiss R, et al. Engineered bidirectional communication mediates a consensus in a microbial biofilm consortium. Proc. Natl. Acad. Sci. U. S. A. 2007;104:17300–17304.

[40] Hays SG, Patrick WG, Ziesack M, et al. Better together : engineering and application of microbial symbiosesMicrobial Consortia Engineering for Cellular Factories: in vitro to in silico systems. Curr. Opin. Biotechnol. 2015;36:40–49.

[41] Pandhal J, Noirel J. Synthetic microbial ecosystems for biotechnology. Biotechnol. Lett. 2014;36:1141–1151.

[42] Fussmann GF, Loreau M, Abrams PA. Eco-evolutionary dynamics of communities and ecosystems. Funct. Ecol. 2007;21:465–477.

[43] Loeuille N, Leibold M a. Evolution in metacommunities: on the relative importance of species sorting and monopolization in structuring communities. Am. Nat. 2008;171:788–799.

[44] Barranguet C, van Beusekom SAM, Veuger B, et al. Studying undisturbed autotrophic biofilms: still a technical challenge. Aquat. Microb. Ecol. 2004;34:1–9.

[45] Kavita K, Mishra A, Jha B. Extracellular polymeric substances from two biofilm forming Vibrio species: Characterization and applications. Carbohydr. Polym. 2013;94:882–888.

[46] Zhang B, Powers R. Analysis of bacterial biofilms using NMR-based metabolomics. NIH Public Access. 2012;4:1273–1306.

[47] Sekar V. P.; Nandakumar, K.; Nair, K. V. K.; Rao, V. N. R. R. V. Early stages of biofilm succession in a lentic freshwater environment. Hydrobiologia. 2004;512:97–108.

[48] Beech IB, Sunner J. Biocorrosion: towards understanding interactions between biofilms and metals. Curr. Opin. Biotechnol. 2004;15:181–186.

[49] Dashti Y, Grkovic T, Abdelmohsen UR, et al. Production of induced secondary metabolites by a co-culture of sponge-associated actinomycetes, Actinokineospora sp. EG49 and Nocardiopsis sp. RV163. Mar. Drugs. 2014;12:3046–3059.

[50] Volk RB, Furkert FH. Antialgal, antibacterial and antifungal activity of two metabolites produced and excreted by cyanobacteria during growth. Microbiol. Res. 2006;161:180–186.

[51] Ahmer BMM. Cell-to-cell signalling in Escherichia coli and Salmonella enterica. Mol. Microbiol. 2004;52:933–945.

[52] González JE, Keshavan ND. Messing with bacterial quorum sensing. Microbiol. Mol. Biol. Rev. 2006;70:859–875.

[53] Hooshangi S, Bentley WE. From unicellular properties to multicellular behavior: bacteria quorum sensing circuitry and applications. Curr. Opin. Biotechnol. 2008;19:550–555.

[54] March JC, Bentley WE. Quorum sensing and bacterial cross-talk in biotechnology. Curr. Opin. Biotechnol. 2004;15:495–502.

[55] Badri D V, Weir TL, van der Lelie D, et al. Rhizosphere chemical dialogues: plant–microbe interactions. Curr. Opin. Biotechnol. 2009;20:642–650.

[56] Shank EA, Kolter R. New developments in microbial interspecies signaling. Curr. Opin. Microbiol. 2009;12:205–214.

[57] Netzker T, Fischer J, Weber J, et al. Microbial communication leading to the activation of silent fungal secondary metabolite gene clusters. Front. Microbiol. 2015;6:299.

[58] Rateb ME, Hallyburton I, Houssen WE, et al. Induction of diverse secondary metabolites in Aspergillus fumigatus by microbial co-culture. RSC Adv. 2013;3:14444–14450.

[59] Watanabe K. Microorganisms relevant to bioremediation. Curr. Opin. Biotechnol. 2001;12:237–241.

[60] Jones WR. Practical applications of marine bioremediation. Curr. Opin. Biotechnol. 1998;9:300–304.

[61] Atlas RM, Atlas MC. Biodegradation of oil and bioremediation of oil spills. Curr. Opin. Biotechnol. 1991;2:440–443.

[62] Díaz E, Jiménez JI, Nogales J. Aerobic degradation of aromatic compounds. Curr. Opin. Biotechnol. 2013;24:431–442.

[63] Ding S-Y, Xu Q, Crowley M, et al. A biophysical perspective on the cellulosome: new opportunities for biomass conversion. Curr. Opin. Biotechnol. 2008;19:218–227.

[64] Stenuit B, Agathos SN. Deciphering microbial community robustness through synthetic ecology and molecular systems synecology. Curr. Opin. Biotechnol. 2015;33:305–317.

[65] van Baarlen P, Kleerebezem M, Wells JM. Omics approaches to study host-microbiota interactions. Curr. Opin. Microbiol. 2013;16:270–277.

[66] Schofield MM, Sherman DH. Meta-omic characterization of prokaryotic gene clusters for natural product biosynthesis. Curr. Opin. Biotechnol. 2013;24:1151–1158.

[67] Kazamia E, Riseley AS, Howe CJ, et al. An Engineered Community Approach for Industrial Cultivation of Microalgae. Ind. Biotechnol. 2014;10:184–190.

[68] Croft MT, Lawrence AD, Raux-Deery E, et al. Algae acquire vitamin B12 through a symbiotic relationship with bacteria. Nature. 2005;438:90–93.

[69] Angelis S, Noivak AC, Sydney EB, et al. Co-Culture of Microalgae, Cyanobacteria, and Macromycetes for Exopolysaccharides Production: Process Preliminary Optimization and Partial Characterization. Appl. Biochem. Biotechnol. 2012;167:1092–1106.

[70] Goers L, Freemont P, Polizzi KM. Co-culture systems and technologies: taking synthetic biology to the next level. J. R. Soc. Interface. 2014;11:65.

[71] Markou G, Nerantzis E. Microalgae for high-value compounds and biofuels production: a review with focus on cultivation under stress conditions. Biotechnol. Adv. 2013;31:1532–1542.

[72] Gebreslassie BH, Waymire R, You FQ. Sustainable Design and Synthesis of Algae-Based Biorefinery for Simultaneous Hydrocarbon Biofuel Production and Carbon Sequestration. Aiche J. 2013;59:1599–1621.

[73] Trzcinski AP, Hernandez E, Webb C. A novel process for enhancing oil production in algae biorefineries through bioconversion of solid by-products. Bioresour. Technol. 2012;116:295–301.

[74] DesRochers TM, Kuo IY, Kimmerling EP, et al. The effects of mycoplasma contamination upon the ability to form bioengineered 3D kidney cysts. PLoS One. 2015;10:1–11.

[75] Schmidtke A, Gaeke U, Weithoff G. A mechanistic basis for underyielding in phytoplankton communities. Ecology. 2010;91:212–221.

[76] Cheirsilp B, Suwannarat W, Niyomdecha R. Mixed culture of oleaginous yeast Rhodotorula glutinis and microalga Chlorella vulgaris for lipid production from industrial wastes and its use as biodiesel feedstock. N. Biotechnol. 2011;28:362–368.

[77] Kitcha S, Cheirsilp B. Enhanced lipid production by co-cultivation and co-encapsulation of oleaginous yeast Trichosporonoides spathulata with microalgae

in alginate gel beads. Appl. Biochem. Biotechnol. 2014;173:522–534.

[78] Tinzl-Malang SK, Rast P, Grattepanche F, et al. Exopolysaccharides from co-cultures of Weissella confusa 11GU-1 and Propionibacterium freudenreichii JS15 act synergistically on wheat dough and bread texture. Int. J. Food Microbiol. 2015;214:91–101.

[79] Wang R, Tian Y, Xue S, et al. Enhanced microalgal biomass and lipid production via co-culture of Scenedesmus obliquus and Candida tropicalis in an autotrophic system. J. Chem. Technol. Biotechnol. 2015;9:Pages.

[80] Cai S, Hu C, Du S. Comparisons of growth and biochemical composition between mixed culture of alga and yeast and monocultures. J. Biosci. Bioeng. 2007;104:391–397.

[81] Xue F, Miao J, Zhang X, et al. A new strategy for lipid production by mix cultivation of Spirulina platensis and Rhodotorula glutinis. Appl. Biochem. Biotechnol. 2010;160:498–503.

[82] Papone T, Kookkhunthod S, Leesing R. Microbial Oil Production by Monoculture and Mixed Cultures of Microalgae and Oleaginous Yeasts using Sugarcane Juice as Substrate. World Acad. Sci. Eng. Technol. 2012;64:1127–1131.

[83] Buzzini P. Batch and fed-batch carotenoid production by Rhodotorula glutinis - Debaryomyces castellii co-cultures in corn syrup. J. Appl. Microbiol. 2001;90:843–847.

[84] Wang E-X, Ding M-Z, Ma Q, et al. Reorganization of a synthetic microbial consortium for one-step vitamin C fermentation. Microb. Cell Fact. 2016;15:21.

[85] Ling J, Nip S, Cheok WL, et al. Lipid production by a mixed culture of oleaginous yeast and microalga from distillery and domestic mixed wastewater. Bioresour. Technol. 2014;173:132–139.

[86] Su CH, Chien LJ, Gomes J, et al. Factors affecting lipid accumulation by Nannochloropsis oculata in a two-stage cultivation process. J. Appl. Phycol. 2011;23:903–908.

[87] Chi ZY, Liu Y, Frear C, et al. Study of a two-stage growth of DHA-producing marine algae Schizochytrium limacinum SR21 with shifting dissolved oxygen level. Appl. Microbiol. Biotechnol. 2009;81:1141–1148.

[88] Orphan VJ. Methods for unveiling cryptic microbial partnerships in nature. Curr. Opin. Microbiol. 2009;12:231–237.

[89] Minty JJ, Singer ME, Scholz SA, et al. Design and characterization of synthetic fungal-bacterial consortia for direct production of isobutanol from cellulosic biomass. Proc. Natl. Acad. Sci. U. S. A. 2013;110:14592–14597.

[90] Oren a. Availability, uptake and turnover of glycerol in hypersaline environments. FEMS Microbiol. Ecol. 1993;12:15–23.

[91] Zhang Z, Ji H, Gong G, et al. Synergistic effects of oleaginous yeast Rhodotorula glutinis and microalga Chlorella vulgaris for enhancement of biomass and lipid yields. Bioresour. Technol. 2014;164:93–99.

[92] Fukami T. Historical contingency in community assembly : integrating niches, species pools, and priority effects. Annu. Rev. Ecol. Evol. Syst. 2015;46:1–23.

[93] Chase JM. Community assembly: When should history matter? Oecologia. 2003;136:489–498.

[94] Paul C, Mausz MA, Pohnert G. A co-culturing/metabolomics approach to investigate chemically mediated interactions of planktonic organisms reveals influence of bacteria on diatom metabolism. Metabolomics. 2012;9:349–359.

[95] Wrede D, Taha M, Miranda AF, et al. Co-cultivation of fungal and microalgal cells as an efficient system for harvesting microalgal cells, lipid production and wastewater treatment. PLoS One. 2014;9:e113497.

[96] Smith MJ, Francis MB. Improving metabolite production in microbial co-cultures using a spatially constrained hydrogel. Biotechnol. Bioeng. 2017;114:1195–1200.

[97] Ponomarova O, Patil KR. Metabolic interactions in microbial communities: untangling the Gordian knot. Curr. Opin. Microbiol. 2015;27:37–44.

[98] Dalmas FR, Astarita L, Defilippis L, et al. Growth inhibition of an Araucaria angustifolia (Coniferopsida) fungal seed pathogen, Neofusicoccum parvum, by soil streptomycetes. BMC Microbiol. 2013;13:168.

[99] Santos C, Caldeira M, Lopes da Silva T, et al. Enhanced lipidic algae biomass production using gas transfer from a fermentative Rhodosporidium toruloides culture to an autotrophic Chlorella protothecoides culture. Bioresour. Technol. 2013;138:48–54.

[100] Byun CK, Hwang H, Choi WS, et al. Productive chemical interaction between a bacterial microcolony couple is enhanced by periodic relocation. J. Am. Chem. Soc. 2013;135:2242–2247.

[101] Lobete MM, Fernandez EN, Van Impe JFM. Recent trends in non-invasive in situ techniques to monitor bacterial colonies in solid (model) food. Front. Microbiol. 2015;6:1–9.

[102] Fukami T. Community assembly along a species pool gradient: Implications for multiple-scale patterns of species diversity. Popul. Ecol. 2004;46:137–147.

[103] Subashchandrabose SR, Ramakrishnan B, Megharaj M, et al. Mixotrophic cyanobacteria and microalgae as distinctive biological agents for organic pollutant degradation. Environ. Int. 2013;51:59–72.

[104] Christenson L, Sims R. Production and harvesting of microalgae for wastewater treatment, biofuels, and bioproducts. Biotechnol. Adv. 2011;29:686–702.

[105] Machado IMP, Atsumi S. Cyanobacterial biofuel production. J. Biotechnol.

2012;162:50–56.

[106] Mata TM, Martins AA, Caetano N. Microalgae for biodiesel production and other applications: A review. Renew. Sustain. Energy Rev. 2010;14:217–232.

[107] Frigon JC, Matteau-Lebrun F, Hamani Abdou R, et al. Screening microalgae strains for their productivity in methane following anaerobic digestion. Appl. Energy. 2013;108:100–107.

[108] Parmar A, Singh NK, Pandey A, et al. Cyanobacteria and microalgae: a positive prospect for biofuels. Bioresour. Technol. 2011;102:10163–10172.

[109] Posten C, Schaub G. Microalgae and terrestrial biomass as source for fuels--a process view. J. Biotechnol. 2009;142:64–69.

[110] Chisti Y. Biodiesel from microalgae. Biotechnol. Adv. 2007;25:294–306.

[111] Vigani M, Parisi C, Rodriguez-Cerezo E, et al. Food and feed products from micro-algae: Market opportunities and challenges for the EU. Trends Food Sci. Technol. 2015;42:81–92.

[112] Cuellar-Bermudez SP, Aguilar-Hernandez I, Cardenas-Chavez DL, et al. Extraction and purification of high-value metabolites from microalgae: Essential lipids, astaxanthin and phycobiliproteins. Microb. Biotechnol. 2015;8:190–209.

[113] Borowitzka MA. High-value products from microalgae-their development and commercialisation. J. Appl. Phycol. 2013;25:743–756.

[114] Liu L, Pohnert G, Wei D. Extracellular Metabolites from Industrial Microalgae and Their Biotechnological Potential. Mar. Drugs. 2016;14:191.

[115] Chen H, Jiang JG. Osmotic responses of Dunaliella to the changes of salinity. J. Cell. Physiol. 2009;219:251–258.

[116] Dragone G, Fernandes BD, Abreu AP, et al. Nutrient limitation as a strategy for increasing starch accumulation in microalgae. Appl. Energy. 2011;88:3331–3335.

[117] Ras M, Steyer JP, Bernard O. Temperature effect on microalgae: a crucial factor for outdoor production. Rev. Environ. Sci. Bio-Technology. 2013;12:153–164.

[118] Sayre R. Microalgae: The Potential for Carbon Capture. Bioscience. 2010;60:722–727.

[119] Yao B, Xi BD, Hu CM, et al. A model and experimental study of phosphate uptake kinetics in algae: Considering surface adsorption and P-stress. J. Environ. Sci. 2011;23:189–198.

[120] Elvira-Antonio N, Ruiz-Marin A, Canedo-Lopez Y. Effect of Nitrogen Content and CO2 Consumption Rate by Adding Sodium Carbonate in the Lipid Content of Chlorella vulgaris and Neochloris oleoabundans. Int. J. Environ. Prot. 2013;3:13–19.

[121] Feng DN, Chen ZA, Xue S, et al. Increased lipid production of the marine oleaginous microalgae Isochrysis zhangjiangensis (Chrysophyta) by nitrogen supplement. Bioresour. Technol. 2011;102:6710–6716.

[122] Jiang Y, Yoshida T, Quigg A. Photosynthetic performance, lipid production and biomass composition in response to nitrogen limitation in marine microalgae. Plant Physiol. Biochem. 2012;54:70–77.

[123] San Pedro A, Gonzalez-Lopez C V, Acien FG, et al. Marine microalgae selection and culture conditions optimization for biodiesel production. Bioresour. Technol. 2013;134:353–361.

[124] Schlagermann P, Göttlicher G, Dillschneider R, et al. Composition of Algal Oil and Its Potential as Biofuel. J. Combust. 2012;2012:1–14.

[125] Campenni' L, Nobre BP, Santos CA, et al. Carotenoid and lipid production by the autotrophic microalga Chlorella protothecoides under nutritional, salinity, and luminosity stress conditions. Appl. Microbiol. Biotechnol. 2013;97:1383–1393.

[126] Fu W, Guomundsson ??lafur, Paglia G, et al. Enhancement of carotenoid biosynthesis in the green microalga Dunaliella salina with light-emitting diodes and adaptive laboratory evolution. Appl. Microbiol. Biotechnol. 2013;97:2395–2403.

[127] Lamers P, van de Laak CCW, Kaasenbrood PS, et al. Carotenoid and fatty acid metabolism in light-stressed Dunaliella salina. Biotechnol. Bioeng. 2010;106:638–648.

[128] Phadwal K, Singh PK. Isolation and characterization of an indigenous isolate of Dunaliella sp. for beta-carotene and glycerol production from a hypersaline lake in India. J. Basic Microbiol. 2003;43:423–429.

[129] Phadwal K, Singh P. Effect of nutrient depletion on β-carotene and glycerol accumulation in two strains of Dunaliella sp. Bioresour. Technol. 2003;90:55–58.

[130] Hard BC, Gilmour DJ. A mutant of Dunaliella parva CCAP 19/9 leaking large amounts of glycerol into the medium. J. Appl. Phycol. 1991;367–372.

[131] Tran D, Doan N, Louime C, et al. Growth, antioxidant capacity and total carotene of Dunaliella salina DCCBC15 in a low cost enriched natural seawater medium. World J. Microbiol. Biotechnol. 2014;30:317–322.

[132] Del Campo JA, García-González M, Guerrero MG. Outdoor cultivation of microalgae for carotenoid production: current state and perspectives. Appl. Microbiol. Biotechnol. 2007;74:1163–1174.

[133] Avila-Leon I, Matsudo M, Sato S, et al. Arthrospira platensis biomass with high protein content cultivated in continuous process using urea as nitrogen source. J. Appl. Microbiol. 2012;112:1086–1094.

[134] Liu J, Fan K, Jiang Y, et al. Production potential of Chlorella zofingienesis as a

feedstock for biodiesel. Bioresour. Technol. 2010;101:8658–8663.

[135] Sekar S, Chandramohan M. Phycobiliproteins as a commodity: trends in applied research, patents and commercialization. J. Appl. Phycol. 2007;20:113–136.

[136] Raja R, Hemaiswarya S, Kumar NA, et al. A perspective on the biotechnological potential of microalgae. Crit. Rev. Microbiol. 2008;34:77–88.

[137] Spolaore P, Joannis-Cassan C, Duran E, et al. Commercial applications of microalgae. J. Biosci. Bioeng. 2006;101:87–96.

[138] Pignolet O, Jubeau S, Vaca-Garcia C, et al. Highly valuable microalgae: biochemical and topological aspects. J. Ind. Microbiol. Biotechnol. 2013;40:781–796.

[139] Dayananda C, Kumudha A, Sarada R, et al. Isolation, characterization and outdoor cultivation of green microalgae Botryococcus sp. Sci. Res. Essays. 2012;5:2497–2505.

[140] de Morais MG, da Silva Vaz B, Etiele Greque de M, et al. Biologically Active Metabolites Synthesized by Microalgae. Biomed Res. Int. 2015;2015:1–15.

[141] Blanco AM, Moreno J, Del Campo JA, et al. Outdoor cultivation of lutein-rich cells of Muriellopsis sp. in open ponds. Appl. Microbiol. Biotechnol. 2007;73:1259–1266.

[142] Li J, Zhu D, Niu J, et al. An economic assessment of astaxanthin production by large scale cultivation of Haematococcus pluvialis. Biotechnol. Adv. 2011;29:568–574.

[143] Caswell M, Zilberman D. Algolculture. An Econ. Anal. Algoculture. Corvallis, Oregon,; 2000.

[144] Ip P, Wong K, Chen F. Enhanced production of astaxanthin by the green microalga Chlorella zofingiensis in mixotrophic culture. Process Biochem. 2004;39:1761–1766.

[145] Del Campo JA, Rodríguez H, Moreno J, et al. Accumulation of astaxanthin and lutein in Chlorella zofingiensis (Chlorophyta). Appl. Microbiol. Biotechnol. 2004;64:848–854.

[146] Choi YE, Yun YS, Park JM. Evaluation of factors promoting astaxanthin production by a unicellular green alga, Haematococcus pluvialis, with fractional factorial design. Biotechnol. Prog. 2002;18:1170–1175.

[147] Zhang BY, Geng YH, Li ZK, et al. Production of astaxanthin from Haematococcus in open pond by two-stage growth one-step process. Aquaculture. 2009;295:275–281.

[148] Harker M, Tsavalos AJ, Young AJ. Autotrophic growth and carotenoid production of Haematococcus pluvialis in a 30 liter air-lift photobioreactor. J. Ferment. Bioeng. 1996;82:113–118.

[149] Pisal D., Lele S. Carotenoid production from microalga, Dunaliella salina. Indian J Biotechnol. 2005;4:476–483.

[150] Gomez PI, Gonzalez MA. The effect of temperature and irradiance on the growth and carotenogenic capacity of seven strains of Dunaliella salina (Chlorophyta) cultivated under laboratory conditions. Biol Res. 2005;38:151–162.

[151] Rad FA, Aksoz N, Hejazi MA. Effect of salinity on cell growth and β -carotene production in Dunaliella sp . isolates from Urmia Lake in northwest of Iran. African J. Biotechnol. 2011;10:2282–2289.

[152] Sathasivam R, Kermanee P, Roytrakul S, et al. Isolation and molecular id entification of β -carotene producing strains of Dunaliella salina and Dunaliella bardawil from salt soil samples by using species- specific primers and internal transcribed spacer (ITS) primers. African J. Biotechnol. 2012;11:16677–16687.

[153] Mojaat M, Pruvost J, Foucault a., et al. Effect of organic carbon sources and Fe2+ ions on growth and β-carotene accumulation by Dunaliella salina. Biochem. Eng. J. 2008;39:177–184.

[154] Yoo C, Jun S-Y, Lee J-Y, et al. Selection of microalgae for lipid production under high levels carbon dioxide. Bioresour. Technol. 2010;101 Suppl:S71-4.

[155] Garbayo I, Cuaresma M, Vilchez C, et al. Effect of abiotic stress on the production of lutein and beta-carotene by Chlamydomonas acidophila. Process Biochem. 2008;43:1158–1161.

[156] Sloth JK, Wiebe GW, Eriksen NT. Accumulation of phycocyanin in heterotrophic and mixotrophic cultures of the acidophilic red alga Galdieria sulphuraria. Enzyme Microb. Technol. 2006;38:168–175.

[157] Kazamia E, Czesnick H, Nguyen TT Van, et al. Mutualistic interactions between vitamin B12 -dependent algae and heterotrophic bacteria exhibit regulation. Environ. Microbiol. 2012;14:1466–1476.

[158] Grant MAA, Kazamia E, Cicuta P, et al. Direct exchange of vitamin B12 is demonstrated by modelling the growth dynamics of algal–bacterial cocultures. ISME J. 2014;1–10.

[159] Xie B, Bishop S, Stessman D, et al. Chlamydomonas reinhardtii thermal tolerance enhancement mediated by a mutualistic interaction with vitamin B12-producing bacteria. ISME J. 2013;7:1544–1555.

[160] Helliwell KE, Scaife MA, Sasso S, et al. Unraveling vitamin B12-responsive gene regulation in algae. Plant Physiol. 2014;165:388–397.

[161] Praveen P, Loh K-C. Photosynthetic aeration in biological wastewater treatment using immobilized microalgae-bacteria symbiosis. Appl. Microbiol. Biotechnol. 2015;99:10345–10354.

[162] Shu C-H, Tsai C-C, Chen K-Y, et al. Enhancing high quality oil accumulation and

carbon dioxide fixation by a mixed culture of Chlorella sp. and Saccharomyces cerevisiae. J. Taiwan Inst. Chem. Eng. 2013;44:936–942.

[163] Narihiro T, Sekiguchi Y. Microbial communities in anaerobic digestion processes for waste and wastewater treatment: a microbiological update. Curr. Opin. Biotechnol. 2007;18:273–278.

[164] Beale D, Kouremenos K, Palombo E. Microbial Metabolomics. Enzo Palombo, editor. Springer International Publishing, Switzerland; 2016.

[165] Frølund B, Palmgren R, Keiding K, et al. Extraction of extracellular polymers from activated sludge using a cation exchange resin. Water Res. 1996;30:1749–1758.

[166] Solomon K V., Haitjema CH, Thompson D a., et al. Extracting data from the muck: Deriving biological insight from complex microbial communities and non-model organisms with next generation sequencing. Curr. Opin. Biotechnol. 2014;28:103–110.

[167] Ebada SS, Edrada RA, Lin W, et al. Methods for isolation, purification and structural elucidation of bioactive secondary metabolites from marine invertebrates. Nat. Protoc. 2008;3:1820–1831.

[168] Kapoore RV, Vaidyanathan S. Towards quantitative mass spectrometry-based metabolomics in microbial and mammalian systems. Philos. Trans. A. 2016;374:1–14.

[169] Goulitquer S, Potin P, Tonon T. Mass spectrometry-based metabolomics to elucidate functions in marine organisms and ecosystems. Mar. Drugs. 2012.

[170] Society M. http://metabolomicssociety.org/resources/metabolomics-databases#home. 2014.

[171] Flemming H, Wingender J. The biofilm matrix. Nat. Rev. Microbiol. 2010;8:623–633.

[172] Xiao R, Zheng Y. Overview of microalgal extracellular polymeric substances (EPS) and their applications. Biotechnol. Adv. 2016;34:1225–1244.

Chapter 2: Materials and Methods

2.1. Introduction

This chapter contains the description of the general materials and methods employed in this research. Brief overviews of microorganisms used in this study and their method of growth are provided. Furthermore, details about biochemical assays and instruments used are outlined. Specific details pertinent to each chapter are provided in the sections named experimental design.

2.2. Microorganisms studied

This chapter provides the general material and methods used for the purpose of the investigation. Included are details on the microorganisms: their provenance and growth/medium requirements. An outline will be provided on each species cultivation method, and on the measured parameters of optical density, cell counts, colony formation units (CFU) and light intensity readings. Specific details pertaining to individual chapters will be provided in the respective sections.

D. salina, *Halomonas* and *S. obliquus* were identified using molecular biological techniques (Appendix A).

2.2.1. *Dunaliella salina* CCAP 19/18

Dunaliella salina 19/18 culture was obtained from the Culture Collection of Algae and Protozoa (CCAP). The cell stocks were maintained in 3 M HEPES medium. The medium consisted of: 87.75 g NaCl (1.5 M NaCl and was varied as required depending on the salinity chosen), 10 mM KCl, 20 mM $MgCl_2$, 10 mM $CaCl_2$, 24 mM $MgSO_4$, 5 mM $NaNO_3$, 24 mM Na_2SO_4, 0.1 mM NaH_2PO_4, 0.0015 mM FeEDTA, 1 ml/L of trace elements (185 mM H_3BO_3, 7 mM $MnCl_2{\cdot}4H_20$, 0.8 mM $ZnCl_2$, 0.02 mM $CoCl_2{\cdot}6H_2O$, 0.4 mL of 0.2 mM in 400 mL, 2 mM $CoCl_2{\cdot}6H_20$ in 225 mL and 0.2 mM $CuCl_2{\cdot}2H_20$ in 900 mL), 20 mM HEPES pH 7.6 and 1 g/L of $NaHCO_3$. The medium was autoclaved at 121°C before use, pH measured and adjusted to 7.5. For agar plates, 15-20 g/L agar was added (Agar No 3)

prior to autoclaving. *D. salina* was stored on agar plates containing 500 µg/L of cefoxamine, to minimise contamination from bacterial cultures.

Stocks were grown in 3 M HEPES (175 g/L of NaCl), in static 250 mL Erlenmeyer flasks, at 25±2 °C, and illuminated at 50-60 µmol m^{-2} s^{-1}.

2.2.2. *Halomonas* (isolated from *D. salina*)

Halomonas was isolated from the *D. salina* cultures and characterized (Appendix A). It was grown in 1.5 M LB medium containing, per litre: 10 g tryptone, 5 g yeast extract and 10 g NaCl. The medium was autoclaved at 121 °C before use. Agar plates were made by adding 15 g/L of agar prior to autoclaving. *Halomonas* was mainly grown on plates. When resuspended in liquid cultures, the cells were grown in 100 mL of LB medium, shaken at 150 rpm at 30 °C or room temperature (depending on the experiment).

2.2.3. *Halobacterium salinarum* NCIMB 764

Halobacterium salinarum NCIMB 764 was ordered from the National Collection of Industrial, Food and Marine Bacteria (NCIMB). The haloarchaeon had been freeze-dried in 1996 and shipped in a glass ampoule. The haloarchaeon was grown in 4.2 M ATCC1863/NCIMB 219 containing, per litre: 7.5 g Casamino acids, 10 g Yeast extract, 3 g Trisodium citrate, 2 g KCl, 20 g $MgSO_4 \cdot H_2O$, 36 mg $FeCl_2 \cdot H_2O$, 0.36 mg $MnCl_2 \cdot 4H_2O$ and 250 g/L of salt (for 4.2 M medium). The medium was autoclaved at 121 °C before use, pH measured and adjusted to 7.4. For agar plates, 20 g/L of agar (Agar No 3) was added prior to autoclaving. Upon arrival, the microorganism was resuspended in 30 mL of 4.2 M medium and grown at 30 °C for a week. Within a week, the microorganism showed signs of growth; aliquots were passaged into 100mL of medium and shaken at 150 rpm at 30 °C. The optical densities were measured, and readings became stable after the 4^{th} week of passages, with reproducible flasks readings. 4.2 M Agar plates at were used to maintain stocks.

2.2.4. Scenedesmus obliquus

Scenedesmus obliquus 276/3A was ordered from CCAP and grown in Bold's Basal Medium (BBM), which contained, per litre: 10 mL, of 10 g $NaNO_3$, 3 g $MgSO_4 \cdot 7H_2O$, 1 g

NaCl, 3 g K_2HPO_4, 7 g KH_2PO_4 and 1 g $CaCl_2 \cdot 2H_2O$ in 400 mL of stock; 1 mL of trace elements solution containing 8.82 g $ZnSO_4 \cdot 7H_2O$, 1.44 g $MnCl_2 \cdot 4H_2O$, 0.71 g MoO_3, 1.57 g $CuSO_4 \cdot 5H_2O$ and 0.49 g $Co(NO_3)_2 \cdot 6H_2O$ per litre of stock; 1 mL of a solution containing 11.42 g H_3BO_3 per litre of stock; 1 mL of a solution containing 50 g EDTA and 31 g KOH per litre of stock; 1 mL of a solution containing 4.98 g $FeSO_4 \cdot 7H_2O$ and 1 mL H_2SO_4 (conc.) per 1 litre of stock. The medium was autoclaved at 121 °C before use, pH measured and adjusted to 6.2. Agar plates were made by adding 15 g/L of agar prior to autoclaving.

S. obliquus cell colony was were kept on the agar plates at room temperature, under 90-100 µmol m^{-2} s^{-1} of irradiance. Prior to experiments, a cell colony would be re-suspended in 30 mL of BBM medium for a week and passaged twice, before working stocks were used to inoculate working flasks. The 250 mL Erlenmeyer flasks, contained 100 mL of BBM, illuminated at 90-100 µmol m^{-2} s^{-1}, shaken at 70-80 rpm and grown at room temperature (22-23°C).

2.2.5. *Rhodosporidium toruloides* NCYC 912

Rhodosporidium toruloides NCYC 912 was grown in Yeast Mold (YM) medium, which consisted of 3 g/L of yeast extract, 3 g/L of malt extract, 10 g/L of dextrose and 5 g/L of peptone. The chemicals were mixed together with the help of a magnetic stirrer and the pH adjusted to 6.2 with 1 M NaOH or HCl as required. The medium was then autoclaved at 121 °C for 15 minutes. The yeast was grown in an INFORS incubator at 30 °C and rotating speed of 100 rpm. For agar plates, 15 g/L of agar was added after pH adjustment. For liquid suspension, a colony of yeast was added into 30 mL of YM and grown over 24 hours. Then passage into 100 mL of medium and place on a shaker. As the growth rate of this microorganism was quite fast, liquid cultures subculturing was required every 4 days, whilst the plates were passaged every 7 days.

2.3. Maintenance of species and growth

2.3.1. Microorganisms Growth monitoring

Method on how to monitor and report microorganism growth data was species-dependent. For *D. salina* only cell counts are provided whilst, for the *S. obliquus* dry cell weight (DCW) is added to the correlation. DWC data was an unsuitable method of

estimation for the *D. salina* cells, due to the high concentration of salts within the samples that would skew the results.

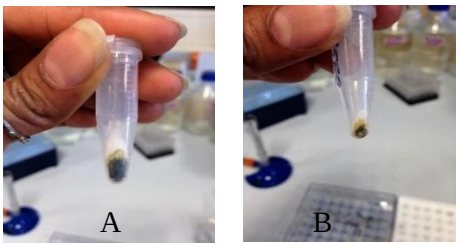

Figure 2.3.1: Salt interference in samples.

Picture A and B show the difficulty in removing the salt without affecting the biomass. A is lyophilised harvested from 3M salts. B is a pellet from the same flask that was washed once with PBS. Although some of the salts were removed, the loss of biomass is quite visible.

To obtain enough biomass for dry weight analysis, 50 mL of cells at various optical densities where harvested as described in section 2.3.1. Subsequently, to remove any traces of salts the cells where washed by adding 1mL of MilliQ-water or PBS 1x buffer (this step was not suitable with the *D. salina* cells, as osmotic shock caused the cells to rupture). Centrifuging the cells for a last time at 17,000 g for 10 minutes allowed pipetting out the wash buffer. The Eppendorfs were stored -20°C until lyophilization for 24 hours at -110 °C. The weight difference between the empty Eppendorf and the lyophilised Eppendorf gave the biomass amount (mg).

Dry weight estimates of *D. salina* cells was disregarded as the high salinities of 1.5-3 M (87.5-175 g/L) skewed the results. Trials were conducted of washing the pellets with PBS and then estimating the dry weights. Problems were encountered, as the cells ruptured due to osmotic shock.

Cell counts using haemocytometer are a good method of estimating the cells, however, prone to human error and time consuming. A method was developed to reduce errors, by which pictures of the algae haemocytometers were taken and analysed with image software tools, such as MATLAB. Thus using more than one method of estimating the cell growth and correlating, these methods should minimise the errors when reporting data. On the other hand, bacteria, haloarchaea and yeast cells are quite small to count under the haemocytometer, therefore OD and colony formation unit (CFU) methods

were used to monitor the growth patterns. Furthermore, the tasks of monitoring the mixed population by cell counts and CFU units is time consuming and prone to error. Therefore, an attempt was made to develop a simple spectrophotometric method that would allow for simultaneous detection of microorganism in co-culture. Details of this method are presented in Appendix B. This method was not used to analyse the data in this thesis, as more work needs to be done to ensure the robustness of the method.

2.3.1.1. Microscope cell counts

10µL was transferred from the cuvette to the haemocytometer and counted under the microscope at ×40 magnification using the clicker counter. Dilutions were required at high cell counts. All 4 quadrants were counted and the number of cells were calculated by:

$$No.of\ cells = \frac{No.of\ cells\ in\ 4\ quadrants}{4} \times 10{,}000\ \times\ dilution\ factor$$

2.4. Light intensity measurements

Light intensity of the cultures was measured using a PAR (photosynthesis activated radiance) irradiance sensor (QSL-2100, Biospherical Instruments Inc., USA). The measurements were taken by submerging the head of the sensor inside the culture flask and by taking surrounding measurements. The values provided are an average of these measurements. The light intensities varied according to the algal species and the experiment, and values will be provided within to experimental design in each chapters, if differing to the stock growth values.

2.3.2. Microbial Harvesting

Depending on the protocol, aliquots of microbial culture were placed in 15/50 mL Falcone tubes and centrifuged at 200 g for 20 minutes for *D. salina* cells or at 3,202 g for 10 minutes for all other microorganisms. Upon removal of the supernatant, the resulting pellet was resuspended in 1 mL of medium and pipetted into 2 mL Eppendorfs. Following centrifugation at 16,500 g for 10 minutes, the remaining supernatant was removed with the help of a pipette without disturbing the cell pellet. The samples were then stored at

-80°C or -20 °C until future analysis. If necessary prior to the analysis, the pellets were freeze dried (ScanVac CoolSafe 110-4) for 24 hours at -110 °C.

2.4.1. Estimation of growth rates

By monitoring the growth through cell/CFU counts and optical density measurements it was possible to estimate the growth rate for individual organisms. The following formula was used for calculating the growth rates.

$$Growth\ rate\ (hrs^{-1}), \mu = \frac{LN(x_i) - LN(x_y)}{t_{\mathrm{xi}} - t_{xy}}$$

$$Average\ growth\ rate\ (hrs^{-1}), \bar{\mu} = \frac{\sum_{i=1}^{n} \mu_i}{t_{\mathrm{t}} - t_o}$$

Where:

x_i and x_y : reading in terms of cell/CFU

t_{xi} : time at point xi

t_{xy} : time at point xy

μ_i: growth rate

t_0 : initial time

t_t : final

Growth rates were estimated for an hourly or daily basis, whilst average growth rates expressed in terms of the elapsed time of the experimental period.

Standard error of the mean, Sx, was calculate as follows:

$$S_x = \frac{\sqrt{\sum_{i=1}^{n}(x_i - \bar{x})^2}}{n - 1}$$

n: number of data points

x: mean of xi

xi: each of the values of the data

Shown on the graphs as ± Sx.

F-test and T-test were used to calculate statistical significance, *p*. Values of $p<0.05$ were considered significant.

2.4.2. Microscope Images

Cell images acquired through an Olympus microscope (60x or 100x magnification) coupled to a computer with ProReg software.

2.5. Analytical methods

The biochemical assays used to analyse intra and extracellular molecules will be outlined in this section. Experimental set-ups, which are specific to each chapter, are outlined in the respective methods sections.

2.5.1. Wellburn assay

The 80% acetone method following the protocol outlined by Wellburn [1]was chosen. The equations for the quantification of chlorophylls a, b and carotenoids are as follows:

$$C_a = 12.21A_{663} - 2.81A_{646}$$

$$C_b = 20.13A_{646} - 5.03A_{663}$$

$$C_{x+c} = (1000A_{470} - 3.27C_a - 104C_b)/198$$

Briefly, 450 µm glass beads (acid washed, 425-600µm, Sigma Aldrich, G8772) and 1.5 mL of 80 %v/v acetone were added to the dried algae pellets. The samples were then bead beaten for 5 cycles (1 minute bead beating followed by 1 minute on ice) using a Disruptor Genie. The procedure was carried out in the dark, in order to avoid degradation of the pigments. Subsequently, the samples were incubated for 20 minutes at 4°C. The extracts were then centrifuged at 16,500 g for 10 minutes, to ensure that the glass beads and any algae debris settled to the bottom of the Eppendorf tube. A 1.4 mL quartz cuvette was used with 80 % acetone as blank. Samples were measured at 470 nm, 646 nm and 663 nm to satisfy Wellburn's equations. The cuvette was washed with 80%v/v acetone, between readings.

2.5.2. Tetrahydrofuran assay

The Tetrahydrofuran (THF) assay was used to extract β-carotene from *D. salina* cells, this method was developed by taking ideas from techniques used in the food industry [2,3]. Briefly, concentrations 0.6, 1.2, 1.8, 2.4 and 3 µg/mL of all-trans-βcarotene (C9750-

Sigma Aldrich) dissolved in THF were used to generate a standard curve. A 1.4 mL quartz cuvette was used for the measurements. 100 % THF was used as a blank. The standards were measured at 457 nm, with the cuvette being washed with THF between readings. The equation for the estimation of β-carotene was: $y = 0.1864x + 0.0025$, where y is the absorbance reading at OD_{457nm} and x β-carotene (µg/mL). β-carotene was extracted from the algae pellets by adding 2 mL of THF and vortexing for 4-6 minutes or until all the biomass was colourless. The procedure was carried out in the dark, in order to avoid degradation of the carotenoid. Finally, the extracts were centrifuged at 16,500 g for 10 minutes, to ensure any debris settled to the bottom of the Eppendorf. The samples were then measured at 457 nm.

2.5.3. Glycerol assay

Concentration of glycerol in cell supernatants was carried out by using a colorimetric assay. Briefly, glycerol standard (Sigma-G7793, 0.26 mg glycerol/mL) was used to make standard concentrations of 6.5, 5.2, 3.9, 2.6, 1.3 and 0 µg. The standards were made in 3 M HEPES or the growth medium used in the investigation. Free glycerol reagent (Sigma- F6428) was taken from the fridge and allowed to reach room temperature before starting the assay. For cuvette assays, 800 µL of reagent alongside 25 µL of standard were pipetted into 1 mL cuvettes, and mixed and incubated for 15 minutes. If a plate reader was used, the ratios were tailored to fit the maximum well capacity. Using the zero to blank the spectrophotometer, the standards were measured at 540 nm. The equation for the estimation of glycerol was y = 0.1267x - 0.1925, where y is the absorbance reading at OD_{540nm} and x glycerol (µg). Cellular supernatant was collected and filtered using 0.22 µm syringe filter before assaying.

2.5.4. Dissolved Inorganic Nitrogen assay

Dissolved inorganic Nitrogen (DIN) protocol was adapted from [4]. Using a 0.22 µm filter, to remove traces of inorganic matter, the supernatant from centrifuged cells was filter sterilised and stored at -20 °C. Firstly, a calibration curve was generated using known amounts of sodium nitrate (same nitrate source in 3 M HEPES and BBM medium) dissolved in nitrate free growth medium.

A stock solution of 500 µM was used to obtain concentrations ranging from 15 µM to 500 µM of sodium nitrate. Readings were done in triplicate batches to ensure the robustness of the assay. The results were then graphed and fitted a best-fit line. The equation generated for the estimation of nitrates in 3 M HEPES medium was y = 0.0012x + 0.0478 and for BBM medium was y = 0.0024x + 0.0056, where y is the optical density reading at OD_{220nm} and x, the amounts of nitrates, was later used to estimate the concentration of nitrate in microalgae supernatant samples.

On the day of analysis, all the samples were thawed and vortexed to ensure homogeneity of the sample. The samples were diluted by a factor of 10 or 20 to ensure that the readings obtained would fall within the boundaries of the calibration curve. Nitrate free BBM medium with 2 % 1 M HCl used as blank and to dilute the samples. Acidification with HCl is recommended to prevent interference from hydroxide or carbonate concentrations present within the sample. The samples were measured in a quartz cuvette at 220 nm for nitrate estimation, and readings at 275 nm were used to correct the nitrate values obtained.

2.5.5. Transesterification of microalgae biomass

For the detection of Fatty Acid Methyl Esthers (FAME) [5], 5 mL of algae biomass was harvested into 15 mL Falcon tubes and centrifuged at 3,202 g for 15 minutes. 4 mL of supernatant was removed and stored for DIN and pH analysis. The remaining 1 mL of supernatant was used to re-suspend the microalgae pellet, which was transferred to a 2 mL Eppendorf Safe-Lock tube. This was then spun down at 16,500 g for 10 minutes and the remaining supernatant removed with the help of a 1 mL pipette. The samples were stored at -20 °C and analysed within one month, or stored at -80 °C for 3-4 months.

The transesterification consisted in extraction and derivatization of the samples in sequential steps. Briefly, 300 µL of toluene was added to the pellets and vortexed for 1 minute. Following, 300 µL of sodium methoxide was added to the mix, vortexed for 1 minute. The mixture was then transferred into 2 mL glass vials with PTFE caps (Sigma-Aldrich, 27134) and incubated for 20 minutes on a heating block at 80 °C. At the end of the incubation period, the vials were left to cool for 10 minutes, after which 300 µL of boron trifluoride was added to each vial, followed by a last incubation of 20 minutes at

80 °C. In the meantime, 2 mL Safe-Lock Eppendorf tubes were prepared with 300 µL of MS grade water and 600 µL of hexane. To terminate the incubation period, each sample was transferred into these Eppendorfs. The resulting biphasic mixture of organic solvents and water was vortexed and centrifuged for 16,500 g at 10 °C, to facilitate phase separation. The top layer (organic solvents) now containing the FAMES was collected into a fresh 2 mL Safe-Lock Eppendorf tube, the bottom layer was discarded. The amount of organic solvent collected was kept equal to for all samples, in order to minimise skewed of the results. For this study, 800 µL of organic solvent were collected and evaporated to dryness using N_2 gas and a Multivap. It is important at this stage not to have any water in the samples, as injection of this in the GC-FID would damage the column. The now dry samples were lastly resuspended in 80 µL of toluene ready for GC-FID analysis.

2.5.6. GC-FID analysis

Prior to injection, the samples were centrifuged for 1 minute at 16,500 g. This ensured any debris within the sample would not be picked up when transferring 30 µL of toluene suspension to the injection vials (PP vial 12x32 mm, crimp seal and snap ring cap 11 mm, Chromatography direct.com) destined to the GC-FID. To quantify and identify the components within the microalgae FAME samples, Supelco 37-FAME MIX calibration standard (Supelco, CRM 47885) was purchased and injected prior to every run. The microalgae FAMEs were identified using a Thermo Finnigan TRACE 1300 GC-FID System (Thermo Scientific, Hertfordshire, UK) onto a TR-FAME capillary column (25 m x 0.32 mm x 0.25 µm). 1 µL of derivatized sample was injected at 250 °C, with a split flow of 75 mL/min and purge flow of 5 mL/min. A constant helium flow of 1.5 mL/min was maintained, and the analysis time resulted in 15 minutes per sample.

2.5.7. Dissolved Inorganic Carbon (DIC)

Procedure was carried out according to Chen et al. [6]. Briefly, from each culture flask, 5mL of medium was taken. The medium was then placed in a glass serum bottle and crimped. The crimping would seal shut the bottle and prevent any carbon dioxide from escaping. Following, 0.4 mL orthophosphoric acid was injected through the self-sealing

rubber seal. The bottle was then shaken to ensure mixing and a 5 mL syringe was inserted into seal. Subsequently, 20 mL nitrogen syringe was bubbled into the bottom of the acidified medium, displacing any gases released from the acidification reaction into the 5 mL syringe. The captured gas samples were quickly sealed and analysed using gas chromatography (GC). Thermos Scientific TRACE 1310 Gas Chromatograph was used for analysis. The samples were injected at 150 ^{o}C through a used was a HaisepQ 60/80 column (2 m, ID 1 mm, 1/16 in OD). Temperature ramps were set at 50 ^{o}C for 2.5 min, 30 ^{o}C/min for 0.7 min, reaching a temperature of 70 ^{o}C, followed by 100 ^{o}C/min for 1.67 min, reaching a final temperature of 240 ^{o}C. The thermal conductivity detector was at 150 ^{o}C. Standards of CO_2 were run in order to establish a calibration curve.

2.5.8. Combined assay for extraction of carbohydrates, proteins and pigments

2.5.8.1. Extraction

Combined extraction of carbohydrate, proteins and pigments was carried out according to Chen et al. [7]. The microalgae samples were extracted using 24.3 µL Phosphate buffer (pH 7.4), 1.8 mL of 25 % methanol in 1 M NaOH and glass beads in 2 mL Safe lock Eppendorf tubes. The cells were bead beaten for 10 minutes (3 cycles, 2 minutes cool down time) using the Disruptor Genie.

2.5.8.2. Carbohydrates

Standards of D-glucose (Sigma Aldrich, G8270) in Milli-Q water were prepared at the following concentrations: 400, 200, 100, 80, 60, 40, 20, 0 mg/mL in 2 mL Eppendorf tubes. From each standard, two aliquots of 200µL were removed and placed in 2 mL PTFE capped glass vials. For carbohydrate analysis, 1 vial was used as a control and the other as a sample. To the control sample, 1.2 mL pre-chilled 75 % H_2SO_4 was added and 0.4 mL of pre-chilled 75 % H_2SO_4 plus 0.8 mL of freshly prepared Anthrone reagent. Following, the samples were incubated at 100 °C for 15 minutes. Absorbance measurements were taken at 578 nm. The same procedure was followed for the samples. After the extraction process two aliquots of 200 µL of extract were removed and analysed.

2.5.8.3. Proteins

The remainder of the extracts were saponified. The extracts were placed in 4 mL PTFE vials and incubated for 30 minutes at 100 °C. From the saponified proteins, samples 0.7mL of supernatant was removed and used for chlorophylls and carotenoids quantification. The remaining saponified samples were moved into 2 mL Eppendorfs and centrifuged at 16,500 g for 10 minutes. Afterward, BCA kit (Pierce™ BCA, Protein Assay kit, 23225) was used to estimate proteins. The BCA kit consisted of Reagent A and Reagent B (a copper solution). Using a 96-well plate, 25 µL per samples in duplicate was pipetted. Similarly to carbohydrates assay, one vial would act as control (add only 200 µL of Reagent A) and the other as sample (Reagent B). The plate was incubated for 30 minutes at 37 °C. Readings were taken using the plate reader facility on the spectrophotometer, at 562 nm. BSA standards, 0-2 mg/mL in 25% methanol in 1M NaOH were prepared and analysed using the kit.

2.5.8.4. Pigments

To the 0.7 mL of saponified extract, 1.05 mL of chloroform:methanol (2:1) was added. The samples were vortexed and centrifuged at 16,500 g for 10 minutes. For chlorophylls analysis the resulting top layer was analysed in a quartz cuvette at 416 nm, 453 nm and 750 nm using methanol as a blank. The bottom layer was analysed using chloroform:methanol (2:1) as a blank. Readings were taken at 430 nm, 450 nm, 480 nm and 750 nm. The following equations were used to calculate the pigments:

$$\text{Chl a } (\mu g/mL) = 6.4 * A_{416} - 0.79 * A_{453}$$

$$\text{Chl b } (\mu g/mL) = 5.87 * A_{453} - 0.24 * A_{416}$$

$$\text{Carotenoids } (\mu g/mL) = A_{450}/0.1364$$

2.5.9. Total Carbohydrates quantification

Phenol-sulphuric method was used to analyse sugars in extracellular supernatant [8]. Briefly, glucose standards were prepared by diluting D-Glucose (Sigma Aldrich, G8270) in MilliQ water to obtain concentrations of 0 (Blank), 10, 20, 40, 80, 100 and 200 µg/mL. Into a 2 mL Eppendorf, 100 µL of each standard were pipetted followed by 100 µL of 5 %w/v of Phenol in water. The mixture was vortex for a several seconds. Subsequently, 1mL of sulphuric acid (conc.) was added and vortexed for several seconds. The mixtures

were incubated at 90 °C for 5 minutes. The samples were left to cool to room temperature before measuring absorbance readings at 495 nm. For analysing the samples, the same procedure was followed, and if needed, the concentrated supernatant was diluted with MilliQ water, in order to produce reading that would fall within the standard curve. All biological triplicates were measured in technical triplicates for this assay.

2.5.10. Total Protein quantification

Folin's phenol method [9] was used to identify proteins in extracellular supernatant samples. The following solutions were made and stored beforehand: NaOH (0.8 M), SDS (10 %) and Copper Tartarate Carbonate (CTC) Solution (0.2 % w/v potassium sodium tartarate tetrahydrate, 0.1 % w/v copper sulphate and 10 % w/v sodium carbonate).
Firstly, BSA standards were prepared by diluting BSA (Sigma Aldrich , A7030) in MilliQ water to obtain concentrations of 0 (Blank), 20, 40, 80, 100 and 200 µg/mL. Into a 2 mL Eppendorf, 300 µL of each standard were pipetted followed by 700 µL of MilliQ water and vortexed. To this, 100 µL of Sodium deoxycholate (0.15 % w/v) was added and vortexed to ensure homogenisation, and incubated for 10 minutes at room temperature. Following, 100µL of Trichloroacetic acid (72% w/v) were pipetted. The mixture was vortexed and centrifuged at 3,000 g for 15 minutes. The resulting pellets were then dried and resuspended in 500 µL of MilliQ water. A fresh solution (Reagent A) of MilliQ water, NAOH (0.8 M), SDS (10 %) and CTC solution was prepared in ratios 1:1:1:1. To the resuspended pellets, 500 µL of Reagent A was added, vortexed and incubated for 10 minutes at room temperatures. Finally, 250 µL of Folin's phenol reagent (diluted with MilliQ water by 1/6) was added. The samples where vortexed and incubated on the bench for 30 minutes. Absorbance measurements were taken at 750 nm, using 0 as a blank. The standard curve was done in triplicate readings. For analysing the samples, the same procedure was followed, and if needed the concentrated supernatant were diluted with MilliQ water, in order to produce readings that would fall within the standard curve. All biological triplicates were measured in technical triplicates for this assay.

2.5.11. SDS-PAGE gels

The protocol was adapted from Sambrook & Russell [10]. The 12 % resolving gel for SDS-PAGE was prepared as follows. In a 50 mL Falcon tube, 6.6 mL of Milli-Q water, 8 mL 30 % acrylamide mix, 5 mL 1.5 M Tris (pH =8.8), 200 µL of 10 % SDS, 200 µL of 10 % ammonium persulfate (prepared fresh) and 8 µL of TEMED were mixed. The mixture was poured into glass mould, leaving 1 cm space at the top for the stacking gel. The resolving gel was overlayed with 1 mL of isopropanol to prevent cracks forming. After the gel had polymerised, the isopropanol was carefully poured off, and the gel was washed with distilled water twice. With the help of a pipette most of the fluid was removed. The stacking gel was prepared by mixing 3.4 mL of Milli-Q water, 830 µL 30 % acrylamide mix, 630 µL 1M Tris (pH = 6.8), 50 µL of 10 % SDS, 50 µL of 10 % ammonium persulfate (made fresh) and 5 µL of TEMED in a 15 mL Falcon tube. The gel was then poured on top of the resolving gel, and a clean Teflon comb inserted carefully, avoiding any air bubbles. The gel was left to solidify for 20 minutes.

2.5.11.1. Preparations of sample and running the gel

Samples were diluted to obtain a concentration of 3µg/mL and 3.75 µg/mL for the *S. obliquus* and *D. salina*, respectively. To the samples 15 µL of SDS gel loading buffer was added. The proteins were then denatured by heating at 95 °C for 5 minutes. After the stacking gel polymerisation was complete, the gel was mounted into the electrophoresis apparatus, and the comb was carefully removed. Before loading the samples, 1x running buffer (Tris-glycine electrophoresis buffer) was poured into the inner and outer reservoir. In the first lane, 20 µL of protein ladder (Fisher BioReagents™ EZ-Run™ Prestained Rec Protein Ladder, 10 to 72 kD, BP3603500) was added, followed by the protein samples. The SDS-PAGE was run at 80-100 V, until the dye enters the resolving gel, and then at 150 V until all the proteins (dye) reach the bottom of the gel.

2.5.11.2. Silver nitrate

Silver nitrate protocol was adapted from Couto et al. [11]. After removing the gels from the tank, it was washed with Milli-Q water and incubated in fix solution (50 %v/v methanol, 10 %v/v acetic acid) overnight. The fix solution was discarded the following morning, and the gels were incubated in fresh fixing solution for 30 minutes. The fix solution was removed, and the gel was washed three time with 50% v/v ethanol

solution; each wash step required a 20 minute incubation period. The gel was then incubated for 1 minute in 0.02 % w/v sodium thiosulfate and washed twice with Milli-Q water. Fresh 0.1 % w/v silver nitrate solution was prepared and added to the gel. The gel was incubated for further 20 minutes and covered with aluminium foil to prevent any light damage. Afterwards the gel was washed with Milli-Q water and developed in 0.04% formalin containing 2 %w/v sodium carbonate plus 0.02 % thiosulfate solution. After 5 minutes the bands began to appear. The reaction was stopped by rinsing the gel with water. Pictures of the gels were taken before storing them in fix solution.

2.5.12. Extraction of metabolites from agar plugs

2.5.12.1. Extraction

The samples were extracted using 100 % methanol. Briefly, 1 mL of 100 % methanol was pipetted into 2 mL Eppendorfs containing the agar plugs. A Genie Disruptor was used to vortex the sample for 5 minutes, followed by incubation for 15 minutes at room temperature. This procedure was repeated twice. After which, the 1 mL of alcohol was removed and placed into a fresh Eppendorf. A second short incubation was followed using 0.5 mL of methanol. So as not to damage the agar further as the debris may affect the GC-MS; the samples were vortexed and left to incubate further for 15 minutes on the bench. The resulting alcohol was removed after spinning the samples at 16,500 g for 10 minutes and pooled with the previously collected one. To evaporate the liquid a speed vacuum (Eppendorf, Concentrator 5301) was used. When it was certain that the samples had dried, these were stored at -20 °C, ready for the derivatization step.

2.5.12.2. Derivatization

Sample preparation was performed following the procedure developed by Kapoore et al [5]. Each sample was derivatized with 40 µL of 20 mg/mL methoxyamine hydrochloride in pyridine solution at 40 °C for 80 minutes. Followed by a second incubation at 40 °C for 80 minutes with 40 µL of MSTFA (N-methyl-N-trimethylsilyltrifluoroacetamide). The samples were centrifuged at 17,000 g for 10 minutes before transferring into GC vials.

2.5.12.3. GC-MS

Thermo Finnigan TRACE DSQ GC-MS System (Thermo Scientific, Hertfordshire, UK) operating in EI mode onto a TRACE TR-5MS capillary column (30 m x 0.25 mm x 0.25 µm) was used for metabolites identification. The derivatized sample volume of 1 µL was injected in split less mode at 230 °C, and the transfer line maintained at 250 °C. The GC was operated at a constant flow of 1 mL/min helium. The temperature program was started at 80 °C for 6 min, followed by ramping at 6 °C/min to final temperature of 290 °C and held constant at 310 °C for 5 min. Data acquisition was performed on a DSQ MS system with a mass range of 50 to 650 m/z.

2.5.12.4. Metabolite identification

The metabolites were identified as TMSi derivatives by comparing their mass spectral and RI index with online databases (The GOLM Metabolome database: http://csbdb.mpimp-golm.mpg.de/ and NIST 05 database). The acquired spectra were deconvolulated by AMDIS (Automated Mass Spectral Deconvolution and Identification System), before comparing with the database. Spectra of individual components were further transferred to the NIST mass spectral search system and matched with NIST main library, RI index library and the GMD (GOLM metabolome database).

2.5.12.5. Data analysis

All GC-MS chromatograms were processed using freely available AMDIS 2.70 software. The peaks were deconvoluted and the retention indices (RIs) were automatically calculated according to the retention time of the alkane mixture by exporting the RI calibration file into AMDIS. AMDIS deconvolution parameters used are as follows: resolution was set to high, sensitivity was high, shape requirement was medium, and component width was at 12 (Validated with 70 metabolite standard mixture). For identification, the minimum match factor was kept at 60, resolution: high; sensitivity: high; shape requirement: medium. Finally, a report was generated in *.xls format and the first hit considered. Compounds found in at least in two out of three biological replicates were considered true hits. Data for retention time, S/N ration, peak tailing, m/z value and peak area was collected manually by exporting to MS Excel 2013.

2.6. References

[1] Wellburn AR. The Spectral Determination of Chlorophylls a and b, as well as Total Carotenoids, Using Various Solvents with Spectrophotometers of Different Resolution. J. Plant Physiol. 1994;144:307–313.

[2] Prado JM, Veggi PC, Meireles MAA. Extraction Methods for Obtaining Carotenoids from Vegetables - Review. 2014;29–66.

[3] Meléndez-Martínez AJ, Vicario IM, Heredia FJ. Review: Analysis of carotenoids in orange juice. J. Food Compos. Anal. 2007;20:638–649.

[4] Collos Y, Mornet F, Sciandra A, et al. An optical method for the rapid measument of nitrate in marine phytoplankton cultures. J. Appl. Phycol. 1999;11:179–184.

[5] Kapoore RV. Mass spectrometry based hyphenated techniques for microalgal and mammalian metabolomics. The University of Sheffield; 2014.

[6] Chen Y, Zhang L, Xu C, et al. Dissolved inorganic carbon speciation in aquatic environments and its application to monitor algal carbon uptake. Sci. Total Environ. 2016;541:1282–1295.

[7] Chen Y, Vaidyanathan S. Simultaneous assay of pigments, carbohydrates, proteins and lipids in microalgae. Anal. Chim. Acta. 2013;776:31–40.

[8] Dubois M, Gilles KA, Hamilton JK, et al. Colorimetric Method for Determination of Sugars and Related Substances. Anal. Chem. 1956;28:350–356.

[9] Lowry O., Rosenbrough NJ, Farr A., et al. Protein Measurement with Folin Phenol Reagent. Readings. 1951;193:265–275.

[10] Sambrook J, Russell DW. Commonly Used Techniques in Molecular Cloning. 3rd ed. Sambrook J, Russell DW, editors. Cold Spring Harbor, NY, USA,: Cold Spring Harbor Laboratory Press; 2001.

[11] Couto N, Barber J, Gaskell SJ. Matrix-assisted laser desorption/ionisation mass spectrometric response factors of peptides generated using different proteolytic enzymes. J. Mass Spectrom. 2011;46:1233–1240.

Chapter 3: Co-culturing of *Dunaliella salina* with bacteria and/or archaea for increased ß-carotene production.

3.1. Introduction

Artificial co-cultures to investigate the synergisms of *Dunaliella salina* with *Halomonas* and *Halobacterium salinarum* were designed for increased β-carotene production. The bacterium, *Halomonas*, and the haloarchaeon, *H. salinarum*, were selected as co-culturing aiders based on natural synergistic partnerships highlighted in the literature.

3.1.1. Hypersaline ecosystem

Hypersaline environments are deemed as extreme environments, due to the low species diversity that are able to thrive within. They can be described as the dominion of the best adapted/evolved microbial species [1,2]. As the word suggests, hypersaline environments are highly saturated with large concentrations of salts, NaCl or other salts, which can be present at concentrations ranging from 15-50% (w/v). Hypersaline environments are usually low in oxygen, due to the solubility of oxygen in high salinity being 2ppm, when compared to seawater at 7ppm [3]. Good examples of hypersaline environments are the Great Salt Lake [4], the Dead Sea, and Solar Salterns [5]. Changes in the climate and seasonality changes affect hypersaline environments significantly. Infrequent heavy rainfall and long periods of drought modify the composition of the environments affecting the communities within, showing shifts in abundance and the extinction patterns of certain species in some lakes and their appearance in others [6].

Not many organisms have evolved to tolerate such harsh environments; however, a group of species has, known commonly as halophiles. Halophiles or halophilic microorganisms are salt loving microorganisms equipped with the necessary tools to counteract the salt stress of these environments. Halophilic organisms can live across a range of salt concentrations from 0.8M-5M (extreme cases) which are prohibitive to other organisms, as shown in Table 3.1.1. Though the taxonomic diversity of such environments is relatively low when compared to conventional ecosystems, isolates derived from the hypersaline environments reveal an interesting array of eukaryotic,

prokaryotic and archaeal microorganisms. The energy dispensed for the osmotic adaptation delimits the biota of highly saturated environments [7]. Isolates can be found not only in saline waterbodies, but in soil, salt deposits, within fermented and salted food [8].

Table 3.1.1: Examples of halophilic and halotolerant microorganisms across a variety of salinity ranges (details from [5,7,9])

Species	Salinity (NaCl)
Bacteria:	
Halomonas elongata	1.36M-4.8M
Halomonas variabilis	1.2 M-4.8M
Halothermothrix orenii	3.4M
Pseudomonas halophile	0.2 M-3.4M
Gracilibacillys halotolerants	0M-3.4M
Halanaerobium praevalens	0.35-5M
Desulfobacter halotolerans	0.1-2.2 M[a]
Desulfovibrio retbaense	4M
Halothiobacillus halophilus	0.8M-4.3 M
Microalgae:	
Dunaliella salina	Up to saturation levels (from 1M to ~4.5M)
Dunaliella bardawil	
Dunaliella virdis	
Dunaliella parva	
Oocystis parva	
Asteromonas gracilis	
Archaea:	
Halobacterium salinarium	Up to saturation levels
Halorhabdus utahensis	4.6M
Haloferax volcanii	2-3 M
Halorubrum sodomese	2.1M
Other organisms:	
Aphanothece halophytica	2.7M-4M
Synechoccus elongates	2.7M-4M
Artemia shrimp	4.5-5M

[a] with addition of 45g/L $MgCl_2 \cdot 2H_2O$.

The halophiles behaviour will also change as a response to the concentration of additional salts, such as magnesium, calcium, and potassium, which are present in addition to NaCl. Hypersaline environments can be subdivided into two main classifications: thalassohaline and athalassohaline [7,8]. Thalassohaline environments results from the evaporation of seawater, inland lakes are a good example of this. Their ionic composition is quite similar to that found in the sea, with high concentrations of NaCl. On the other hand, athalassohaline environments have naturally evolved as salt brines based on the local geology. They vary in ionic composition to seawater, and are

quite diverse amongst themselves; alkaline soda lakes, and the Dead Sea are good examples [5,7,10].

Investigations conducted by Rodriguez-Valera *et al.* [2] shed light on the population distribution trends to be expected with varying concentrations of salt. Organisms below approximately 15% salt were those encountered in most seawater bodies, whilst over the threshold of 15% mainly halophilic organisms where encountered. Within the 15-30% range large populations of the microalga, *Dunaliella sp.*, were recorded in association with halophilic bacteria. Furthermore, at higher gradients of salts reaching about 50% total salts (much greater than NaCl saturation levels) only three species were isolated, *Halomonas elongata, Halomonas variabilis* and *Halorhabdus utahensis* (see Table 3.1.1).

In highly saline environments prokaryotes and haloarchaea account for the majority of the population; amongst which some eukaryotes can be found. The osmotic stresses that the organisms are subjected to are counteracted by the production of 'compatible solutes' called osmolytes; whereas other microorganisms, such as the archaea, counterbalance the NaCl by accumulation of KCl and can even live trapped in salt crystal structures. At high salinity concentrations, the range of microorganisms able to thrive decreases. As a result, the eukaryotes, with the exception of those in the *Dunaliella* genus, are not present. Prokaryotes and haloarchaea are still found at salt concentrations as high as 5M [3].

Hypersaline waterbodies, such as the Dead Sea, are known to have a distinctive water colouration of red-pink. This colouration previously solely attributed to the presence of *Dunaliella* species, is now attributed to the agglomeration of a number of bacteria and haloarchaea. These microorganisms live in association with the halophilic green algae. The reason for the colouration is thought to be due to the bacteriorhodopsin pigment accumulated within haloarchaea such as, *Halobacterium* [8], alongside accumulation of β-carotene by the *Dunaliella salina,* or *Dunaliella bardawi,l* which changes their appearance from green to orange, contributing to the waters colouration [11].

Though all the microorganisms are halotolerant and halophilic, the mechanisms in which they withstand osmotic shock differs [7]. However a common denominator exists, where the sodium ions are excluded from the cytoplasm, through potent transport

mechanisms based on Na^+/H^+ antiporters, which expel any Na^+ ions from within the cell [7,12,13]. The range of metabolic processes that are known not to occur at higher salinities (above 1.5 M-2.5M), include autotrophic nitrification, methanogenesis based on the reduction of CO_2 and H_2, methanogenesis from acetate and sulphate-reducing bacteria oxidation of acetate by sulphate-reducing bacteria. Looking from a community/consortia perspective, work undertaken in the 1980s by Borowitzka [14] reported that the prevalent species of *Halobacterium* and *Halococcus* lived in symbiosis with *Dunaliella sp.*, which provided the necessary glycerol as a carbon source for their growth.

3.1.2. Halophilic microalga: *Dunaliella salina*

Dunaliella salina is a unicellular halophilic microalga belonging to the Chlorophyceae class and family Volvocales [15,16]. Theodoresco Dunal first discovered this alga in 1838. The alga has also been isolated from other hypersaline environments around the world, such as in Romania, Algeria, and Lorraine (France). The absence of an array of grazers and of competition from other algal species for the nutrients increased the probability of *Dunaliella* species surviving in hypersaline environments [4].

Some strains belonging to the genus *Dunaliella,* including *D. tertiolecta*, *D. parva, D. viridis*, are large unicellular flagellates (12-16µm x 6-9µm) whilst, *D. bardawil* and *D. salina* measure about 12µm x 8µm. All the *Dunaliella* species have the ability to thrive in medium containing a large concentration of NaCl, reaching from 1M to higher molarities of 4-5M [1,4,15,17].

Dunaliella cells do not possess a cell wall. The cell is enclosed within a thin plasma membrane, which allows the cell to shift morphology during osmotic changes. This can be seen, when the cells accumulate or secrete glycerol, to withstand harsh changes in salinity. In a similar fashion other pathways, such as control of ionic fluxes across the plasma membrane, osmotic salt-induced gene expression and accumulation of salt-induced proteins aid the microalga to thrive. As a result of exposure to high light intensities, some species of *Dunaliella* cells produce large amounts of intracellular β-carotene [15].

Dunaliella species are not the only organisms capable of producing β-carotene. Amongst the microalgae, *Haematococcus pluvialis*, is known for its ability to synthesize β-

carotene; however, it is largely cultivated for the extraction of astaxanthin. *Spirulina platensis* is another candidate, with yields of 0.8-1%w/w [18]. *Dunaliella bardawil* and *D. salina* are the preferred strains due to the high accumulation, up to 10% dry weight, and also because the β-carotene produced contains a large percentage of 9-*cis* isomer [5,19]. The fungus *Blakeslea*, yellow, orange and dark-green vegetables and fruits are also sources of these carotenoids. So why is there a preference for the derivatives from *Dunaliella* species? This is down to the fact that the carotenoid extracts contain substantial amounts of *cis* and *trans*-isomers plus an array of other carotenoids with wider applications. Furthermore, the advantage of using microalgae for the production of β-carotene, rests on the fact of high yield per output, bio-adaptability, and the halotolerant nature of *Dunaliella* decreases the risk of contamination from other microorganisms. Furthermore, the high amount of protein obtained from *Dunaliella* cells is used as a food additive whilst spent biomass is used a fertilizer or feedstock.

3.1.3. β-carotene from *D. salina*

Dunaliella salina has been the preferred industrial workhorse for the production of β-carotene. The algae accumulate β-carotene within their lipid globules in the inter thylakoid spaces of the chloroplast [20,21]. However, β-carotene is not produced naturally in high amounts, but results when the alga is subjected to stress, such as high light intensity, depletion of nutrients (nitrates, phosphorous and sulphur), high salinity concentrations (3-5M NaCl) and temperature fluctuations [22].

Hyperosmotic shock, high irradiance and nutrient deficiency slows down biomass generation [20]. Following a high salt shock, the *Dunaliella* cells require a period of acclimatisation, after which they start accumulating carotenoids, including largely β-carotene. This suggests that perhaps certain enzymes need to be activated, in order for the cells to acclimatise readily [16]. Phadwal and Singh [21] showed that the induction of β-carotene leads to a decrease in the content of total chlorophylls, this is probably due to the alga directing its pathways to counteract damage by radiation. It is possible to conjecture that perhaps the low solubility of the CO_2 in high salinities may have an effect on the photosynthetic efficiency of the algae. Furthermore, the production of β-carotene from *D. salina* isolates increased with nitrate, sulphur and phosphate limitation

[21]. To obtain high titres, the microalgae were grown in unstressed condition, prior to applying an abiotic stress [23].

Biotechnological industry is interested in maximising the production of β-carotene by *D. salina*. β-carotene can be synthesised artificially, however the ratio of 9-*cis* and all-*trans*-isomers cannot be replicated effectively [24]. Furthermore, the β-carotene derived from the microalgae is the best suited for human consumption. Upon assimilation of β-carotene the body converts this into vitamin A (retinol). In light of this, a preliminary investigation was undertaken to find out whether *D. salina* would produce β-carotene in a highly competitive environment, which would result in indirect nutrient stressing as displayed in Table 3.1.2.

Table 3.1.2: Overview of reported amounts of β-carotene accumulation in *D. salina*

Species	**Light intensity**	**Salinity (NaCl)**	**T (°C)/pH**	**β -carotene**	**Ref.**
D. salina	180µmol/m^2/s	5-20%	26/-	170µg/mg	[16]
D. salina UTEX 2538	200µmol/m^2/s	2 M	25/7.5	80g/m^3/d	[24]
Sambhar Salt Lake, Rajasthan	56.84→118.18µmol m^2/s	2 M	25/7.5	1.15→ 4.21pg/cell	[25]
Germany SAG 19.3	~50 µmol/m^2/s	2 M	25/-	1.65→7.05pg/cell	[26]
Germany SAG 19.3	111 µmol/m^2/s	2 M	35/-	1.65→8.26pg/cell	[26]
Germany SAG 42.88	52.84 µmol/m^2/s	2 M	25/7.5	3.99pg/cell	[21]
Chile CONC-007	40→100µmol photons/m^2/s	2 M	26/-	72.7pg/cell	[27]
CCAP 19/18	40→100µmol photons/m^2/s	2 M	15/-	31.6 pg/cell	[27]
Urmia Lake, Iran	100µmol photons/m^2/s	1.5-3 M	25/(7.5,8.5,10)	0.19→8.94-11.4pg/cell	[28]
Thailand, BuriRam KU01	72.34 µmol/m^2/s	0.5-4M	25/-	56.25pg/cell	[29]
CCAP 19/18	400 µE/m^2/s	1.5	25/-	70pg/cell	[30]

Despite the capacity of D. salina to produce β-carotene, commercial production is limited to a fairly small volume due to the relatively low productivity. However, the yields are still considered large by algae manufacturing standards.

3.1.4. Other pigments

Although *D. salina* cells are highly in demand for the production of β-carotene, other pigments such as chlorophylls and zeaxanthin can be found within the cells. Chlorophylls are pigments that characterise plants and microalgae found in the thylakoid sacs of the chloroplast. The effect of co-culturing *D. salina* on the distribution of chlorophyll a and b and total carotenoids within the cells was investigated. Chlorophyll a, the main photosynthetic pigment absorbs energy from wavelengths of blue-violet and orange-red light and is found in all photosynthetic eukaryotes, cyanobacteria and prochlorophytes. It also plays a vital role in primary electron transport chain (ETC). Chlorophyll b, on the other hand is the accessory pigment which collects energy and routes it to chlorophyll a. Whilst, chlorophyll a regulates the reaction centre of the antenna array of core proteins, chlorophyll b regulates the size of the antenna. As chlorophyll a is the main pigment for successful photosynthesis, it is usually found in a ratio of 3:1 to chlorophyll b, however this can vary depending on the heath of the cell [31].

3.1.5. Glycerol accumulation

Dunaliella are able to withstand changes in salinities, thanks to the modifications they make in order to survive. These alterations occur at both morphological and metabolic levels. *Dunaliella* cells naturally accumulates and secretes glycerol during hyperosmotic and hypoosmotic shock [15,20]. For example, when subjected to hyperosmotic shock, the cells shrinks within 5 minutes. Ion exchange across the plasma membrane expels intracellular water into the surrounding medium. Following this, over a couple of hours, the cells start generating glycerol, allowing the cells to resume their original size and structure. If the cells were exposed over a prolonged period of time (12-24 hours), they will initiate protein accumulation [32]. The accumulation of glycerol is also common to halotolerant green algae, for example *Asteromonas gracilis*, as means to withstand osmotic shock. Concomitantly, the photosynthetic activity and respiration of the cells decreased with increasing salinity and glycerol production [33]. The amount of glycerol accumulation within the cell can reach amounts of 90% of the cell weight in *D. salina* [18].

The accumulation of glycerol within the *Dunaliella* cells involves the action of glycerol-3-phosphate dehydrogenase (GPDH), also found in higher plants and other algae [34] and glycerol-3-phosphate phosphatase [32,35]. Two possible pathways exist; the first pathway uses directly the photosynthetic fixation of CO_2, whilst the other hydrolyses already existing starch repositories to glucose, which is then converted into fructose-1,6-diphospate. This is consequently converted to dihydroxyacetone phosphate (DHAP), and then to glycerol-3-phosphate by GPDH, to be finally converted into glycerol by glycerol-3-phosphate phosphatase. Conversely, if hypoosmotic shock occurs, the cells accumulate water from the environment whilst conducting ion exchange. As in the case for hyperosmotic shock, this process occurs within the time space of 5 minutes. The glycerol, which was within the cell, is dissipated into the environment, in order for the cell to return to its original state [15]. If the salinity decrease is not too severe, the glycerol is removed through oxidation to DHA and phosphorylated to DHAP. The glycerol accumulated within the cell is not toxic, and being an end product metabolite, it does not pose any limitations to the other pathways.

3.1.6. Moderately Halophilic Bacterium: *Halomonas*

Moderately halophilic bacteria are found predominantly in salt lakes or saline soils and have also been isolated from salted food products, with many thriving within the threshold of approximately 2.5M NaCl. Moderate halophiles are also of interest in biotechnological applications. Work has been conducted in adapting these microorganisms to withstand harsher environments. *Salinivibrio costicola*, *Halomonas elongata*, and *Halomonas israelensis* are amongst the species widely studied [36].

In order to thrive in high salt environment, just like osmotolerant algae and fungi, halotolerant bacteria are able to readily adapt to a wide range of physical condition fluctuations. The bacteria are equipped with machinery to facilitate ionic exchange across the membrane. During this process, organic solutes accumulate which provide the cells with the ability to resist osmotic shock. Work conducted by Vreeland et al. [37] has shown that when *Halomonas elongata* cells are subjected to salinity increases they produce ectoine and glycine betaine as compatible solutes, in the same way *that Dunaliella* uses glycerol.

As for other microorganisms, the growth conditions, in which moderately halophilic bacteria are able to thrive, depend on the pH and the temperature of the medium. *Actinopolyspora halophile* is an example of an extremophile bacterium, which grows optimally at NaCl concentrations of 4 M [36]. Amongst the moderately halophilic bacteria, applications have included denitrification [38].

3.1.7. Haloarchaeon: *Halobacterium salinarum*

Haloarchaea constitute a large portion of the biota that inhabits hypersaline environments. As these organisms are highly salt tolerant, they require a minimum of 1.5 M NaCl, however, they are able to withstand salinities up to the saturation levels of 5.2 M [8]. Haloarchaea are believed to be responsible for the orange-pink colour that depicts many hypersaline lakes. Haloarchaea produce a red-to-pink pigment, called bacterioruberin C_{50}, which is stored in the microorganisms' membrane. Common places where haloarchaea may be found include salt salterns, soda lakes, salt deposits and food products. Studies have shown that bacterial species have been implicated in the role of supplying vitamins, commonly cobalamin to microalgae species. A good example of this is the *A. operculatum* associated bacteria, which was found to supply this vitamin [39]. These finding have been compared to *Halobacterium sp.*, and speculation is that *Halobacterium* cells are able to supply vitamins in exchange for photosynthate from the microalgae.

Within the haloarchaea some strains have been sought for denitrification purposes in wastewater scenarios. Good examples of this are *H. halobium* and *H. denitrificans*. Studies undertaken by Orellana et al. [40] have shed light onto the relationship that exists between *D. salina* and *Halobacterium*. The studies revealed that when the *Dunaliella* cells underwent programmed cell death, that the glycerol expelled into the medium was taken up by the haloarchaea. The glycerol is assimilated by the haloarchaea and catabolised through phosphorylation to glycerol-3-phosphare, leading to the formation of DHAP [41]. In the case of *H. salinarum*, the glycerol is converted into DHA. The findings indicated that *H. salinarum* benefitted from *D. salina* lysate, and that in turn it re-mineralised the culture medium for the benefit of the microalgae [40].

3.1.8. Biotechnological application of halophilic microorganisms

As monocultures, various halophilic microorganisms have been used in biotechnological applications.

Table 3.1.3: Biotechnological application of halophilic microorganisms

Product	Organism	Biotechnology potential/use	Industrial sector
β-carotene	*Dunaliella* species	Used as antioxidant and food colouring	Food, cosmetics, assays
Carotenoid pigments	*Dunaliella* species Halobacteriaceae *H. pluvialis*	Used as antioxidant and food colouring	Food, cosmetics, assays
Ectoine and hydroxyectione	*Halomonas elongata*, *Marinococcus* M52	Act as moisturiser	Cosmetics
Glycerol	*Dunaliella* species *Astermonas gracilis*	Bulking agent	Pharmaceutical, food, cosmetics
Poly-β-hydroxyalkanoate	*Hf. mediterranei*	Thermoplastic polymer, resistant up to 180°C. Biodegradable	Medical and pharmaceutical
Salt-tolerant enzymes	Numerous haloarchaea and halobacteria	Added value product into foods, not used at the moment	Food and consumables
Soy sauce, fish sauce	Numerous haloarchaea and halobacteria	Food additive	Food, leisure
Bacteriorhodopsin	*H. salinarium*	Potential to be used as holographic material, in photoelectric converters.	IT, electronics, process, commercial and industrial tech
Extracellular polysaccharides (EPS	*Hf. mediterranei*	Attachment surface, gum	Food, cosmetics
Biomass	Microalgae species, plus other halophiles	Bulking agent, fertiliser, feed for aquaculture/animals	Farming, food, nutraceutical
Phycocyanian	*Spirulina sp.*	Colouring, used in assays and also as a dye	Analytical, food, textiles

3.1.9. Current co-culture studies with *Dunaliella salina*

Studies into co-cultures have gained a high interest in the last decade. Examples of successful co-cultures were provided in Chapter 1. In this section, the associations that have been tested with *Dunaliella salina* and other microorganisms are summarised. Keshtacher-Liebson et al. [42] investigated the effect of *Halomonas* on *D. bardawil,* and reported that the presence of the bacteria facilitated the growth of the algae in iron depleted medium. The bacteria released siderophores that acted as iron transporters, allowing the algae to grow: this was later shown with *Dunaliella salina* [43]. Studies into the allelopathy effects from dinoflagellates on *D. salina* have been conducted by Dong et al. [44]. The inhibitory effects of *Karenia mikimotoi* on *D. salina*, were more pronounced when exudates from the dinoflagellates were obtained at the exponential

phase. Furthermore, *Bacillus solisals* was isolated from non-axenic cultures of *D. salina* [45]. Whilst, Orellana et al. [40] have studied the effect of *H. salinarum* on cell death in *D. salina* strains. Isolation work conducted on the solar salterns fed by the Bay of Bengal in India, showed that in thalassohaline environments, *D. salina* cells were associating with *Halomonas* and *H. salinarum* [46]. There is limited literature on co-culture work with *D. salina* despite this alga being an industrial workhorse for β-carotene production. A better understanding of the methods by which it interacts with other organisms such as *Halomonas* and *H. salinarum* in terms of bioproduction would be beneficial.

3.2. *Dunaliella salina* consortium for increased production of β-carotene

The co-culture of *Dunaliella salina* with *Halomonas* and *H. salinarum* is investigated (Figure 3.2.1). Work undertaken in this field has led to the hypothesis that both *Halomonas* and *H. salinarum* are able to assimilate glycerol as a carbon source [5–7]. It is a common belief that the glycerol produced by the *Dunaliella* cells may, through cell apoptosis [40] or cell leakage, as shown in mutant strains of *D. parva*, be released into the surrounding medium [47].

On the other side, studies support the idea that the heterotroph *H. salinarum* re-mineralises the carbon present within the growth medium using the glycerol leaked from the algae, and making it available for the *D. salina* species; justifying a mutualistic relationship [40,48]. Work has been undertaken in depicting how these interactions behave; however, no clear elucidation has been given on the exact metabolites exchanged.

The success of co-cultures is in the exchange of metabolites between interacting organisms [49–51]. Furthermore, there is belief that vitamins like cobalamin (B_{12}) and biotin (B_7) may be released by *Halomonas* when in association with the *D. salina* cells; however, this has not been clarified to date, as *D. salina* can synthesise its own vitamins [52].

The growth rate, total biomass and behaviour under stress conditions for the production of β-carotene will be assessed for the co-cultures of *D. salina* and *Halomonas*, and for *D. salina* and *Halobacterium salinarum*. The aim is to prove that a co-culture approach

will yield higher biomass and thus higher accumulation of β-carotene compared to the axenic growth. Based on these results, a possible 3-way consortium will be trialled: the outcome of this will be dictated by the behaviour of the two co-cultures.

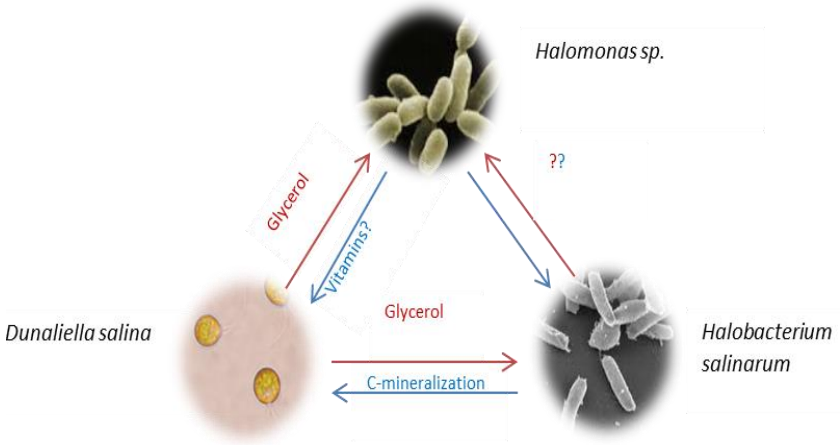

Figure 3.2.1: Representation of *Dunaliella salina*, *Halomonas* and *H. salinarum*. The red arrows represent any biomolecules released by each species, whilst the blue stand for molecules acquired.

3.3. Experimental Design

3.3.1. Communal medium

The first step was to establish a communal growth medium. As the cells here are halophilic, a common salinity denominator had to be established. Therefore, all the microorganisms were subjected to grow over a range of salinities. Their growth performance was monitored in terms of optical density and cell counts (algae species). *D. salina* cells were grown as outlined in section 2.2.1. The growth performance of the cells was monitored at 1.5 M, 2 M. 2.5M, 3 M and 3.5 M, NaCl. As halophilic microalgae are known to have slower growth rates, compared to freshwater species, a larger starting inoculum of 0.2-0.25 OD_{595nm} was used instead of the more conventional 0.08 OD_{595nm}. Algae cells were harvested throughout the duration of the experiment as described in section 2.3.1. The samples were analysed for chlorophylls (section 2.5.1) and β-carotene production (section 2.5.2).

Halomonas was inoculated in 150mL of LB broth, at 1.5 M, 2 M and 3 M NaCl concentrations, in 250mL Erlenmeyer flasks. In a similar fashion, *Halobacterium salinarum*, was inoculated in 2 M, 3 M and 4.2 M Halophile Medium (as described in

section 2.2.3). Optical density readings were taken at 595 nm, 680 nm and 750 nm. Flasks were set up in triplicate for each condition.

3.3.2. Co-culture of *D. salina* and *Halomonas*

Here we hypothesise, that adding *Halomonas* to *D. salina* will increase the microalgal biomass and overall β-carotene production. Three experimental set-ups were tested: direct mixing, bead entrapment and medium spiking. Growing the microorganisms in the same vessel (direct mixing, as opposed to bead entrapment and medium spiking), will provide understanding on whether certain molecules are triggered when the microbes are in closer proximity.

3.3.2.1. Direct mixing

At high population densities, bacteria are known to release substances into the environment. The chemical cues are believed to help mediate cell-to-cell associations within the assemblage. Here, we investigated if the association of *D. salina* with *Halomonas* significantly increased the growth rate and biomass of the microalgae by directly mixing the microorganism in the same growth flask.

As *Halomonas* is endogenous to *D. salina* cells, the microalgae growth medium 3 M HEPES was chosen for co-culturing, alongside a supplemented growth medium, which will be referred to as 3 M HEPES+. The supplemented medium contained 1 g/L of yeast extract to provide an initial boost to the bacterial population, thus instigating quorum sensing. Both organisms were co-inoculated at a ratio of 1:1. There is a risk of the bacterial population overtaking the algal cells in the 3 M HEPES+ medium, however, literature suggests that an equilibrium stage may be established, soon after all the bacterial substrate is consumed [53]. For ease of reference, the table below provides the conditions of the monoculture and co-cultures tested.

Table 3.3.1: Summary of the flask labels and nomenclature used in text, figures and graphs

Flasks Label	*D. salina*	*Halomonas*	3 M HEPES	3 M HEPES+
DS	✓	×	✓	×
DS:HALO	✓	✓	✓	×
DS:HALO+	✓	✓	×	✓

D. salina flasks were inoculated at a seeding density of 0.2 OD_{595nm}, in 100mL of medium, in 200mL static Erlenmeyer flasks at 22-23°C, light intensity of 50-60µmol m^{-2} s^{-1}. *Halomonas* was first grown separately in 100mL of 3 M LB medium, on a 200rpm rotary shaker at 30°C. When the bacterial culture reached logarithmic phase, an aliquot of the culture was taken from the culture flasks. The density of the aliquot was adjusted to 0.2 OD_{595nm}, to equal that of the microalgae. To remove any residual trace of the 3 M LB medium, the *Halomonas* inoculum was spun down at 17,000xg and washed once with 3 M HEPES or 3 M HEPES+ medium, according to the final growth medium.

The set-up consisted of static flasks, with triplicates for each condition. Every day for the duration of the experimental period, the flasks were shaken manually. Optical density, cell counts and CFU counts were performed to monitor the population dynamics of the two microorganisms. The CFU agar plates also helped to monitor the axenic nature of the monoculture flasks throughout the experimental period. Biomass samples were collected and stored at -20°C for future pigment analysis

3.3.2.2. Encapsulating *Halomonas* in sodium alginate beads for co-culture experiments

Here, the bacterial culture was encapsulated in porous sodium alginate beads, to attest whether the synergism between algae and the bacteria is hindered if the two were segregated. This type of co-culturing has been used in wastewater treatment and to study co-cultures [54–56]. The porous surface of the sodium alginate beads allows the bacteria to release any biomolecules into the culture medium. However, compared to direct mixing where the two-microorganisms come into direct contact, there is the risk that part of the biomolecules may be retained within the alginate bead itself. Furthermore, trapping the bacteria in the bead may shield the microorganism from recognising the presence of the microalgae, and thus not have a significant effect on the biomass yield. The bacterial species was chosen as the candidate to be encapsulated, as the effect on the growth of the *D. salina* algae species was to be monitored.

3.3.2.2.1. Bead encapsulation

The protocol proposed by Kitcha and Cheirsilp [54] was modified for the purpose of this work. Briefly, sodium alginate 4% w/v and 0.2 M $CaCl_2$ solutions were prepared and autoclaved at 121°C for 20 minutes, and cooled to room temperature. Trials were

carried out to determine at which ratio would be best to entrap the bacterial species within the beads, as the high salinity of the growth medium may interfere with the sodium alginate matrix. Trials were run at 1:1, 1:2 and 1:3 ratios of 3 M LB broth to sodium alginate. The best mixing ratio was found to be 1:3 where the sodium alginate beads would readily solidify with reasonable uniformity. A syringe was used to take up the mixture and to create droplets that were released into $CaCl_2$ solution. The beads upon contact with the $CaCl_2$ solidified. The bead size ranged from 2-5mm in diameter. The beads were left to rest for 1 hour in the solution to harden. They were then filtered and washed with deionised water, in order to remove any traces of $CaCl_2$. The washed beads were then allowed to rest in the growth medium overnight, prior to commencing the experiment.

3.3.2.2.2. Flask set-up

Halomonas was grown in 3 M HEPES+, at 200rpm in 250mL Erlenmeyer flasks containing 100mL of working culture. The bacteria were harvested when an OD_{595nm} of 0.45-0.5 was reached. The assumption was that at this OD, the bacteria would have started to release metabolites into the growth culture, as according to the literature at higher densities quorum sensing is triggered, as population increases [57]. According to the growth data obtained for the culture at this point in time, maximum growth is seen at that point for the 3 M cultures, after which the culture reaches stationary phase, followed by death phase.

Halomonas was mixed at a ratio of 1:3 (bacteria: sodium alginate) to obtain a final inoculum equivalent to 0.2-0.22 OD_{595nm}. To factor in the presence of the beads on the *D. salina* cells, parallel blank beads were added to the monoculture flasks.

The following day the beads were introduced into five 250mL Erlenmeyer flasks with 125mL of *D. salina* at OD_{595nm} of 0.2-0.25. Three control flasks consisting only of *D. salina* and blank beads equivalent in amounts to the *Halomonas* beads were set up alongside. An illustration depicting the experimental set-up is provided in Figure 3.3.1.

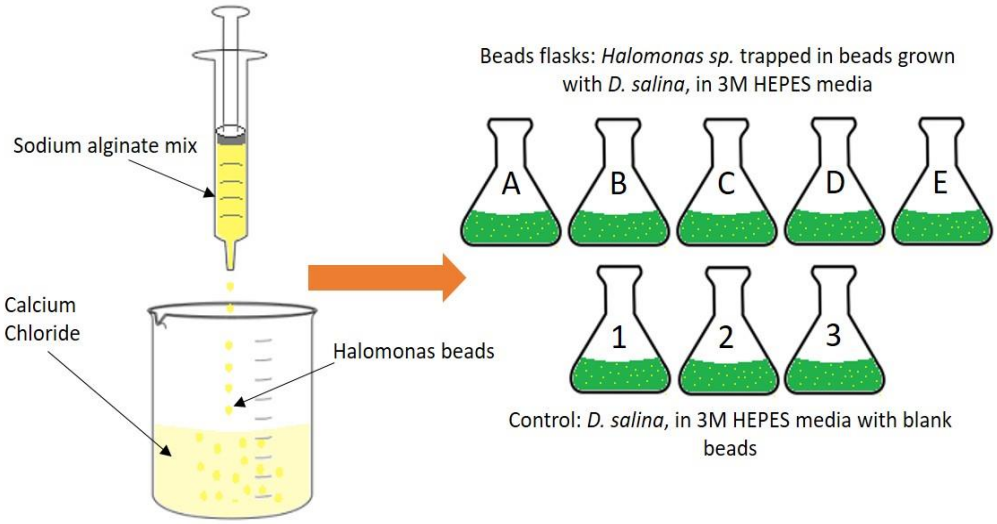

Figure 3.3.1: Encapsulation of *Halomonas* in alginate beads and flask set-up for experiment

The static flasks were then placed under a 50-60 µmol m^{-2} s^{-1} light at room temperature of 25-26 ˚C. Optical density measurements and sampling were done simultaneously every 2-3 days. The growth of the algae was monitored over a period of 27 days. On the 17th day, the flasks were moved onto stronger light intensity 120-130 µmol m^{-2} s^{-1}, to stress the cells in accumulating higher amounts of β-carotene.

3.3.2.3. Spiking experiment

A third experiment was carried out, in order to check whether the biomass of *D. salina* would be affected by the supernatant of the bacterial culture only.

D. salina and *Halomonas* were grown as detailed in section 2.2.1 and 2.2.2. Upon the bacterium reaching a density of 0.45 OD_{595nm}, the cells were centrifuged and the supernatant collected and filter sterilised using a 50mL syringe and a Millipore 0.22 µm filter. The filtrate was checked for the presence of *Halomonas sp.*, using the spectrophotometer and by incubating triplicate agar plates. The *Halomonas* supernatant was not autoclaved to avoid the degradation of secreted molecules. Thereafter, 50mL Falcon tubes containing 0 % (Control), 10 %, 25 %, 50 %, 75 % and 100 %(v/v) of filtered supernatant and brought to volume by adding 3 M HEPES medium were inoculated with *D. salina* (0.2 OD_{595nm}). The Falcon were sealed with Parafilm to prevented contaminants from entering the tube. Each condition was set up in triplicate. During this period, measurements of growth in terms of optical density and cell counts were performed, alongside sampling for pigments.

3.3.3. Co-cultures of *D. salina* and *Halobacterium salinarum*

The supplemented medium (3 M HEPES+) was not suitable for *H. salinarum* growth, therefore, a combination medium was used, where 10% of 3 M ATCC 1863 medium was added to the 3 M HEPES, referred to as HEPES 1863.

3.3.3.1. Direct mixing

D. salina flasks were inoculated in 3 M HEPES medium at a seeding density of 0.2 OD_{595}, in 100 mL of medium, in 200 mL static Erlenmeyer flasks at 22-23 °C, light intensity of 50-60 µmol m^{-2} s^{-1}. *H. salinarum* stocks were grown in 3 M ATCC 1863 medium on a rotatory shaker placed at room temperature. When the *H. salinarum* reached exponential phase, an inoculum equivalent to that of the microalgae was centrifuged at 17,000xg. This was then washed in HEPES 1863. The set-up consisted of static flasks, with triplicates for each condition, as outlined in Table 3.3.2. The co-culture flask (DS:HB) was inoculated at a ratio of 1:1 (OD_{595nm}).

Table 3.3.2: Summary of the flask labels and nomenclature used in text, figures and graphs

Flasks Label	*D. salina*	*H. salinarum*	HEPES	HEPES 1863
DS	✓	×	✓	×
DS:HB	✓	✓	×	✓

Every day for the duration of the experimental period, the flasks were shaken manually. Optical density, cell counts and CFU counts were performed to monitor the population dynamics of the two microorganisms. Agar plates were made from 3 M ATCC 1863 medium alongside 3 M LB agar plates. The ATCC plates would facilitate the growth of *H. salinarum*, whilst the LB plates were spread to check whether *Halomonas*, endogenous to the microalgae species, would also thrive on the added supplements. On a similar note, the axenicity of the monoculture was monitored for the duration of the experimental period. Sampling was conducted for monitoring growth and evaluating β-carotene.

3.3.4. Direct Mixing: subjecting the co-cultures to abiotic stresses.

Dunaliella salina has been used widely in industry for the production of β-carotene [14,26,58]. Axenic culturing methods have been preferred as a method in which to cultivate microbes for biotechnological application. However, contamination from

bacteria cannot be avoided, especially in large scale facilities. Therefore, instead of looking at bacterial as a contaminant, it may be worth to check if the presence of some bacteria can be exploited for biotechnological use.

Here, we investigate the effect of *Halomonas* or *H. salinarum* on *D. salina*, when the co-cultures are subjected to abiotic stresses. The monoculture and co-culture in the lab were subject to salt [25], light [59] and nitrogen stress [21], as these have been highlighted in the literature as ways in which to trigger the accumulation of β-carotene in *D. salina.*

For all three abiotic stresses, measurements were taken in terms of cell number and optical density, alongside measurements of pigments: chlorophyll a, chlorophyll b and β-carotene. The extracellular supernatant was measured for the presence of glycerol and dissolved inorganic nitrogen. Additionally, pictures were taken at each sampling point, to check for any algae morphology changes. The pictures will also shed light on whether the presence of the bacterium would make the algae behave differently when subjected to stress and tie in with the pigment data.

Direct mixing was chosen as the method to be tested, as the *D. salina* cells were able to sustain a steady growth rate during the experimentation period.

Figure 3.3.2: Workflow for two-stage stress experiment.

The co-culture is set up, stressed and the impact of the bacteria/haloarchaea on the production of β-carotene was compared to a control monoculture, which has undergone the same treatments.

3.3.4.1. Method

Dunaliella salina cells were grown at 50-60 µmol m^{-2} s^{-1}, at 25 °C in static 250 mL Erlenmeyer flasks. A first flask of *D. salina* cells grown in 3 M HEPES was inoculated. This flask acted as a control to all other flasks and was not be subjected to any of the stresses. To differentiate between the monoculture flasks, this flask was called Control. Similarly to the direct mixing experiment, outlined in section 3.3.2.1, this experiment consisted of a monoculture flask (DS), a co-culture flask (DS:HALO) and a co-culture flask grown in

supplemented medium (DSHALO+). For all stressed experiments, the flasks were inoculated with a starting density of 0.2 OD_{595nm}. On the 1st day of set-up, *Halomonas*, (in logarithmic phase) was inoculated at a ratio of 1:1. On day 7, 10 and 14, the experimental monoculture (DS) and co-culture (DS:HALO and DS:HALO+) cells were centrifuged, resuspended in 'stress medium' (Table 3.3.3).

Table 3.3.3: Summary of the flask labels and nomenclature used in text, figures and graphs

Flasks Label	*D. salina*	*Halomonas*	HEPES	HEPES+	Stressed
Control	✓	×	✓	×	×
DS	✓	×	✓	×	✓
DS:HALO	✓	✓	✓	×	✓
DS:HALO+	✓	✓	×	✓	✓

The same set-up for the direct mixing experiment (3.3.2.1) was used for the co-culture of *D. salina* and *H. salinarum*. Table 3.3.4 gives an overview of the flasks involved in the experiment. Briefly, six 500 mL Erlenmeyer flasks were inoculated with 450 mL volume of *D. salina*, with a starting density of 0.2 OD_{595nm}. The same size inoculum of *H. salinarum* was co-inoculated in the co-culture flasks. All the flasks were left to acclimatise for 1 hour. Three of the 500 mL flasks were subdivided into 200 mL Erlenmeyer flasks with 150 mL working volume and subjected to 24 hours salt, 48 hours light and 5 days nitrogen stress. The remainder was subdivided and left to acclimatise for 3 days before subjecting to stress.

Table 3.3.4: Summary of the flask labels and nomenclature used in text, figures and graphs

Flasks Label	*D. salina*	*H. salinarum*	HEPES	HEPES 1863	Stress
Control	✓	×	✓	×	×
DS	✓	×	✓	×	✓
DS:HB	✓	✓	×	✓	✓

In both set-ups, in order to keep the treatment of the cells the same at all times, all the flasks including the Control, underwent centrifuging and re-suspending in new medium. This was to remove any effects that shear stress from centrifuging might have on the cells. All flasks were set up in triplicate. At the set-up as static, the flasks were shaken once a day manually.

3.3.4.1.1. Salt stress

The flasks were subjected to osmotic shock from 3 M to 4.2 M NaCl.

3.3.4.1.2. Light stress:

During light stress, the cells were subjected to 180-200 µmol m^{-2} s^{-1} light, instead of 50-60 µmol m^{-2} s^{-1}.

3.3.4.1.3. Nitrogen stress

The cells were re-suspended in nitrogen-free medium, therefore none of the co-culture flasks were supplemented with yeast extract.

3.3.5. Morphological changes

Here, we observed the behaviour of *D. salina* with and without the presence of *Halomonas* and *H. salinarum*. Images were taken with the aid of a microscope. An Olympus microscope with 60x magnification lens was used, connected to ProReg software on the computer. The images were analysed for cell dimensions using a MATLAB and R-studio software.

3.4. Results

The aim of this investigation was to discover whether the presence of *Halomonas* or *H. salinarum* would lead to an increase in *D. salina* biomass and β-carotene accumulation. Results in sections 3.4.2-3.4.7 will detail the co-culture work conducted with *Halomonas* only. Whilst 3.4.7-3.4.8 will dwell on the results with *H. salinarum* incorporated into the co-culture study.

3.4.1. Communal medium

Firstly, a communal medium recipe was developed to attest at which salinity all three microorganisms could co-exist. As salinity was the common denominator, various molarities of NaCl were tested: with 3 M NaCl, being the best-suited salinity for the co-culture study.

3.4.1.1. Dunaliella salina growth and pigments

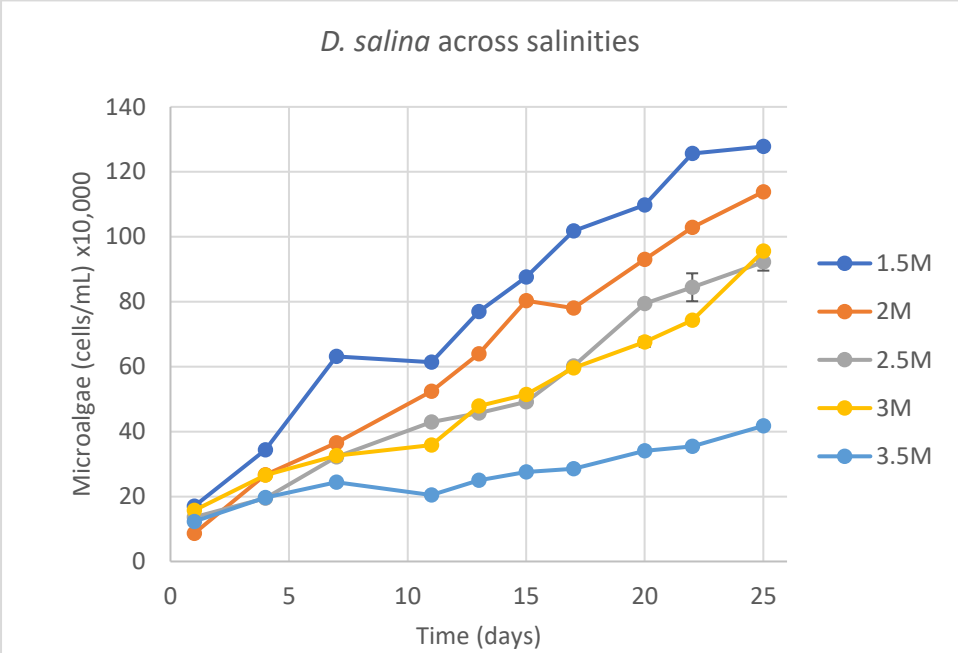

Graph 3.4.1: Monitoring the growth of *D. salina* across salinities through cell counts. Standard error plus and minus bars for biological triplicates. Average of three biological replicates plotted with the error bars, representing the standard error about the mean.

The average growth rates for the flasks were 0.074 day^{-1}, 0.089 day^{-1}, 0.070 day^{-1}, 0.065 day^{-1} and 0.042 day^{-1}, starting from 1.5 M to 3.5 M.

Pigment extractions as shown in Graph 3.4.2. With the exception of the cells at 1.5 M, the chlorophyll a of *D. salina* flasks at higher salinities decreased with time.

A

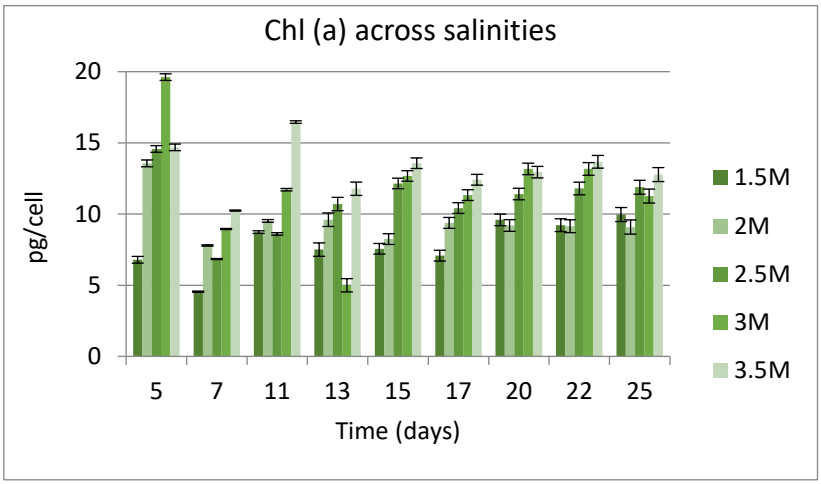

B

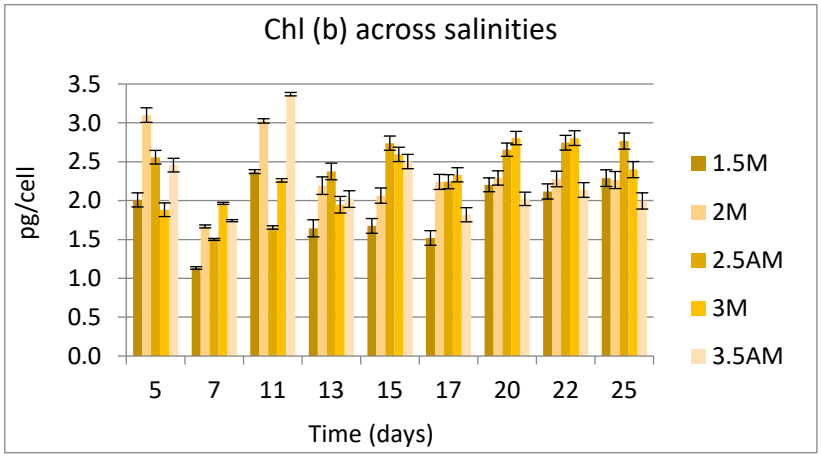

C

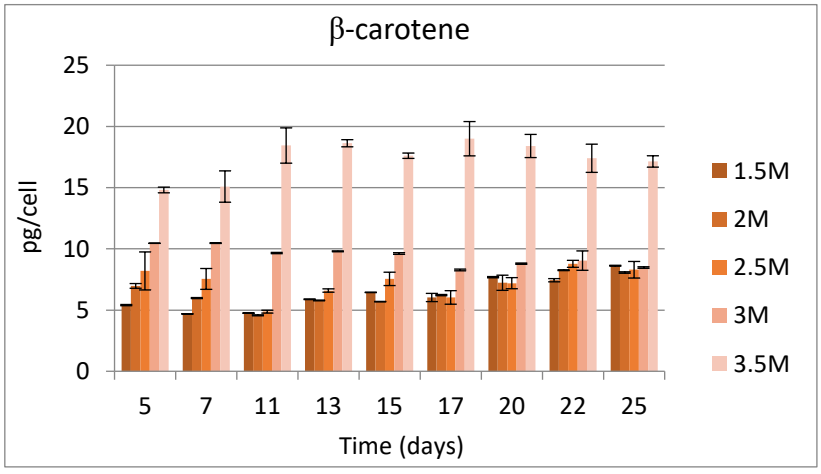

Graph 3.4.2: Pigment extraction of *D. salina* monoculture across a range of salinities. (A) Chlorophyll a, (B) Chlorophylls b, and (C) β-carotene. Average of three biological replicates plotted with the error bars, representing the standard error about the mean.

3.4.1.2. *Halomonas*

Halomonas was grown in 150 mL LB at different NaCl concentrations of 1.5 M, 2 M and 3 M (section 2.2.2), until the culture reached stationary or death phase.

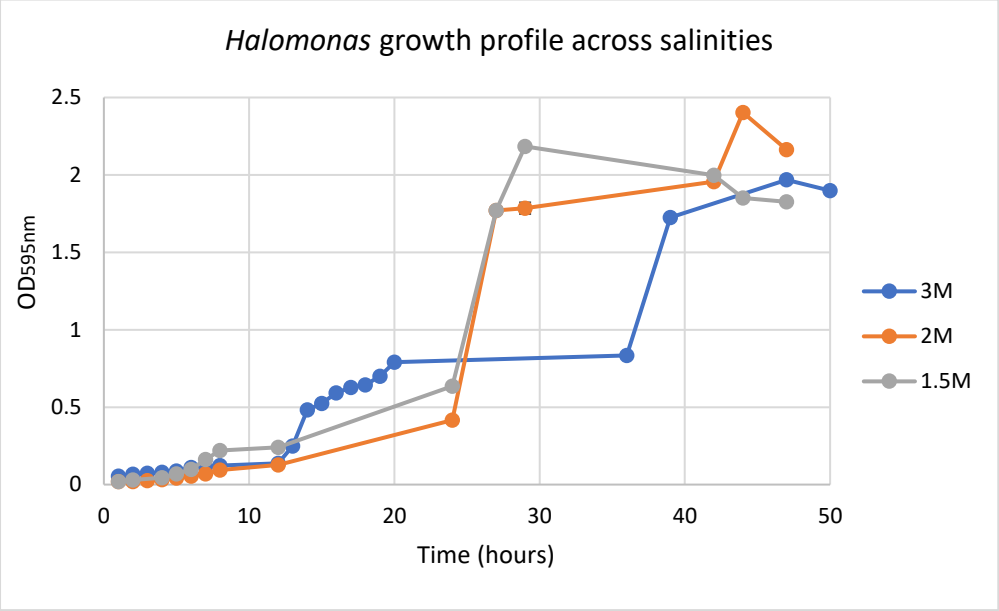

Graph 3.4.3: Growth curve of *Halomonas* over a period of 50 hours across various salinities of LB media. Average of three biological replicates plotted with the error bars, representing the standard error about the mean.

Average growth rate was calculated as 0.215 h^{-1}, 0.147 h^{-1} and 0.124 h^{-1} for 1.5 M, 2 M, and 3 M cells, respectively. The slower growth rate of the bacterium at 3 M, would delay any possible overyielding effects on the microalgae.

The 1.5 M and 2 M flasks were inoculated at 0.019 OD_{595nm}, whilst the 3 M flask was inoculated with a higher density of 0.056 OD_{595nm}, as the cells when inoculated at lower concentrations in the 3 M flasks did not grow (Graph 3.4.4). Stalling the growth, with osmotic shock may affect the production of quorum sensing molecules, which are believed to develop when bacteria are at large concentrations [60,61].

3.4.1.3. *Halobacterium salinarum*

The haloarchaea, *H. salinarum*, was grown over a period of 11 days in ATCC 1863 medium, at three salinity concentrations: 4.2 M, 3 M and 2.5M. The original archaeal culture had been growing at 4.2 M NaCl and had to acclimatised to 3 M. Colonies from 4.2 M agar plates were spread on 3 M agar plates and incubated at 30°C. The surviving cells on the 3 M plates were then spread on subsequent 3 M plates: this procedure took

4-6 weeks. Initially, the 3 M agar plates were incubated at 30 °C to then be subsequently acclimatised at room temperature. After which, colonies were resuspended first in 30 mL of 3 M ATCC 1863 medium broth, to then be subcultured into 100 mL of growth medium. The same procedure was conducted with 2.5 M plates; however, the culture did not survive when inoculated in liquid cultures.

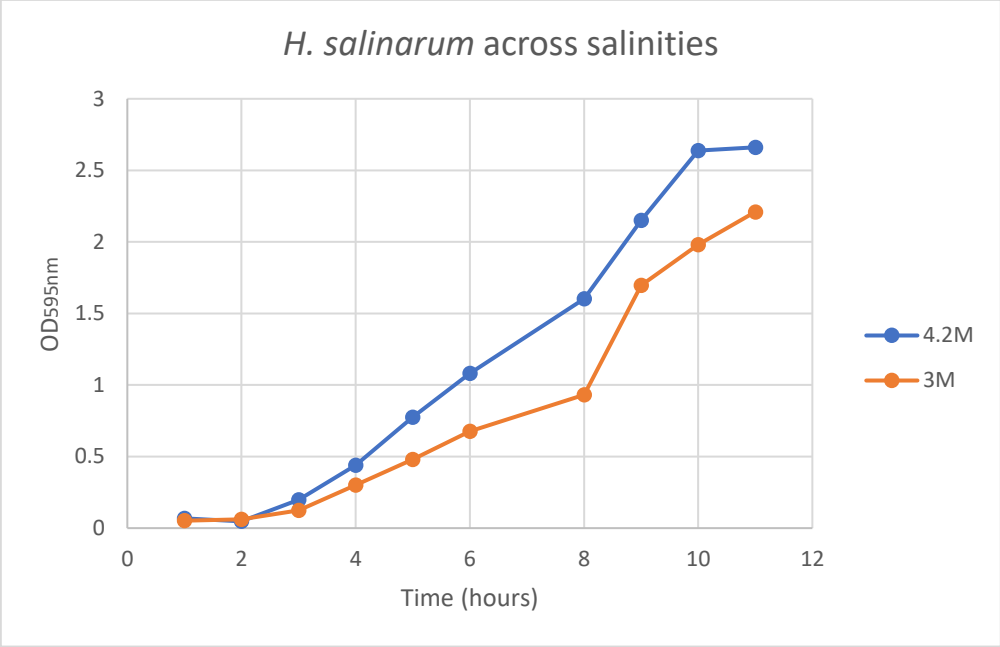

Graph 3.4.4: Growth curve and growth rate for monoculture of *H. salinarum* over a period of 11 days. Average of three biological replicates plotted with the error bars, representing the standard error about the mean.

The data shows that the archaea grows best at 4.2 M (average growth rate 0.4 day^{-1}); however, it was possible to adapt it to grow at 3 M (average growth rate 0.37 day^{-1}). The 2.5 M treatment showed no growth, even when dense inoculums 0.1 OD_{595nm} were tested.

3.4.2. Co-cultures of *D. salina* and *Halomonas*

3.4.2.1. Direct mixing

Algae cell counts provided a better picture of *D. salina* growth because when the bacterial population was high, the turbidity of the samples can affect spectrophotometer readings.

A

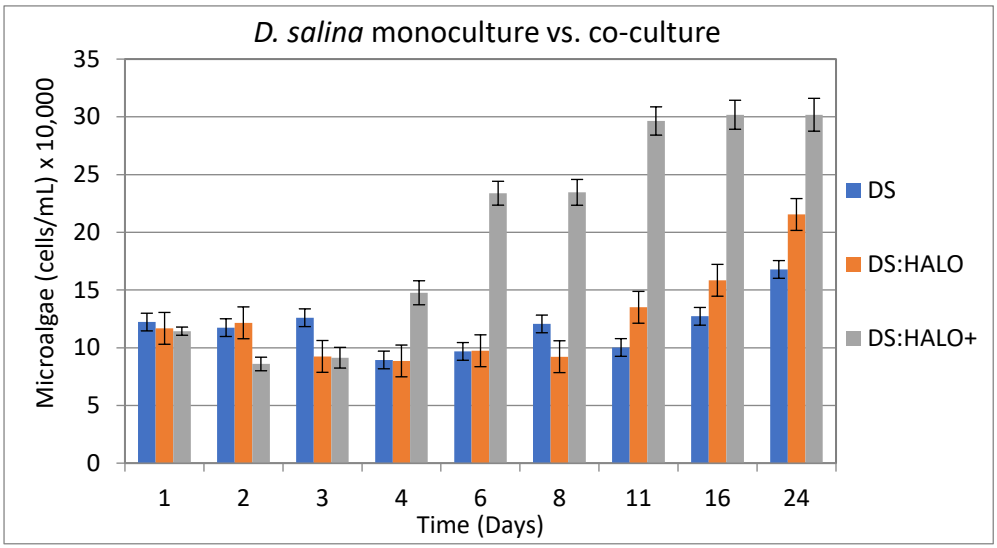

B

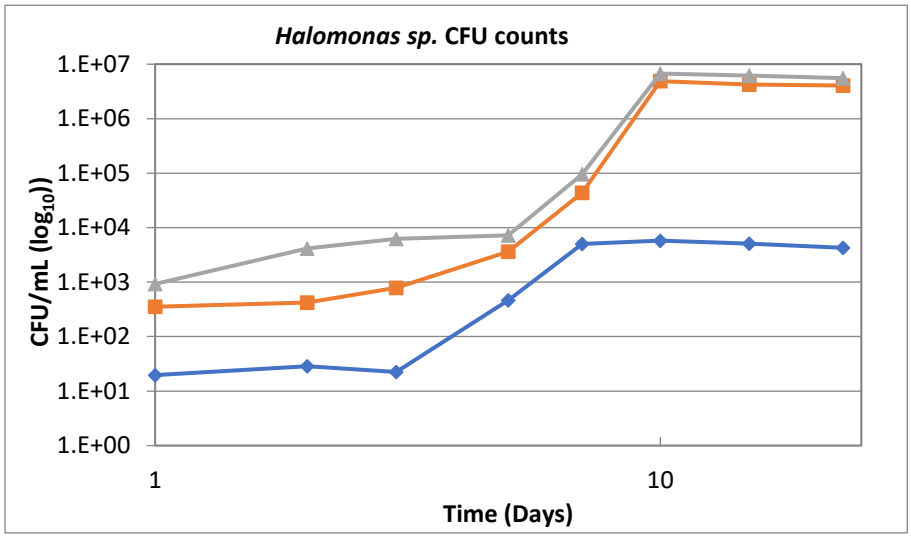

Graph 3.4.5: Growth cure and growth rate of *D. salina* monoculture vs. *D. salina* co-cultures (A). CFU/mL of *Halomonas* given in (B). Average of three biological replicates is plotted with the error bars, which represent the standard error about the mean (not visible).

Growing *D. salina* with *Halomonas* boosts the growth rate of the algae after 4-5 days, as shown in Graph 3.4.6, A and B. The overall growth rates for the flasks was calculated as

0.0138 day^{-1}, 0.0266 day^{-1} and 0.0422 day^{-1} for the DS, DS:HALO and DS:HALO+ flasks, respectively.

3.4.2.2. Encapsulating Halomonas in sodium alginate beads

As the *Halomonas* were trapped in the beads, sampling for just the algae cells was simple.

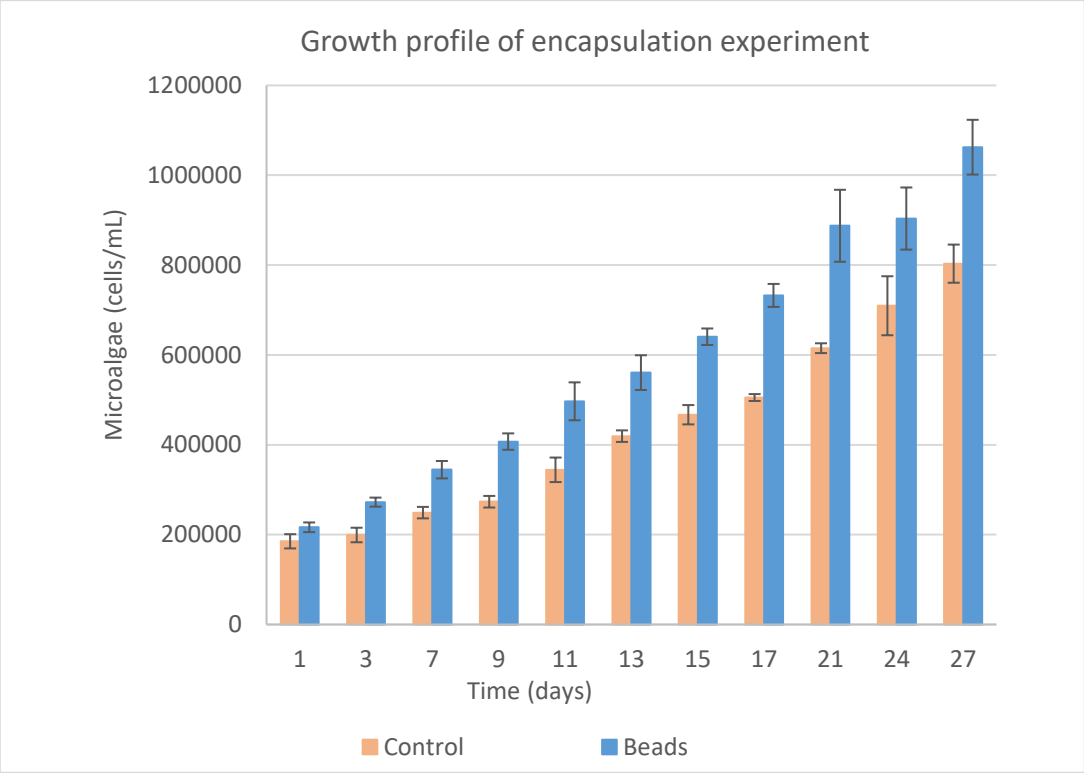

Graph 3.4.6: Growth rates and cell concentration for monoculture and bead-co-culture data over a period of 27 days. Average of three biological replicates is plotted with the error bars which represent the standard error about the mean.

The average growth rate was calculated for both flasks, with the control rate equal to 0.066 day^{-1} and the co-culture rate measuring 0.077 day^{-1}, for the period of 15 days, prior to light stress. After that, the growth rate for both flasks was calculated as 0.04 day^{-1}, for a period of 5 days.

3.4.2.3. Spiking experiment

The effect of the *Halomonas*, exudate on the *D. salina* growth is quite apparent. The *D. salina* was in all medium compositions from 0% to 100% with overall growth rates for the period of 15 days of 1.58 day^{-1}, 1.59 day^{-1}, 1.60 day^{-1}, 1.61 day^{-1}, 1.62 day^{-1} and 1.63 day^{-1}, respectively. Higher cell concentrations were achieved for the 75 % and 100 % growth conditions, with cells approximating $8x10^5$ cells/mL opposed to $5x10^5$ cells/mL in the control flasks (0% condition).

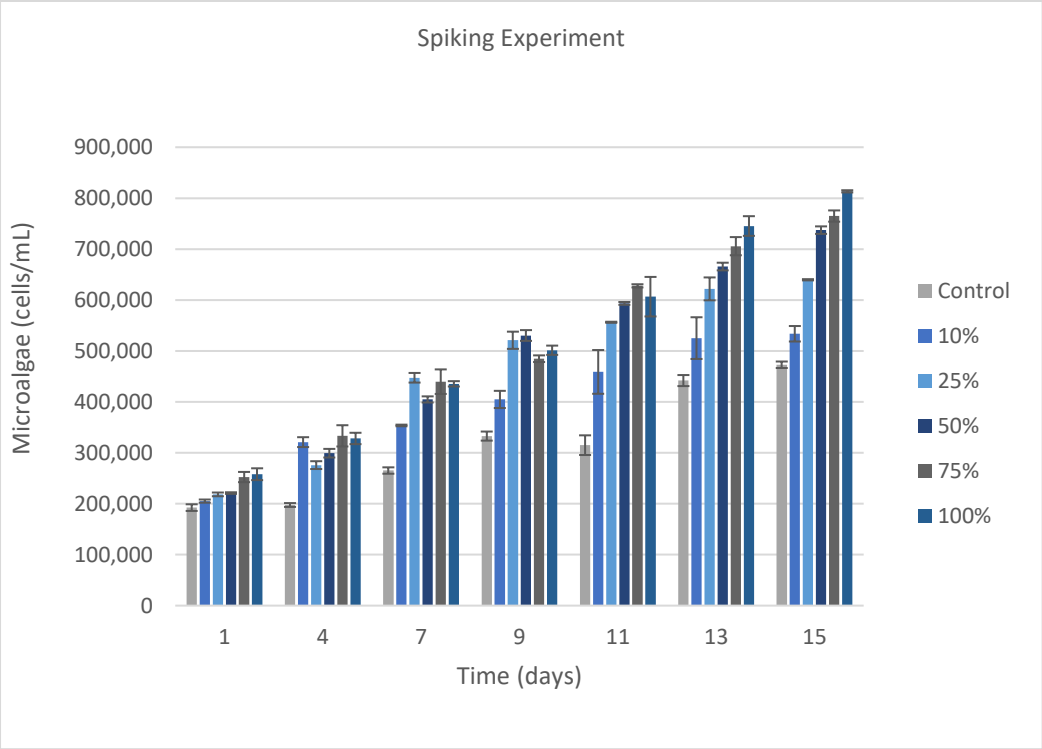

Graph 3.4.7: Concentrations of *D. salina* cells in spiking experiment. Values reported for all condition from 0% to 100% *Halomonas* supernatant mixes. Average of three biological replicates is plotted with the error bars which represent the standard error about the mean.

Overall, the *D. salina* cells that were grown in the presence of *Halomonas* supernatant surpassed the cell densities obtained for the control flask. For the 25 % and 50 % flasks, the cell counts were highest, $5x10^4$ cells/mL higher compared to the other conditions with the first 10 days of growth; to be overtaken by the 75 % and 100 % set-ups, with final counts at $7.6x10^5$ cells/mL and $8.1x10^5$ cells/mL. It is possible to speculate that *D. salina* may have depleted the nutrients provided by the *Halomonas* supernatant, thus slowing growth.

3.4.3. Effect of *Halomonas* on *D. salina* β-carotene production

This section will investigate whether co-culturing *D. salina* with *Halomonas* causes the algae cells to accumulate more β-carotene. The results will provide levels of β-carotene in terms of accumulation per cell and also in terms of overall production rate for the experimental time.

3.4.3.1. Direct mixing

During the direct mixing experiment, *D. salina* and *Halomonas* were co-cultured in 3 M HEPES and 3 M HEPES+ medium for a period of 24 days (Graph 3.4.9).

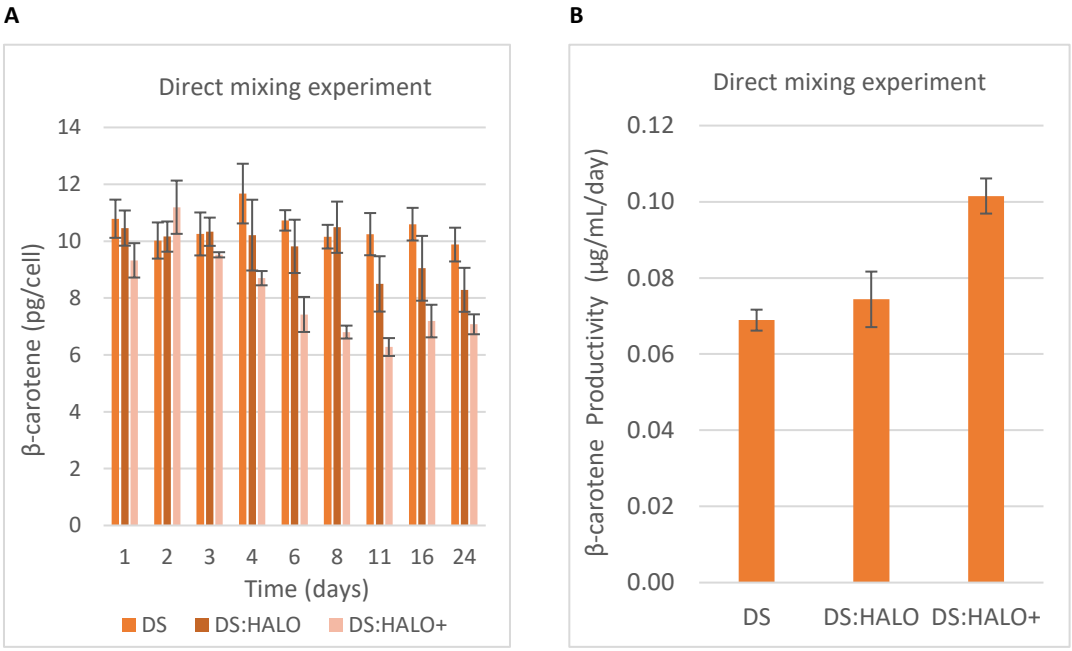

Graph 3.4.8: β-carotene production (A) per cell and overall (B) production over time in direct mixing experiment. Average of three biological replicates is plotted with the error bars, which represent the standard error about the mean.

β-carotene productivity increased by 7 % in DS:HALO flasks, and by 47 % in DS:HALO+ flasks.

3.4.3.2. Encapsulating Halomonas in sodium alginate beads

β-carotene productivity was monitored over a period of 15 days. The results show a productivity increase by 14% using bacterium encapsulated beads in co-culture with *D. salina*.

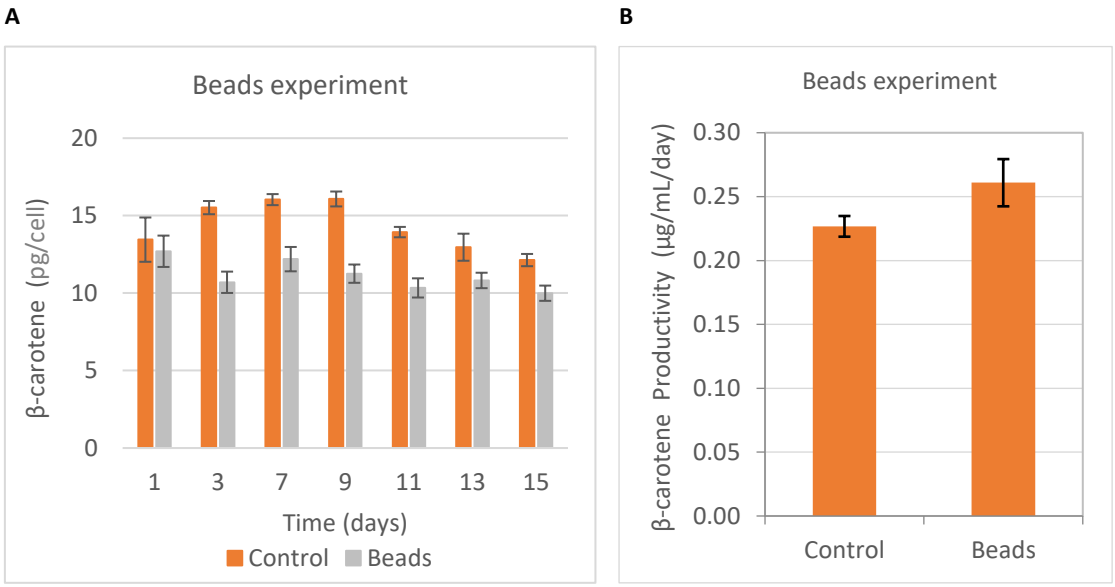

Graph 3.4.9: β-carotene production (A) per cell and (B) production over time for bead experiment. Average of three biological replicates was plotted with the error bars, which represent the standard error about the mean.

3.4.3.3. Spiking experiment

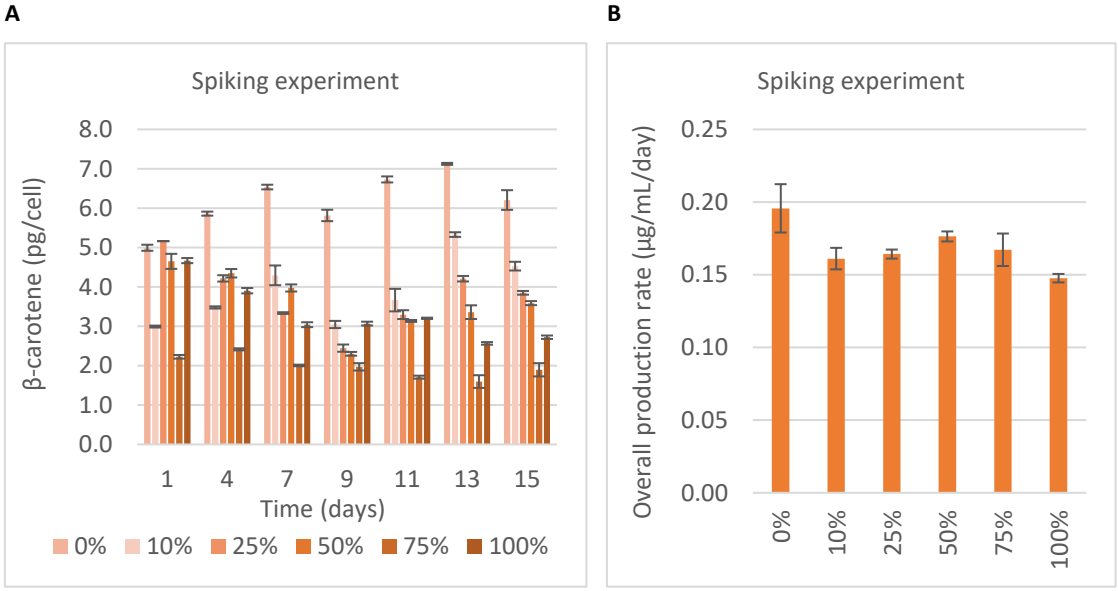

Graph 3.4.10: β-carotene accumulation per cell (A) and overall production (B) over time for spiking experiment. Average of three biological replicates plotted with the error bars, representing the standard error about the mean.

The results for the media spiking experiment (Graph 3.4.11) show that the level of β-carotene for the control flask (0 %) is higher compared to the spiked flasks. The overall production for the period of 15 days for the control flasks is approximately 0.2 µg/mL/day, in the range of 0.16 µg/mL/day for 10 % to 75 % and 0.14 µg/mL/day for the 100 %. The presence of *Halomonas* seems to be fundamental in order obtain significant levels of biomass that would offset lower intracellular β-carotene accumulation.

3.4.4. Effect of *Halomonas* on *D. salina* pigmentation

The chlorophyll a and b and the total carotenoid contents from the samples collected from the experiments outlined in section 3.4.2 in this chapter. The quantitation of these pigments will provide an indication on the effect of *Halomonas*, with respect to photosynthesis and perhaps help understand the cell growth dynamics seen in the results in section 3.4.2 and 3.4.3.

3.4.4.1. Direct mixing

In direct mixing, both microorganisms were mixed together in the same culture flask at a ratio of 1:1 based on the optical density at OD_{595nm}.

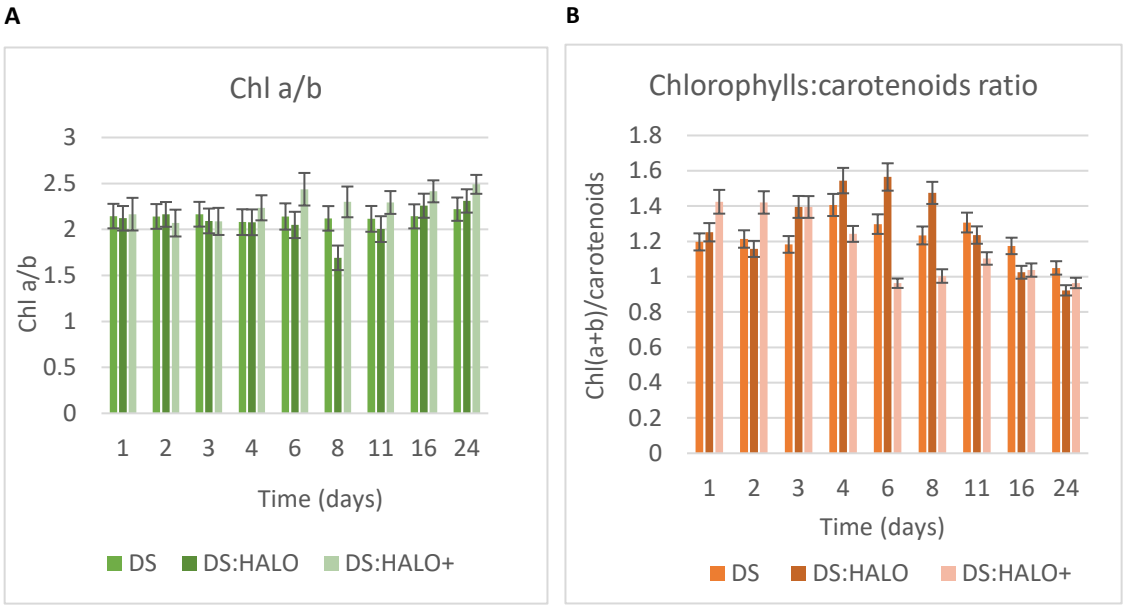

Graph 3.4.11: Relationship of Chlorophylls a to b (A)and total chlorophylls with relation to total carotenoids (B) for direct mixing experiment. Average of three biological replicates plotted with the error bars, representing the standard error about the mean.

The chlorophyll profile was as expected and shows that the ratio of chl a:b is close to 3, with the DS HALO+ flasks showing a slightly larger, but not significant amount of chl a,

when compared to the DS and DS:HALO flasks. This could perhaps be a factor contributing to the increase in biomass. The total chlorophylls to carotenoids ratio further shows that the amounts of carotenoids in the DS:HALO+ flasks are a fraction smaller compared to the other two conditions.

3.4.4.2. Encapsulating Halomonas in sodium alginate beads

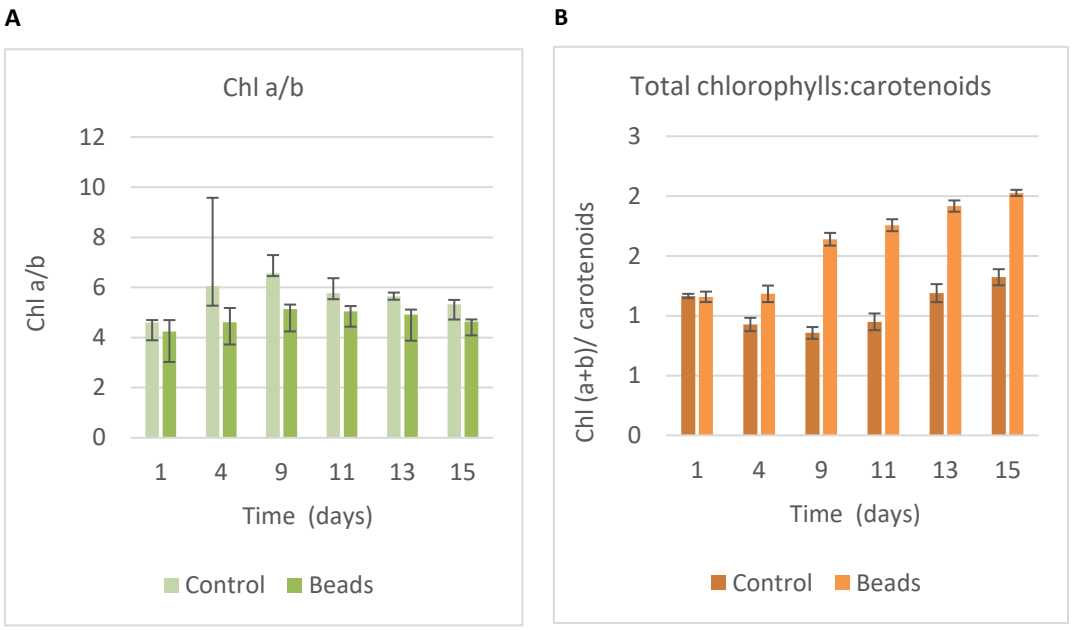

Graph 3.4.12: Relationship of Chlorophylls a to b (A) and total chlorophylls with relations to total carotenoids (B for Beads experiment. Average of three biological replicates plotted with the error bars, representing the standard error about the mean.

In the encapsulated bead experiment, the ratio again of chl a:b shows that the majority of the chlorophylls within the cell is chl a. However, the values obtained are higher than the usual ratio of 3:1.

3.4.4.3. Spiking experiment

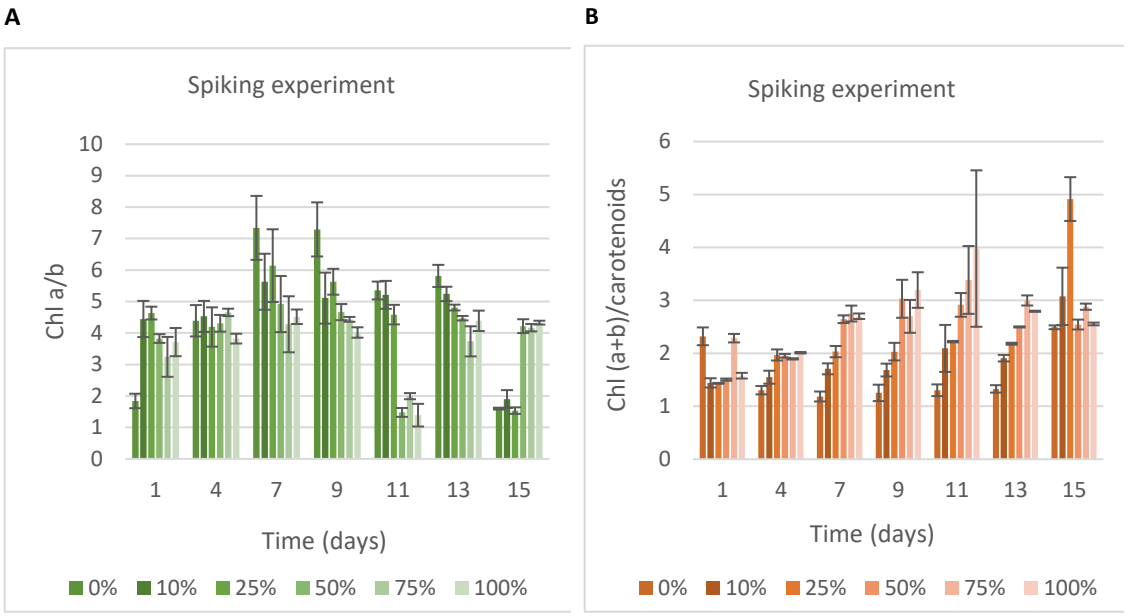

Graph 3.4.13: Relationship of Chlorophylls a to b (A) and total chlorophylls with relations to total carotenoids (B) for Beads experiment. Standard error plus and minus bars for biological triplicates.

The spiking experiment results show again quite high levels of chl a compared to chl b. Graph A also indicates that on the 11th day the ratio of chl a:b drops in the 50 %, 75 % and 100 % sample to then increase again on the 15th day, this phenomenon mirrored in conditions 0 %, 10 % and 25 %.

The readings were not discarded, as the results obtained were the same for all biological triplicates, belonging to those conditions. The ratio of chlorophylls to total carotenoids, however show the same trend as in the other experiments, with the exception of day 15. The percentage of chlorophylls is higher in the flasks with higher amounts of *Halomonas* exudates.

3.4.5. Direct Mixing: subjecting *Dunaliella salina* and *Halomonas* to abiotic stresses.

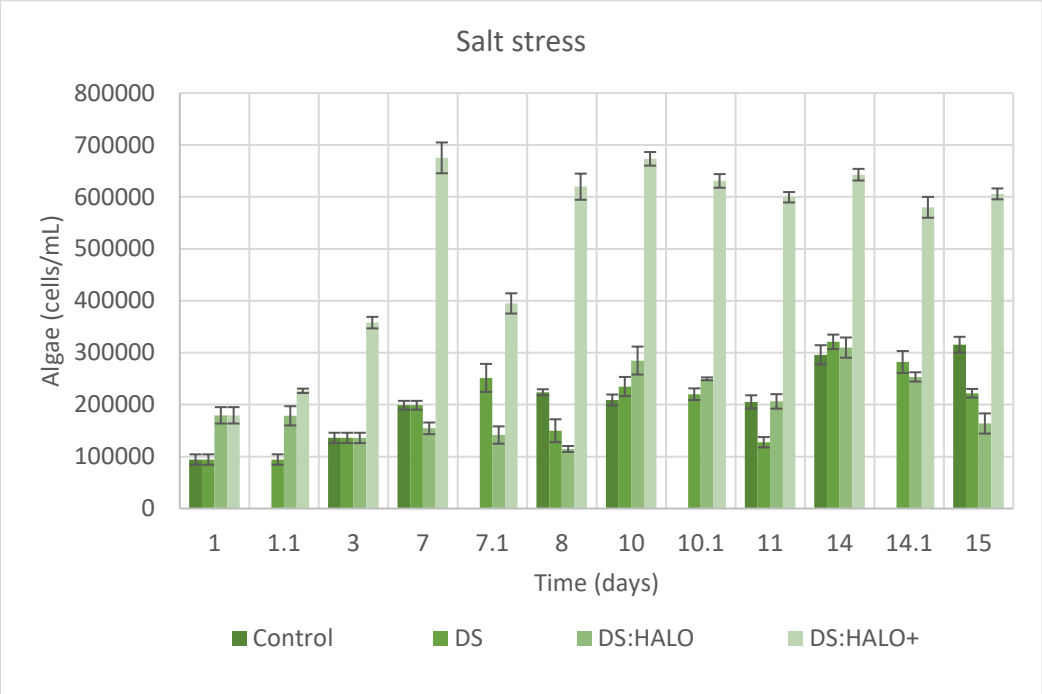

Graph 3.4.14: Effect of salt stress on microalgae cell numbers. Average of three biological replicates plotted with the error bars, representing the standard error about the mean.

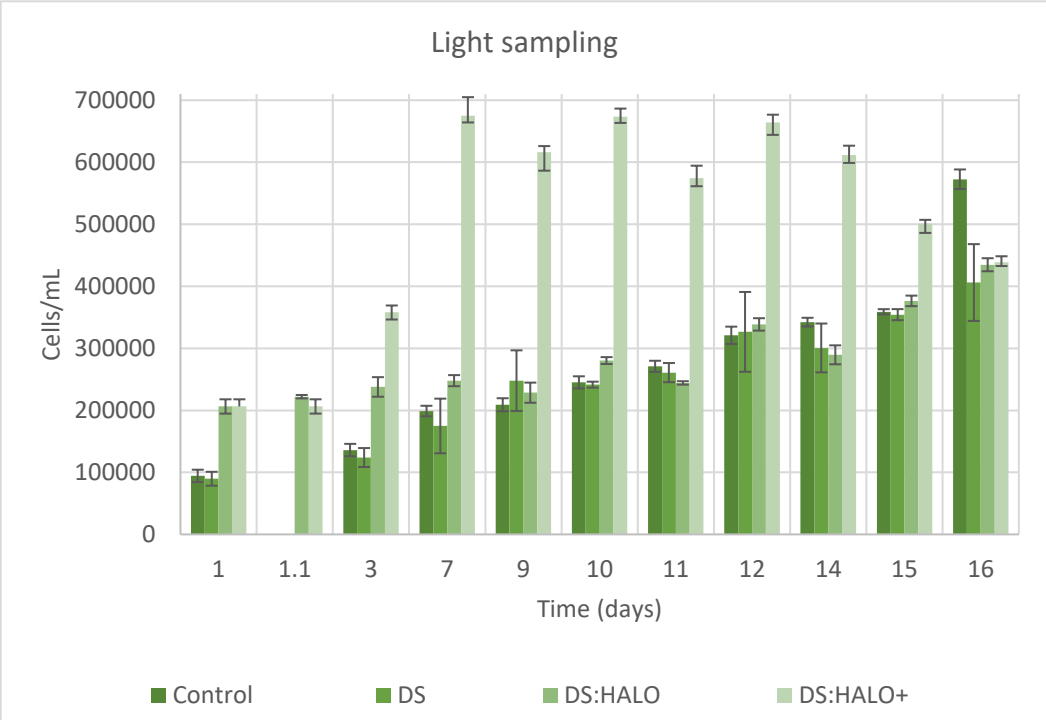

Graph 3.4.15: Effect of light stress on microalgae cell numbers. Average of three biological replicates plotted with the error bars, representing the standard error about the mean.

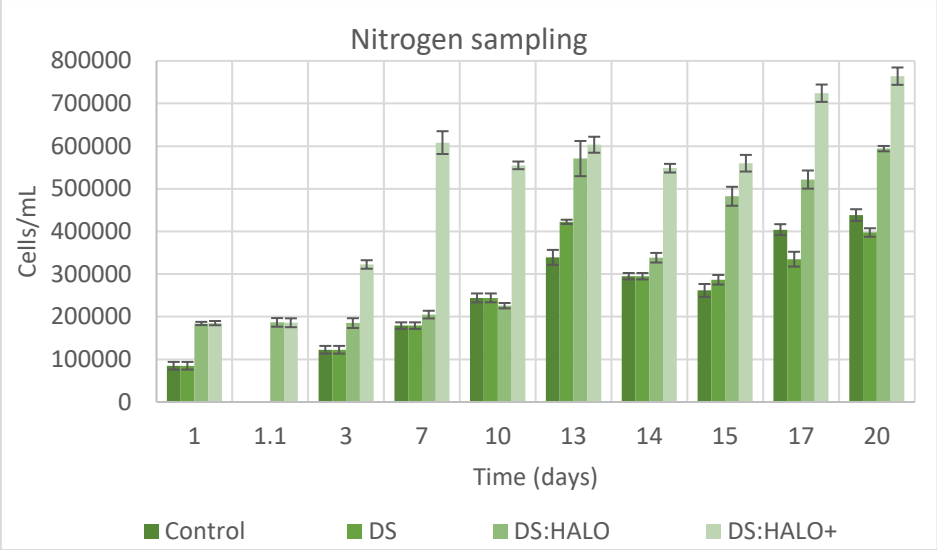

Graph 3.4.16: Effect of nitrogen stress on microalgae cell numbers. Average of three biological replicates plotted with the error bars, representing the standard error about the mean.

The presence of the *Halomonas* led to an increase in overall microalgae cell numbers. The salt stressed flasks of DS:HALO+ on average showed values of 650,000-700,000cells/mL, more than a 2-fold increase when compared to the Control and the DS stressed flasks. Similarly, in both Light and Nitrate stress flasks the cell numbers where higher, in the region of 800,000cells/mL.

3.4.5.1. β- carotene production

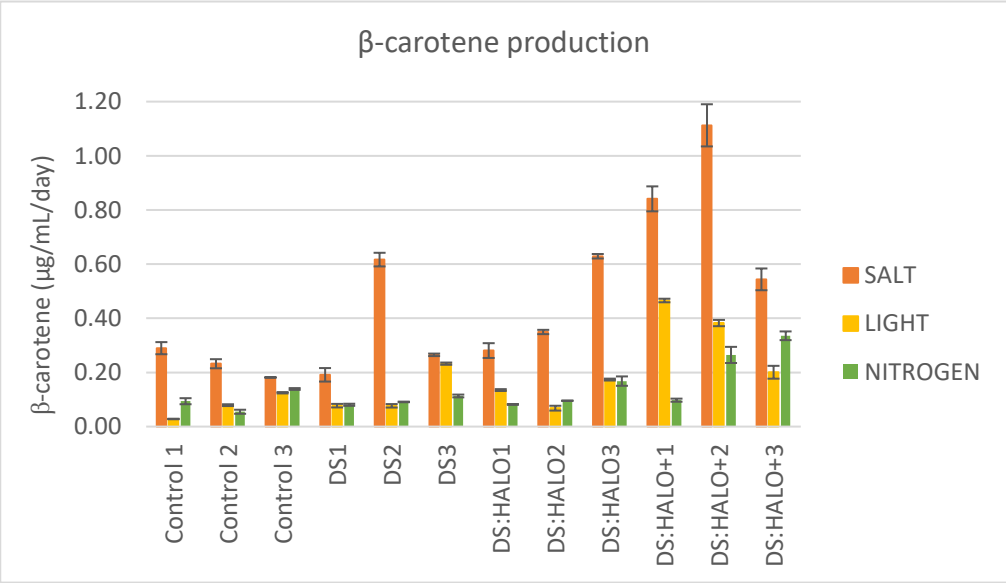

Graph 3.4.17: Effects of abiotic stresses β-carotene production (µg/mL/day). Average of three biological replicates plotted with the error bars, representing the standard error about the mean.

The results obtained for β-carotene production (Graph 3.4.18)show a net increase in the DS:HALO+ flasks for all conditions. The DS:HALO+ flasks show overall production levels higher when compared to the DS flasks, due to the higher concentrations of cells. T-test indicates that the productivities for both light and salt stress are robust methods ($p<0.05$ with nitrogen starvation perhaps requiring more time to see better results ($p=0.09$. On the other hand, accumulation of β-carotene per cell basis of the DS:HALO+ flasks do not show significant variations from the DS flask, with ($p>0.05$) for all flasks. This study further demonstrates that associating *Halomonas* with *D. salina* leads to an increase in microalgae cell number during normal co-culture conditions and when the co-culture is subjected to stress. This agrees with the literature surveyed, showing that microorganisms that are part of a co-culture/consortium are better able to adapt and are more resilient to environmental conditions [56].

3.4.5.2. Glycerol consumption

Glycerol is one of the main compounds playing a role in the interaction between *D. salina* and *Halomonas* The supernatant medium was analysed for content of glycerol, by performing a simple colorimetric assay, as described in section 2.5.3.

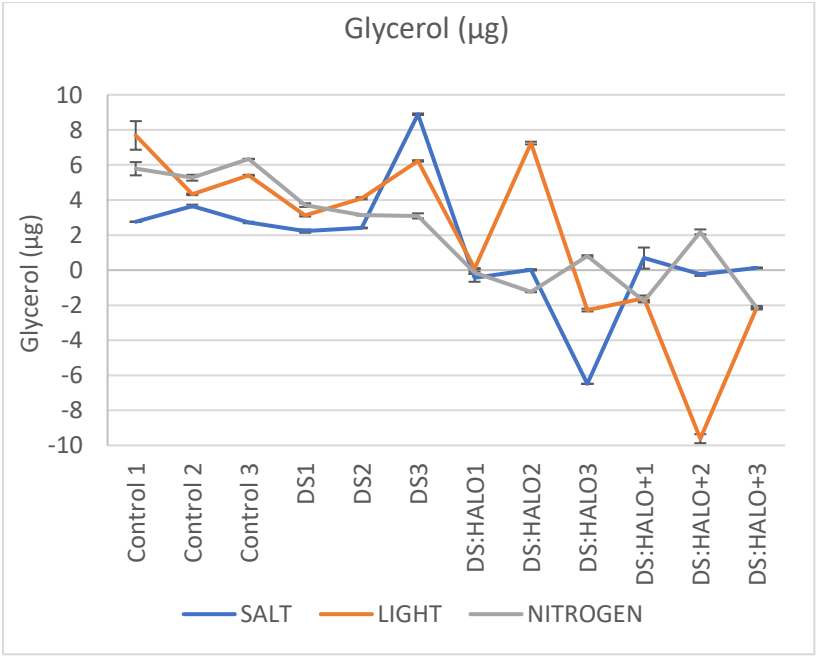

Graph 3.4.18: Glycerol content in supernatant. All values for the stressed flasks have been subtracted from the control values. Average of three biological replicates plotted with the error bars, representing the standard error about the mean.

The control's initial value of glycerol was measured in the flasks prior to adding *Halomonas* and stressing the flasks. When comparing the runs for the data, the DS:HALO+ flasks showed a lower amount of glycerol present within the supernatant. On the other hand, the flasks on the 3rd run for DS show amounts of glycerol surpassing the Control concentration. It is possible that around the 14th day of salt stress, the cells leak amounts of glycerol in the medium to counteract osmotic shock [47]. Similarly, in the light stress, the DS:HALO flask shows an increase in glycerol output, as the cells are subjected to light. This phenomenon may induce them to release all intracellular glycerol in amounts that surpass the demand from *Halomonas*

3.4.6. Dissolved inorganic nitrogen

Nitrate levels were monitored for all stressed samples. Dissolved inorganic nitrates were estimated using the method outlined in section 2.5.4.

Depletion of nitrates within the medium has been shown to induce *D. salina* cells into producing β-carotene. Here, we investigate if the presence of *Halomonas* affects the amounts of nitrate present, other than nitrogen starvation itself.

Graph 3.4.20 to 3.4.22 provide details for the initial amounts of nitrate (these are the nitrate measured in the growth medium prior to inoculation and measured nitrate levels, which have been estimated at the end of the stress period for that given scenario. The consumed values were calculated by deducting the measured nitrate levels from the initial levels.

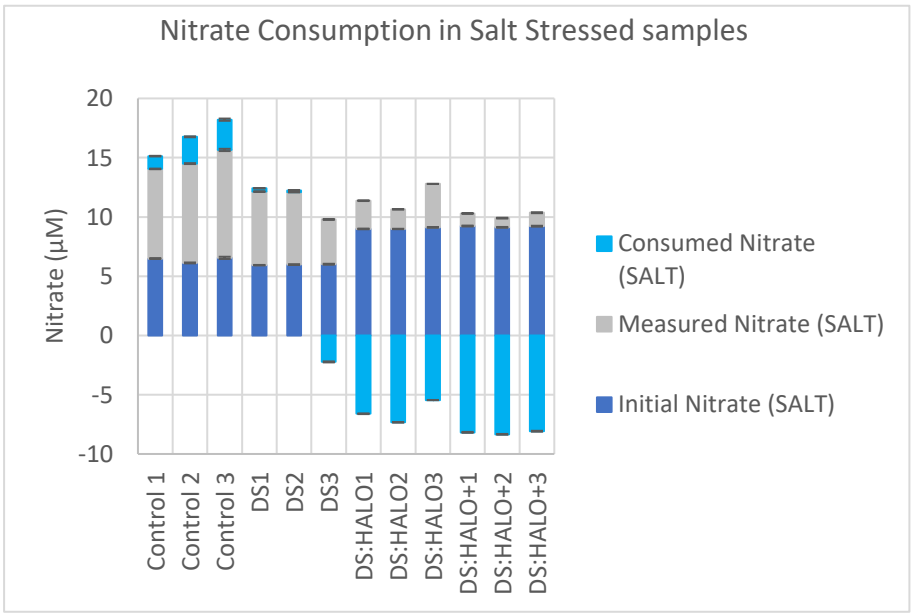

Graph 3.4.19: Nitrate consumption for all salt stressed flasks. Standard errors for plus and minus values for triplicate. Average of three biological replicates plotted with the error bars, representing the

standard error about the mean.

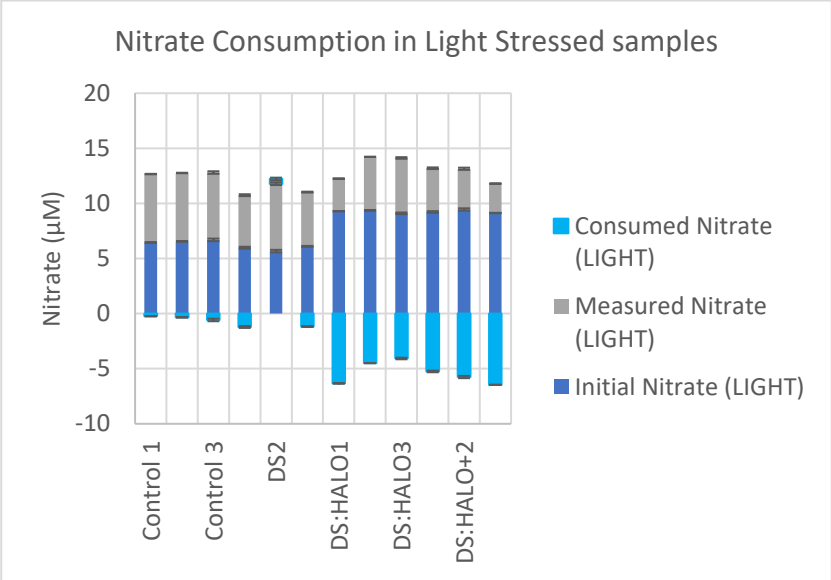

Graph 3.4.20: Nitrate consumption for all light stressed flasks. Standard errors for plus and minus values for triplicate. Average of three biological replicates plotted with the error bars, representing the standard error about the mean.

The nitrate levels in all scenarios involving high presence of *Halomonas* are lower compared to the Control and the DS stressed flasks. The use of nitrogen is linked to cell growth in both species, thus having the additional presence of *Halomonas* within the mix may contribute to further diminishing the amounts within the medium. The nitrate data for *D. salina* cells suggests that with the presence of *Halomonas*, the algae cells may be experiencing a nitrogen depletion effect alongside salt and light stress.

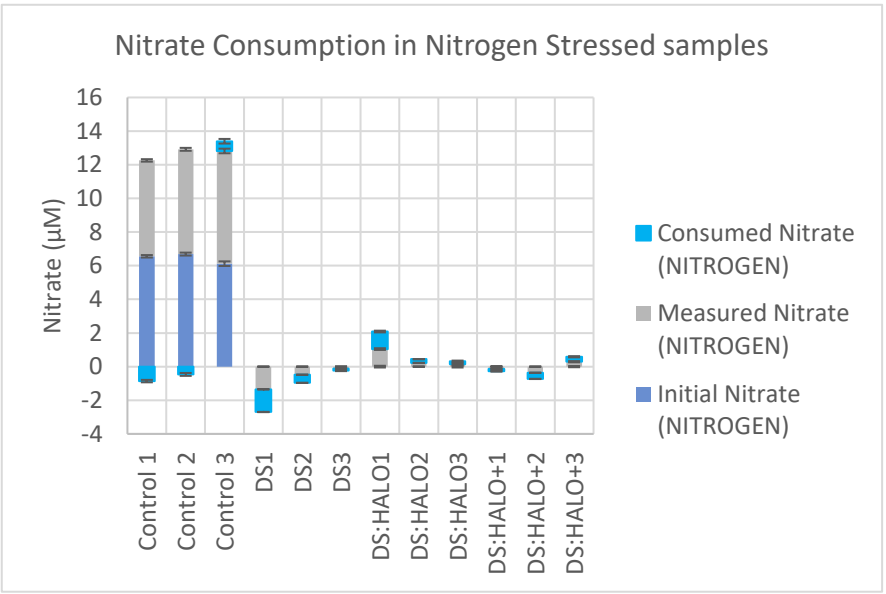

Graph 3.4.21: Nitrate consumption for all nitrogen stressed flasks. Average of three biological replicates plotted with the error bars, representing the standard error about the mean.

All the nitrogen depleted flasks show nitrate concentration levels in the range of zero. The DS:HALO 1 flasks show higher amounts, perhaps as residues coming from the stock flasks which were grown with the additional yeast extract. However, it is possible that

the *Halomonas* or the *D. salina* may be nitrifying the medium, to minimise the stress on the other species.

3.4.6.1. Chlorophylls

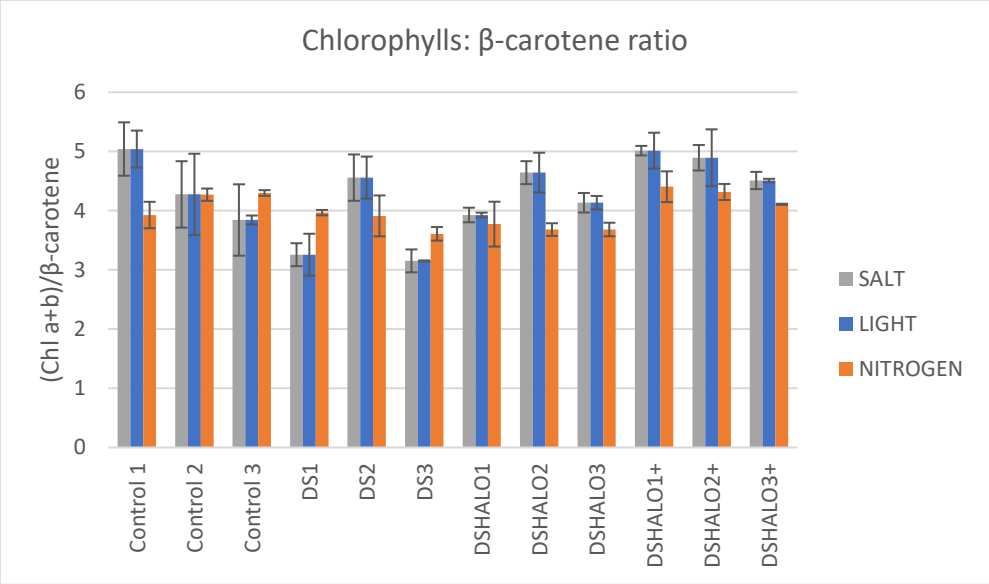

Graph 3.4.22: Total chlorophylls to β-carotene ratio in stressed *D. salina* cells (pg/cell) ratios for salt, light and nitrogen stress. Average of three biological replicates plotted with the error bars, representing the standard error about the mean.

The ratios of total chlorophylls to β-carotene show that in both salt and light stress, concentrations of total chlorophylls in the cells is either the same as the controls or higher. This shows salt and light stress on the co-cultures, has less effect when *Halomonas sp*. is present. However, nitrogen stress has an effect on the co-culture. Nitrogen is a factor that also contributes to the well-being of the *Halomonas*, thus with lower nitrogen levels, they would utilise nitrogen themselves without passing any nitrogen to the algae.

3.4.7. Co-cultures of *D. salina* and *H. salinarum*

3.4.7.1. Direct mixing

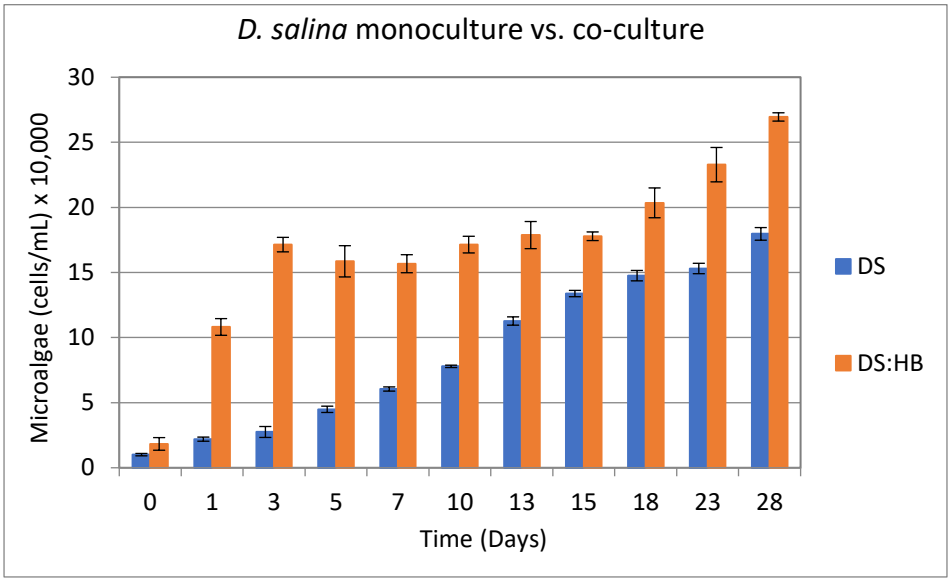

Graph 3.4.23: Growth curve and growth rate of *D. salina* monoculture and co-culture. Average of three biological replicates plotted with the error bars, representing the standard error about the mean.

The addition of *H. salinarum*, at first glance, shows an increase in cell numbers. At the end of the experimental run, the DS:HB flask has $2.6x10^5$ cells/mL compared to the $1.8x10^4$ cells/mL: a significant 52% increase with $p<0.05$. In the first five days, the growth rate of the monoculture and the co-culture averaged 0.38 day^{-1} and 0.66 day^{-1}, respectively. As shown by the CFU counts (Graph 3.4.25) this was an effect caused by the presence of both *Halomonas* and the *H. salinarum*.

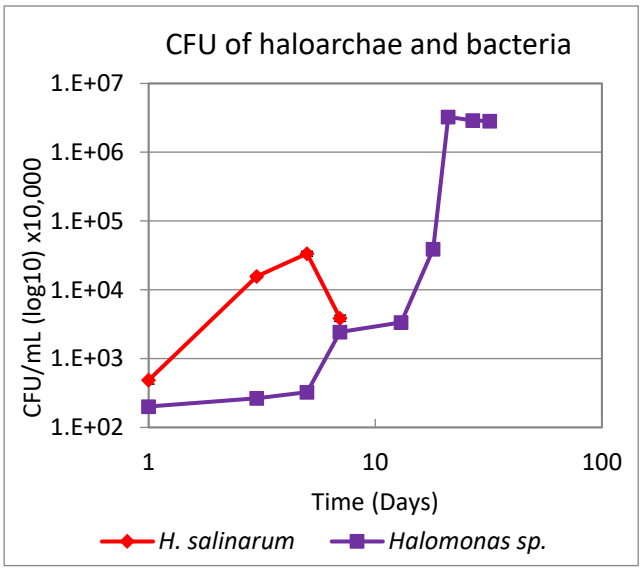

Graph 3.4.24: *H. salinarum* and *Halomonas*, CFU/cell in DS:HB flasks. Average of three biological replicates plotted with the error bars, representing the standard error about the mean.

Complete removal of *Halomonas* within the *D. salina* culture was not possible. The addition of a 10 % ATCC 1863 to the medium encouraged the growth of the bacteria within the co-culture flasks, as well. This was further spurred by the short life-span of the haloarchaon. As the *H. salinarum* withered (Graph 3.4.25) the *Halomonas* grew consuming its spoils. However, this can only be verified by a spiking test with *H. salinarum* dried biomass to supplement the growth of *Halomonas*.

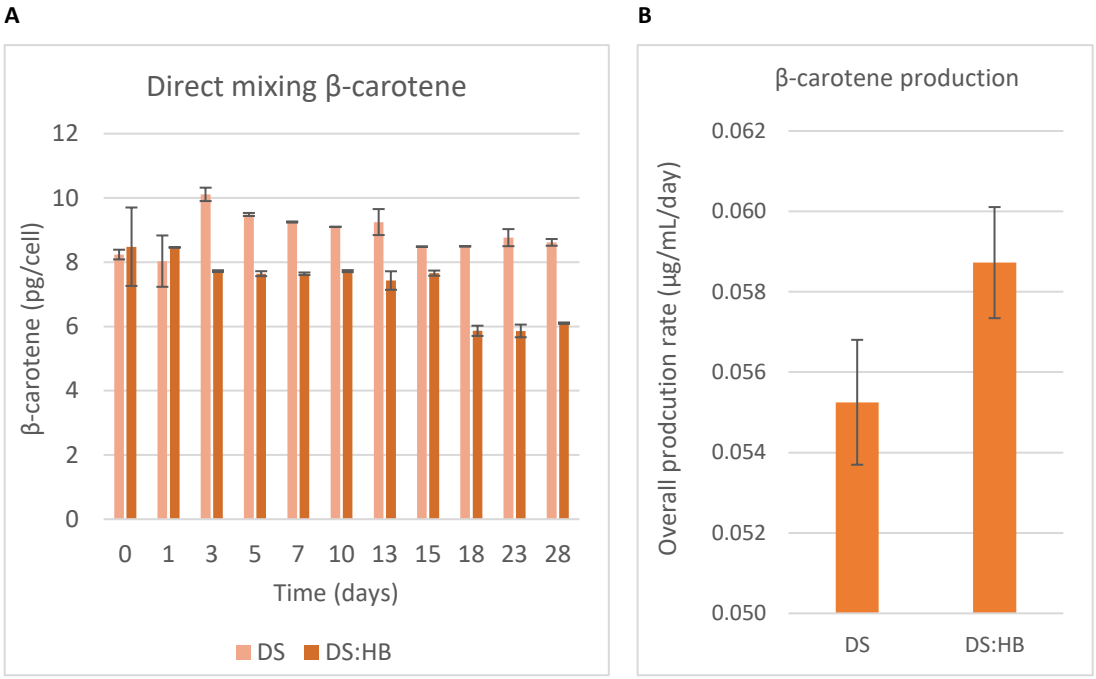

Graph 3.4.25: β-carotene content (A)per cell and (B) concentration for monocultures of *D. salina* and co-cultures of *D. salina* with *H. salinarum* in HEPES 1863 medium. Average of three biological replicates plotted with the error bars, representing the standard error about the mean.

In the above graph (3.4.26), point 0 on the x-axis represents sampling done just after inoculation within 30 minutes. The β-carotene overall production in the direct mixing experiment, showed an increase of 5% in productivity when the microalgae were grown with *Halomonas* and *H. salinarum*.

3.4.8. Direct Mixing: subjecting *Dunaliella salina* and *H. salinarum* to abiotic stresses.

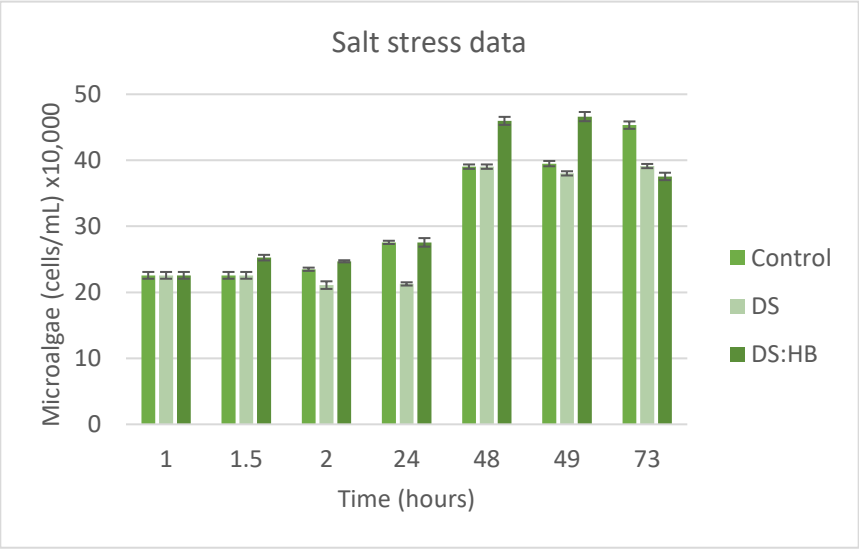

Graph 3.4.26: Counts of *D. salina* cells, during salt stress. Control, is the *D. salina* cells grown in 3 M HEPES, DS is the algae monoculture at 4.2 M and DS:HB is the co-culture at 4.2 M. Average of three biological replicates plotted with the error bars, representing the standard error about the mean.

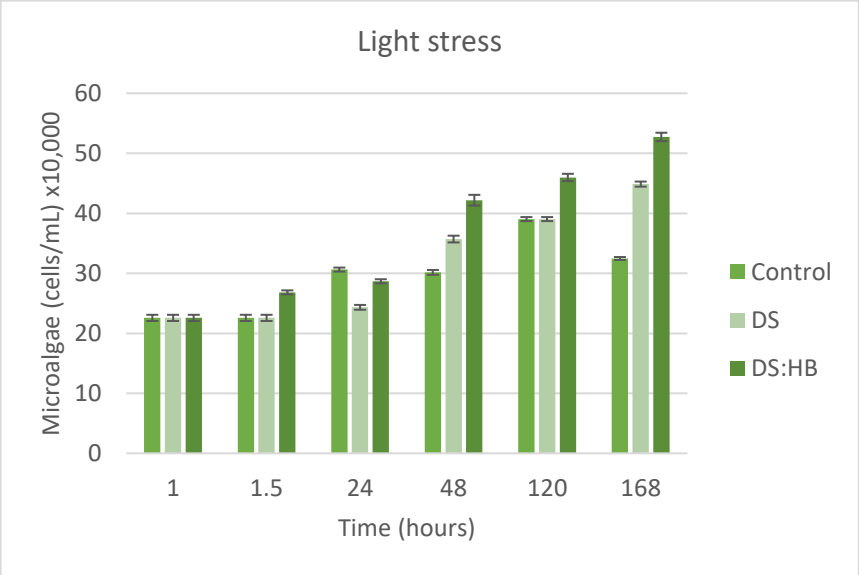

Graph 3.4.27: Counts of *D. salina* cells, during Light stress. Control, is the *D. salina* cells grown in 3 M HEPES, DS is the algae monoculture and DS:HB is the co-culture subjected to high light (value). Average of three biological replicates plotted with the error bars, representing the standard error about the mean.

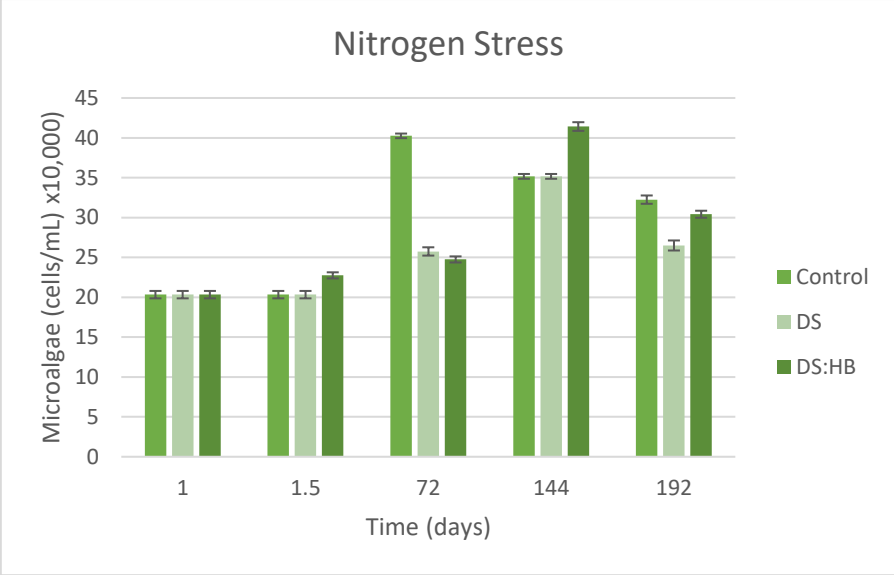

Graph 3.4.28: Counts of *D. salina* cells, during Nitrogen stress. Control, is the *D. salina* cells grown in 3 M HEPES, DS is the algae monoculture and DS:HB is the co-culture subjected to nitrate deprivation. Average of three biological replicates plotted with the error bars, representing the standard error about the mean.

Graphs 3.4.27-3.4.29 show the concentration of cells during the direct mixing stress experiment. In contrast to the co-culture with *Halomonas* and *D. salina* alone, the salt stress effects the co-culture. The first stress period of over 24 hours shows that the microalgae cells in the DS:HB flask are higher compared to the stressed monoculture, DS, however, the concentration of $2.7x10^5$ cells/mL is the same as that of the control. Furthermore, the co-culture conducted a few days' later shows that salt stress leads to a decrease in the number of algal cells, from 4.5 to 3.7 $x10^5$ cells/mL. As the *H. salinarum* was hard to acclimatise to 3 M HEPES 1863, a sudden osmotic shock may also effect the haloarchaeon, making the consortia vulnerable. In contrast, light stress shows an increase in cell concentration. After 48 hours of stress, the first batch of cell numbers reached $4.2x10^5$ cells/mL and in the second batch, the number further increases to $5.2x10^5$ cells/mL. Similar, to the salt stress, nitrate stress causes a stress to both the *D. salina* and the *H. salinarum*, offsetting the benefits that *Halomonas* would have on the co-culture.

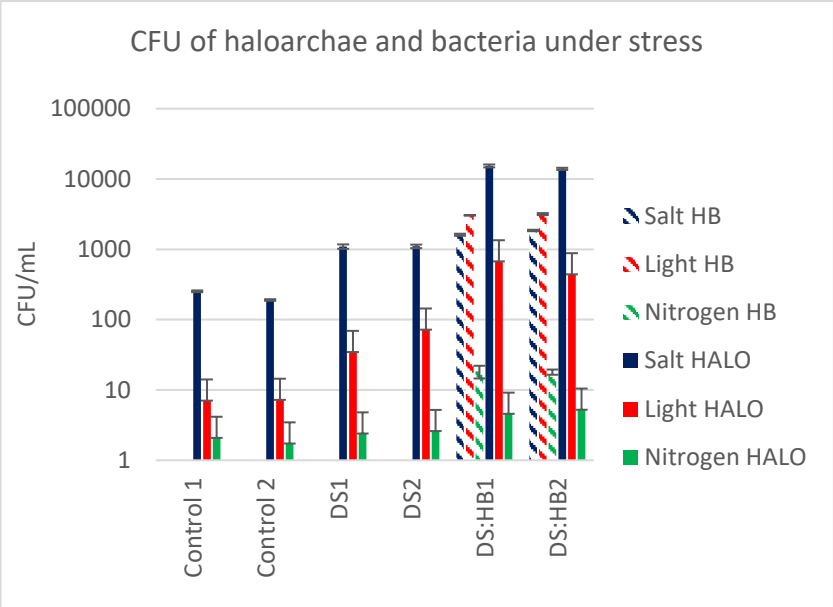

Graph 3.4.29: Loading of *H. salinarum* and *Halomonas* at the sampling point. Average of three biological replicates plotted with the error bars, representing the standard error about the mean.

Nitrate stress has the largest effect on both aiders. Followed by salt stress, which limits the *H. salinarum* activity.

3.4.8.1. β-carotene and pigments accumulation and production

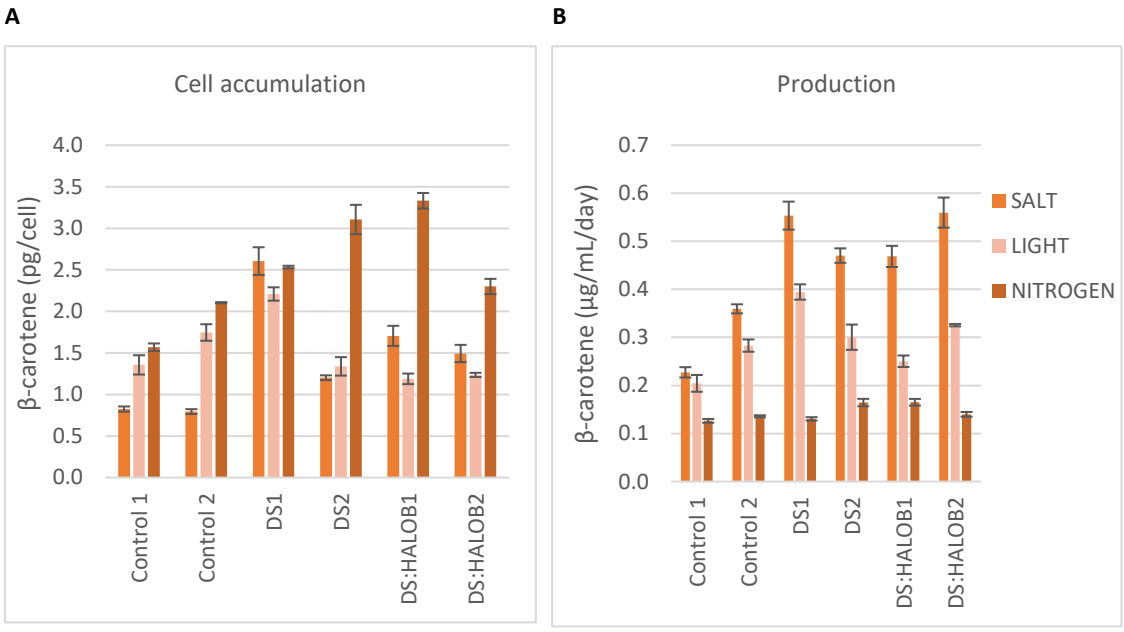

Graph 3.4.30: Effects of abiotic stresses *D. salina* cells ability to synthesise (A) β-carotene (pg/cell) and production (µg/mL/day) (B). Average of three biological replicates plotted with the error bars, representing the standard error about the mean.

The data in Graph 3.4.32 demonstrates that in the current consortia, the nitrate stress had more effect on the microalgae and the *H. salinarum* together, compared to the other stresses. As the *H. salinarum* also accumulated bacteriorhodopsin when stressed

this may be translated into the β-carotene readings at a cellular basis (A. Although the best overall productivity is seen in the salt stressed co-cultures, the β-carotene levels obtained are not significantly different to the ones obtained by the monoculture.

A

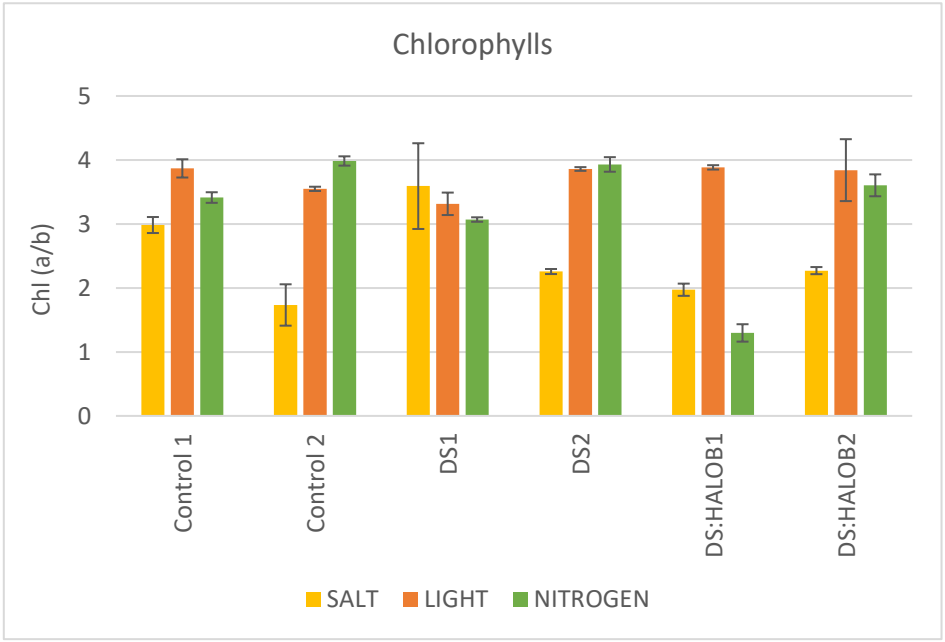

B

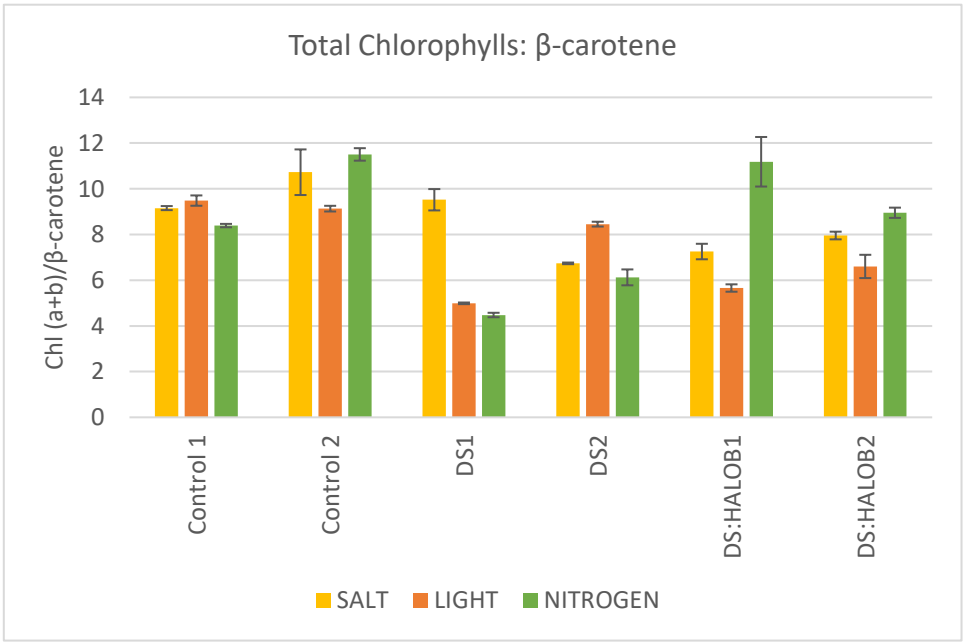

Graph 3.4.31: Relationship of chlorophylls a to b (A and total chlorophylls with relations to total β-carotene (B for direct mixing experiment. Average of three biological replicates plotted with the error bars, representing the standard error about the mean.

Changes in chlorophyll throughout the stress experiment show that both light and nitrogen stress induced the *D. salina* cells to divert pathways into carotenogenesis. Salt stress does not seem to impact on the chlorophyll levels within the cells as substantially.

3.4.8.2. Glycerol in supernatant

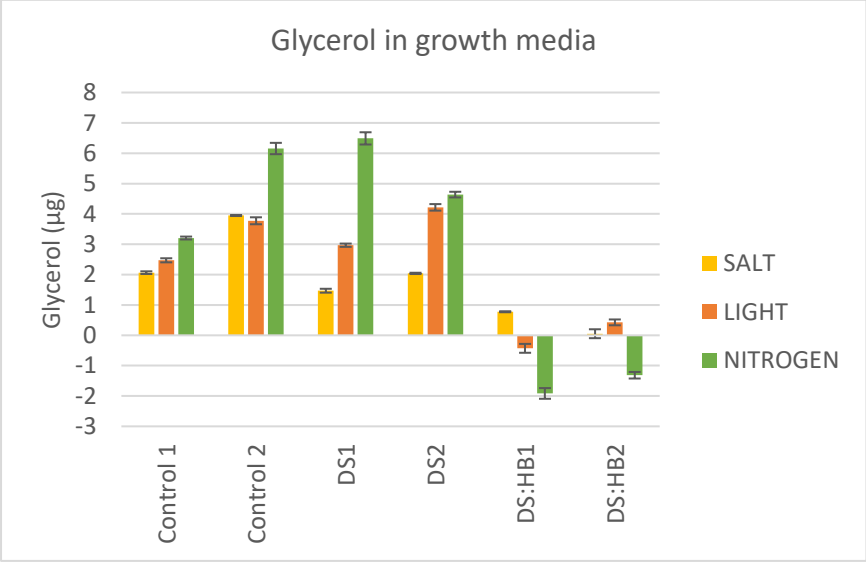

Graph 3.4.32: Glycerol consumption (µg). Measurements taken from extracellular medium. Average of three biological replicates was plotted with the error bars, which represent the standard error about the mean.

The absence of glycerol in the supernatant of the consortia medium when compared to the stressed monocultures levels indicated that both aiders have used this as a carbon source.

3.4.8.3. Dissolve inorganic nitrogen

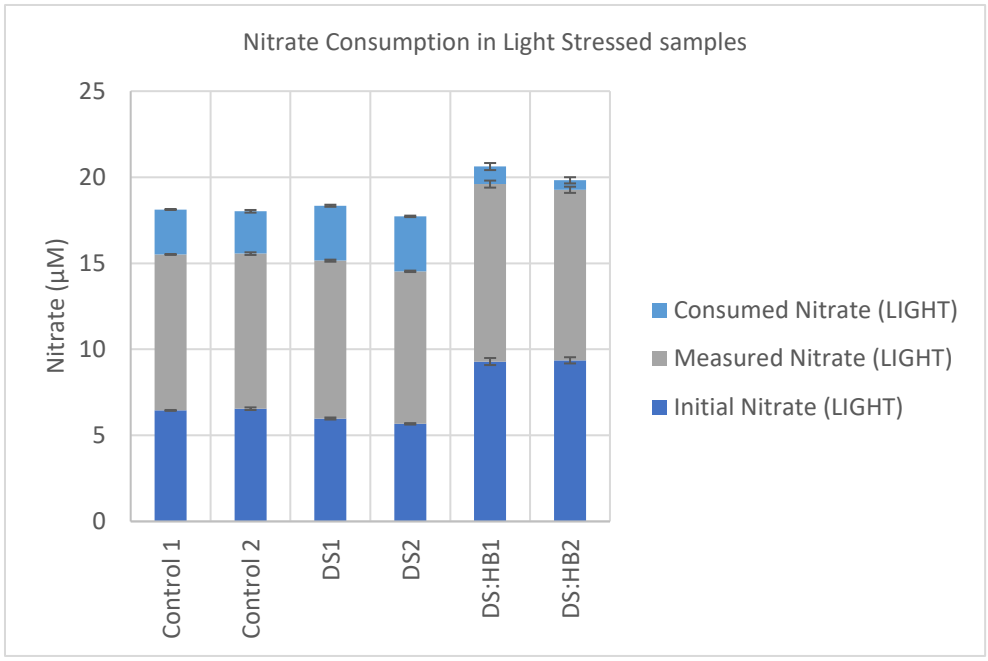

Graph 3.4.33: Nitrate consumption for all light flasks. Average of three biological replicates plotted with the error bars, representing the standard error about the mean.

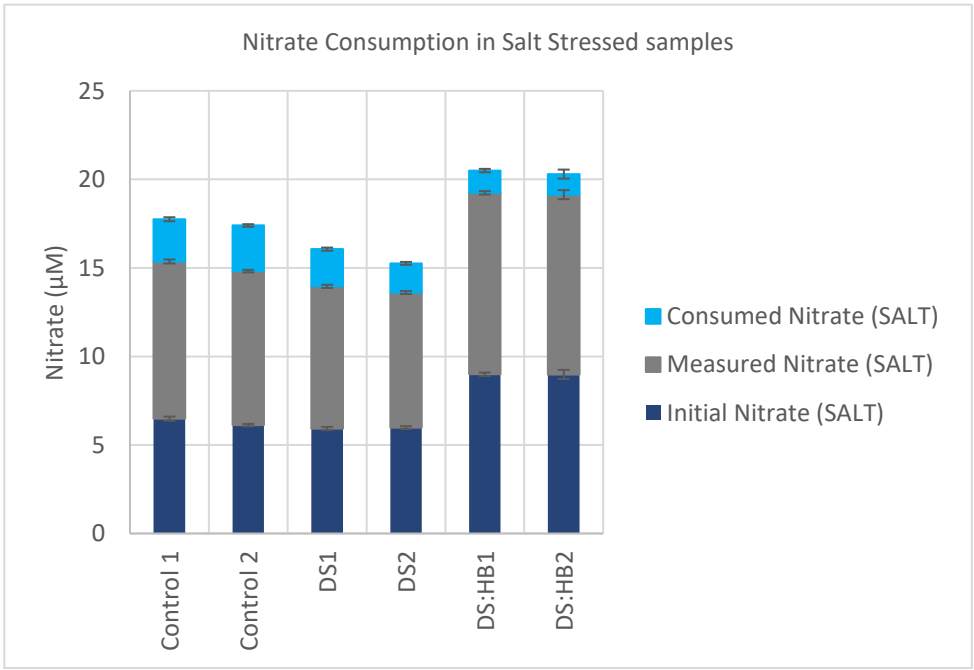

Graph 3.4.34: Nitrate consumption for all salt flasks. Average of three biological replicates plotted with the error bars, representing the standard error about the mean.

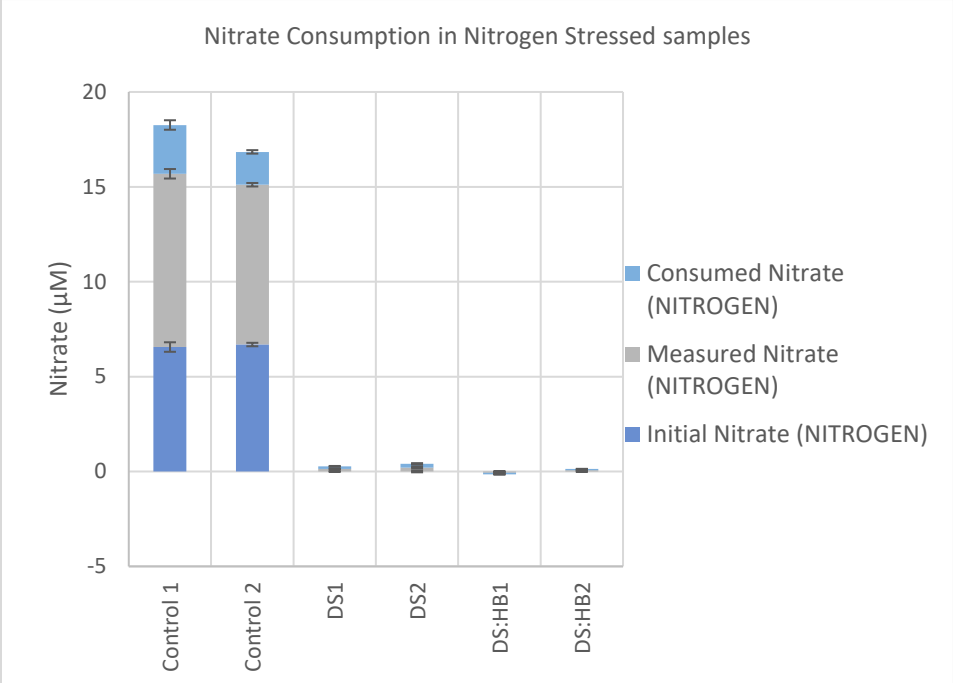

Graph 3.4.35: Nitrate consumption for all nitrogen flasks. Average of three biological replicates plotted with the error bars, representing the standard error about the mean.

The measured nitrate values after the experiments show higher values compared to the initial one for all non-nitrate stressed flasks. These levels are slightly higher in the co-culture flask. This can be attributed to the nitrate present in the supplement.

3.4.9. Morphological changes

3.4.9.1. Direct mixing: effect of Halomonas on D. salina

D. salina is an alga that is known to change shape during glycerol accumulation [22]. In the reported literature, the observations have been done on monocultures, when the cells have been subjected to stress.

Figure 3.4.1: *D. salina* monoculture and co-culture flasks with *Halomonas sp*. Flask pictures were taken every day inside the laminar flow hood using an iPhone. Cell pictures were taken with a microscope at 60X magnification.

Here, we observed the behaviour of *D. salina* monoculture and with *Halomonas* The pictures belong to the flasks in the Direct Mixing (section 3.3.2) experiment. Figure 3.4.1 shows how the *D. salina* monoculture (DS) and the *D. salina* co-cultures, DS:HALO and DS:HALO+, change in pigmentation over the experimental period. The visual changes tally in with the β-carotene and chlorophylls data from the results section (3.4.3 and 3.4.4).

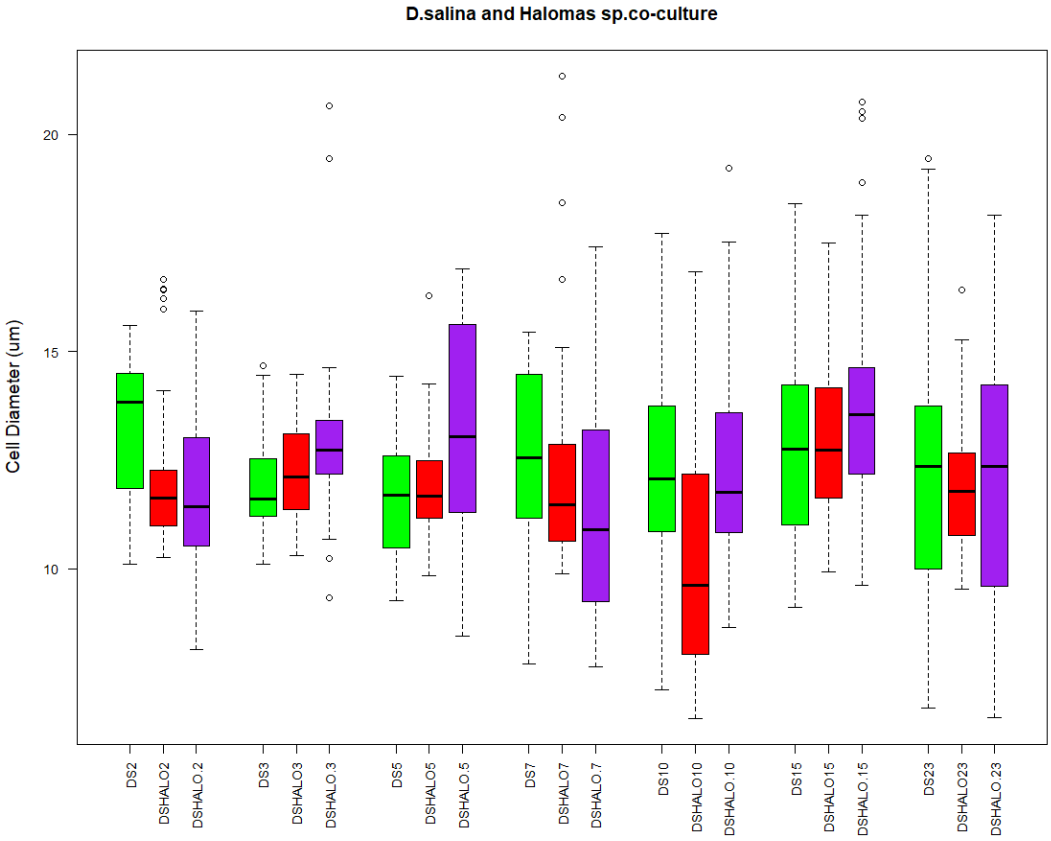

Graph 3.4.36: Box plot chart showing the size distributions of *D. salina* cells when in monoculture and co-culture with *Halomonas* cells over a period of 33 days. Labels: Flask and date, e.g. DS2 – *D. salina* on Day 2.

The boxplots presented in Graph 3.4.37 and 3.4.38 showed the variation in *D. salina* cells diameter when in co-culture, under non-stressed conditions. The medium cells size of 12-13 µm, represented by the thick horizontal line, did not show any significant variation. The exception for the *D. salina: Halomonas sp*. on day 10 (DSHALO10), with the majority of cells measuring 10 µm. The size of the plots and their elongations vary throughout the course of the experiments, indicating that the *D. salina* cell size varies with time. The upper and lower whiskers of the boxplots represent the sizes that are outside the normal distribution. These stretch over a large area, indicating that at a given time, various cell sizes are present within the flask. The outliers indicate that some cells measured up to 20µm.

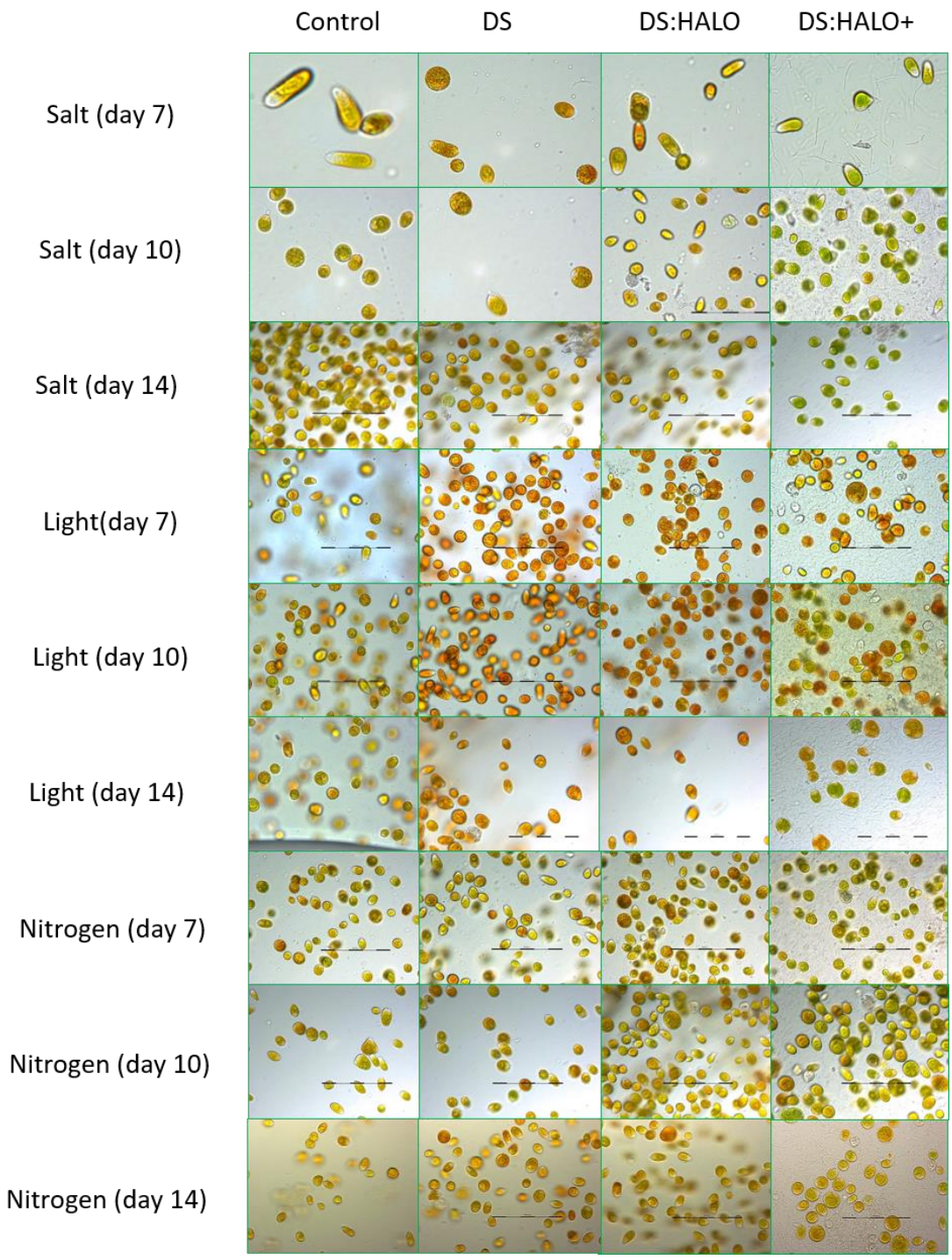

Figure 3.4.2: Microscope pictures (60X Olympus) of stressed *D. salina* and *Halomonas*. Control cells were not subjected to stress, the DS (*D. salina* only), DS:HALO (*D. salina*: *Halomonas)* and DS:HALO+ (same as DS:HALO plus bacterial supplement) were subjected to abiotic stress. The days indicate the day on which the *Halomonas* was inoculated into the microalgae cultures.

β-carotene accumulation is clearly visible in the *D. salina* monoculture (DS) as stark contrast to the co-culture cells in DS:HALO+.

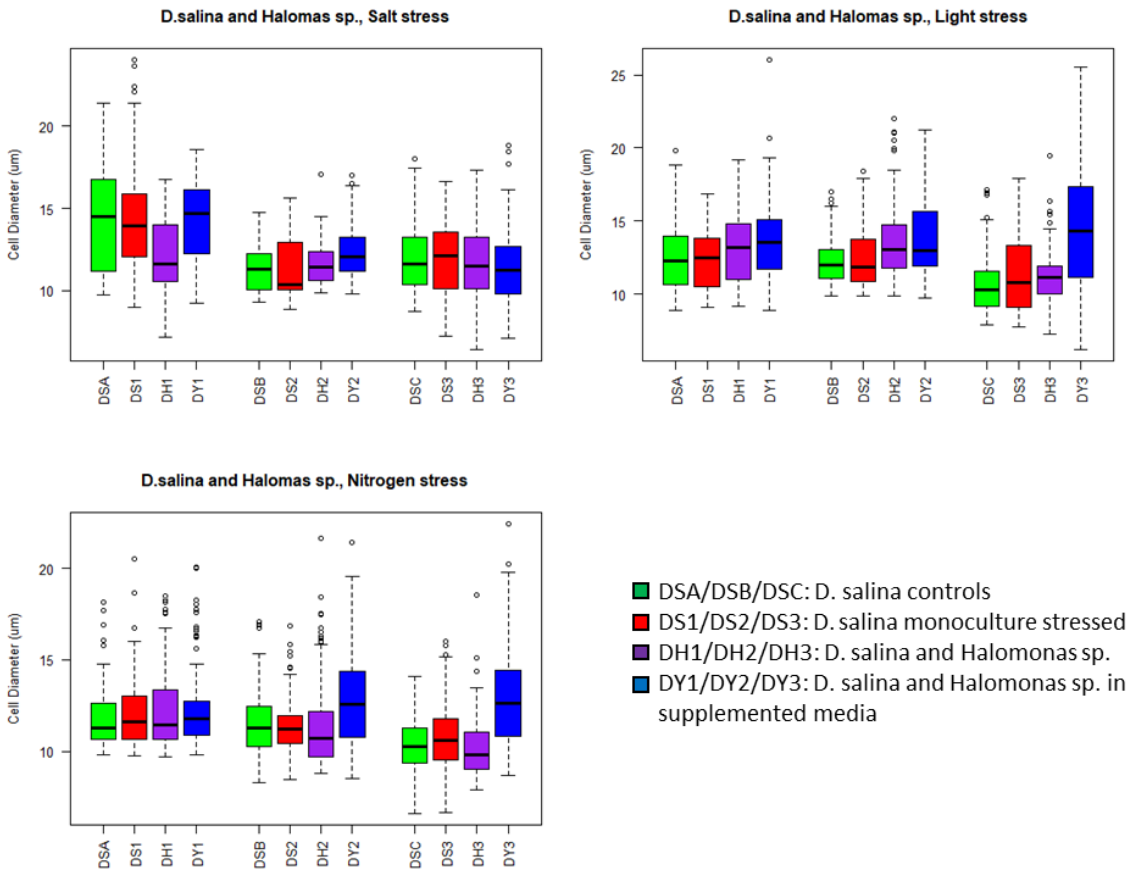

Graph 3.4.37: Boxplots depicting the effects of abiotic stresses on monoculture and co-cultures of *D. salina* and *Halomonas*. Labels: Flask and date, e.g. DS2 – *D. salina* on Day 2.

Similar to the data obtained in Graph 3.4.38, the boxplot in Graph 3.4.39 depicts the size distribution of *D. salina* cells in monoculture and co-cultures subjected to abiotic stress (section 3.3.4). The cells in association with *Halomonas* in supplements medium (DY show a trend of being large when subjected to light and nitrogen stress, 12-16 µm, with numerous outliers of 20 µm. This effect is seen in the cells, which are in association with *Halomonas sp*. and under stress. This implies that the presence of the bacteria may in fact contribute to the size of the algal cells during abiotic stress, however, the mechanisms behind this need to be elucidated.

3.4.9.2. Direct mixing: effect of H. salinarum on D. salina

The observations here cover the direct mixing experiments conducted on the *H. salinarum* and *D. salina* co-culture, which has been referred to as a consortium due to the presence of the *Halomonas* (section 3.3.3).

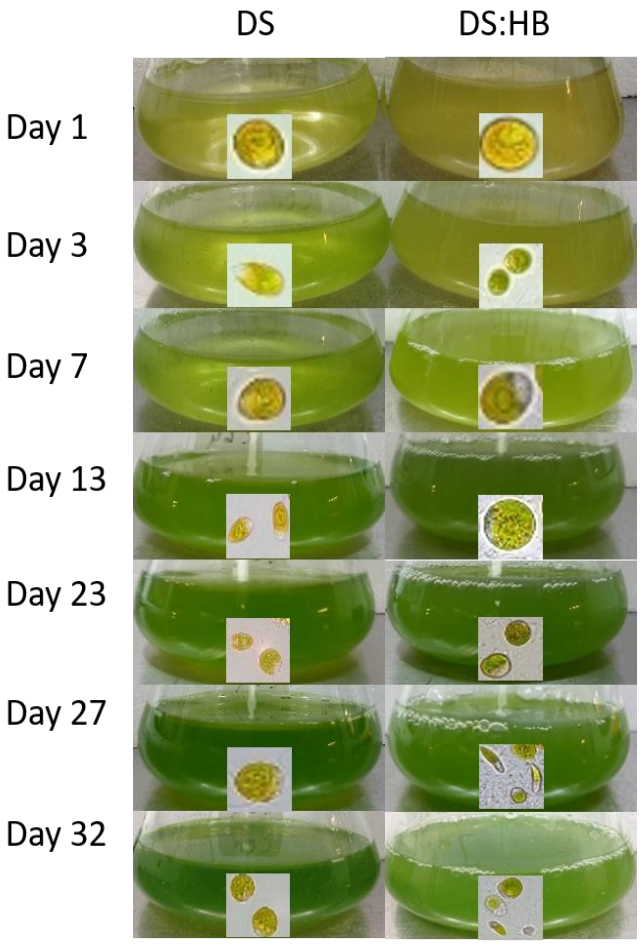

Figure 3.4.3: *D. salina* monoculture and co-culture flasks with *H. salinarum*. Flask pictures were taken every day inside the laminar flow hood using an iPhone. Cell pictures were taken with a microscope at 60X magnification.

Similarly to the *D. salina* and *Halomonas* co-culture, the consortium flasks show vivid shades of green between the 23rd and 27th day of growth. However, after the 27th day, the *D. salina* cells change their morphology from spherical to elongate. This sudden change in the shape of the microalgae is reflected in the pigmentation of the flask. It is a known fact that *D. salina* cells change in shape, however, this observation has only been seen when *H. salinarum* has been added to the microbial assemblage.

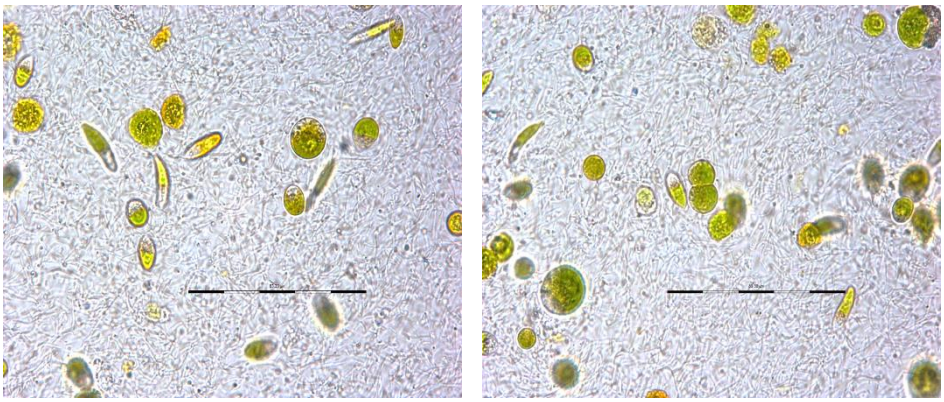

Figure 3.4.4: Drastic changes in *D. salina* morphology in the presence of *H. salinarum* and *Halomonas* (60x magnification).

The papers from Orellana et al. [40] indicated that *H. salinarum* had a role in the cell death of the microalgae. Perhaps, this sudden change experienced by some of the microalgae is an indication of this effect. This is clearly visible in Figure 3.4.4. The green microorganisms are the *D. salina* cells, whilst the hair-like strands are *Halomonas sp*. *H. salinarum* is not visible as a higher magnification is required

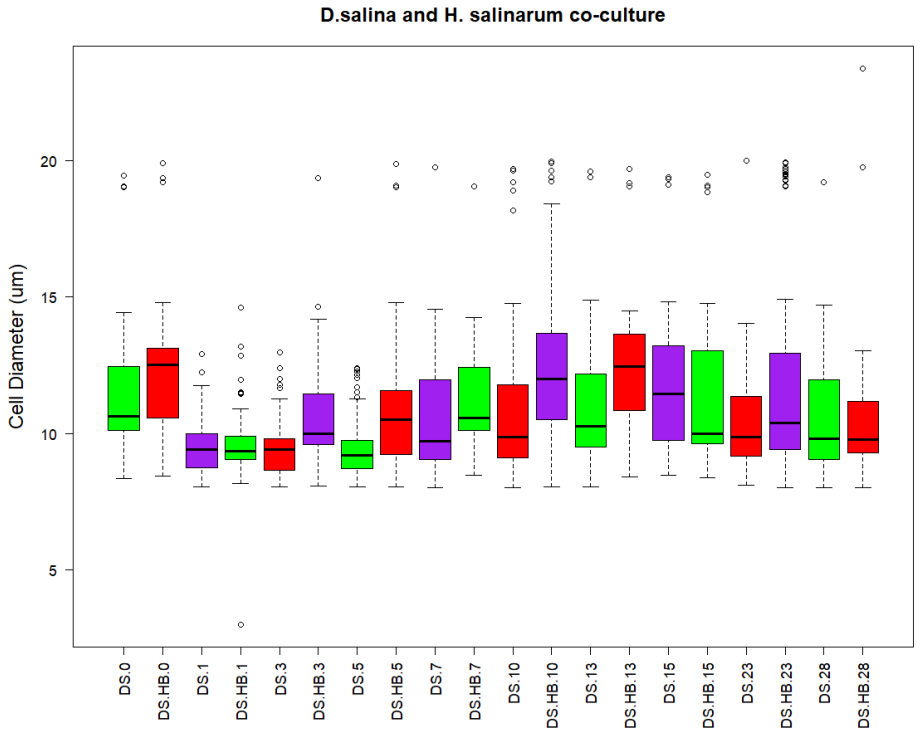

Graph 3.4.38: Box plot chart showing the size distributions of *D. salina* cells when in monoculture and co-culture with *H. salinarum.*

The box plots presented in Graph 3.4.39 show that when co-culture with *H. salinarum*, the cell size medium is 12µm. Less variation, when compared to 3.4.37 plots, is seen in the size distribution of the cells. The occurrence of outliers, diameters of 20µm, is more pronounced with time.

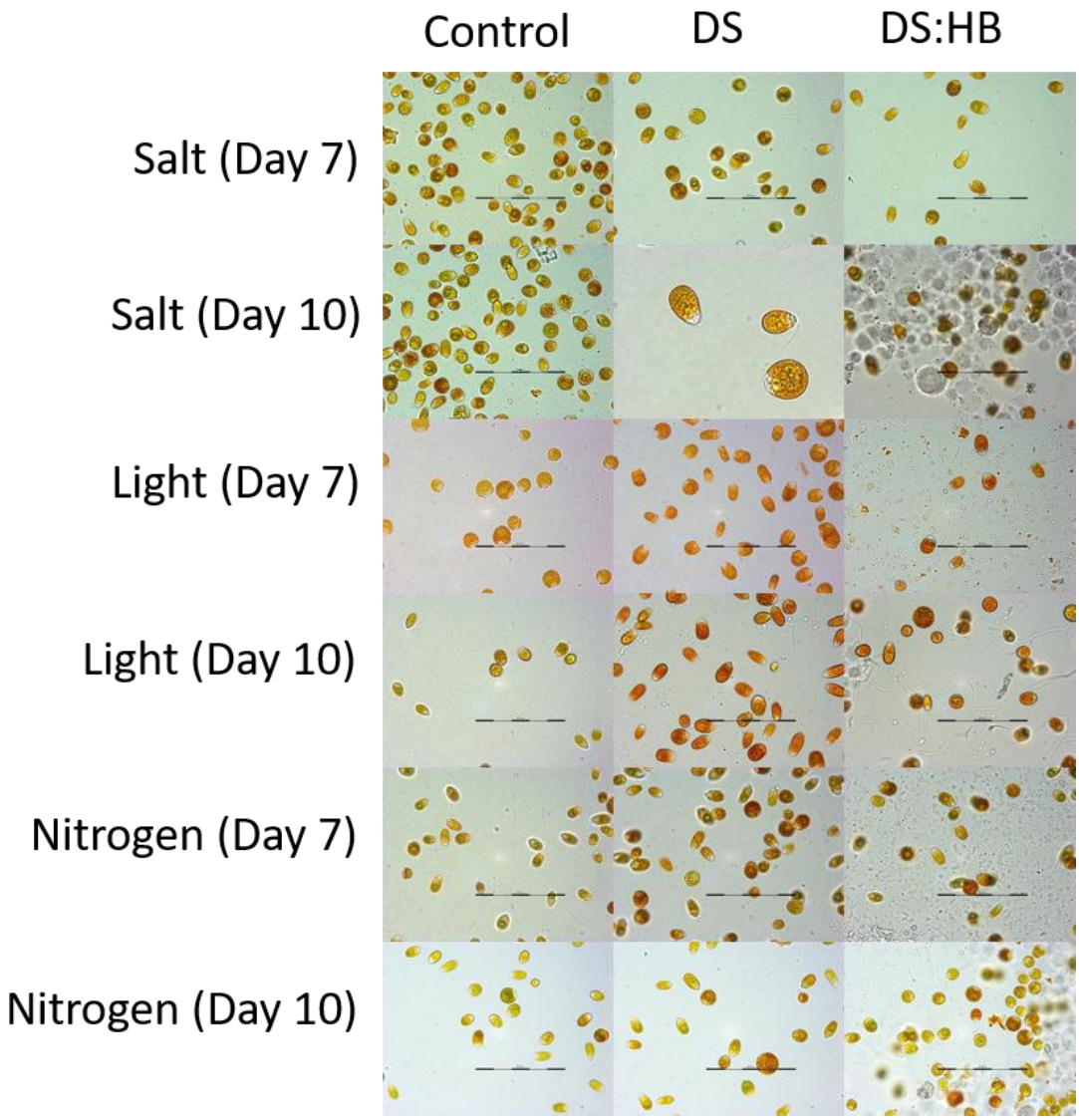

Figure 3.4.5: *D. salina* and *H. salinarum* cells from Control flasks, stressed monoculture and co-culture flasks.

β-carotene accumulation is clearly visible in the *D. salina* monoculture (DS. The DS:HB flask show traces of the carotenoid, showing that the presence of *H. salinarum* during abiotic stress does not protect the microalgae. This is the opposite too what was observed with *Halomonas*

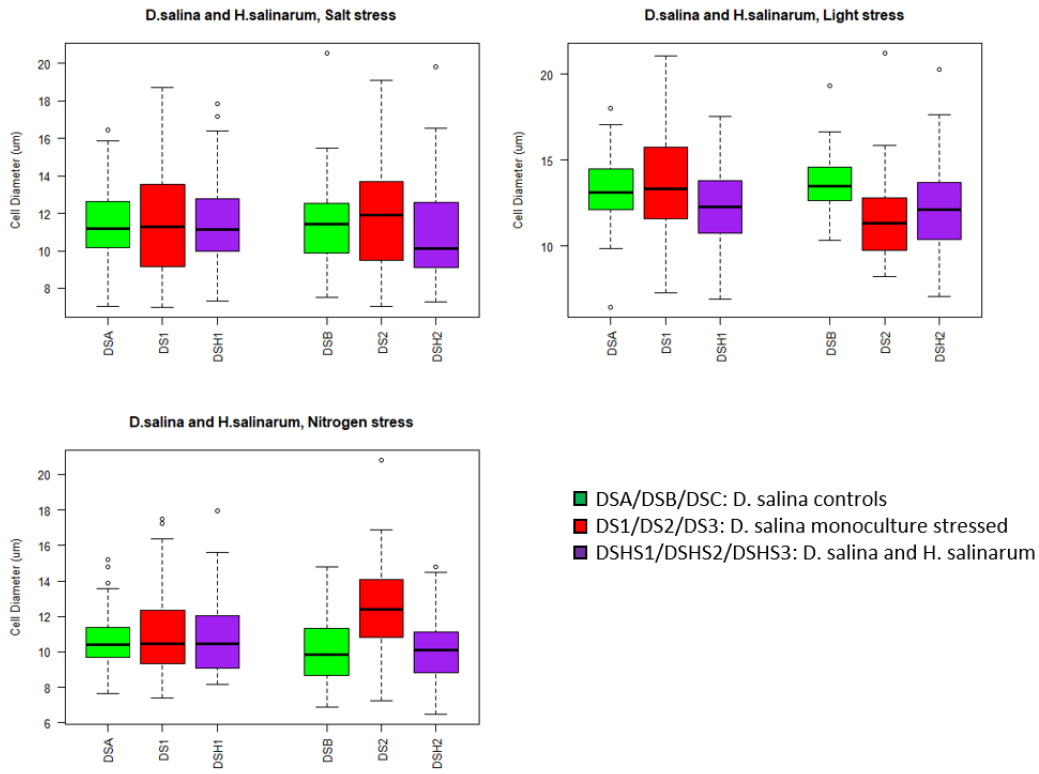

Graph 3.4.39: Box plot chart showing the size distributions of *D. salina* cells when in monoculture and co-culture with *H. salinarum* cells when subjected to abiotic stress.

The size of *D. salina* does not undergo any significant changes, whilst in the consortium. The size range shown is between 10-15µm, prevalently. The pigment characterisation, conducted in section 3.3.4, show that the nitrogen samples have more β-carotene. However, as mentioned, the bacteriorhodopsin in the *H. salinarum* cultures may be skewering the results. Visually, the light stressed cultures show higher amounts of β-carotene within the cells compared to the other conditions.

3.5. Discussion

The aim of this investigation was to discover whether the presence of *Halomonas* or *H. salinarum* would lead to an increase in *D. salina* biomass and β-carotene production.

The first part of the investigation involved choosing a communal medium where all three microorganisms could co-exist. With salinity being the common denominator affecting them all, various molarities of NaCl were tested. The results showed that 3 M was the best-suited salinity for the co-culture study.

The salinity test results for *D. salina* (Graph 3.4.1) showed that in the first seven days, the growth rate was highest in 1.5 M HEPES, with incremental salinity slowing the growth rate [28]. This was because *D. salina* cells accumulated glycerol to counteract osmotic shock, and β-carotene, as stores for excess CO_2 [62]. A closer look at the growth rates of *D. salina* cells showed the growth curve of the flasks grown at 1.5 M, 2 M and 2.5 M approaching a stationary phase at the end of the 20 days of cultivation. However, the 3 M and 3.5 M flasks, though with lower overall growth rates showed a trend of increasing growth rate. This was particularly true for the 3 M flasks. Furthermore, it was observed that at 1.5 M and 2 M, the cultures adhered to the bottom of the flask. As the health of the cells would affect the outcome of the co-culture, the lower salinity ranges were diregarded. The trade-off of *D. salina*'s slower growth, however, was compensated by slower growth rates of both *Halomonas* and *H. salinarum* cultures in 3 M NaCl medium, making it unlikely for the *D. salina* cells to be outnumbered.

The construction of an artificial co-culture, in this case, mimicking the natural environment required a communal growth environment allowing both populations to coexist at equilibrium. Based on the findings, a communal medium was developed, where 1g/L of yeast extract or 10% of the ATCC1863 Halophile medium was added to the 3 M HEPES algal medium to supplement the growth of *Halomonas* and *H. salinarum*, respectively.

The first set of experiments focused on assessing the effect of *Halomonas* on *D. salina* in terms of biomass and β-carotene productivity. *Halomonas* is ubiquitous in *D. salina* cultures and its presence was monitored in the monoculture flasks. The first part of the investigation involved testing if physical contact and/or segregation of the two species in co-culture would yield higher biomass yields, as the methods of co-culturing have

been shown to impact on the behaviour of microorganisms [63]. Three methods: direct mixing, bead entrapment and supernatant spiking were chosen to test the hypothesis.

Direct mixing of *Halomonas* and *D. salina* (Graph 3.4.6 – A) showed an initial boost in the growth of the cells which resulted in higher cell numbers. The number of *D. salina* cells at the end of the co-culture period, was approximately 301,800 cells/mL for the DS:HALO+ flasks. The DS:HALO flasks reached a total cell count of 215,400 cells/mL with the monoculture reaching a density of 167,805 cells/mL. The number of *D. salina* cells in the DS:HALO+ flasks increased by 79.9 % compared to the monoculture flasks, whilst the DS:HALO flasks shows a final cell count increment of 28.4 %. Thus, we can conclude that the presence of the bacterial cells, leads to an increase in *D. salina* cell numbers. Graph 3.4.6 (B) depicted the CFU/mL of *Halomonas* along the growth curve. The axenic monoculture of *D. salina* showed presence of *Halomonas* with time, however, these numbers are negligible compared to the concentrations found in both co-culture conditions. The *Halomonas* growth reached a plateau; indicating an equilibrium between algae and bacterium was established. The higher loading of *Halomonas* in the co-culture flasks suggested that at high concentrations, the bacterium released biomolecules that aided microalgae propagation [64].

The subsequent method involved trapping *Halomonas* in porous sodium alginate beads prior to co-culturing with *D. salina*. The cell numbers in the co-culture flasks again exceeded those in the monoculture flasks. Similar results were also obtained by growing the microalgae in bacterial exudate. Therefore, we can conclude that the presence of the *Halomonas* does indeed improve cell proliferation of *D. salina*.

Although all three methods showed an increase in *D. salina* cells, the direct mixing experiment, however, had a more pronounced effect on the growth of the microalgae. The results showed that when *D. salina* and *Halomonas* were in physical proximity, the algal cell were able to maintain a steadier higher growth rate compared to the control. Indeed, the direct mixing flasks outcompeted the control cultures by a factor of 1.8, compared to 1.6 and 1.4 times in the encapsulated bead and spiking experiments, respectively. It can be speculated that the biomolecules released by *Halomonas* (when grown on its own) may indeed contain a source of nutrients for the algae, or that the bacterial respiration is able to provide the necessary CO_2 for *D. salina* to use as carbon

source [65]. There is reason to believe that the partnership established between these two microorganisms is based on a trigger-response mechanism. That is to say, that *D. salina* and *Halomonas* react to each other when they can clearly detect their symbiotic partner.

Similar results were obtained when co-culturing *D. salina* with *H. salinarum* (Graph 3.5.1). The *D. salina* cells in co-culture were $2.6x10^5$ cells/mL compared to the $1.8x10^4$ cells/mL ($p<0.05$). Over the period of 28 days of co-culturing, the CFU data of both *H. salinarum* and *Halomonas* (Graph 3.4.25) showed that in the first 5 days a combined effect of the haloarchaea and the bacterium spur the microalgae's growth. However, after the 5^{th} to 7^{th} day, the *H. salinarum* cells withered, leaving only *Halomonas* Therefore, it was hard to conclude that the boost in microalgae growth was due to the presence of *H. salinarum* alone. However, when comparing the data from Graph 3.5.2, the effect of the *Halomonas* on the *D. salina* took 3-4 days, whereas with the presence of *H. salinarum*, changes in *D. salina* cell numbers are evident within 24 hours. Therefore, it was possible to assume that the addition of *H. salinarum* played a major role in the growth dynamics of the microalgae.

The β-carotene data presented in both direct mixing experiments (section 3.4.4 and 3.4.6) showed that the presence of *Halomonas* and *H. salinarum* did not improve β-carotene accumulation within the cells. However, the resulting increase in algal cells resulted in higher productivity of the β-carotene.

The chlorophyll content was found to be inversely proportional to carotenoid production [66]. This was because the cells enter a 'stressed' stage deviating energy from the photosynthetic pathway into the sustenance pathways. In the encapsulated bead experiment the ratio of chl a:b, showed that the majority of the chlorophylls within the cell was chl a. However, the values obtained are higher than the usual ratio of 3:1. This could be an effect of the beads on the way the microalgae assimilated the light. The beads may be an obstruction, diminishing the amount of light available. Thus, by increasing chlorophyll a, the cells are maximising light collecting capabilities. As in the direct mixing experiment, the amount of total chlorophylls in the cells with the beads, is almost double that of the monoculture cells. This indicates again that the cells with *Halomonas* present are producing more photosynthetic pigments. This could be due to

a stimulus received by the *D. salina* cells, in response to the presence of the bacterial metabolites [65].

The initial investigation showed that the presence of an aiding organism does increase the biomass output of *D. salina*. To further stress the co-culture and check its resilience to stress and maximise β-carotene levels, a two-stage experiment was carried out. The microorganisms were first grown in unison and were later subjected to osmotic shock, light stress and nitrogen deprivation. All these methods were proven to induce β-carotene in *D. salina* cells [16,21,24–27].

The results from abiotic stress experiment showed that *Halomonas* did indeed protect the microalgae cells (section 3.4.5). As seen in the literature microorganisms that are part of co-cultures or consortia are more resilient to stress [56]. The flasks of DS:HALO+ showed lower β-carotene levels and higher total chlorophylls compared to the DS flasks. Nevertheless, the higher biomass yields of *D. salina* in co-culture offset the lower carotenoids accumulation (Graph 3.4.15 -3.4.17). This confirmed the hypothesis that the bacterium supplemented microalgae growth [48,65].

Subjecting the co-culture to salt stress yielded a higher productivity of β-carotene (1.12 µg/mL/day), almost twice the highest productivity of β-carotene production (0.61 µg/mL/day) for the monoculture flasks subjected to salt stress. Nitrogen stress productivity (0.33 µg/mL/day) and light stress productivity (0.21 µg/mL/day) were lower than the higher monoculture value, but higher than the respective monoculture flasks. When looking at intracellular accumulation, the values were between those published (Table 3.1.2).

The consortia of *D. salina, Halomonas and H. salinarum* resulted in a 52% increase in microalgae biomass (cells/mL) compared to the monoculture flask (Graph 3.4.24). The consortia was subsequently subjected to abiotic stress. The stress experiment showed that when subjected to osmotic shock (Graph 3.4.27), the co-culture, after 1 hour of acclimatisation, yielded $2.7x10^5$ cells/mL compared to the stress monoculture of $2x10^5$ cells/mL. However, the cells that were acclimatised for 3 days showed higher microalgae cell numbers to start off, but decreased at the end of the culturing period. Thus, the presence of *H. salinarum* may hinder *D. salina* when subjected to osmotic shock. As mentioned at the beginning of this chapter, *H. salinarum* was acclimatised to grow in 3

M medium. Furthermore, the lifespan of the bacterium from ATCC 1863 medium to HEPES 1983 decreased by a week's time. In contrast, light stress (Graph 3.4.28) does not perturb neither the algae nor the haloarchaea/bacteria that are present within the growth flask, as the number of algae cells increases to reach $5.2x10^5$ cells/mL compared to $4.4x10^5$ cells/mL in the stress monoculture flask (DS).

The nitrogen stress experiment (Graph 3.4.29) showed that over a period of 72 hours the yield of microalgae in the control flasks ($4x10^5$ cells/mL) was higher than both stressed flasks (DS and DS:HB). The microalgae in the DS:HB flaks later reach similar values of 4 $x10^5$ cells/mL. The loading of the haloarchaea and bacteria measured provides an indication on how these microorganisms behaved when subjected to each stress (Graph 3.4.30). The results indicated that under nitrate stress, *H. salinarum* and *Halomonas* decreased considerably, compared to other conditions. It is possible to infer that nitrogen is necessary for the welfare of *H. salinarum* and *Halomonas.* Furthermore as for the osmotic shock experiment, the findings suggested that when *H. salinarum* was affected by the stress, the entire consortia reported damage.

Chlorophyll analysis for both co-culture set-ups showed variation of chl a:b ratio in relation to β-carotene. As expected for most flasks, the ratio of chl a to b is almost three times. However, in the case of salt stress, some of the flasks show an almost 1:1 ratio. As expected, monoculture stressed cells show higher amounts of β-carotene, when compared to the co-culture cells. These findings tallied in with the visible changes seen in the microalgae cells when observed under the microscope (Figure 3.4.1 and 3.4.3).

As for the *Halomonas* and *D. salina* co-culture, extracellular glycerol released by the microalgae may be a source of carbon for the *H. salinarum*. The control flasks in Graph 3.4.33 show that *D. salina* released glycerol into the medium in non-stressed settings. The stressed monoculture flasks (DS) secreted glycerol into the growth medium, with amounts similar to the Control flasks. The salt stressed flasks showed that some of the available glycerol had been consumed, whilst the glycerol levels within the nitrogen stressed flasks was completely depleted. The lack of nitrogen spurred the haloarchaea and bacteria to consume the available glycerol [41,47,48].

The morphological investigation of *D. salina* cells provided a visual representation of how *Halomonas* and *H. salinarum* interacted with *D. salina*. The *D. salina* cell sizes

reported in Graph 3.4.37, 10-15 µm, coincided with reported values [1,4,15,17]. It is clear from the data that size distribution of *D. salina* cells changes regardless to them being in co-culture. Approaching the last day of the experiment, an array of sizes were measured: with older cells probably being the larger outliers and younger cells taking up the lower quartile measurements [22]. Furthermore, as shown in Figure 3.4.2 and 3.4.4, during abiotic stress the presence of *Halomonas* only aided *D. salina* (cells are greener) whilst when in consortium with *H. salinarum*, this effect was minimised (more orange-red cells).

3.6. Conclusions

The co-culture investigation carried out in this chapter demonstrated that by adding *Halomonas* with *D. salina* at a ratio of 1:1, an increase in the algal growth rate is observed. The same effect was experienced in consortium with *H. salinarum*, however, the effects were more pronounced in the bacterium only set-up. The presence of both bacterium and haloarchaon hindered the accumulation of intracellular β-carotene in the *D. salina* cells, however, the increase in biomass led to an increase in productivity. This finding suggested that the aiding microorganisms allowed the microalgae cells to withstand nutrient limitations that may arise over prolonged periods of growth. This was not the case when the co-culture was subjected to osmotic shock, light and nitrate stress. The adaptability of *Halomonas sp*. to the sudden changes did not interfere with its ability to aid the microalgae during abiotic stresses. However, when in consortium with *H. salinarum*, the effects of the *Halomonas* on the microalgae were hindered. The co-culture with *Halomonas* showed significant increase in β-carotene productivity when the co-culture was subjected to both light and salt stress ($p<0.05$, whereas there were no significant differences in the association with *H. salinarum*.

Biomolecules released by *Halomonas* may indeed contain a source of nutrients for the algae, or that the bacterial respiration is able to provide the necessary CO_2 for *D. salina* to use as carbon source [39,51,65]. There is reason to believe that the partnership established between these two microorganisms is based on a trigger-response mechanism. That is to say, that *D. salina* and *Halomonas* react to each other when they can clearly detect their symbiotic partner.

Results from the analysis of extracellular polymeric substances (EPS and detection quorum sensing are provided in Chapter 5. These results may aid in better understanding the relationship between *D. salina* and *Halomonas*

3.7. References

[1] Brock TD. Ecology of Saline Lakes. In: Shilo M, editor. Strateg. Microb. Life Extrem. Environ. Weinheim-New York: Verlag Chemie; 1979. p. 22–47.

[2] Rodriguez-Valera F, Ventosa A, Juez G, et al. ECOLOGY Variation of Environmental Features and Microbial Populations. Microb. Ecol. 1985;11:107–115.

[3] Grant WD. Life at low water activity. Philos. Trans. R. Soc. Lond. B. Biol. Sci. 2004;359:1249-1266; discussion 1266-1267.

[4] Brock TD. Salinity and the Ecology of Dunaliella from Great Salt Lake. J. Gen. Microbiol. 1975;89:285–292.

[5] Oren A. Halophilic Microorganisms and their Environment. 5th ed. Dordrecht/Boston/London: Kluwer Academic Publishers; 2002.

[6] Bardavid RE, Khristo P, Oren A. Interrelationships between Dunaliella and halophilic prokaryotes in saltern crystallizer ponds. Extremophiles. 2008;12:5–14.

[7] Oren A. Diversity of halophilic microorganisms: environments, phylogeny, physiology, and applications. J. Ind. Microbiol. Biotechnol. 2002;28:56–63.

[8] Ventosa A. Unusual micro-organisms from unusual habitats : hypersaline environments. In: Logan NA, Lappin-Scott HM, Oyston PCF, editors. SGM Symp. 66 Prokaryotic Divers. - Mech. significance. Cambridge University Press; 2006. p. 223–255.

[9] Ghasemi MF, Shodjai-Arani A, Moazami N. Optimization of bacteriorhodopsin production by Halobacterium salinarium PTCC 1685. Process Biochem. 2008;43:1077–1082.

[10] Oren A. The dying Dead Sea: The microbiology of an increasingly extreme environment. Lakes Reserv. Res. Manag. 2010;15:215–222.

[11] Oren A, Stambler N, Dubinsky Z. On t h e red c o l o r a t i o n of saltern c r y s t a l l i z e r p o n d s. Int. J. Salt Lake Res. 1992;1:77–89.

[12] Katz A, Kaback HR, Avron M. Na + / H + antiport in isolated plasma membrane vesicles from the halotolerant alga Durtaliella salzkza. FEBS Lett. 1986;202:141–144.

[13] Katz A, Pick U. Plasma membrane electron transport couple to Na(+) extrusion in the halotolerant algal Dunaliella. Biochim. Biophys. Acta (BBA-Bioenergetics}. 2001;1504:423–431.

[14] Borowitzka LJ, Borowitzka MA, Moulton TP. The mass culture of Dunaliella salina for fine chemicals : From laboratory to pilot plant. Hydrobiologia. 1984;116–117:115–121.

[15] Chen H, Jiang JG. Osmotic responses of Dunaliella to the changes of salinity. J. Cell. Physiol. 2009;219:251–258.

[16] Borowitzka MA, Borowitzka LJ, Kessly D. Effects of salinity increase on carotenoid accumulation in the green alga Dunaliella salina. J. Appl. Phycol. 1990;2:111–119.

[17] Oren A. A hundred years of Dunaliella research: 1905-2005. Saline Systems. 2005;1:2.
[18] Dufossé L, Galaup P, Yaron A, et al. Microorganisms and microalgae as sources of pigments for food use: A scientific oddity or an industrial reality? Trends Food Sci. Technol. 2005;16:389–406.
[19] Gómez PI, Barriga A, Cifuentes AS, et al. Effect of salinity on the quantity and quality of carotenoids accumulated by Dunaliella salina (strain CONC-007) and Dunaliella bardawil (strain ATCC 30861) Chlorophyta. Bio Res. 2003;185–192.
[20] Hadi MR, Shariati M, Afsharzadeh S. Microalgal Biotechnology: Carotenoid and Glycerol Production by the Green Algae Dunaliella Isolated from the Gave-Khooni Salt Marsh, Iran. Biotechnol. Bioprocess Eng. 2008;13:540–544.
[21] Phadwal K, Singh P. Effect of nutrient depletion on β-carotene and glycerol accumulation in two strains of Dunaliella sp. Bioresour. Technol. 2003;90:55–58.
[22] Ben-Amotz A, Polle JE., Subba Rao DV. The Alga Dunaliella. 2009.
[23] Lamers PP, Van De Laak CCW, Kaasenbrood PS, et al. Carotenoid and fatty acid metabolism in light-stressed Dunaliella salina. Biotechnol. Bioeng. 2010;106:638–648.
[24] García-González M, Moreno J, Manzano JC, et al. Production of Dunaliella salina biomass rich in 9-cis-beta-carotene and lutein in a closed tubular photobioreactor. J. Biotechnol. 2005;115:81–90.
[25] Phadwal K, Singh PK. Isolation and characterization of an indigenous isolate of Dunaliella sp. for beta-carotene and glycerol production from a hypersaline lake in India. J. Basic Microbiol. 2003;43:423–429.
[26] Pisal D., Lele S. Carotenoid production from microalga, Dunaliella salina. Indian J Biotechnol. 2005;4:476–483.
[27] Gomez PI, Gonzalez MA. The effect of temperature and irradiance on the growth and carotenogenic capacity of seven strains of Dunaliella salina (Chlorophyta) cultivated under laboratory conditions. Biol Res. 2005;38:151–162.
[28] Rad FA, Aksoz N, Hejazi MA. Effect of salinity on cell growth and β -carotene production in Dunaliella sp . isolates from Urmia Lake in northwest of Iran. African J. Biotechnol. 2011;10:2282–2289.
[29] Sathasivam R, Kermanee P, Roytrakul S, et al. Isolation and molecular id entification of β -carotene producing strains of Dunaliella salina and Dunaliella bardawil from salt soil samples by using species- specific primers and internal transcribed spacer (ITS) primers. African J. Biotechnol. 2012;11:16677–16687.
[30] Mojaat M, Pruvost J, Foucault a., et al. Effect of organic carbon sources and Fe2+ ions on growth and β-carotene accumulation by Dunaliella salina. Biochem. Eng. J. 2008;39:177–184.
[31] Sironval C. Chlorophyll metabolism and t h e l e a f c o n t e n t in s o m e other tetrapyrrole p i g m e n t s. Photochem. Photobiol. 1963;2:207–221.
[32] Chen H, Lao YM, Jiang JG. Effects of salinities on the gene expression of a (NAD+)-dependent glycerol-3-phosphate dehydrogenase in Dunaliella salina. Sci. Total Environ. 2011;409:1291–1297.
[33] Ben-Amotz a, Grunwald T. Osmoregulation in the Halotolerant Alga Asteromonas gracilis. Plant Physiol. 1981;67:613–616.
[34] Radakovits R, Jinkerson RE, Darzins A, et al. Genetic Engineering of Algae for Enhanced Biofuel Production. Eukaryot. Cell. 2010;9:486–501.

[35] Chen H, Jiang JG, Wu GH. Effects of Salinity Changes on the Growth of Dunaliella salina and Its Isozyme Activities of Glycerol-3-phosphate Dehydrogenase. J. Agric. Food Chem. 2009;57:6178–6182.
[36] Ventosa A, Nieto JJ, Oren A. Biology of moderately halophilic aerobic bacteria. Microbiol. Mol. Biol. Rev. 1998;62:504–544.
[37] Vreeland RH, Anderson R, Murray RG. Cell wall and phospholipid composition and their contribution to salt tolerance of *Halomonas elongata*. J. Bacteriol. 1984;160:879–883.
[38] Peyton BM, Mormile MR, Petersen JN. Nitrate Reduction with Halomonas campisalis: Kinetics of Denitrification at pH 9 and 12.5% NaCl. Water Res. 2001;35:4237–4242.
[39] Croft MT, Lawrence AD, Raux-Deery E, et al. Algae acquire vitamin B12 through a symbiotic relationship with bacteria. Nature. 2005;438:90–93.
[40] Orellana M V, Pang WL, Durand PM, et al. A role for programmed cell death in the microbial loop. PLoS One. 2013;8:e62595.
[41] Falb M, Müller K, Königsmaier L, et al. Metabolism of halophilic archaea. Extremophiles. 2008;12:177–196.
[42] Keshtacher-Liebson E, Hadar Y, Chen Y. Oligotrophic bacteria enhance algal growth under iron-deficient conditions. Appl. Environ. Microbiol. 1995;61:2439–2441.
[43] Baggesen C. A study of microalgal symbiotic communities with the aim to increase biomass and biodiesel production. PhD Thesis. 2014.
[44] Dong H, Jiao L, Qiang H, et al. Interspecific competition and allelopathic interaction between Karenia mikimotoi and Dunaliella salina in laboratory culture. Chinese J. Oceanol. Limnol. 2016;34:301–313.
[45] Wang Y, Zhang C-H, Wang S, et al. Accumulation and transformation of different arsenic species in nonaxenic Dunaliella salina. Huan Jing Ke Xue. 2013;34:4257–4265.
[46] Keerthi S, Koduru UD, Nittala SS, et al. The heterotrophic eubacterial and archaeal co-inhabitants of the halophilic Dunaliella salina in solar salterns fed by Bay of Bengal along south eastern coast of India. Saudi J. Biol. Sci. 2015;
[47] Hard BC, Gilmour DJ. A mutant of Dunaliella parva CCAP 19/9 leaking large amounts of glycerol into the medium. J. Appl. Phycol. 1991;367–372.
[48] Oren A. Availability, uptake and turnover of glycerol in hypersaline environments. FEMS Microbiol. Ecol. 1993;12:15–23.
[49] Dashti Y, Grkovic T, Abdelmohsen UR, et al. Production of induced secondary metabolites by a co-culture of sponge-associated actinomycetes, Actinokineospora sp. EG49 and Nocardiopsis sp. RV163. Mar. Drugs. 2014;12:3046–3059.
[50] Bertrand S, Azzollini A, Schumpp O, et al. Multi-well fungal co-culture for de novo metabolite-induction in time-series studies based on untargeted metabolomics. Mol. Biosyst. 2014;10:2289–2298.
[51] Kazamia E, Czesnick H, Nguyen TT Van, et al. Mutualistic interactions between vitamin B12 -dependent algae and heterotrophic bacteria exhibit regulation. Environ. Microbiol. 2012;14:1466–1476.
[52] Kumudha A, Sarada R. Characterization of vitamin B12 in Dunaliella salina. J. Food Sci. Technol. 2016;53:888–894.

[53] Grant MAA, Kazamia E, Cicuta P, et al. Direct exchange of vitamin B12 is demonstrated by modelling the growth dynamics of algal–bacterial cocultures. ISME J. 2014;1–10.
[54] Kitcha S, Cheirsilp B. Enhanced lipid production by co-cultivation and co-encapsulation of oleaginous yeast Trichosporonoides spathulata with microalgae in alginate gel beads. Appl. Biochem. Biotechnol. 2014;173:522–534.
[55] de-Bashan LE, Hernandez J-P, Morey T, et al. Microalgae growth-promoting bacteria as “helpers” for microalgae: a novel approach for removing ammonium and phosphorus from municipal wastewater. Water Res. 2004;38:466–474.
[56] Natrah FMI, Bossier P, Sorgeloos P, et al. Significance of microalgal-bacterial interactions for aquaculture. Rev. Aquac. 2014;6:48–61.
[57] Stacy AR, Diggle SP, Whiteley M. Rules of engagement: defining bacterial communication. Curr. Opin. Microbiol. 2012;15:155–161.
[58] Fu W, Guomundsson ??lafur, Paglia G, et al. Enhancement of carotenoid biosynthesis in the green microalga Dunaliella salina with light-emitting diodes and adaptive laboratory evolution. Appl. Microbiol. Biotechnol. 2013;97:2395–2403.
[59] Lamers P, van de Laak CCW, Kaasenbrood PS, et al. Carotenoid and fatty acid metabolism in light-stressed Dunaliella salina. Biotechnol. Bioeng. 2010;106:638–648.
[60] Brenner K, You L, Arnold FH. Engineering microbial consortia: a new frontier in synthetic biology. Trends Biotechnol. 2008;26:483–489.
[61] Williams P. Quorum sensing, communication and cross-kingdom signalling in the bacterial world. Microbiology. 2007;153:3923–3938.
[62] Arun N, Singh D. Differential response of Dunaliella salina and Dunaliella tertiolecta isolated from brines of Sambhar Salt Lake of Rajasthan (India) to salinities: A study on growth, pigment and glycerol synthesis. J. Mar. Biol. Assoc. India. 2013;55:65–70.
[63] Goers L, Freemont P, Polizzi KM. Co-culture systems and technologies: taking synthetic biology to the next level. J. R. Soc. Interface. 2014;11:20140065–20140065.
[64] Natrah FMI, Bossier P, Sorgeloos P, et al. Significance of microalgal- bacterial interactions for aquaculture. Rev. Aquac. 2014;6:48–61.
[65] Croft MT, Warren MJ, Smith AG. Algae need their vitamins. Eukaryot. Cell. 2006;5:1175–1183.
[66] Capa-Robles W, Paniagua-Michel J, Soto JO. The biosynthesis and accumulation of β-carotene in Dunaliella salina proceed via the glyceraldehyde 3-phosphate/pyruvate pathway. Nat. Prod. Res. 2009;23:1021–1028.

Chapter 4: Co-cultures for enhanced lipid production

4.1. Introduction

Alternative and renewable energy sources are being sought to replace the depleting reserves of fossil fuels [1,2] to curb the alarming increase of greenhouse gases (GHGs) in the atmosphere [3]. This has been the priority of many countries, with new legislations enforced. In 1992 the United Nations Framework Convention on Climate Change (UNFCCC) established the Kyoto Protocol [4], a global agreement whereby 192 member states agreed to reduce their emission targets. It was agreed that carbon dioxide (CO_2), methane (CH_4), nitrous oxide (N_2O), hydrofluorocarbons (HFCs), perfluorocarbons (PFCs), and sulphur hexafluoride (SF_6) were the six gases to be curbed, if global warming was to be delayed. In a similar fashion, individual countries have outlined their own emission policies, such as the Climate Change Act 2008 [5]. This act stipulated that the United Kingdom (UK) had to ensure that the net carbon output for the six Kyoto GHGs for the year 2050, are lowered by 80 % compared to the levels in 1990.

The main challenge consisted of meeting the rising population's energy demands whilst complying to stringent emissions directives [6]. Plus, the alternative energy had to be suitable for the existing fuel distribution infrastructure [7,8]. Atmospheric carbon dioxide (CO_2) capture, storage and utilisation are essential in the achievement of environmental sustainability [9]. Therefore, new production routes needed to be carbon neutral or, preferably, carbon negative [10]. Advances in engineered CO_2 abatement and storage solutions, include processes such as physicochemical adsorption and injection into ocean/geological depth, which though successful have the inherent danger of harming the environment [9].

Biological fixation, involving CO_2 capture and utilization from higher plants and microbes were later seen as better alternatives [11–13]. The biomass generated in the process can be processed as fuel feedstocks, yielding not only lipids for biodiesel production, but carbohydrates, pigments and other biomolecules of interest to the medical, pharmaceutical and food industry. Liquid fuels such as biodiesel and bioethanol are of

great interest to industry, due to their ease of incorporation into the current energy infrastructure. Bioethanol and biodiesel are prevalently produced using first and second generation feedstocks; agricultural crops and lignocellulosic biomass, respectively [1,10,14,15]. However, first generation feedstocks posed a dilemma regarding their use as food or fuel sources whilst second generation required large areas of arable land. Fuel generation relies mainly on gasification, pyrolysis and torrefaction; *i.e.* methods that generate GHG's [16]. Thus, a third generation of feedstock, microalgal crops were introduced. Despite the fact that microalgae feedstock posed a feasible solution to overcome these challenges, there are still some drawbacks.

Table 4.1.1 compares the energy feedstock potentials of each feedstock generation, highlighting the higher energy yield per hectare of algal crops. Higher energy yield correlate with high photosynthetic efficiency of microalgae when compared to terrestrial plants. Studies have shown that from an average of 200-300W/m^2 of incoming solar energy, only 1W/m^2 is photosynthetically converted by switchgrass, reputed to be the quickest growing terrestrial plant; whereas, microalgae have the potential of achieving 10% conversion rates [17–19].

Table 4.1.1: Comparison of feedstocks for potential energy generation (adapted from Stephenson et al., [3])

Biofuel Generation	**First (agricultural crops)**	**Second (lignocellulosic)**	**Third (algae)**
Primary	Bioethanol Biodiesel	Bioethanol Solid fuel Hydrogen gas	Biodiesel Hydrogen gas
Secondary	Biomethane Distillers grain Animal feed	Biomethane Wood Fuel	Biodiesel, Bioethanol, Bio-oil, Biomethane High value products Animal Feed
Species Used	Maize/ Corn Oil Palm Sugarcane	Poplar Miscanthus Switchgrass	*Dunaliella sp.* *Nannochloropsis sp.* *Botryococcus sp.* *Chlorella sp.*
Product cost (US $/L) (potential)	0.40-0.50	0.55-0.70	0.50-1.00
Potential Fuel Yield (L/ha/y)	200-7,500	5,000-12,000	50,000-120,000
Land Requirements	Fertile land	Marginal land	Non-arable land
Other Requirements	Freshwater, Fertilisers Sunlight/ Irradiance CO_2 source	Freshwater, Fertilisers Sunlight/ Irradiance CO_2 source Extensive processing	Sunlight/ Irradiance CO_2 source Water source (species variable)

A question that springs to the mind, whilst looking at the data above, is why are we not using microalgae derived biofuels to power our transportation infrastructure? The answer is simply because of the high costs associated with the production process. Thus in order to offset this, researchers have proposed to treat microalgae feedstocks like petroleum and to apply the biorefinery concept where multiple products are extracted from the same crude material [20].

The use of microalgal based co-cultures or consortia has been deemed suitable for such purpose. The benefits of having a consortium, opposed to a monoculture, are increase in biomass yield, resistance to commination and a self-sustaining assemblage would decrease costs associated with nutrients because of the advantage of using co-cultures in bioremediumtion for biomass generation [21]. The challenges is in creating such a system that would also improve lipid profiles, as explored in the work detailed in the Experimental Design section.

4.1.1. Microalgae for biofuels

Originally biofuels were derived from crops destined for food use, such as wheat, barley, maize and sugarcane [22]. Fuel deriving from edible feedstocks was later termed first generation biofuels. Therefore, lignocellulosic biomass, also known as second-generation fuels was used. This biomass consisted of by-products from cereal straw, sugarcane and forest residues, certain organic solid wastes and dedicated feedstock such as grasses and short rotation forests [23]. Lignocellulosic biomass is cheaper than first generation crops and grown on non-arable land. However, the large amounts of water and fertilisers required for their growth to meet biofuel demand off-sets the carbon balance [24], making the switch to second-generation biofuels questionable. To surmount the bottlenecks of arable land and fertiliser requirements, research has to pursue alternative methods for the production of biofuels. Biological microorganisms such as oleaginous microalgae, bacteria and yeasts have been highlighted as potential candidates for biofuel production [25].

Microalgal lipids are suitable for biodiesel production and for direct incorporation into the energy infrastructure [26]. Their cultivation does not require arable land and large

amounts of fertilisers [27]. Additionally microalgae have been used for bioremediumtion due to their ability to acquire nutrients from wastewater streams [28,29]. The diversity and adaptability of these organisms allows for cultivation in salty, fresh and brackish waters. Wijffels and Barbosa [30] have highlighted that for 1L of microalgal biofuel, only 1.5 L of water is required (assuming 50 % dry wt of the algae biomass is lipids), instead of the 10,000 L of water used for the cultivation of land crops for the same end use. The use of herbicides and pesticides is not required for the growth of microalgae, reducing the impact on the environment and on net GHGs emissions [31]. Furthermore, microalgae can be considered perennial crops with biomass yields increasing and decreasing depending on the availability of sunlight and nutrients [32]. The added benefit of carbon sequestration from microalgae makes their use as biofuel feedstocks even more desirable.

4.1.2. Biodiesel

Microalgae offer a better alternative to conventional fossil fuels in terms of environmental sustainability, due to their non-toxic nature and biodegradability. Furthermore, microalgal biofuels when combusted produce less particulate emissions, carbon monoxide and soot [33]. With a few modifications to engines, microalgal biodiesel can be incorporated into the current energy infrastructure. Microalgae can be used as feedstock for the generation of multiple fuels, such as bioethanol, syngas, biodiesel and others as discussed by Suali and Sarbatly [34].

Some fuels are generated from the transesterification of lipids, as in the case for biodiesel, or treatment of the biomass. Others are fermented into bioethanol, adiabatic digestion for biogas [15,27,35] or photo-biologically produced hydrogen [26]. The conversion of the oils extracted from microalgae into biodiesel when compared to other feedstocks required less energy. The key was to select oleaginous algae strains, that are capable of producing high outputs of lipids [27]. The most commonly used marine algal cultures for the production of biodiesel are *Botryococcus braunii*, *Chlorella vulgaris*, *Chaetoceros muelleri*, *Dunaliella salina*, *Nannochloropsis oculata*, *Nannochloropsis salina, Arthrospira maxima*, and *Scenedesmus quadricauda* [36], to name a few, of which

Table 4.1.2 provides the percentage of oil content estimated within dry microalgal biomass. Microalgae are also a source of proteins and carbohydrates, spent biomass is suitable to be used as rich nitrogen and phosphorus crop fertiliser or livestock feed [15,26].

Table 4.1.2: Microalgae oil content, envisaging biodiesel production

Microalga	Total Lipids (% dry wt)	Induction method	Reference
B. braunii	60-86	Potassium phosphate 0.058 g/L, Magnesium sulphate 0.09 g/L in BG-11	[37,38]
C. vulgaris	55.9 56.6	Nitrogen limitation, 0.313 g/L KNO_3, iron limitation	[39]
N. oculata	36	0.22mm $N{\cdot}L^{-1}$ f/2 medium	[40]
I. zhangjiangensis	53	Nitrate concentration, 9 g/L, 24h intervals	[41]
Nannochloris sp.	31-68	CO_2 enrichment	[42]
P. tricornutum	20-30	12:12 L:D cycle	[43]
Schizochytrium limacinum	50-77	Glycerol substrate	[44]
Tetraselmis sueica	15-23	12:12 L:D cycle	[43]
Auxenochlorella protothecoides	60	Heterotrophic with glucose	[45]
C. protothecoides (UTEX 256)	53	Glycerol substrate	[46]
Isochrysis galbana	20-30	12:12 L:D cycle	[43]
S. obliquus	22-43	Nitrate, phosphate and sodium thiosulphate deficiency	[38]

However, high costs of cultivation, lower lipid production by microalgae when scaled-up, contamination and competition from other oleaginous microorganisms are limiting factors that need to be surmounted before microalgae could be considered as true sustainable method of biodiesel production [47,48].

4.1.2.1. *Brief overview on transesterification*

Microalgae triglycerides are converted into alkyl esters or biodiesel through the process known as transesterification (ester exchange reaction) [36,49]. The process is represented in the general equation provided by Borges and Diaz, Mata et al., Meher et al. and Ejikeme et al. [36,49–51], as seen in Equation 4.1.1.

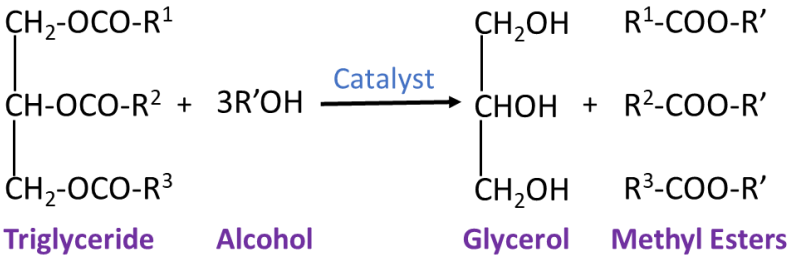

Equation 4.1.1: Transesterification of triglycerides (overall reaction).

In order to reduce the viscosity of the triglycerides, an alcohol, for example methanol is commonly used in place of water [50]. For this investigation methanol in presence of boron trifluoride catalyst (Methanol-BF_3) was used.

4.1.2.2. *Microbial Lipid accumulation*

Microorganisms capable of accumulating more than 20 % of their dry weight are termed oleaginous [52,53]. Many microalgal species fall into this category, as shown in Table 4.1.2. Lipids deriving from microorganisms fit into three distinct categories: phospholipids, glycolipids and triglycerides (TAGs). For biodiesel generation high amounts of TAGs are desirable. Therefore, oleaginous microalgae, yeast, bacteria and fungi have been investigated to be used as 'cell-factories' [54].

4.1.2.2.1. Microalgae lipids

Microalgae produce storage lipids in the form of TAGs or neutral lipids, which are transesterified into biodiesel [55–57]. Lipid globules are formed within the microalgae cells when subjected to abiotic stress factors. Nutrient starvation causes the cells to increase the flux through the metabolic pathway from which they synthesise neutral lipids. Some common methods to induce lipid accumulation consist in depriving light, carbon, nitrogen and/or phosphorous levels within the culturing medium. Nevertheless, nutrient starvation slows down cell division, thus having a detrimental effect on biomass generation [58]. The lipids stored, similarly to starches, acts as reserves on which the

microalgae can rely on when growth is retarded [54]. The constituent amount of lipids varies amongst the microalgae species, the amounts range from 5 to 77 %wt [26]. The composition of these will vary according to environmental constrains such as nutrients, temperature, light intensity, ratio of dark to light cycle and aeration of the culture [59]. For example, Rodolfi et al. [42] were able to achieve a biomass productivity of 0.17-0.2 g/L/day with 25-30 % biomass lipid by culturing *Nannochloropsis sp*. in 250ml flasks, at 25°C with a continuous light source and flushed with CO_2 enriched air.

Scenedesmus obliquus is a fresh-water green algae belonging to the Chlorophyceae. It exists as single-cells or in formations knows as coenobium, of four or eight cells, with cells measuring on average 10µm [60]. Microalgae of the *Scenedesmus* genera (Table 4.1.3) are defined as oleaginous microalgae due to the 40-50% lipids accumulated when stressed [61].

Table 4.1.3: Lipid inducing techniques used on *Scenedesmus* species.

Strain	**Period of growth in original medium**	**Source of N, S or P**	**Stress**	**Reported Lipids yield/concentration**	**Reference**
S. obliquus CNW-N	Detmer's Medium - 4 days	1g/L $Ca(NO_3)_2$ (6mM)	N- for 5days	140.35 mg/L/d	[62]
S. obliquus CNW-N	Detmer's Medium -12 days	1g/L $Ca(NO_3)_2$ (6mM)	N- for 12days	78.7 mg/L/d	[63]
S. obliquus SAG 276-3a	N11 medium - 30days	1.5g KNO_3 (14.8mM)	N- (substitute KNO_3 with KCl)	58.6 mg/L/d	[38]
Scenedesmus sp. LX1	50% BG medium- 16days	0.75g/L NaNO3 (8.8mM)	NaNO3 reduced 0.25mg/L after 13 days	80 mg/L/d	[64]
Scenedesmus sp. LX1	50% BG medium- 16 days	0.02g/L K_2HPO_4	NaNO3 reduced 0.1mg/L for 13 days	150 mg/L/d	[64]
S. obliquus UTEX 393	n.d.*	KNO3 10 mM (1g/L)	300hrs (12days)	40 %dry wt	[61]
S. obliquus UTEX 393	15day (until 1g/L reached)	KNO3 (1.6g/L) 16.8 mM	15days	35 %dry wt	[65]
Scenedesmus obliquus	BG11- for 14 days	1.5g/L $NaNO_3$ (17.8mM)	0.025g/L for 14 days	32 %dry wt	[66]
S. obliquus (XJ-15)	BG-11 for 8-10days	0.9g/L NaNO3 (10.7mM)	No $NaNO_3$, Varied T(°C): 17, 25, and 33 °C	47.6 % lipids (77 % TAGs)	[67]

*n.d. not disclosed by the authors, [a] maximum yield achieved in study

4.1.2.2.2. Yeast lipids

Among other oleaginous microorganisms are yeasts, which are eukaryotic microorganisms capable of growing either aerobically or anaerobically, using nitrogen and carbon sources for their growth and releasing CO_2 into the atmosphere. Used widely in industry for fermentation process, yeasts convert low value products, such as glycerol, into lipids for biodiesel application [68]. Compared to microalgae, yeasts have a high growth rate and are resistant to viral infections [69]. However, when compared to microalgae, yeasts require complex medium requirements [70] leading to high production costs. Oleaginous yeasts are used for the production of lipids, suitable for the biofuels industry [69], with the majority of strains containing 90 % TAGs in their storage lipid [54]. Lipid accumulation can be triggered by nitrogen limitation [53] with triglyceride profiles varying from species to species [69]. However, yeasts on their own would not be suitable for sustainable biofuel production in terms of achieving a circular CO_2 economy. Therefore, research has steered towards associating algae and yeast, with the interest of harnessing the best of both worlds for increasing biomass and biofuels production [70].

Similar to *S. obliquus*, the yeast proposed here, *Rhodosporidium toruloides*, is able to accumulate up to 60 % dry wt in lipids, alongside β-carotene, torulene and torularhodin. In recent years the entire genome of *R. toruloides* has been sequenced [71]. Lipid yield of *R. toruloides*, when compared to *S. obliquus* are quite high with values in the range of 0.4 g/L/h [72], 0.54 g/L/h [73].

4.1.3. Microalgae co-cultures for lipid production

The first chapter of the thesis highlighted the importance of finding co-culture partners that would work in mutual symbiosis. The examples provided show that in nature mixtures of microalgae, cyanobacteria, bacteria, yeast and fungi co-exist. Microalgae and bacteria partnerships have been shown to be 'ideal' combinations when it comes to co-cultures. The underlying principle of exchanging metabolites being the basis of their relationship. The availability of CO_2 plays a major role in the growth and reproduction of microalgae, therefore, associating oleaginous microalgae and yeast may offer a method in which to increase lipid outputs.

Challenges in current microalgal cultivation include the optimisation of culturing conditions to improve parameters such as CO_2 availability, nutrient optimisation to enhance biomass yield and consequently lipid production. For a fruitful co-culture, as outlined in Chapter 1, the synergistic effect of carbon dioxide and oxygen exchange alongside biomolecules exchange will dictate the outcome of the co-culture. Lipid productivity during co-cultures with high concentration of carbon sources [74] is higher compared to those under lower carbon availability [75]. This indicates that high capital costs may be incurred, unless wastewater streams can be used as feed. The question remains whether algae-yeast co-cultures are able to outcompete lipid production from microalgae monoculture.

4.1.4. Co-culturing *Scenedesmus obliquus* and *Rhodosporidium toruloides*

Microalgae have naturally evolved to respond to environmental cues through synergistic and antagonistic relationships established within their niche. The work presented in this chapter focuses on the interactions of *Scenedesmus obliquus* CCAP 276/3A with *Rhodosporidium toruloides* NYCY 192 in a co-culture set-up. The aim was to investigate if associating an aerobic oleaginous yeast with a lipid-producing microalga lead to an increase in microalgal cell growth and lipid productivity.

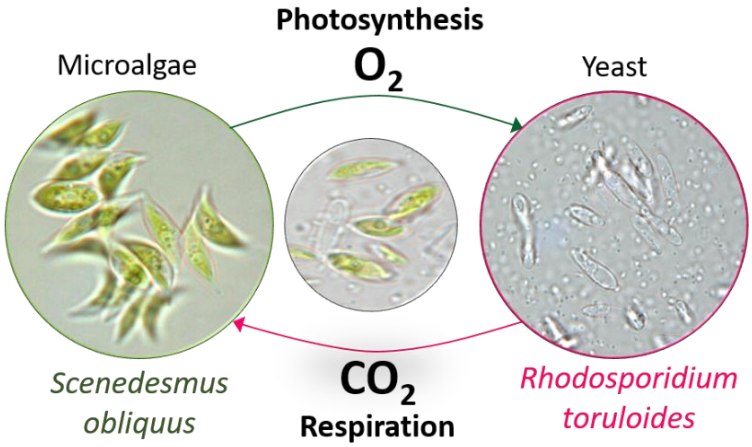

Figure 4.1.1: Illustrating the gas exchange between algae and yeast.

Exchange of carbon dioxide and oxygen are the basis on which the algae-yeast co-culture would thrive. However, some molecules such as glycine and palmitic acid are also believed to contribute to the well being of both species

The proposed microbial association has not been previously tested. Furthermore, the various growth media reported literature were found to be high in carbon and nutrient sources. The rich growth medium would then favour the growth of the oleaginous yeast, unavoidably leading to an increase in lipids. The chosen medium here will test if the co-culture functioned based on a 'true-established' synergism without relying on large amounts of supplement.

In this study, the microalgae is considered the main partner, therefore decisions have been made with respect to its well being. The communal medium developed is not high in sugars or nitrogen, but only contains enough supplements to investigate whether the yeast truly supports the growth of the microalga. Furthermore, a two-stage cultivation system, co-culture growth and then stressed has not been used in other algae-yeast co-culture studies reported (Figure 4.1.1).

The co-culture proposed does not exist in nature, with the underlying risk of not working. These effects have been accounted for by testing for priority effects and sample introduction of the yeast to the microalgae [76,77].

4.2. Experimental Design

4.2.1. *Scenedesmus obliquus* growth in Bold's Basal medium

Primarily, as in Chapter 3, each of the microorganisms selected for this study were grown separately. Firstly, *S. obliquus* growth in terms of cell counts and dry weight was assessed in Bold's Basal Medium (BBM), DIN (see section 2.4.8) and pH readings were taken throughout the experimentation period. *S. obliquus* was grown as described in section 2.2.4.

4.2.2. *R. toruloides* growth in Yeast Mold and BBM modified medium

R. toruloides was grown as described in section 2.2.5. *R. toruloides* cells appear 'milky' in colour at inoculation phase to later develop a pink-orange hue. This is due to the accumulation of β-carotene within the cells. *R. toruloides* was acclimatized to grow at room temperature. This was achieved by passaging the cells over a period of 4-5 weeks on YM agar plates. Briefly, YM agar plates were steaked with dilutions of 10^4 and 10^6 of

yeast cells obtained from the YM culture flask at 30 °C, on the 24th hour of growth, when the cell entered log-phase. Some plates were incubated at 30 °C, to maintain a back-up in the event of failure. The other plates were incubated on the lab bench at room temperature. Amongst the plates at room temperature, on the 5th day single colonies were chosen from the plates and passaged. This process was conducted every 5-6 days until it was clear that cells were able to grow successfully on the lab bench.

By surveying the literature belonging to co-cultures of yeast or bacteria and microalgae, it was noticeable that yeast extract was chosen as the added supplement for yeast to grow in microalgal medium [78]. However, adding yeast extract into microalgal cultures may stimulate the growth of any small percentage of bacteria present within. Therefore, various amounts of yeast extract starting from a concentration of 1 g/L, as suggested in literature to lower amounts of 0.3 g/L were tested. The aim was to check if the growth rate of *R. toruloides* could be slowed down enough, for it to have an effect on the microalgae cultures. The modified medium will be referred to as BBM+, any number beforehand will indicate the concertation of yeast extract (0.3BBM+ = 0.3 g/L yeast extract in BBM).

4.2.3. Lipid accumulation in *S. obliquus*

After selecting the communal medium in which to grow the co-culture, a lipid inducing technique was selected. Looking at literature, various methods are implemented to instigate microalgal lipid accumulation, such as phosphorous [64,79], sulphur and nitrogen starvation [39,80–82]. Table 4.1.3 highlights that nitrogen starvation has been the preferred method for inducing the production of lipids within *Scenedesmus* cells. The same mechanism has been shown to induce lipid accumulation in some yeasts [83], including *R. toruloides* [80,81].

Before starting with the co-culture experiment, *S. obliquus* monoculture was evaluated for lipid production in terms of Fatty Acid Methyl Esters (FAME). Graph 4.3.2 showed that DIN within the *S. obliquus* culture took approximately 50 days to reach minimum amounts. However, the cells were not fully stressed for lipogenesis. Therefore, it was decided to change the growth medium to nitrate free medium.

Figure 4.2.1: Representation of the *S. obliquus* nitrogen starvation two-stage experiment.

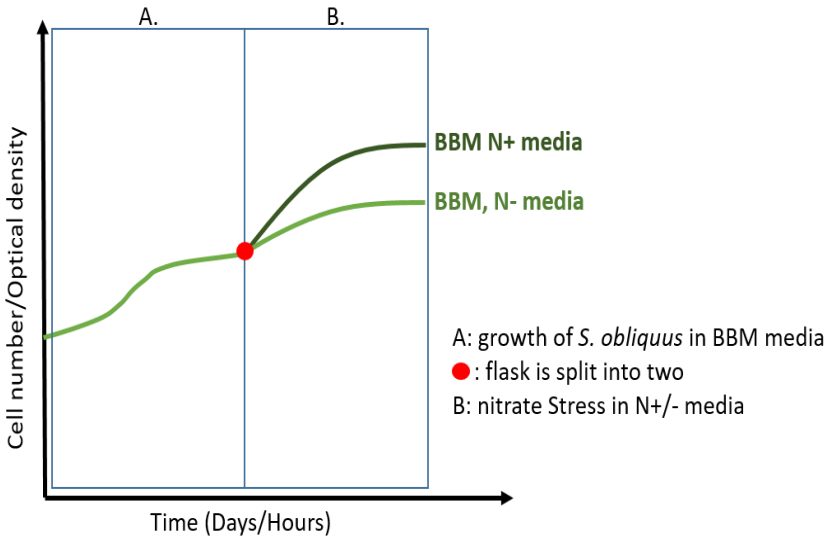

In part A, the microalgae was grown in BBM. In part B, the total algal biomass was split in two. One-half was inoculated into fresh BBM (N+) flask whilst the other was inoculated into nitrogen-depleted medium (N-).

As illustrated in Figure 4.2.1, a two-stage experiment was set-up. The first part (A) involved growing the microalgae in standard BBM. When the microalgae reached an optical density of 0.6-0.8OD_{595nm}, half of the biomass was resuspended in fresh BBM N+ medium, whilst the other was resuspended in nitrate deficient BBM (BBM N-). The nitrate stress reduced the N available to *S. obliquus* cells from 3mM to 0mM $NaNO_3$.

Briefly, *S. obliquus* was grown in triplicate 500 mL culture flasks with 350 mL of BBM, as the conditions described in section 2.2.4. The microalgal cells were grown for 12 days in BBM, before starting the experiment. On the 12th day, optical density for each flask was recorded alongside the pH and DIN measurements. The flasks were split into two by volume and the algae biomass was collected through centrifugation at 2,500 g for 15 minutes. The pellets for the BBM N- medium were washed once with BBM N- medium, to remove any traces of nitrate. The microalgae were then inoculated into triplicate 500mL culture flasks with 350mL of BBM medium N+/-. Sampling was carried-out for OD, cell counts and for FAME analysis using GC-FID.

4.2.4. Effect of yeast inoculum on growth phase of the microalgae

The co-culture of *S. obliquus* and *R. toruloides* is not a naturally established association. The inoculation ratio and phase, at which the inoculum is added to the main culture,

play a significant part in the success of the co-culture study [76]. Similarly, the inoculation ratio, *i.e.* the amounts of algae to yeast would have an effect on the way the co-culture behaves. Inoculation studies have shown that keeping the range of 3:1 and 2:1 (algae: microorganism) has had positive results, with respect to microalgae growth, with no prominent underyielding effects [84,85].

A study was carried out to test if indeed adding the yeast at different time points of microalgae growth, would affect the growth performance of *S. obliquus*. For this study, it was decided to inoculate the yeast when the *S. obliquus* at different growth stages (Figure 4.2.2). *S. obliquus* as grown at as per the conditions detailed in section 2.2.4. Prior to each inoculation point, the yeast was activated by growing it in 1 g/L of modified BBM (1BBM). Yeast inoculums were harvested when the OD_{595nm} of 0.5-0.6 was reached (start of log-phase). The first inoculum of yeast at a ratio of 3:1, based on optical density, was added on the first day (START); the second inoculum was added on the 3rd day (MIDDLE) whilst on the 6th day a fresh inoculum was added to the flask (END). Alongside the inoculum, sterilized yeast extract solution was added to obtain a concentration of 1 g/L within the flask.

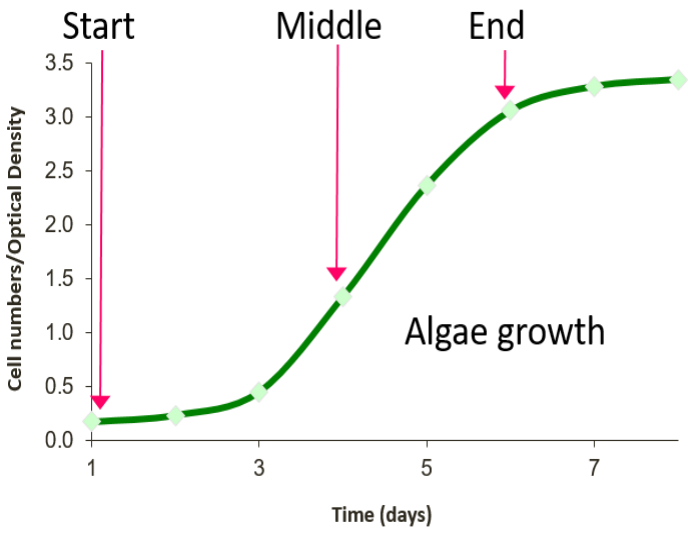

Figure 4.2.2: Growth phase inoculation diagram.

The arrows indicate the points at which the yeast inoculum was added to the microalgae culture.

4.2.5. Co-culture of *S. obliquus* and *R. toruloides* for increased lipid production: two-stage system.

Based on the literature in Table 1.3.1 (Chapter 1), co-culture studies on algae-yeast direct mixing experiments do not include a stress-inducing step. That is to mean that both microorganisms were grown in communal medium and the lipids deriving from these associations were evaluated. The results obtained by co-culturing the two microorganisms indicated that a two-stage system might be the best way to trigger lipogenesis. Two-stage system will involved growing the algae and the yeast together and then subjecting them to nitrate stress.

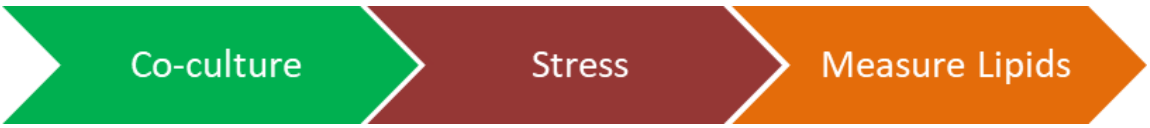

Figure 4.2.3: Flowchart for two-stage set-up for lipid stress in microbial cultures.

Three flasks for each conditions were set-up: algae monoculture, yeast monoculture and co-culture flasks. Firstly, six 500 mL Erlenmeyer flasks, containing 400 mL of BBM were inoculated to give 4 x10^5 microalgae cells/mL (0.1-0.15 OD_{595nm}). The flasks were grown until the cell density reached 1x10^6 cells/mL (0.4-0.5 OD_{595nm}), at which point the yeast culture at a ratio of 2:1 (algae: yeast) was added. Yeast extract solution was added to obtain a concentration of 0.3g/L in the co-culture flasks. In parallel, three more flasks were inoculated with the same size of yeast inoculum into 0.3BBM + medium. The preliminary data indicated that the yeast reached its maximum growth rate within 24 hours, therefore on the 32nd hour, the half flasks were subjected to nitrate stress. The experiment was evaluated through means of OD readings, cell/CFU counts, DIN, biochemical assay for protein, carbohydrates, pigments, and for FAMEs. Sampling points are shown in Figure 4.2.4.

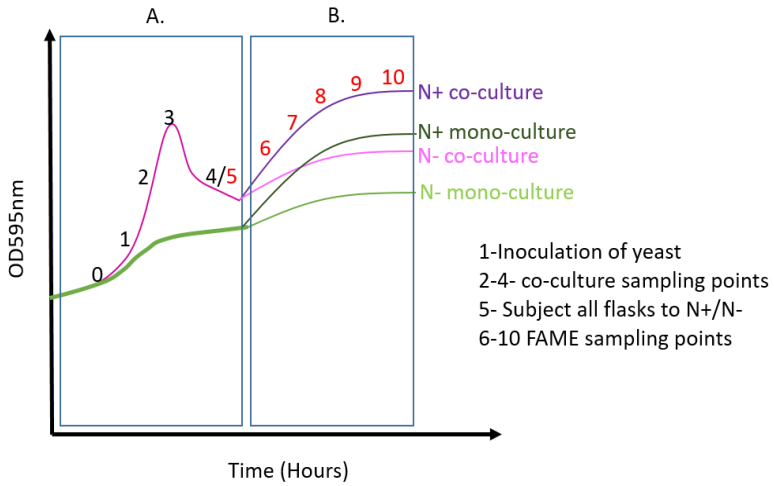

Figure 4.2.4: Diagram showing the sampling points for the two-stage experiment. All runs in triplicate flasks. Two stages: (A) co-culture and (B) nitrate stress.

4.2.6. Gas exchange

Carbon dioxide and oxygen exchange play a vital role in the outcome of co-culture studies [86]. The evolution of carbon dioxide was measured in terms of dissolved inorganic carbon (DIC, see section 2.4.11) and CO_2 evolution using a gas analyser (BlueInOne FERM, Blue Sense) coupled to a computer with BlueVis software. All the cultures were grown in BBM with 1g/L of yeast extract, in 1L tight-sealed Duran bottles, fitted with an inlet and outlet port cap. The algal gas evolution was first measured for 120-150 hours, followed by the yeast for 70-72 hours and lastly the co-culture for 72 hours. This was performed by first growing the algae up to OD_{595nm} of 0.6 and then inoculating the yeast at a 2:1 (algae: yeast) ratio through the sampling port, as shown in Figure 4.2.5 below. Air at a flowrate of 0.1 L/min was pumped into the vessel to encourage mixing and facilitate exiting gas through the port. The gas analyser was connected to computer that would provide the measurements of carbon dioxide evolution in real time. The sampling point was used to withdraw 6 mL of culture at per each time-point and OD, pH and DIC were measured.

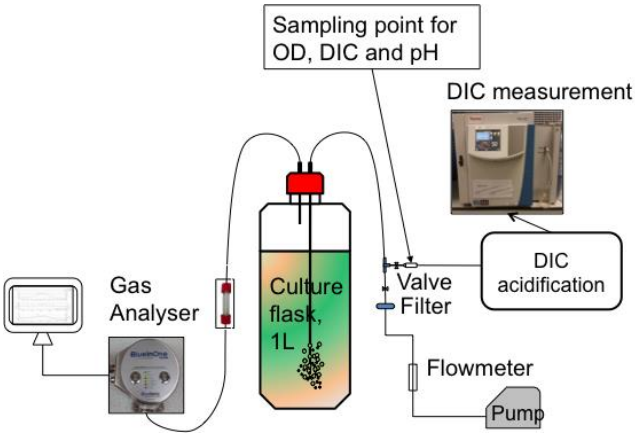

Figure 4.2.5: Gas exchange experimental set-up

4.3. Results

4.3.1. *Scenedesmus obliquus* growth in Bold's Basal medium

The algae were inoculated at a seeding density of 2.4 x10^5 cells/ml, equivalent to an optical density of 0.08-0.09. This inoculum size was found to be sufficient, to allow the algae to propagate successfully (Graph 4.3.1).

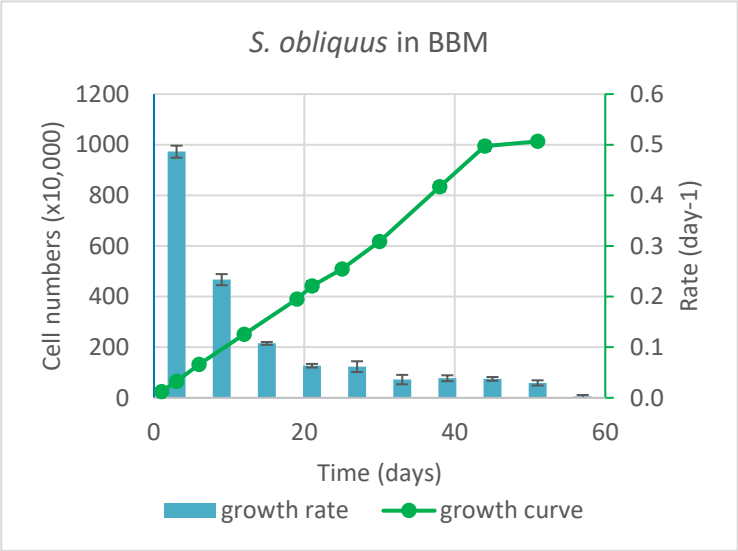

Graph 4.3.1 *S. obliquus* specific growth curve and rate in BBM medium. The error bar represent standard error for biological triplicates.

Maximum growth rate of 0.486 day^{-1}, and an average rate of 0.111 day^{-1}. Overtime, the DIN value measured approaches zero, correlating to slower growth rates (Graph 4.3.2A). The pH values increased from 6.2 to 6.9 (Graph 4.3.2B), indicating that the available carbon dioxide and nitrogen sources were consumed.

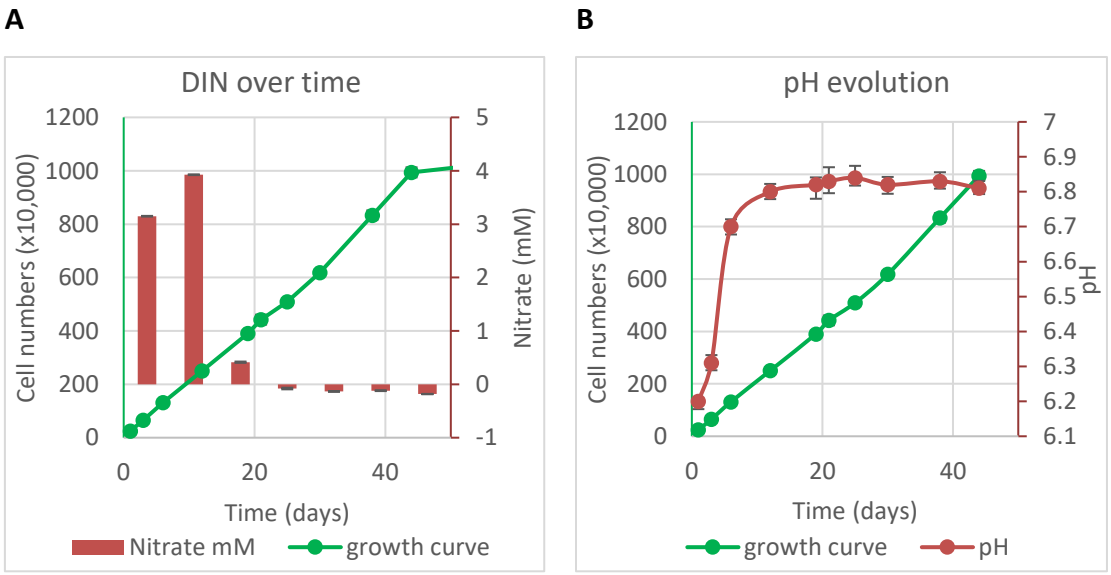

Graph 4.3.2: Measurements of the evolution of (A) dissolved inorganic carbon and (B) pH over a 50 days growth period. Standard error plus and minus for biological triplicates.

4.3.2. *R. toruloides* growth in Yeast Mold and BBM modified medium

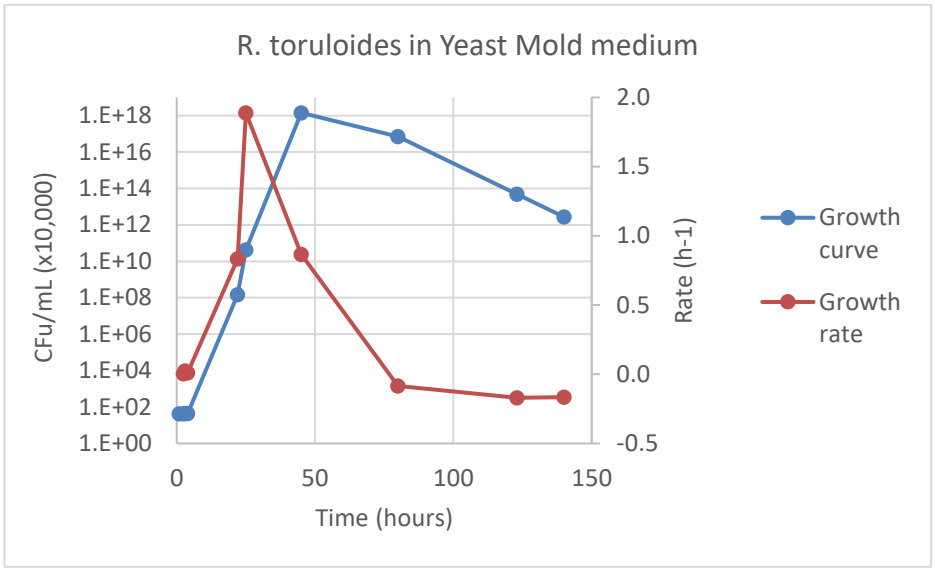

Graph 4.3.3: Growth curve and rate (d^{-1}) for *R. toruloides* grown in Yeast Mold Medium, at 30°C on a shaker at 100rpm. Standard error plus and minus for biological triplicates.

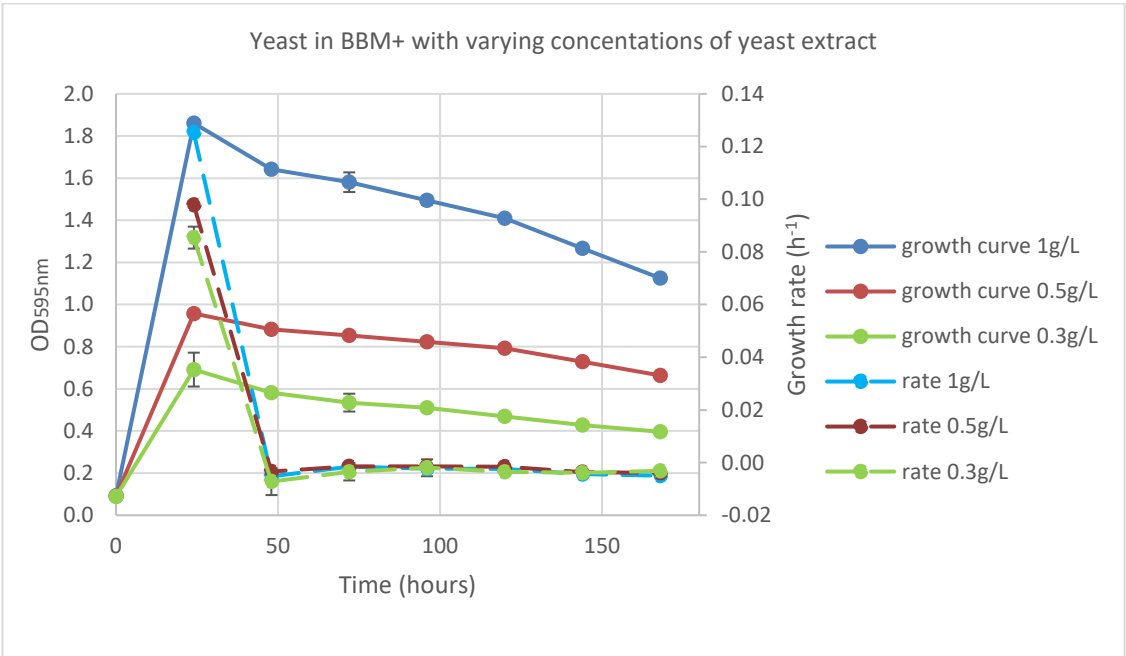

Graph 4.3.4: Testing the ability of *R. toruloides* to grow in BBM modified medium. Standard error plus and minus for biological triplicates.

Concentrations of added yeast extract were tested ranging from 1 g/L to 0.3 g/L. The yeast was grown until the lag-phase was reached. The results display standard error bars for plus and minus values for biological triplicates.

Compared to the growth curve obtained for the *R. toruloides* grown in YM medium (Graph 4.3.3), the maximum yield of yeast using BBM modified medium is seven times

less with 1 g/L of supplement, and even lower with decreasing amounts of yeast extract. At 0.3 g/L an OD_{595nm} of 0.6 was reached (Graph 4.3.4). As the aim of the investigation is to study the effects that the microorganisms have on each other, the lower concentration was chosen. Furthermore, having lower amounts of yeast extract in communal medium would not only detract any disturbances from bacterial population but also ensure that the yeast does not cause any underyielding effects [87] onto the microalgae population.

4.3.3. Lipid accumulation in *S. obliquus*

Axenic *S. obliquus* was first evaluated to accumulation of FAME prior to starting the co-culture experiments (Figure 4.2.1). The two-stage experiment, involved growing the microalgae in standard BBM, to then resuspend half of the biomass in nitrogen deficient medium (0 mM $NaNO_3$) and the other half in fresh BBM (0.25 g/ 3 mM $NaNO_3$).

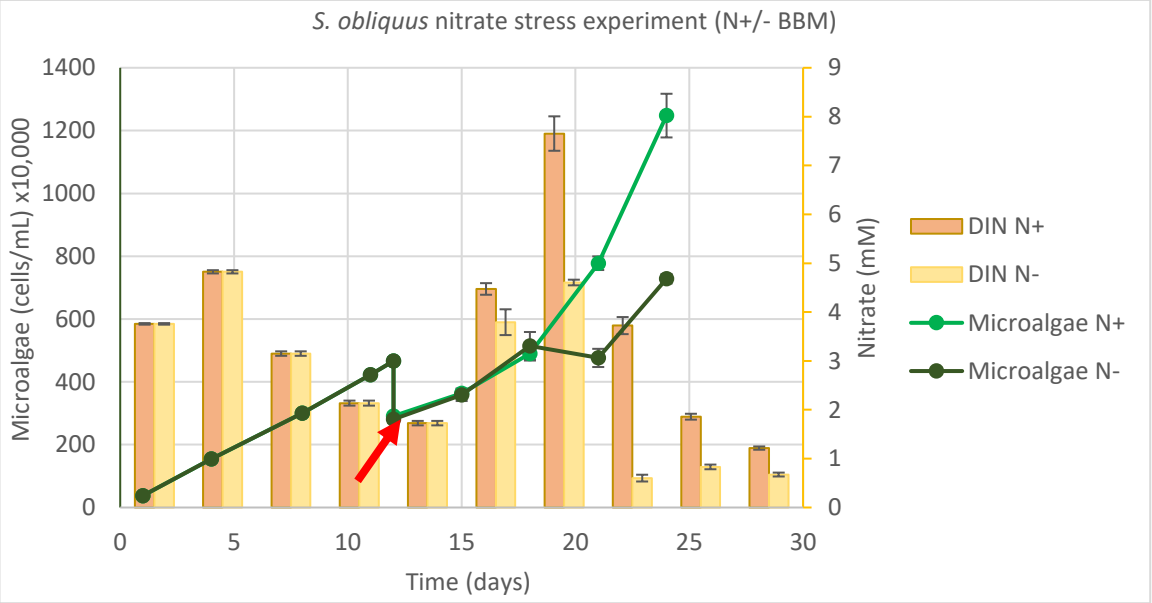

Graph 4.3.5: Cell growth and DIN evolution during nitrate stress. Standard error bars represent plus and minus error for biological triplicate flasks. The red arrow indicates when nitrate stress starts.

Cell counts and DIN measurements were taken for 30 days. The red arrow indicates when the cells were subjected to nitrate stress. The stressed cell slow down in growth rate with diminishing nitrates in the medium. The final cell count is $1.2x10^7$ cells/mL for the non-stressed flasks and $7.2x10^6$ cells/mL for the stressed flask. Measured pH values for the BBM N+ medium measured approximately 7.5±0.2, whist the values recorded for the BBM N- medium ranged in the region of 6.6±2, from a starting pH of 6.2.

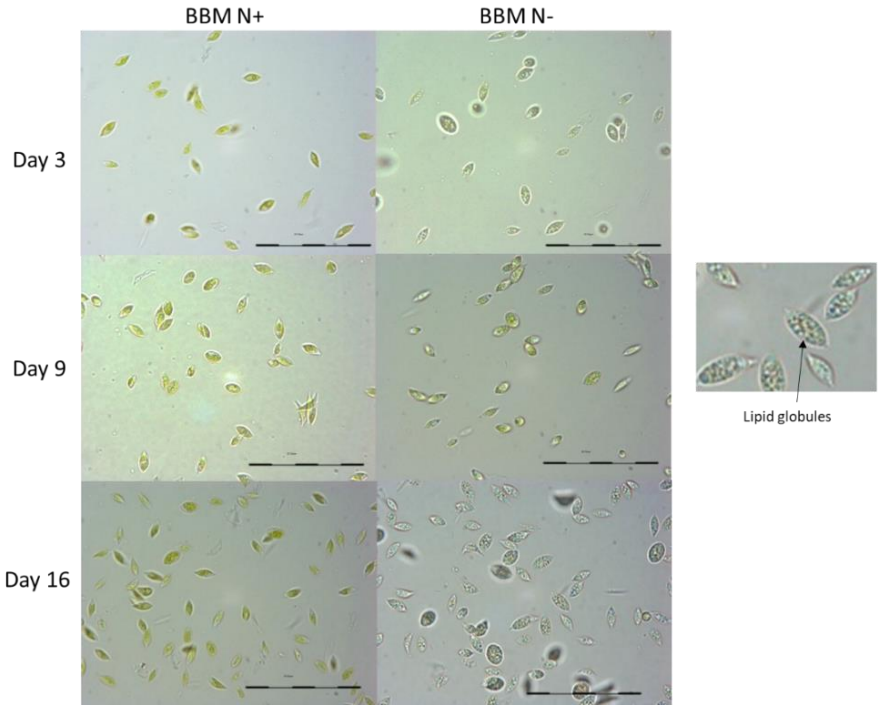

Figure 4.3.1: Microscope pictures (100X), showing S, *obliquus* cells grown under non-stress (BBM N+) and under nitrate stress conditions (BBM N-).

Lipid globules are more visible within the cells (enlarged picture on the side), when approaching day 16 of nitrate stress. Cells measured 7-8µm.

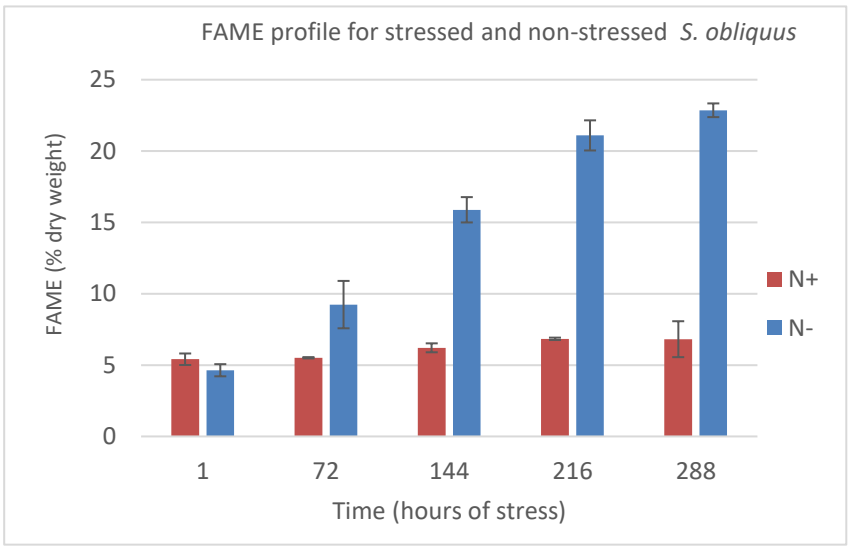

Graph 4.3.6: Percentage of FAMEs present within S. obliquus cells. N+ indicates the cells that were not starved for nitrogen; N- represents nitrogen depleted growth. Standard error represented with plus and minus bars for biological triplicates, with $p<0.05$.

Nitrogen depleted *S. obliquus* accumulated up to 20-22 %dry wt in FAMEs (Graph 4.3.6).

A significant increase when compared to the 6% obtained from unstressed conditions.

4.3.4. Effect of yeast inoculum on growth phase of the microalgae

A study was carried out to test if indeed adding the yeast at different time points of microalgae growth, would affect the growth performance of S. obliquus. A basis of 1 cell/mL = 1 CFU/mL was used to convey data in terms of total biomass.

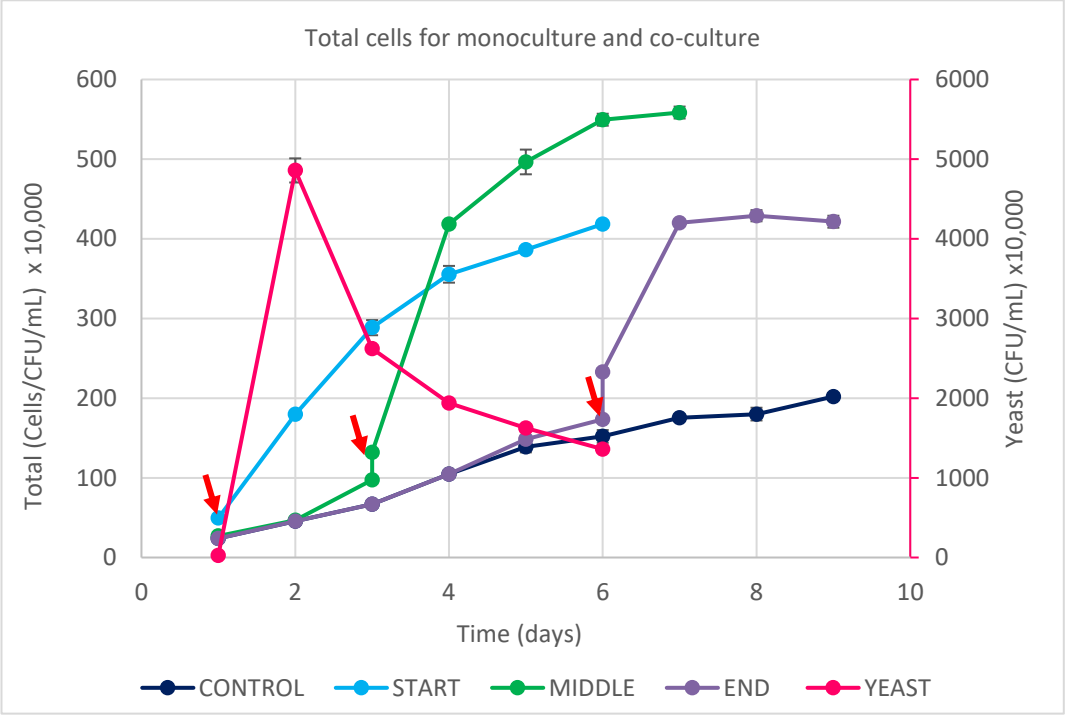

Graph 4.3.7: Total cell count for mono and co-culture flasks. Standard error for duplicate flasks (not visible). Red arrow indicates when the yeast inoculum was added at a ratio of 3:1 (algae: yeast).

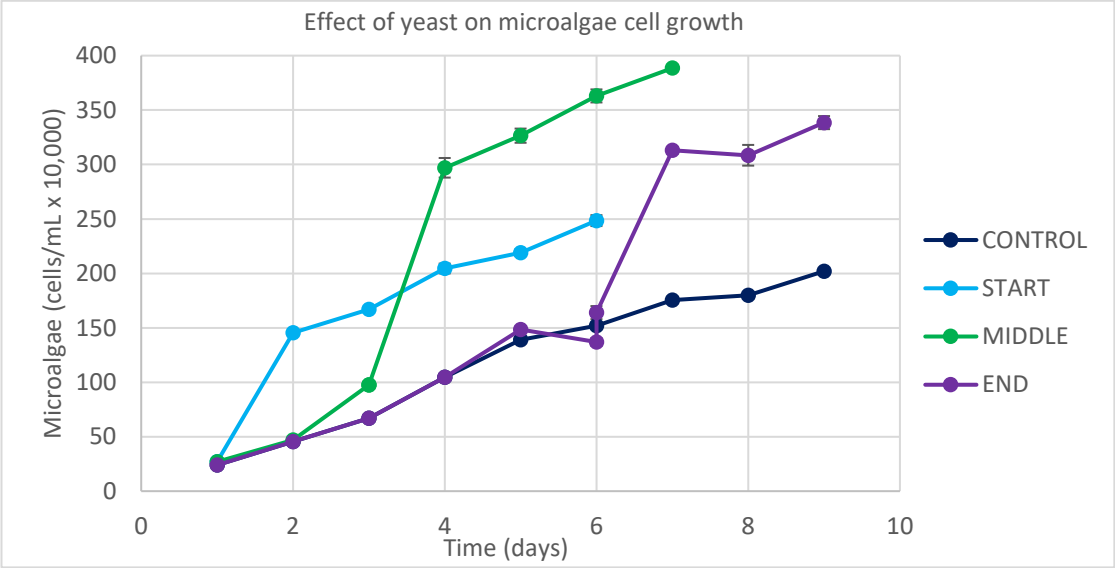

Graph 4.3.8: Effect of yeast on the growth rates of the microalgae cells. Standard error for duplicate flasks (not visible). For all flasks, p>0.05, with Middle p=0.06.

The average growth rate for control 0.266 d^{-1}, start 0.444 d^{-1}, middle 0.520 d^{-1} and end flask 0.339 d^{-1}.

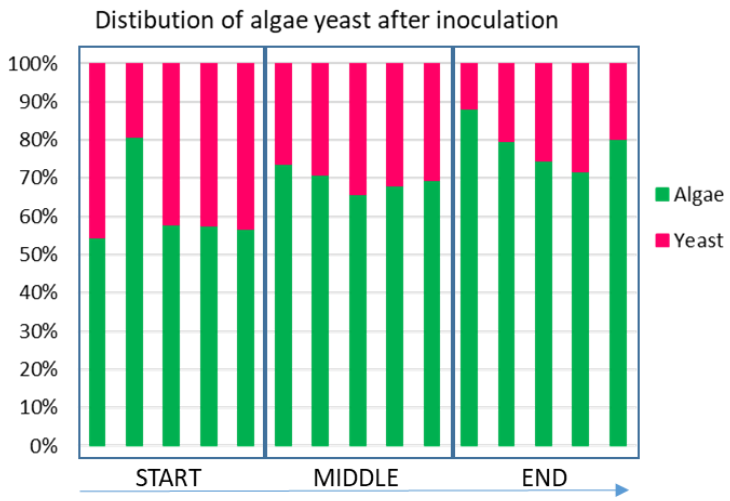

Graph 4.3.9: Microalgae and yeast cell or CFU numbers over the course of the co-culture experiment.

Visual representation of the population dynamics in the flask at the various time points in co-culture.

Table 4.3.1: pH measurements yeast inoculum experiment

pH	Control	Start	Middle	End	Yeast
Initial	6.2	6.2	6.3	6.2	6.1
Final	6.6	8.4	8.4	8.4	7.6

Adding the yeast to the microalgae co-culture increases the alkalinity of the medium.

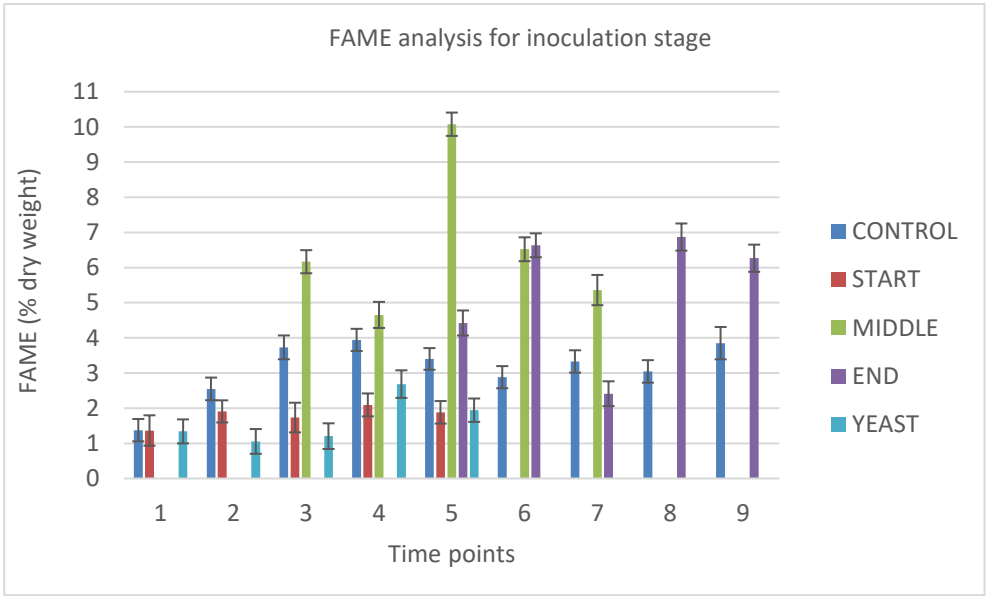

Graph 4.3.10: Productivity of FAMEs for co-cultures inoculated at ratio of 2:1, algae: yeast at different points of growth of the microalgae cells. Standard errors for duplicate flasks.

For all flasks, t-Test: Two-Sample Assuming Unequal Variances shows $p<0.05$. FAME accumulation in Middle inoculated flasks was the highest throughout the co-culture period, with maximum value of 10 %d/w.

4.3.5. Co-culture of *S. obliquus* and *R. toruloides* for increased lipid production: two-stage system.

The previous results lead to the conclusion that the presence of the yeast alone, does not pose enough stress on the microalgae to instigate lipid synthesis. The next step involved linking the element of co-culture, shown to increase microalgae biomass with nitrate stress, shown to increase lipid synthesis.

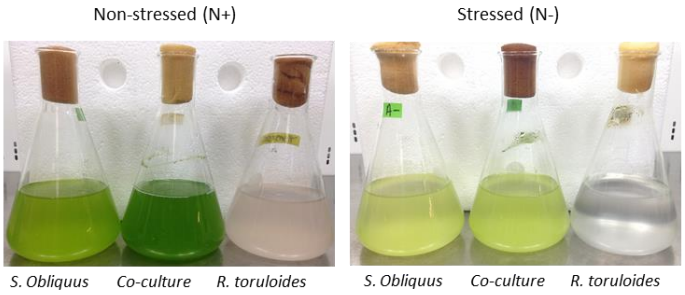

Figure 4.3.2: Flasks of *S. obliquus*, co-culture and *R. toruloides* non-stressed (left) and stressed (right). Picture taken after the cells had been stressed for 192hours.

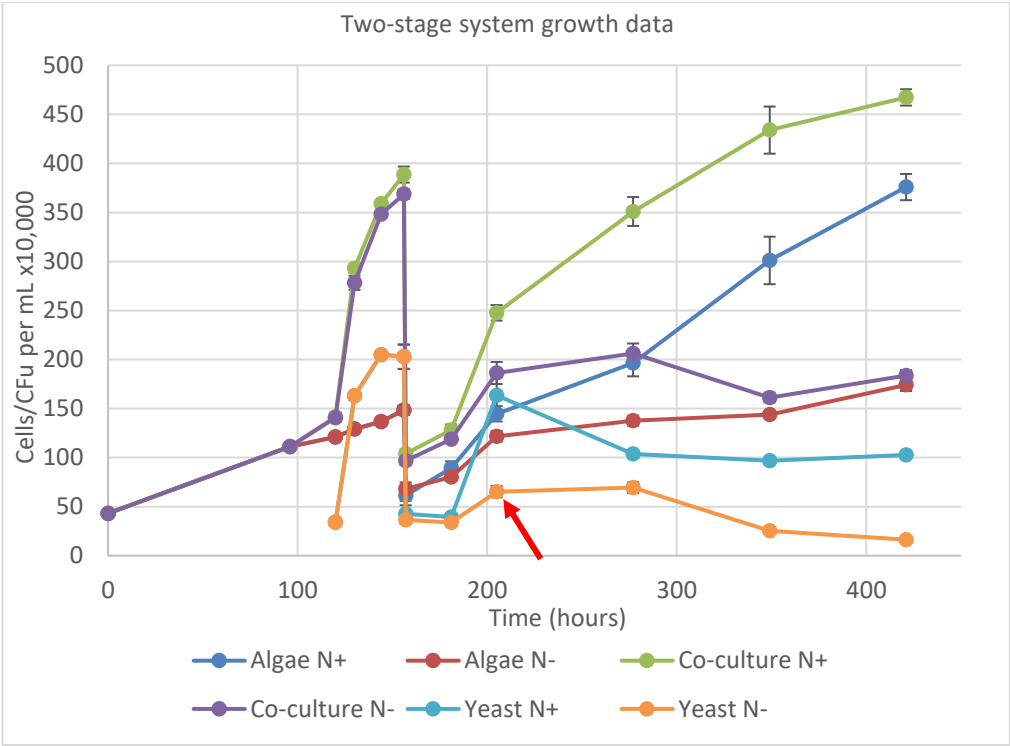

Graph 4.3.11: Growth curve of two-stage system. Standard error for triplicate biologicals replicates.

Stage (A) is before 186 hours. Stage (B) after inflexion point (red arrow). From time 0-100hrs all the flasks were grown as monoculture (not visible due to overlapping lines). Standard errors are representative of triplicate flasks.

The co-culture data obtained for the two-stage experiment agrees with the data obtained in the previous study. The mid-phase inoculation method was used. This

resulted in an increase of algae cells when in co-culture with the yeast cells (Graph 4.3.11 and Table 4.3.2).

Table 4.3.2: Average growth values co-culture stage and stress stage for all flasks.

Growth rate (day^{-1}) for total cells/CFU						
Stage	Algae N+	Algae N-	Co-culture N+	Co-culture N-	Yeast N+	Yeast N-
A	0.148	0.148	0.546	0.521	1.37	1.37
B	0.234	0.140	0.215	0.129	0.237	0.024
Growth rate (day^{-1}) for algae cells						
A	0.148	0.148	0.282	0.274	-	-
B	0.234	0.140	0.231	0.147	-	-
Growth rate (day^{-1}) for yeast CFU						
A	-	-	1.329	1.214	1.37	1.37
B	-	-	0.18	0.035	0.237	0.024

Higher growth rate of the co-culture flasks correlates with high cell numbers as shown in the previous experiment (Graph 4.3.8). During the co-culturing period, the ratio of algae to yeast varies. At all stages, the yeast grows then dies within the period of the experiments (Graph 4.3.12).

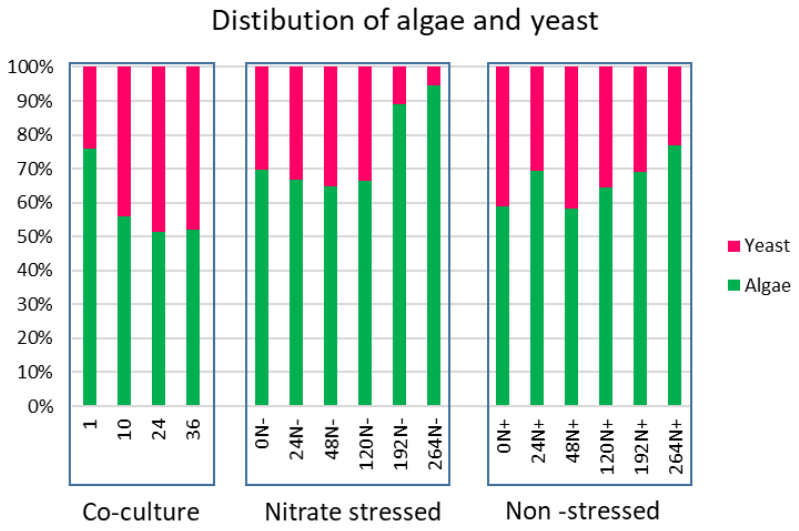

Graph 4.3.12: Percentage of microalgae and yeast cell over the course of the experiment for the co-culture flasks.

All flasks were stressed for 264 hours (11 days). The data for both non-stressed and stressed microalgae is provided for the duration of the stress (Graph 4.3.13). Accumulation of FAME in Co-culture N- vs Algae N- and Co-culture N+ ($p>0.05$).

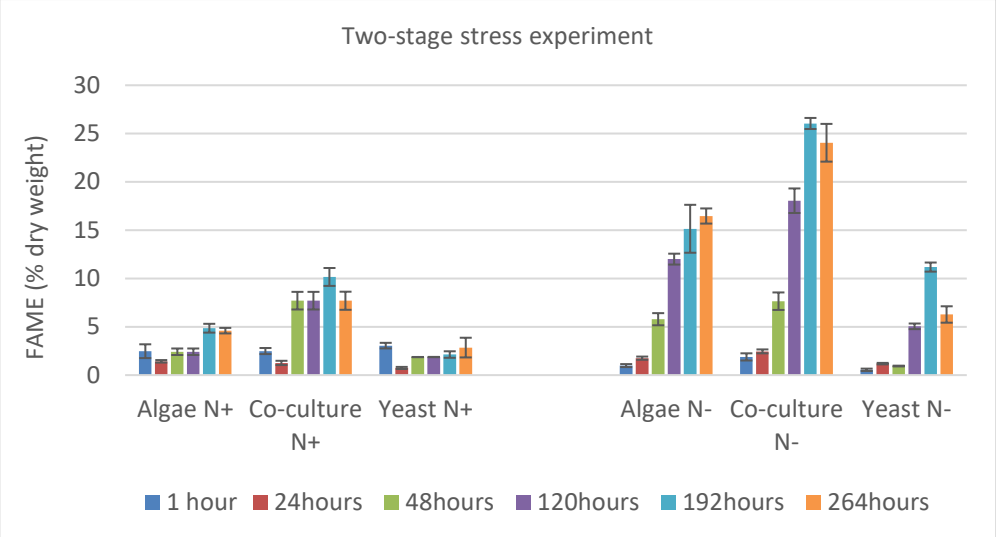

Graph 4.3.13: FAME (% dry weight) for monoculture and co-cultures during the stress period. Standard error for triplicate biologicals replicates.

The increase in FAME in co-cultures is higher compared to the monocultures, however is the effects are not statistically significant (Table 4.3.3).

Table 4.3.3: Biochemical composition of algae monoculture, co-culture and yeast monoculture flasks.

Time point	Time (hrs)	Algae monoculture			Co-culture			Yeast monoculture		
		% dry weight			% dry weight			% dry weight		
		Carbs.	Proteins	FAME	Carbs.	Proteins	FAME	Carbs.	Proteins	FAME
0	0	30.52	19.74	3.05	35.89	19.04	3.97	42.02	17.43	3.18
1	10	32.08	16.31	1.68	23.75	23.90	0.78	16.57	26.71	1.52
2	24	28.06	19.31	2.68	35.58	27.76	2.85	30.73	54.41	3.16
3	36	28.73	19.52	2.75	37.08	31.32	1.86	17.14	40.29	1.13
6N+	85	29.23	21.01	2.42	41.03	37.30	7.71	37.12	42.79	1.87
7N+	157	30.51	30.23	4.30	29.51	51.08	10.37	25.42	59.89	4.51
8N+	229	23.33	18.99	4.85	30.59	47.09	10.16	15.20	8.75	2.13
9N+	301	23.90	15.12	4.60	24.04	36.92	7.70	12.03	47.23	2.85
6N-	85	27.38	27.26	5.79	33.56	20.37	7.65	37.32	3.04	0.94
7N-	157	32.12	33.44	12.00	41.72	12.55	18.05	43.66	23.41	5.05
8N-	229	25.30	12.50	15.15	29.20	19.68	26.04	58.56	31.18	11.18
9N-	301	17.80	42.55	16.47	22.39	45.43	24.05	53.04	34.68	6.28

For all compounds ($p>0.05$) when comparing stressed monoculture of algae to co-culture values. Time points 0-3 measurements to the co-culture before stress, 6-9

measurements for the non-stressed flasks (N+) and 6-9 nitrate stress flasks (N-). Highest FAME values highlighted in red.

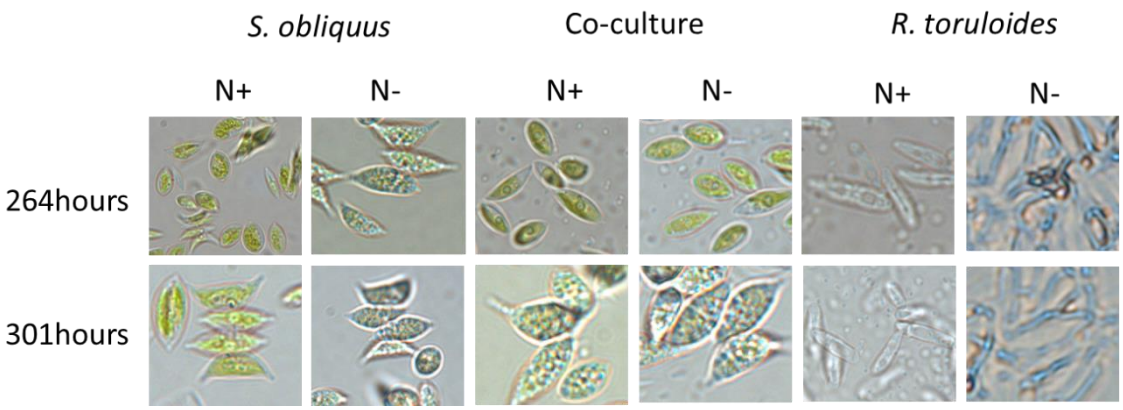

Figure 4.3.3: Pictures 100X magnification, showing *S. obliquus* in monoculture and co-culture with *R. toruloides*, taken at later stage of growth, when lipid globules (FAMEs) are clearly visible.

Microscope pictures (Figure 4.3.3) show the stressed and non-stressed cells for monocultures and co-culture set-ups. The lipid globules are visible in the *S. obliquus* cells in both monoculture and co-culture flasks, which are stressed. The yeast cells can be seen to be healthy when not stressed (N+) a stark contrast to the damaged cells when stressed (N-).

4.3.6. Gas Exchange

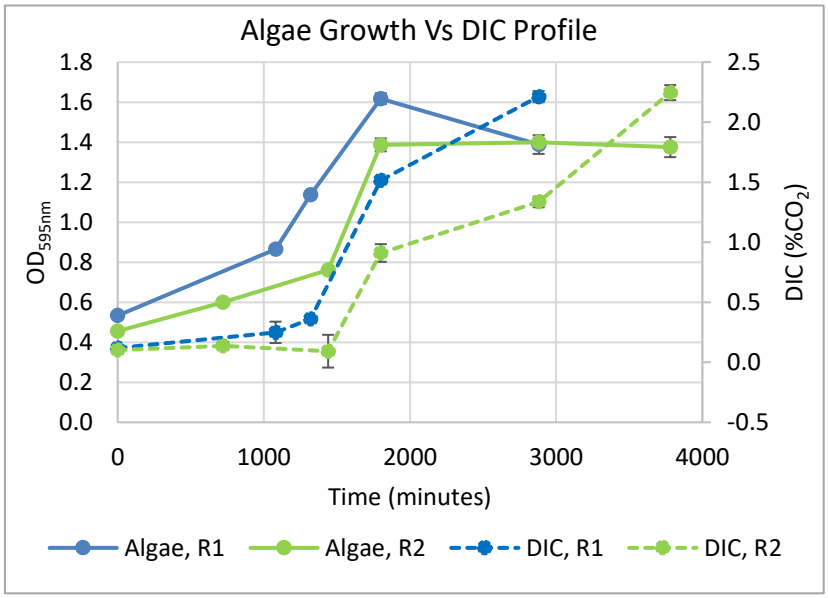

Graph 4.3.14: DIC evolution for microalgae monoculture BBM+ medium. DIC readings correspond to the dotted lines. Biological duplicates per run.

The data obtained for the monoculture of the microalgae, shows an increase in the CO_2 evolution over time (Graph 4.3.14). This does not agree with the fact that they respire

CO_2 and give off oxygen. The supplement in the medium increased the bacterial population over time, which may contribute to the carbon dioxide released.

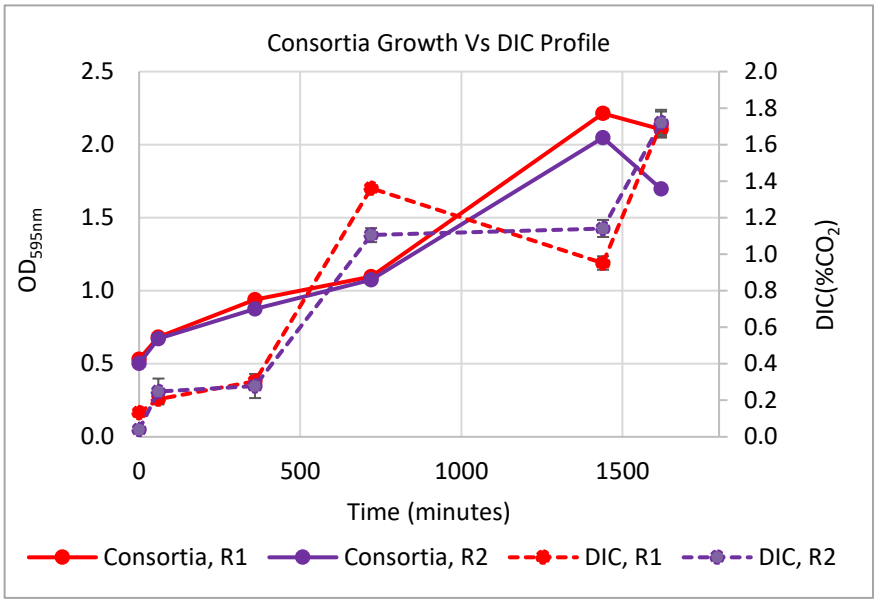

Graph 4.3.15: DIC evolution for microalgae co-cultured microalga and yeast in BBM+ medium. DIC readings correspond to the dotted lines. Biological duplicates per run.

DIC sampling was carried out after adding the yeast to the culture flask. The increase in CO_2 is seen at 720hours, which looking at the graph 4.3.4, shows yeast growth in the region reaching OD_{595nm} of 1.

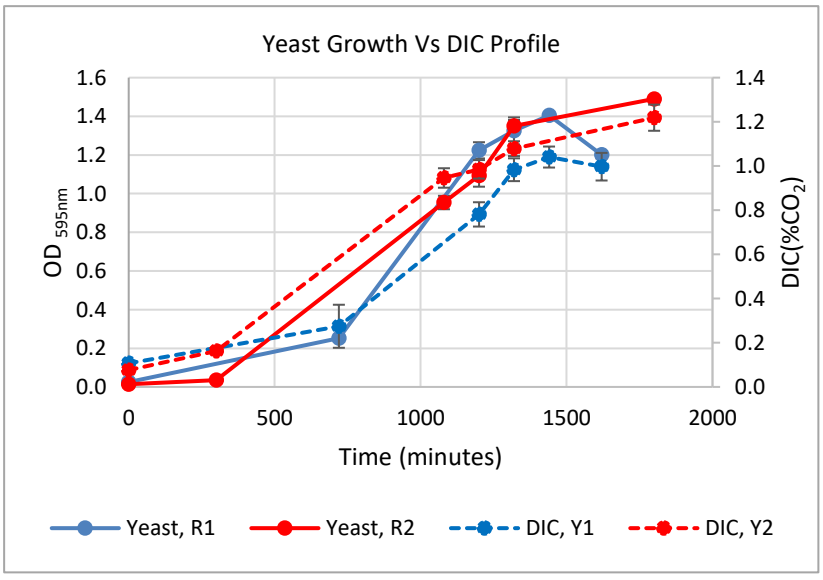

Graph 4.3.16: DIC evolution for yeast growth in BBM+ medium. DIC readings correspond to the dotted lines.

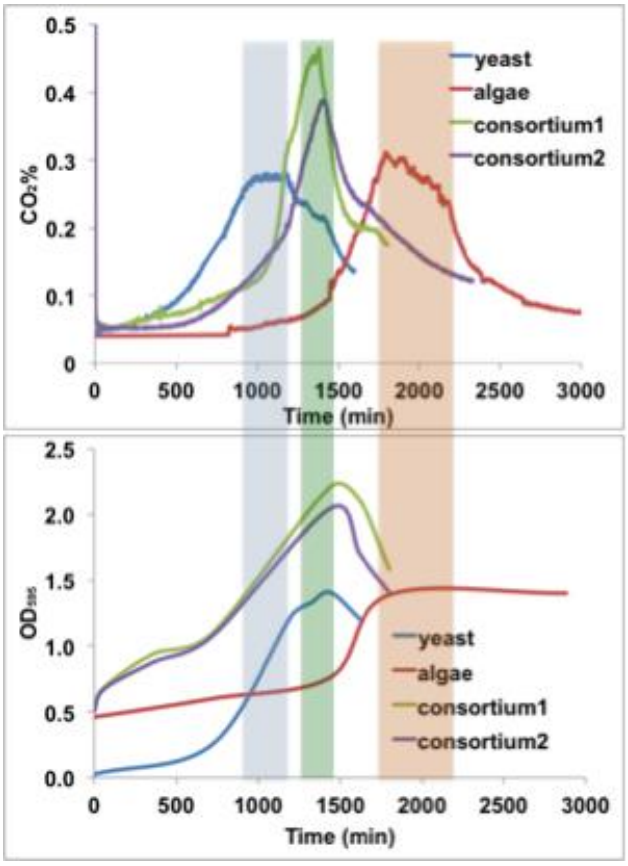

Graph 4.3.17: Gas analyser results

Gas analyser results on top and growths in terms of optical density at the bottom. The highlighted regions show the corresponding growths to CO_2 evolution.

The carbon dioxide evolution for the yeast data (blue line) coincides with the growth and DIC data in Graph 4.3.16, at around 1000 minutes. This same peak is visible in the co-culture runs (green and purple lines), but with a delay of 200-300 minutes. This delay could be attributed to the presence of the algae in the same vessel. Puzzling is the fact that the algal flasks, shows an increase of carbon dioxide levels (red lines). This peak occurs after 1700 minutes, the large stationary phase indicates that the microorganisms within the flasks are respiring. This event occurs for around 500 minutes, about 20 hours, perhaps the time it takes for a bacterial population to grown and wither.

4.4. Discussion

The aim of this investigation was to establish whether the co-culture of *S. obliquus* and *R. toruloides* would lead to an increase in microalgal biomass and consequently lipid production. The results show that a synergistic relationship does exist between the two microorganisms, however, unlike natural co-cultures maintaining the balance between the two partners proved to be more problematic. Firstly, the growth of each microorganism was evaluated as well as the lipid production of *S. obliquus* was measured in monocultures. As the microalga is the main partner of this investigation,

everything was designed keeping the algae growth in focus. This was achieved by sacrificing some of the lipid producing attributes of the yeast cells; not an uncommon factor when designing co-culture set-ups [88,89].

The data in Graph 4.3.1 showed that over a period of 50 days *S. obliquus* grew at a steady pace with a specific growth rate (μ) ranging from 0.48 to 0.002 day^{-1}. As lipogenesis occurs when microalgal cells are stressed [90], *S. obliquus* was subjected to nitrogen stress. Table 4.1.3 showed that the lipids increased with decreasing concentration of nitrate within the medium [38,62,64], this agreed with the results in Graph 4.3.6. To counteract the damage from nitrogen-deprived medium, the microalgae converged its pathways into storage lipid production. As the amount of available nitrogen diminished intracellular lipid production increased.

The maximum yield of FAMEs obtained was 22 %dry weight over a 12 day stress period, lower compared to the reported value of 33.2 %dry weight obtained with *S. obliquus* CCAP 276/3A grown in wastewaters [91]. However, in the lower limits of 22-27 %dry wt of *Scenedesmus* strains grown in synthetic medium. The pH evolution graph showed (Graph 4.3.2 B) an increase in the pH value, from starting pH of 6.2 (to which BBM was adjusted prior autoclaving) with advancing algal cell numbers, to settle at final values of 6.7 to 6.8, due to consumption of carbon dioxide and the replacement of this with oxygen molecules [92].

As the *R. toruloides* growth in YM medium would outcompete the microalgae, a modified medium, 0.3BBM+ was used. The medium decreased the maximum growth rate of the yeast from 1.88 h^{-1} to 0.08 h^{-1}. A balanced co-culture was key to the outcome for the experiment. At a high growth rate, the yeast would have underlying effects and shaded the microalgal cells [93]. Additionally, large amounts of carbon dioxide would either acidify the growth chamber or escape to the surroundings. In a few words, the algae would not grow better. Additionally, using nutrient rich medium would feed any bacterial cells associated with the microalgae, hindering the co-culture work.

Firstly, the effect of the yeast culture on the microalgae growth rate is depicted in Graph 4.3.7 and 4.3.8. On average, the growth rate for the Control flasks was 0.266day^{-1}, for the Start flasks 0.444 day^{-1}, for the Mid-flask 0.520 day^{-1} and 0.339 day^{-1} for the End flask.

In terms of growth rate, adding the yeast at the start of the co-culture (Start flask), provided a sudden burst to the number of algal cells; from an initial inoculum of $2.4x10^5$ cells/ml over the space of a day, the cells increase to $1.45x10^6$ cells/mL, a 6-fold increase compared to Control flasks. Thereafter, the microalgal growth rate decreases, perhaps the CO_2 available for the algae cells outweighs the demand and dissipated out of the flask. Likewise, the number of cells benefitting from such availability was lower when compared to mid-phase or end-phase cultures. The addition of the yeast had a greater effect on the Middle flask; shown by the boost in growth rate of microalgae cells from $9.8x10^5$ cell/mL to $3x10^6$ cells/mL, which is a 3-fold increase compared to the Control flasks. The End flask increased from $1.04x10^6$ cells/mL to $2.48x10^6$ cells/mL, a 2-fold increase compared to the Control flask. The statistical significance of the findings, is just shy of the values of $p<0.05$, with $p=0.06$ for the Middle flasks and the End flasks with $p=0.07$.

Though all flasks increased in cell numbers at the beginning of the inoculation, the effects were short lived, as the growth rate decreased with increasing pH (Table 4.4.1) couple with the yeast withering. All co-culture flasks increased from pH 6.2 to pH 8.3-8.5 (low alkaline). Similarly, the yeast monoculture pH increased but with a ceiling value of 7.5. This large change cannot be justified by decrease in available dissolved carbon dioxide alone [92] . The change in pH could be due to cell leakage, death and/or yeast extract degradation: however, there is not clear conclusion.

A closer look at the dynamics within the flasks (Graph 4.3.9) showed that the distribution of algae cells to yeast cells is close to be 1/3 of the total population. When looking at the growth of the yeast cells on their own, the CFU growth rates are higher, than when in co-cultures. The CFU rates were calculated as 0.405 day^{-1}, 0.399 day^{-1}, 0.398 day^{-1}, and 0.647 day^{-1}, for the Start, Middle, End and Yeast monoculture, respectively. Overall, all the co-culture flasks have shown an increase in microalgae cell numbers with the addition of the yeast. Significant changes in terms of cell numbers are shown in the End and Middle flasks. In graph 4.3.10, we analyse whether this has translated into higher production of lipids. The results show that an increase FAMEs productivity occurs for the Middle culture flasks. However, these values are significantly lower than the previously reported values for co-culture of yeast and algae (Table 4.1.3).

The highest amount of FAMEs obtained is in the region of 10% dry weight when in co-culture, however *S. obliquus* stress experiment showed that when stressed the microalgae can reach levels of FAMEs within the 20-22 % dry weight region. One of the reasons for the poor production of FAMEs is that *S. obliquus* required a form of stress, for example, nitrogen stress to induce the production of lipids. Furthermore, previous co-culture studies reported using rich medium (sugars in the form of syrups) that would boost the growth of the yeast with lipids accumulation up to 60 % of dry weight [71]. In contrast, the medium supplements used in this study only aid the yeast over a short time period. By slowing down the yeast growth, the trade-off has been its ability to produce high amounts of lipids [94,95]. This suggested that the published lipid accumulation results are largely contributed by the yeast. In this study, the addition of large concentrations of supplements was avoided in order to study the actual synergy, if any, that takes place between the two microorganisms.

It must be noted that bacteria are present within the co-culture set-up. The bacteria are endogenous to the microalgae cultures and efforts have been done to keep the number low. However, when adding yeast supplements to the medium, the bacterial population rapidly grows. A higher increase in bacteria would skew the results in terms of biomass calculations and decrease the effects that the two main microorganisms would have on each other. The presence of the bacteria may not be detrimental for the microalgae; however, it would pose problems in terms of evaluating the efficacy of the current study. The published literature does not highlight the presence of bacteria; however, during the trials conducted in the laboratory, it is hard to believe that these did not interfere.

The co-culture two-stage stress experiment showed the dynamics of the algae and yeast when subjected to stress (Graph 4.3.11). During stage (A), the average growth rate in the co-culture flasks (N+/-) was 3.6 times higher compared to the monoculture Algae flasks (N+/-), perhaps due to the higher rates of the yeast growth in the first 32 hours. However, the microalgae present in the co-culture twice as fast compared to the monocultures. In stage (B), the overall growth rates of the microalgae monocultures flasks increased due to new medium supplement (Algae N+), and as expected the growth rate of the Algae N- flasks decreased as the cells started accumulating storage lipids. This trend was replicated by the microalgae cells present in co-culture N-. Similarly, the yeast

growth rate decrease by almost 10-fold when stressed. Graph 4.3.12 shows ratio of yeast to algae during in co-culture flasks. The nitrate flasks show a net decrease for yeast cells after 120 hours, whilst the non-stress culture the yeast continues to grow. As the yeast cells die, so does the available CO_2 decrease. This is a flaw in the design, where a possible continued growth of the yeast would aid *S. obliquus* in growing also under stress conditions.

The biochemical composition of the flasks in terms of carbohydrates, protein and FAMEs is displayed in Table 4.3.3. Samples for the respective time points listed in the first column were analysed. During the co-culture period, from time point 0 to 3, the levels of carbohydrates within the microalgae cells is around 30% dw, with proteins in the range of 20% dw and FAMEs in the lower values of 2-3 %dry wt. The values for the FAME in the co-culture as well, are quite low: as no stress has been induced onto any for the flasks. The composition of the yeast during this time shows trends of carbohydrates decreasing with increasing proteins, whilst the amount of FAMEs generated is negligible. The data from time point 6-9 provide an overview on what is happening to the cells during non-stress (N+) nitrates stress (N-). In terms of carbohydrates, both monoculture and co-culture accumulate maximum amounts, 32 %dry wt and 42 %dry wt after 120 hours of nitrate stress. The maximum FAME accumulation in the stressed co-cultured cells was equal to 26 %dry wt, with the monocultures only reaching 16 %dry wt, and the yeast 11 %dry wt. Whilst, after 48 hours of co-culturing the non-stressed flasks accumulated 10 %dry wt at the point when yeast growth is at its maximum (around 24-32hours).

It is safe to assume that the majority of the lipids in the stressed co-culture belong to the algae. As *S. obliquus* is capable of mixotrophic growth, it should not be discounted that the microalgae is able to consume the organic carbon and nitrogen provided by the yeast debris. The same may apply to the monocultures of yeast, as the stress does not seem to hinder the presence of cells within the flask. The levels of carbohydrates, proteins and FAMEs in co-cultures, are shown to be higher compared to the monoculture of the microalgae, however results are not significant ($p>0.05$).

One noticeable feature was that the microalgae cells in co-culture dissociate into unicellular cells, whilst most of the cells in the monoculture of *S. obliquus* maintained their 4-cell colony. This may be caused by some of the molecules released by *R. toruloides*, or be a method used by the microalgae as a response to a foreign microorganism.

The DIC data showed the presence of CO_2 in all culture conditions. Finding high levels of CO_2 within the algae flasks, was puzzling as these microorganism use CO_2 to perform photosynthesis (Graph 4.3.14). However, upon closer observation of the flasks, it was clear that the added yeast extract had spurred the growth of the low population of bacteria found within the culture flasks. Therefore, the bacteria may be contributing to the added DIC within the medium. On the other hand, the carbon present within the yeast extract may be contributing to the amounts registered. The data obtained for the yeast monoculture, showed that DIC within the medium increased after 500 minutes of culturing (Graph 4.3.16). The same trend was seen in the co-culture flasks (Graph 4.3.15). Thus, within the co-culture set-up the CO_2 levels increased and decreased. The overall DIC within the co-culture flasks shows a trend of being generated by both the yeast and the bacteria present within the culture. The time points for each CO_2 peak and trough indicate that this may be the case.

Graph 4.3.17 show that carbon dioxide evolution data collected using the gas analyser. The peak for the yeast flasks as expected, occurred between 500 to 1000 minutes, as seen in the DIC data, the same peak is delayed in the co-cultures. The lag can be attributed to a slower yeast growth in the presence of the microalgae. However, in all runs the amount of carbon dioxide recorded in the co-culture flasks was more than what was generated by the yeast alone. This can again be attributed to the presence of the bacteria, which though hindered by the presence of a competitor are still able to thrive. The DIC data and the Gas analyser data tell the same story. Improvements to the set-up can be carried out in order to minimise the impact the bacterial population has on the algae by changing medium composition and introduction of yeast timing alongside the supplements. Other methods have been used in the literature to study the exchange of gases between algae and yeast. Puangbut and Lessing [96] cultivated the microalgae *Chlorella sp.* (KKU-S2) and the yeast *Torulaspora maleeae* (Y30) in separate reactors and

connected the gas emitted from the yeast reactor to obtain an overall lipid yield of 8.33g/L, of which 1.339g/L belonged to *Chlorella sp.* (KKU-S2). Santos et al. [97] use the fermentation off gas of *R. toruloides* as inlet gas for *Chlorella protothecoides* cultivation, with increase in biomass to 0.015g/L/h and lipid productivity of 2.2mg/L/hr. The results here show that also when directly mixed element of gas, or even substance exchange, which can be harnessed for biomass and lipid production.

4.5. Conclusion

The objective of this chapter was to demonstrate that a co-culture between *S. obliquus* and *R. toruloides* would lead to an overall increase in microalgae biomass and lipid productivity. The results show a higher concentration of FAME in the stressed co-culture, with values of 26 %dry wt compared to 16 %dry wt in the algae monoculture, however, this was not statistically significant ($p>0.05$). The inoculum size and stage of inoculation characterized the way in which the co-culture behaved. Furthermore, the DIC results indicated that gas exchange indeed played a significant role in establishing a synergy between algae and yeast. Improvements to this co-culture system can be made by not having to sacrifice yeast growth and lipid synthesis ability.

4.6. References

[1] Fernandes DLA, Pereira SR, Serafim LS, et al. Second Generation Bioethanol from Lignocellulosics: Processing of Hardwood Sulphite Spent Liquor. In: Lima MAR, editor. Bioethanol. InTech; 2012. p. 123–125.

[2] IEA. IEA Energy Technology Essentials. 2007.

[3] Stephenson PG, Moore CM, Terry MJ, et al. Improving photosynthesis for algal biofuels: toward a green revolution. Trends Biotechnol. 2011;29:615–623.

[4] UNFCCC. Fact sheet: The Kyoto Protocol. UNFCC. 2011;Fact sheet:1–8.

[5] Defra. Climate Change Act 2008. 2004 p. 111–128.

[6] Cox PM, Betts RA, Jones CD, et al. Acceleration of global warming due to carbon-cycle feedbacks in a coupled climate model. Nature. 2000;408:184–187.

[7] Leite GB, Abdelaziz AEM, Hallenbeck PC. Algal biofuels: challenges and opportunities. Bioresour. Technol. 2013;145:134–141.

[8] FAO. Sustainable Bioenergy: A Framework for Decision Makers. 2007.

[9] Zeng X, Danquah MK, Chen DX, et al. Microalgae bioengineering: From CO2 fixation to biofuel production. Renew. Sustain. Energy Rev. 2011;15:3252–3260.

[10] Yuan JS, Tiller KH, Al-Ahmad H, et al. Plants to power: bioenergy to fuel the future. Trends Plant Sci. 2008;13:421–429.

[11] Velea S, Dragos N, Serban S, et al. BIOLOGICAL SEQUESTRATION OF CARBON DIOXIDE FROM THERMAL POWER PLANT EMISSIONS , BY ABSORBTION IN MICROALGAL CULTURE MEDIA. Rom. Biotechnol. Lett. 2009;14:4485–4500.

[12] Sydney EB, Sturm W, de Carvalho JC, et al. Potential carbon dioxide fixation by industrially important microalgae. Bioresour. Technol. 2010;101:5892–5896.

[13] Salih FM. Microalgae Tolerance to High Concentrations of Carbon Dioxide: A Review. J. Environ. Prot. (Irvine,. Calif). 2011;02:648–654.

[14] Jaliliannosrati H, Kiakalaieh A, Zarei A. Comparison of Bioethanol and Biodiesel Feedstock with Futuristic- Look at Biofuel. Int. Conf. Environ. Energy Biotechnol. 2012;33:144–148.

[15] Posten C, Schaub G. Microalgae and terrestrial biomass as source for fuels--a process view. J. Biotechnol. 2009;142:64–69.

[16] Slade R, Bauen A, Shah N. The greenhouse gas emissions performance of cellulosic ethanol supply chains in Europe. Biotechnol. Biofuels. 2009;2:15.

[17] Richmond A. Microalgal biotechnology at the turn of the millennium: A personal view. J. Appl. Phycol. 2000;12:441–451.

[18] Li Y, Horsman M, Wu N, et al. Biofuels from Microalgae. Biotechnol. Prog. 2008;815–820.

[19] Huntley ME, Redalje DG. CO2 mitigation and renewable oil from photosynthetic microbes: a new appraisal. Mitig. Adapt. Strateg. Glob. Chang. 2007;12:573–608.

[20] Cuellar-Bermudez SP, Aguilar-Hernandez I, Cardenas-Chavez DL, et al. Extraction and purification of high-value metabolites from microalgae: Essential lipids, astaxanthin and phycobiliproteins. Microb. Biotechnol. 2015;8:190–209.

[21] Kazamia E, Riseley AS, Howe CJ, et al. An Engineered Community Approach for Industrial Cultivation of Microalgae. Ind. Biotechnol. 2014;10:184–190.

[22] Nigam P, Singh A. Production of liquid biofuels from renewable resources. Prog. Energy Combust. Sci. 2011;37:52–68.

[23] Nanda S, Dalai AK, Kozinski JA. Butanol and ethanol production from lignocellulosic feedstock: Biomass pretreatment and bioconversion. Energy Sci. Eng. 2014;2:138–148.

[24] Sims REH, Mabee W, Saddler JN, et al. An overview of second generation biofuel technologies. Bioresour. Technol. 2010;101:1570–1580.

[25] Alam F, Mobin S, Chowdhury H. Third generation biofuel from Algae. Procedia Eng. 2015;105:763–768.

[26] Chisti Y. Biodiesel from microalgae. Biotechnol. Adv. 2007;25:294–306.

[27] Parmar A, Singh NK, Pandey A, et al. Cyanobacteria and microalgae: a positive prospect for biofuels. Bioresour. Technol. 2011;102:10163–10172.

[28] Mahapatra DM, Chanakya HN, Ramachandra T V. Bioremediation and lipid synthesis through mixotrophic algal consortia in municipal wastewater. Bioresour. Technol. 2014;168:142–150.

[29] Abdel-Raouf N, Al-Homaidan a. a., Ibraheem IBM. Microalgae and wastewater treatment. Saudi J. Biol. Sci. 2012;19:257–275.

[30] Wijffels RH, Barbosa MJ. An Outlook on Microalgal Biofuels. Science (80-.). 2010;329:796–799.

[31] Griffiths MJ, Dicks RG, Richardson C, et al. Advantages and Challenges of Microalgae as a Source of Oil for Biodiesel. In: Montero MS and G, editor. Biodiesel - Feed. Process. Technol. InTech; 2011. p. 178–200.

[32] Malcata FX. Microalgae and biofuels: A promising partnership? Trends Biotechnol. 2011;29:542–549.

[33] Brennan L, Owende P. Biofuels from microalgae-A review of technologies for production, processing, and extractions of biofuels and co-products. Renew. Sustain. Energy Rev. 2010;14:557–577.

[34] Suali E, Sarbatly R. Conversion of microalgae to biofuel. Renew. Sustain. Energy Rev. 2012;16:4316–4342.

[35] Frigon JC, Matteau-Lebrun F, Abdou RH, et al. Screening microalgae strains for their productivity in methane following anaerobic digestion. Appl. Energy. 2013;108:100–107.

[36] Mata TM, Martins AA, Caetano N. Microalgae for biodiesel production and other applications: A review. Renew. Sustain. Energy Rev. 2010;14:217–232.

[37] Tran H, Known ZK, Oh Y, et al. Statistical Optimization of Culture Media for Growth and Lipid Production of Botryococcus braunii LB572. Biotechnol. Bioprocess Eng. 2010;15:277–284.

[38] Mandal S, Mallick N. Microalga Scenedesmus obliquus as a potential source for biodiesel production. Appl. Microbiol. Biotechnol. 2009;84:281–291.

[39] Yeh KL, Chang JS. Nitrogen starvation strategies and photobioreactor design for enhancing lipid production of a newly isolated microalga Chlorella vulgaris ESP-31: Implications for biofuels. Biotechnol. J. 2011;6:1358–1366.

[40] Huang XX, Huang ZZ, Wen W, et al. Effects of nitrogen supplementation of the culture medium on the growth, total lipid content and fatty acid profiles of three microalgae (Tetraselmis subcordiformis, Nannochloropsis oculata and Pavlova viridis). J. Appl. Phycol. 2013;25:129–137.

[41] Feng DN, Chen ZA, Xue S, et al. Increased lipid production of the marine oleaginous microalgae Isochrysis zhangjiangensis (Chrysophyta) by nitrogen supplement. Bioresour. Technol. 2011;102:6710–6716.

[42] Rodolfi L, Chini Zittelli G, Bassi N, et al. Microalgae for oil: strain selection, induction of lipid synthesis and outdoor mass cultivation in a low-cost photobioreactor. Biotechnol. Bioeng. 2009;102:100–112.

[43] Lee SJ, Go S, Jeong GT, et al. Oil production from five marine microalgae for the production of biodiesel. Biotechnol. Bioprocess Eng. 2011;16:561–566.

[44] Johnson MB, Wen ZY. Production of Biodiesel Fuel from the Microalga Schizochytrium limacinum by Direct Transesterification of Algal Biomass. Energy & Fuels. 2009;23:5179–5183.

[45] Abdollahi J, Dubljevic S. Lipid production optimization and optimal control of heterotrophic microalgae fed-batch bioreactor. Chem. Eng. Sci. 2012;84:619–627.

[46] Che Y, Walker TH. Biomass and lipid production of heterotrophic microalgae Chlorella protothecoides by using biodiesel-derived crude glycerol. Biotechnol. Lett. 2011;33:1973–1983.

[47] Kligerman DC, Bouwer EJ. Prospects for biodiesel production from algae-based wastewater treatment in Brazil: A review. Renew. Sustain. Energy Rev. 2015;52:1834–1846.

[48] Wen X, Du K, Wang Z, et al. Effective cultivation of microalgae for biofuel production: a pilot-scale evaluation of a novel oleaginous microalga Graesiella sp. WBG-1. Biotechnol. Biofuels. 2016;9:123.

[49] Ejikeme PM, Anyaogu ID, Ejikeme CL, et al. Catalysis in Biodiesel Production by Transesterification Process-An Insight. E-Journal Chem. 2010;7:1120–1132.

[50] Meher LC, Vidya Sagar D, Naik SN. Technical aspects of biodiesel production by transesterification - A review. Renew. Sustain. Energy Rev. 2006;10:248–268.

[51] Borges ME, Díaz L. Recent developments on heterogeneous catalysts for biodiesel production by oil esterification and transesterification reactions: A review. Renew. Sustain. Energy Rev. 2012;16:2839–2849.

[52] Kitcha S, Cheirsilp B. Enhanced lipid production by co-cultivation and co-encapsulation of oleaginous yeast Trichosporonoides spathulata with microalgae in alginate gel beads. Appl. Biochem. Biotechnol. 2014;173:522–534.

[53] Ratledge C. Regulation of lipid accumulation in oleaginous micro-organisms. Biochem. Soc. Trans. 2002;30:1047–1050.

[54] Donot F, Fontana A, Baccou JC, et al. Single cell oils (SCOs) from oleaginous yeasts and moulds: Production and genetics. Biomass and Bioenergy. 2014;68:135–150.

[55] Smith VH, Sturm BSM, DeNoyelles FJ, et al. The ecology of algal biodiesel

production. Trends Ecol. Evol. 2010;25:301–309.

[56] Weyer KM, Bush DR, Darzins A, et al. Theoretical Maximum Algal Oil Production. BioEnergy Res. 2009;3:204–213.

[57] Thompson P. Algal Cell Culture. In: Doelle HW, Rokem JS, Berovic M, editors. Biotechnol. - Vol. I Fundam. Biotechnol. EOLSS Publications; 2009. p. 67–109.

[58] Halim R, Danquah MK, Webley P a. Extraction of oil from microalgae for biodiesel production: A review. Biotechnol. Adv. 2012;30:709–732.

[59] Raja R, Shanmugam H, V G, et al. Biomass from Microalgae: An Overview. Oceanogr. Open Access. 2014;02:1–7.

[60] Pawlak B, Kopec J. Size distributions of Scenedesmus obliquus cells : experimental results from optical microscopy and their approximations using the φ -normal distribution. Oceanologia. 1998;40:345–353.

[61] Breuer G, Lamers PP, Martens DE, et al. Effect of light intensity, pH, and temperature on triacylglycerol (TAG) accumulation induced by nitrogen starvation in Scenedesmus obliquus. Bioresour. Technol. 2013;143:1–9.

[62] Ho S-H, Chen C-Y, Chang J-S. Effect of light intensity and nitrogen starvation on CO2 fixation and lipid/carbohydrate production of an indigenous microalga Scenedesmus obliquus CNW-N. Bioresour. Technol. 2012;113:244–252.

[63] Ho SH, Chen WM, Chang JS. Scenedesmus obliquus CNW-N as a potential candidate for CO2 mitigation and biodiesel production. Bioresour. Technol. 2010;101:8725–8730.

[64] Xin L, Hong-ying H, Ke G, et al. Effects of different nitrogen and phosphorus concentrations on the growth, nutrient uptake, and lipid accumulation of a freshwater microalga Scenedesmus sp. Bioresour. Technol. 2010;101:5494–5500.

[65] Breuer G, Lamers PP, Martens DE, et al. The impact of nitrogen starvation on the dynamics of triacylglycerol accumulation in nine microalgae strains. Bioresour. Technol. 2012;124:217–226.

[66] El-Baz F, Abdo S, Ali G. Enhancement of oil accumulation in microalga Scenedesmus obliquus. Int. J. Pharm. Sci. Rev. Res. 2016;35:110–115.

[67] Xia L, Song S, Hu C. High temperature enhances lipid accumulation in nitrogen-deprived Scenedesmus obtusus XJ-15. J. Appl. Phycol. 2016;28:831–837.

[68] Meesters PAEP, Huijberts GNM, Eggink G. High-cell-density cultivation of the lipid accumulating yeast Cryptococcus curvatus using glycerol as a carbon source. Appl. Microbiol. Biotechnol. 1996;45:575–579.

[69] Sitepu IR, Garay L a, Sestric R, et al. Oleaginous yeasts for biodiesel: current and future trends in biology and production. Biotechnol. Adv. 2014;32:1336–1360.

[70] Braunwald T, French WT, Claupein W, et al. Economic Assessment of microbial

Biodiesel Production Using Heterotrophic Yeasts. Int. J. Green Energy. 2014;5075:141027055806000.

[71] Lee J, Chen WW. The Production, Regulation and Extraction of Carotenoids from Rhodosporidium toruloides. J. Mol. Genet. Med. 2016;10:14–16.

[72] Fei Q, O'Brien M, Nelson R, et al. Enhanced lipid production by Rhodosporidium toruloides using different fed-batch feeding strategies with lignocellulosic hydrolysate as the sole carbon source. Biotechnol. Biofuels. 2016;9:130.

[73] Li Y, Zhao Z (Kent), Bai F. High-density cultivation of oleaginous yeast Rhodosporidium toruloides Y4 in fed-batch culture. Enzyme Microb. Technol. 2007;41:312–317.

[74] Cheirsilp B, Suwannarat W, Niyomdecha R. Mixed culture of oleaginous yeast Rhodotorula glutinis and microalga Chlorella vulgaris for lipid production from industrial wastes and its use as biodiesel feedstock. N. Biotechnol. 2011;28:362–368.

[75] Shu CH, Tsai CC, Chen KY, et al. Enhancing high quality oil accumulation and carbon dioxide fixation by a mixed culture of Chlorella sp. and Saccharomyces cerevisiae. J. Taiwan Inst. Chem. Eng. 2013;44:936–942.

[76] Fukami T. Historical contingency in community assembly : integrating niches, species pools, and priority effects. Annu. Rev. Ecol. Evol. Syst. 2015;46:1–23.

[77] Loeuille N, Leibold M a. Evolution in metacommunities: on the relative importance of species sorting and monopolization in structuring communities. Am. Nat. 2008;171:788–799.

[78] Yen HW, Chen PW, Chen LJ. The synergistic effects for the co-cultivation of oleaginous yeast-Rhodotorula glutinis and microalgae-Scenedesmus obliquus on the biomass and total lipids accumulation. Bioresour. Technol. 2015;184:148–152.

[79] Wu S, Hu C, Jin G, et al. Phosphate-limitation mediated lipid production by Rhodosporidium toruloides. Bioresour. Technol. 2010;101:6124–6129.

[80] Zhu Z, Zhang S, Liu H, et al. A multi-omic map of the lipid-producing yeast Rhodosporidium toruloides. Nat. Commun. 2012;3:1112.

[81] Liu H, Zhao X, Wang F, et al. Comparative proteomic analysis of Rhodosporidium toruloides during lipid accumulation. Yeast. 2009;26:545–551.

[82] Shen Y, Yuan W, Pei Z, et al. Heterotrophic Culture of Chlorella protothecoides in Various Nitrogen Sources for Lipid Production. Appl. Biochem. Biotechnol. 2010;160:1674–1684.

[83] Cescut J, Fillaudeau L, Molina-Jouve C, et al. Carbon accumulation in Rhodotorula glutinis induced by nitrogen limitation. Biotechnol. Biofuels. 2014;7:164.

[84] Wang R, Tian Y, Xue S, et al. Enhanced microalgal biomass and lipid production

via co-culture of Scenedesmus obliquus and Candida tropicalis in an autotrophic system. J. Chem. Technol. Biotechnol. 2015;9:Pages.

[85] Xue F, Miao J, Zhang X, et al. A new strategy for lipid production by mix cultivation of Spirulina platensis and Rhodotorula glutinis. Appl. Biochem. Biotechnol. 2010;160:498–503.

[86] Shu C-H, Tsai C-C, Chen K-Y, et al. Enhancing high quality oil accumulation and carbon dioxide fixation by a mixed culture of Chlorella sp. and Saccharomyces cerevisiae. J. Taiwan Inst. Chem. Eng. 2013;44:936–942.

[87] Corcoran A., Boeing WJ. Biodiversity Increases the Productivity and Stability of Phytoplankton Communities. PLoS One. 2012;7:e49397.

[88] Padmaperuma G, Kapoore RV, Gilmour DJ, et al. Microbial consortia: a critical look at microalgae co-cultures for enhanced biomanufacturing. Crit. Rev. Biotechnol. 2017;0:1–14.

[89] Goers L, Freemont P, Polizzi KM. Co-culture systems and technologies: taking synthetic biology to the next level. J. R. Soc. Interface. 2014;11:20140065–20140065.

[90] Markou G, Nerantzis E. Microalgae for high-value compounds and biofuels production: a review with focus on cultivation under stress conditions. Biotechnol. Adv. 2013;31:1532–1542.

[91] Das D. Algal Biorefinery: An Integrated Approach. 2015.

[92] Chi Z, O'Fallon J V, Chen S. Bicarbonate produced from carbon capture for algae culture. Trends Biotechnol. 2011;29:537–541.

[93] Richmond A. Principles for attaining maximal microalgal productivity in photobioreactors: an overview. Hydrobiologia. 2004;512:33–37.

[94] Duffy JE, Cardinale BJ, France KE, et al. The functional role of biodiversity in ecosystems: incorporating trophic complexity. Ecol. Lett. 2007;10:522–538.

[95] Matthiessen B, Hillebrand H, Ptacnik R. Diversity and community biomass depend on dispersal and disturbance in microalgal communities. Hydrobiologia. 2010;653:65–78.

[96] Puangbut M, Leesing R. Integrated Cultivation Technique for Microbial Lipid Production by Photosynthetic Microalgae and Locally Oleaginous Yeast. World Acad. Sci. Eng. Technol. 2012;64:975–979.

[97] Santos C, Caldeira M, Lopes da Silva T, et al. Enhanced lipidic algae biomass production using gas transfer from a fermentative Rhodosporidium toruloides culture to an autotrophic Chlorella protothecoides culture. Bioresour. Technol. 2013;138:48–54.

Chapter 5: Extracellular signals

5.1. Introduction

Co-cultures have been successfully used in biomanufacturing [1], food production [2], bioremediation and biofuel production [3,4]. However, their success is not yet fully understood [1] as extra-species cell-to-cell interactions have proven a challenge to understand and characterise. The challenge is to understand to which microorganism a particular molecule belongs. Furthermore, biomolecular signals change from scenario to scenario, making the fingerprinting even more arduous. However, the potential in co-culturing for industrial application for large-scale production is driving research in this field with the aim of devising microbial platforms for multi-fit purposes [5].

Deciphering cell-to-cell interactions holds the key to unravelling the conundrum [6], which govern microbial networks. Research demonstrated that cells can mediate amongst themselves with the aid of biomolecules. Molecules are released for a specific purpose, be this communication, a command signal or a nutrient [7]. Various factors can cause the triggering of the molecules, be this abiotic or biotic stresses. Symbiotic and antagonistic interactions will also see the release of different molecules from a specific species [8].

In Chapter 3, the *D. salina*, *Halomonas* and *H. salinarum* consortia revealed that the association between algal and bacterium/archaeon lead to an increase in the propagation of the microalgal cells. In a similar manner, the presence of the yeast *R. toruloides "*boosted" the growth of *S. obliquus* (Chapter 4). Both studies have shown that associating microalgae with other organisms improved biomass yields. However, it was unclear which parameters governed these associations. Extracellular biomolecules and perhaps gaseous exchange are the first things that came to mind. For example, in the *D. salina* study, microalgal glycerol was a source of carbon for both aiding heterotrophic microorganisms, and in return, these provide the microalga with nutrients to withstand environmental stresses. In the second scenario, the DIC results showed that carbon dioxide and oxygen exchange played a major role in the association of algae and yeast. However, these cannot be the only factors that fashion species interactions:

therefore, an analysis of the extracellular supernatant resulting from some of the co-culture scenarios was carried out. The exopolymeric substances (EPS) derived from the supernatant of directly mixed liquid cultures were analysed for their total carbohydrate and protein contents. The presence of quorum sensing (QS) signals from *Halomonas*, *H. salinarum* and *R. toruloides* were also investigated when in co-culture.

Lastly, a novel approach to trap and monitor the intracellular signalling was proposed to better understand the interactions between *S. obliquus* and *R. toruloides*. Liquid medium used for growth was replaced by its solid form (agar). During co-cultivation in liquid medium, microbial metabolites were secreted into the growth medium. The large volumes used in cultivation diluted the concentrations of secreted metabolites further. To be able to isolate these small molecules, various steps of sample concertation were required. These procedures may lead to the loss or breakdown of the product, thus affecting the reproducibility of the results across biological samples. By replacing the liquid medium with agar, it was possible to trap metabolites in concentrations suitable for GC-MS identification.

5.1.1. Exopolymeric substances (EPS)

Exopolymeric substances (EPS) are released into the environment for various purposes, including, cell protection, signalling, pathogen–host interactions, disease management and creating micro-environments [9]. Within the EPS we find macromolecules such as protein, carbohydrate, uronic acid, humic substances and nucleic acids [10]. The EPS found within a culturing environment, will differ as a direct effect from species, strain, substrate types, nutrition, temperature, pH, salinity, mixing and the age of the cultures [10]. Examples of EPS are provided in Table 5.1.1.

Table 5.1.1: Examples of Extracellular compounds derived from microbial organisms

Extracellular compounds	Examples	Examples of species which release these compounds	Ref.
EPS	Carbohydrates (glucose, galactose, arabinose, xylose, mannose)	Many algae: *Dunaliella sp., Chlorella sp., Chlamydomonas sp., Oocystis sp., B. braunii, Scenedesmus sp., Spondylosium panduriforme, Hyalotheca dissiliens.* Biofilms	[10,11] [12]
	Glycoprotein	Common in green algae (*D. tertiolecta, C. vulgaris*)	[10]
	Proteins	Bacteria, yeast and algae	
	Silica-associated extracellular proteins	Diatoms: *A. coffeaeformis, Amphora sp., and C. closterium.* Red algae: *R. maculate, P. cruentum and Porphyridium*	
Exoenzymes	Alkaline phosphates	*Proteus mirabilis* (bacteria)	[13]
	Proteases	*Sporidiobolus ruineniae* (yeast) *Burkholderia cenocepacia* (bacteria) *Chlamydomonas coccoides* and *D. salina*	[14] [15] [16]
Organic acids	Lactic acids	*S. incrassatulus*	[16]
	Aminolevulinic acid	*Rhodopseudomonas palustris, E. coli*	[17]
	Glycolic acid	*Tetraselmis gracilis, Chlorella cells*	[16]
	Folate acid (Vit B_{12})	*Mesorhizobium loti* (bacterium) *D. salina* (algae)	[18,19] [20]
Allelopathic chemicals	Fatty acids	*Ochromonas Danica* *Platymonas viridis* and *Nephrochloris salina*	[16]
	Polyunsaturated Aldehydes	Diatoms: *Thalassiosira sp., Skeletonema marinoi*	[21–23]
	Alkaloids	*Calothrix sp, Nostoc sp , Nodularia sp.*	[16,22]
	Peptides	*Anabaena flosaquae* and other Cyanobacteria	[22]
	Methanol	Cyanobacteria: *Synechococcus spp.* 8102/8103T, *Richodesmium erythraeum, and Prochlorococcus marinus* Diatom: Phaeodactylum tricornutum, Coccolithophore: *Emiliania huxleyi*, *Cryptophyte: Rhodomonas salina*, Green alga: *Nannochloropsis oculata*	[24]
	Glycerol	*D. salina*	[25]

Furthermore, Mahapatra & Banerjee [26] provided a detailed compendium on distribution of the most common fungal EPS compounds. The work conducted by Flemming & Wingender [27] elucidated on the role of EPS in complex dynamic systems such as biofilms. The EPS material do not only act as a communication network, but also provide stability and external digestive system by keeping extracellular enzymes close to the cells, enabling them to metabolise dissolved, colloidal and solid biopolymers. Similarly, Decho [28] highlighted the role of EPS as a food network in marine microbial communities.

Quorum sensing, allelopathic, inter-kingdom metabolites, cell-to-cell signalling, are different ways in which microorganisms are known to interact with each other within a consortium (Table 5.1.1). These signals are dispersed/secreted into the growth environment by bacteria, fungi, algae, yeast and other microorganisms. The release of these signals will vary in composition and concentration, depending on the growth environment and the intent for which they were dissipated [10,29].

5.1.2. Metabolites

Metabolites have various functions, including fuel, structure, and signalling, stimulatory and inhibitory effects on enzymes, catalytic activity of their own (usually as a cofactor to an enzyme), defence, and interactions with other organisms (e.g. pigments, odorants, and pheromones). In a similar fashion, quorum signals are secreted into the environment and include auto inducers I and II [30].

5.1.3. Quorum sensing

The survival of the consortium will depend on two major features: the first being the ability of the cells to communicate within and between species based on population density (quorum sensing) through molecular signals or exchange of metabolites, and the second being division of labour [7,31–33]. Quorum sensing is a term coined to describe population density driven cell-to-cell signalling in prokaryotes [30]. This method of networking is largely used by bacteria to coordinate communal behaviour, for example in biofilm formations [34]. This is achieved by the release of signalling micromolecules called autoinducers, which increase in abundance in correlation to bacterial population [35]. When this occurs within a mixed community, the other organisms, be they plant cells, mammalian cells and/or algae may secrete molecules that may hinder or enhance

the quorum sensing molecules [36]. Amongst QS molecules a well characterized group are N-acylhomoserine lactones (AHLs) used by Gram-ve proteobacteria, such as *Halomonas* [34].

5.1.4. Allelochemicals

Allelochemicals are biomolecules released by an organism into its surrounding to help it grow, survive and/or reproduce. These can range from fatty acids to alkaloids, peptides and amino acid molecules. The release of these compounds is affected by abiotic and biotic factors, suggesting the possibility of controlling, and perhaps, directing a consortium's behaviour. Allelochemicals can also be used to pinpoint and determine species abundance, allowing for bioassay and chemical analysis methods to be developed for the monitoring of mixed cultures [22,37]. Some allelochemicals can be beneficial, whilst others are toxic [38]. These signalling mechanisms can give an indication regarding the behaviour of single species within a community and the changes that may result due to environmental factors, competition, and space allocation; all this while providing information on how to 'drive' the consortium production. Microalgae are known to release allelochemicals into the growth environment to hinder/aid or communicate with intra and extra-species [16,39,40].

5.2. Experimental Design

Specific details relevant to the experimental design are provided in this section. Protocols for analytical techniques are compiled in Chapter 2: these will be referred to throughout the text.

5.2.1. Liquid Cultures

The EPS analysis presented in this section was carried out on liquid medium cultures.

5.2.1.1. Exopolymeric substances in liquid cultures

The EPS synthesised by microbes vary greatly in composition depending upon their environment [10,29]. The supernatant for co-cultures of *D. salina* and *Halomonas*, and *S. obliquus* and *R. toruloides* were further investigated, as these two co-cultures showed a significant increase in microalgae biomass. Here the focus is to characterise the EPS collected in terms of total carbohydrates and proteins.

5.2.1.1.1. Collecting the supernatant

The microorganisms for the *D. salina* co-culture study were grown as monoculture and co-cultures as described in section 2.2.1. *D. salina* was grown in 3 M HEPES, followed by the co-culture with *Halomonas* in 3 M HEPES+. The bacterium was grown in the modified medium in order to assess its EPS production behaviour in such medium. Likewise, the *S. obliquus* co-culture was grown as detailed in section 2.2.4: with the yeast and co-culture growing in supplemented medium BBM+ and the algae in BBM medium. The flasks were harvested (section 2.3.1). The supernatant was collected and sterilised using 0.22 µm Millipore filter to being stored at -20 °C. Up to 300 mL of supernatant was collected in triplicates for microalgae containing flasks (monoculture and co-culture) and 200 mL for bacteria and yeast monoculture flasks, biological triplicates were analysed.

5.2.1.1.2. Dialysing and concentrating the supernatant

All supernatants were dialysed using Snakeskin® Dialysis Tubing (Thermo Scientific 68035), 3500MWCO. Dialysis was conducted to minimise the impact of salts on the analytical assays. The conductivity of the dialysed samples was measured to estimate the concentration of salts. All samples for *D. salina* were dialysed from 3 M to less than 200 mM salts and samples generated from *S. obliquus* co-culture were dialysed even further in the range of 30-40 mM. All dialysed samples were frozen -20 °C and lyophilised. The resulting EPS was then resuspended in 1mL of MilliQ water and stored at -20 °C for future analysis.

5.2.1.1.3. Analysis of supernatant

Total carbohydrates and proteins were evaluated from the resulting EPS, methods outlined in section 2.5.9 and 2.5.10 respectively. SDS-gels were run to identify any significant changes in extracellular proteins (see 2.5.11 protocol).

5.2.1.2. Screening for quorum sensing and inhibiting molecules

As detailed in section 5.1.3 quorum sensing molecules are believed to shape the outcome of a consortium; with bacteria and yeast known to release these with rising populations [7]. In order to investigate, whether there were any changed in the QS molecules released by *Halomonas and R. toruloides* a bioassay that would enable the detection of quorum sensing (QS) and quorum sensing inhibiting (QSI) molecules, in monoculture and co-culture exudates.

Bioassay for pure cultures and co-culture of *D. salina* with *Halomonas* and *H. salinarum*, alongside the *S. obliquus* and *R. toruloides* were performed. The supernatants deriving from experiment 3.3.4 (DS co-culture stress) and from the co-culture of yeast and algae in section 4.2.5 were tested using *Chromobacterium violaceum* CV026 biosensor system as detailed in Lv et al., and Anbazhagan et al., [36,41].

Chromobacterium violaceum (CV) is an organism that detects AHL molecules by synthesising endogenous C6-HSL compound to the receptor protein CViR, thus when in contact with QSI from other organisms, the cells turn from purple to white. The mutant, *C. violaceum* 026 (CV026), on the other hand, is unable to synthesise the C6-HSL compound, but is able to respond to the C6-HSL and C4 HSL compounds, providing a visual indication by the cells turning from white to purple. The strains of *C. violaceum* (ATCC 12472) were obtained from Professor Paul Williams' laboratories at The University of Nottingham.

5.2.1.2.1. CV026 biosensor assay

Both CV026 and CV were maintained in glycerol stock at -80 °C, with 25 µg/ml of kanamycin added to the 026 strain. Fresh LB plates of CV026 and incubated at 30 °C. Single colonies from each plate were resuspended in 5 mL of LB broth and incubated at 30 °C for 24 hours in a shaking incubator, at 150 rpm. The following day, the cells were measured at OD_{600nm} using a spectrophotometer. The cells were resuspended in the required volume of 0.5 %w/v in 20 mL of LB agar (soft agar), to obtain an optical density of 0.01 OD_{600nm}.

The 20 mL of the soft agar containing the cells were overlayed onto pre-made 20 mL of R2A agar plates. The plates were left to solidify before punching 3mm diameter wells, using cut pipette tips, as shown in the schematic below.

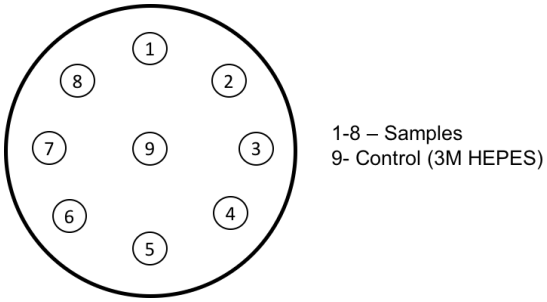

Figure 5.2.1: Picture representing the overlaid R2A plates with CV026/CV cells in soft LB agar.

The cell free supernatant from the experimental cultures was dispensed in volumes of 100 µL per well. The plates were then placed in a static incubator, at 30 °C for 24 hours.

5.2.2. Solid Cultures

Work undertaken here was performed on agar.

5.2.1.3. Metabolites detection in co-culture agar plates

The method used for isolation of EPS would not allow for the trapping of smaller molecules, <1kDA, such as metabolites. Furthermore, some molecules may be lost or degraded during the process of dialysis and lyophilisation. Within the liquid cultures, the metabolites would be diluted and during the concentration steps be denatured or escape into the surroundings. Looking at the literature various techniques have been used to understand the interactions between microorganisms, such as: pelletisation [42], biofilm matrices [41], bead encapsulation [43] , and agar-plate culturing [44].

For the purpose of this investigation, the co-culture of *S. obliquus* and *R. toruloides* was cultured on agar. This co-culture was chosen, as the 3M salts in the *D. salina* agar created complications in terms of plating and extraction. Developing the method for the freshwater co-culture would provide an indication on how to tackle the hypersaline one in the future. Preliminary work to check for extraction efficiency of amino acid standards from agar plugs was carried out using Direct Infusion Electrospray ionisation (DESI-MS). The data gathered from the DESI-ESI helped to design the experiment and to test the methods used for the extraction of the samples. GC-MS was later used for metabolites analysis as deemed a more robust method of analysis [23,45]

5.2.1.2.2. Duo-plates: co-culture agar plates

Duo-plates consisted of a concentric agar plate made with the aid of stainless steel moulds (autoclavable), with the middle consisting of BBM agar (Bold's Basal agar) surrounded by YM (Yeast Mold agar) medium or BBM+ (0.3 g/L of yeast extract) agar. The respective agars were made as described in 2.2.4 and 2.2.5.

Briefly, the stainless-steel mould (ID: 44mm, OD: 4.7mm, thickness: 3mm) was autoclaved, dried and placed in the middle of the petri dish. BBM agar was melted with the use of a microwave and 6.5mL placed in the middle of the stainless-steel moulds. After the agar solidified the stainless-steel moulds were removed and 13mL of YM or BBM+ pre-melted agar was pipetted into the surrounding area. This was left to cool down in the laminar flow hood for 35 minutes or until the steam had escaped. The dishes

were then sealed and stored in a dark cupboard at room temperature. Prior to use the plates were UV sterilised.

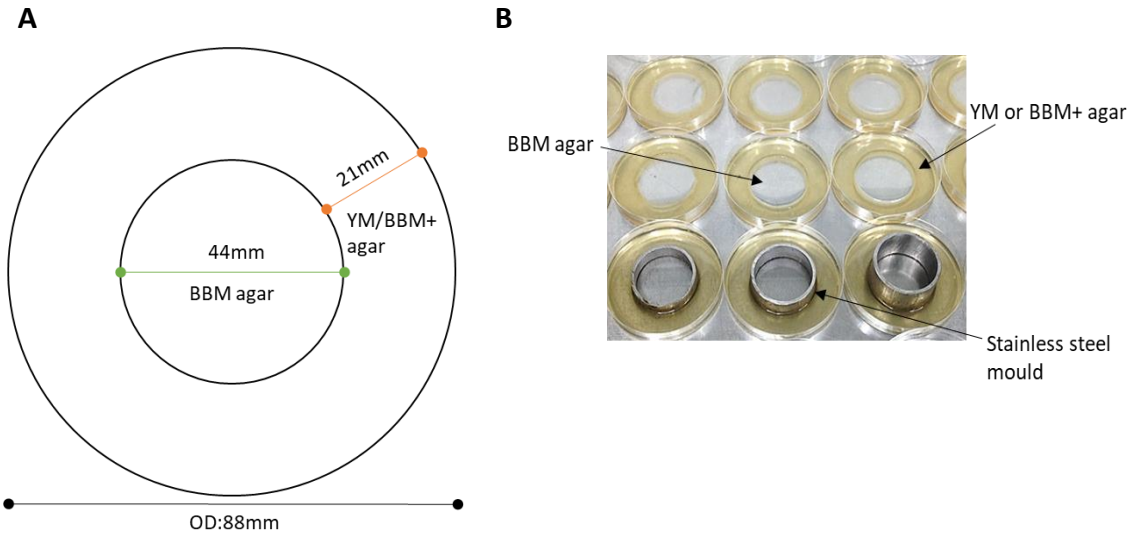

Figure 5.2.2: (A) Schematic representation of the co-culture plate. (B) Picture of the duo-plates.

6.5mL of BBM agar was placed in the middle of the well, surrounded by 13mL of YM agar or BBM+ agar. The algae would be spread in the middle, whilst the yeast would be inoculated on the outskirts.

5.2.1.2.3. Inoculation and sampling of the plates

Trials were conducted to check which best concentration and volume combination of microalgae and yeast would be suitable for spreading. Spreading the algae straight from the culture flasks proved to be erroneous, as the diluted samples would take time to propagate. Furthermore, any traces of bacteria overtook the algae by feeding on the yeast extract or the rich medium in YM agar from the surrounding agar. Thus, concentrated aliquots of algae in the exponential phase were tested. The results obtained indicated that this method would be suitable. Additionally, a quick survey revealed that the YM agar would be best suited for the purpose of this study.

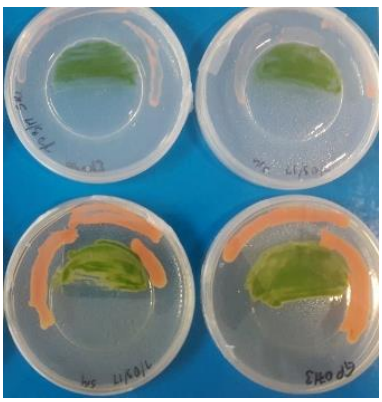

Figure 5.2.3: Evaluating best agar combination for co-culture growth

This test demonstrated that the algae co-cultured on the duo-plates with the yeast on YM medium grew better and faster when compared to the BBM+ agar for yeast growth. Santos et al. [46] *showed that CO_2 released was proportional to the growth rate of yeasts. Therefore, high proliferation leads to an increase of available CO_2 for the algae to use.*

The plates were inoculated as follows. *S. obliquus* was first grown in liquid medium detailed in section 2.2.4. Upon reaching an OD_{595nm}=0.6, 1 mL/plate of culture was spun down. The supernatant was removed and the cells were washed with fresh medium. The cells were then spun down again, the supernatant was discarded and cells resuspended in 40 µL of fresh medium (per plate). Similarly, *R. toruloides* was grown in YM medium (section 2.2.5) until an OD_{595nm} of 0.5 was reached. The OD was first adjusted to 0.1 and then concentrated. The concentrated cells were then resuspended in 10 µL per sample. After inoculation, all Petri dishes were sealed with Parafilm, to prevent contamination. Additionally, five Petri dishes containing 19.5 mL agar of distilled water and yeast medium agar respectively were made. Plugs from these plates served as negative controls for the experiment. The co-culture plates were illuminated at 105-115 µmol m^{-2} s^{-1} and grown at room temperature, 23 $\pm$ 1 ℃. The plates were cultured for 11 days; sampling on day 0 (just after inoculation), 3, 5, 7, 9 and 11.

Table 5.2.1: Legend for the duo-plate co-culture experiment

Plate label	SO	SOY	Y
S. obliquus	√	√	×
R. toruloides	×	√	√

Table 5.2.1 provides the nomenclature used in this chapter for the duo-plate co-culture experiment. A tick mark indicates that the organism was present, whilst a cross indicates the absence of it on the co-culture plate.

5.2.1.2.4. Sampling for metabolites

Sample plugs were collected using autoclaved 1 mL pipette tips whose ends were cut to measure 4-5 mm. Two technical replicates per plate were sampled, for which three plugs were pooled together and stored in 2 mL Safe-Lock Eppendorfs at -80 ˚C. The same was done for the negative control plates. Representative plugs per plate were weighed for establishing the concentration of metabolites in said volume. Yeast-Algae (Y-A plate) duo-plates were inoculated in biological quintuplets, whereas biological triplicates were arranged for Algae only (A-plates) and Yeast only (Y-plate) plates as shown in Figure 5.2.4.

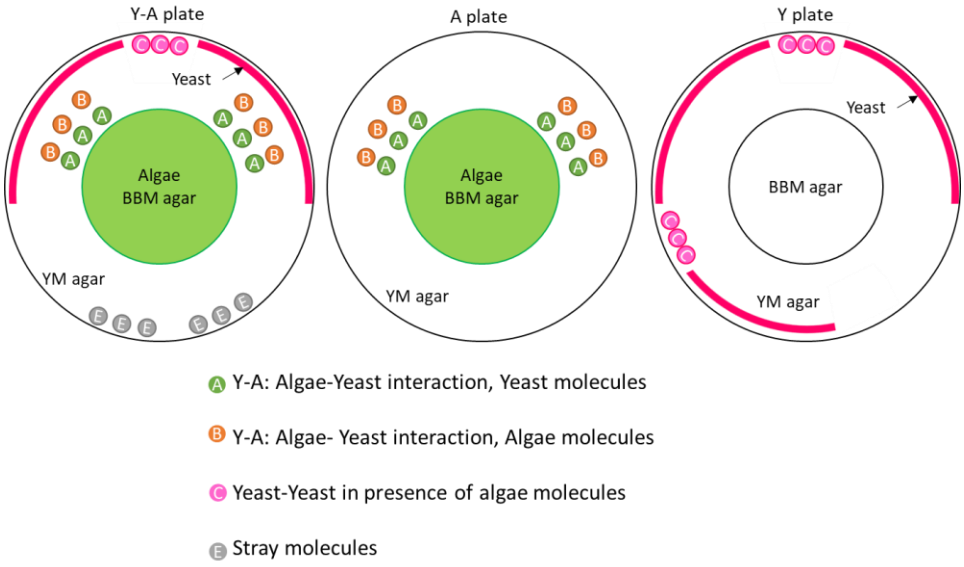

Figure 5.2.4: Co-culture of algae and yeast on duo-plates. A, B, C and E indicate sampling points.

The sampling points indicated were chosen in order to trap the most significant interactions between the microorganisms. Sampling points A and B trapped molecule exchange between *S. obliquus* and *R. toruloides*. Sample point C accounted for the molecules exchanged between yeast colonies in the presence of algae, whilst point E looked at stray-molecules released from the algae in presence of the yeast. The control plates, A-plate and Y-plate, were sampled using the same method, in order to establish any difference in metabolite profiles. The plugs were extracted, derivatized and injected into GC-MS for the detection of metabolites (see section 2.5.12 for details).

5.2.1.2.5. Sampling for optical density

Optical density measurements were taken for both algae and yeast grown on the plates. In a similar way to the sampling for metabolites, plugs were cut out using a 1 mL pipette from areas where each of the microorganisms had grown. As the growth was not uniform, the plugs were taken from various regions in the plate to account for any variations. Each plug was resuspended in 1 mL of growth medium. These were then vortexed until the cells would detach from the agar surface. Once the microorganism has dislodged, readings were taken with the spectrophotometer, at OD_{750nm}, OD_{680nm} and OD_{595nm}.

5.2.1.4. Duo-plates with gaps

The results obtained in Chapter 4, showed that gaseous exchange played a role in spurring the growth rate of the algae. Here, we investigate if this is true for the duo-plates scenario. As the plates are sealed with Parafilm, no gas should escape or enter the chamber. The gap separated the two microorganisms, mimicking transwell or segregated culturing techniques [47,48]. The optical density of the flasks was measured over time.

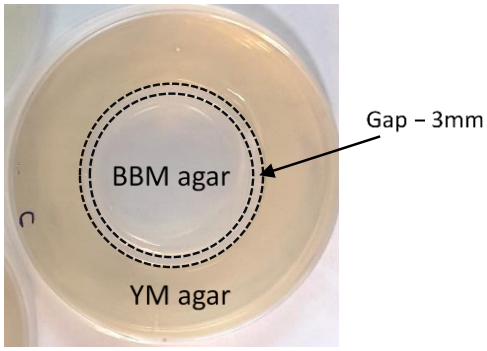

Figure 5.2.5: Duo-plates with gaps.

The agar plate was made following the procedure in section 5.3.3.1, with a modification. In this case, both the BBM agar and the YM agar were added into the mould at the same time. After everything had solidified, the mould was removed, leaving a 3mm gap between the two phases. The plates were inoculated and sampled in the same way as described in section 5.2.1.2.3 and 5.2.1.2.5.

5.3. Results

5.3.1. Liquid Cultures

5.3.1.1. Extracellular polysaccharides in liquid cultures

Extracellular supernatant from the two co-culture studies was analysed for total carbohydrates and total proteins. Subsequently, the proteins were run on SDS-gels to check if there were any distinguishable variations between the monoculture and the co-culture set-ups.

Graph 5.3.1: Total carbohydrates for all co-culture set-ups. (A) *D. salina* co-cultures and in (B) *S. obliquus* co-culture data. Standard error for triplicate biologicals replicates.

The results in Graph 5.3.1 showed the variation in extracellular carbohydrates between algae and bacteria or yeast: with carbohydrates in the hypersaline study 10 times larger than in the freshwater study. As the Snakeskin® Dialysis Tubing only retained molecules smaller than 3,500 kDa, it is possible to assume the carbohydrates detected are long-chain polysaccharides.

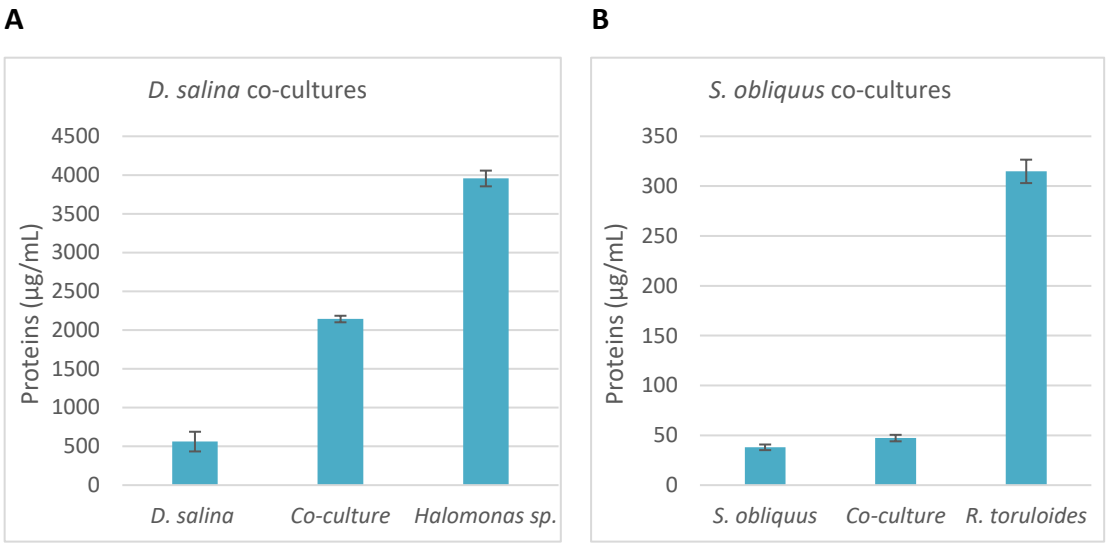

Graph 5.3.2: Total proteins for all co-culture set-ups. (A) *D. salina* co-cultures and in (B) *S. obliquus* co-culture data. Standard error for triplicate biologicals replicates.

EPS proteins are shown in Graph 5.3.2. The concentration of proteins between the hypersaline and the freshwater co-cultures differ by a magnitude of 10. However, the ratio between the protein secretion in *D. salina/Halomonas* co-culture is 1:4:8, whilst in the *S. obliquus/R. toruloides*, the same is 1:1:6.

5.3.1.2. Protein gels

SDS-protein gels were run to check if there were any differences between monoculture and co-culture flasks.

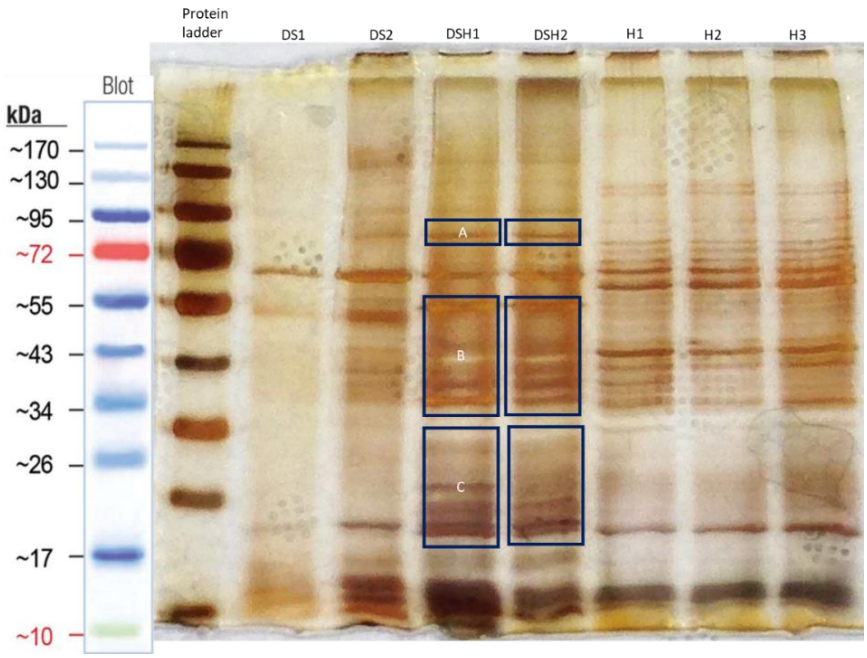

Figure 5.3.1: Protein gel for *D. salina* monoculture and co-culture system.
DS1 and DS2: D. salina monoculture,
DSH1 and DSH2: D. salina and Halomonas co-culture,
H1, H2, H3: Halomonas monoculture.

Figure 5.3.1 shows the difference in protein bands between the monoculture of algae and bacteria and their co-culture. In the region of 95 kDa (A), between 55k-34 kDa and between 25-20 kDa, protein expression in the co-culture is quite prominent. These regions are not present in either monoculture flasks. Indicating that their presence is purely due to the interaction between the two species.

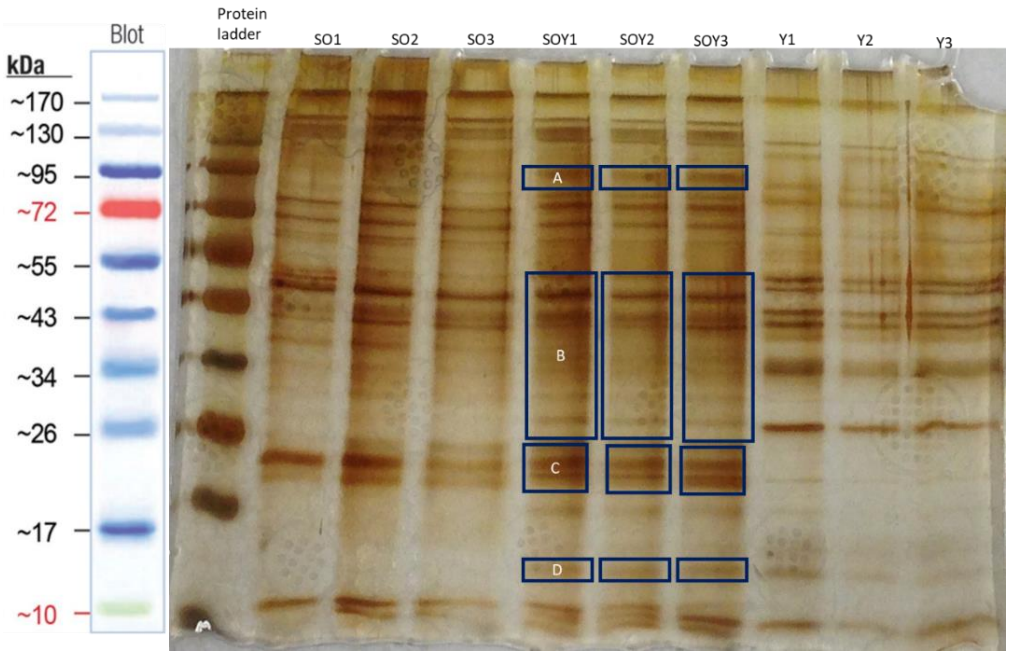

Figure 5.3.2: Protein gel for *S. obliquus* monoculture and co-culture system.

SO1, SO2 and SO3: S. obliquus monoculture, SOY1, SOY2 and SOY3: S. obliquus and R. toruloides co-culture, Y1, Y2, and Y3: R. toruloides monoculture.

Many of the proteins present in the co-culture reflect traits from both strains. The banding patterns in the co-culture flasks of *S. obliquus* and *R. toruloides* (Figure 5.3.2) shows higher expression of proteins, at 95 kDa (A), between 55 kDa and 43 kDa (B), in the region of 25 kDa (C) and below 17 kDa (D).

5.3.1.3. Screening for quorum sensing and inhibiting molecules

Quorum sensing and inhibiting molecules for both co-culture set-ups were investigated. A control assay was performed in order to verify if the strains were behaving accordingly. The results shown in the Figure 5.3.3 indicate that the CV026 when in contact with the supernatant from the CV strains turns purple. This indicates the presence of quorum sensing molecules, such as AHLs. The white hues around the CV stains indicate the presence of QSI molecules as well.

Figure 5.3.3: *Chromobacterium violaceum* bioassay.

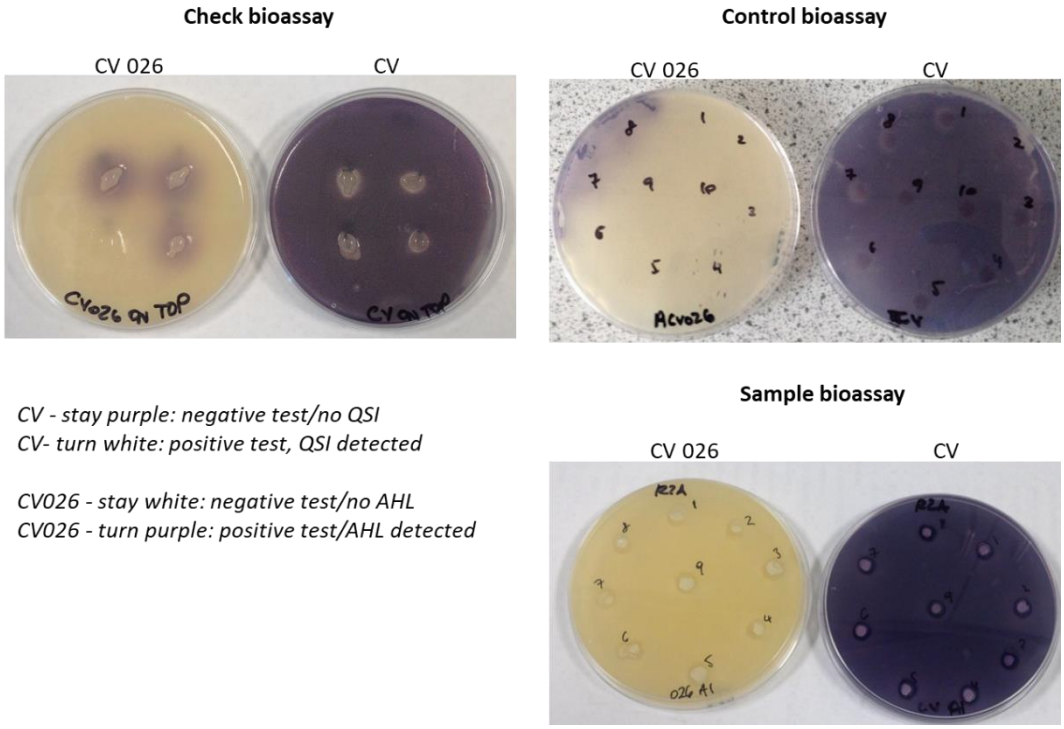

A first test was carried out to test the viability of the assay (Figure 5.3.3, Check Bioassay). Exudates of *C. violaceum* (known to release AHL signals) and *C. violaceum* 026 (no AHL) were spiked into the QS bioassay plates. The CV026 plates showed the presence of AHL molecules as the *C. violaceum* 026 cells turned from white to purple. Whereas, the *C. violaceum* cells lost pigmentation (purple to white) when detecting QSI signal [36]. The Control bioassay plates showed that AHL molecules were present in *Halomonas*, when grown in LB medium (7-8 control bioassay CV026 plate). *R. toruloides* (6-5) showed a faint hue in CV plate (purple).

The assay was run for all conditions presented in experiment 3.3.4 and 4.2.5, to check whether the AHL and/or QSI molecules would be detected when Halomonas, H. salinarum and *R. toruloides* were in co-culture. However, no quorum sensing or inhibition was detected (all plates looked like Sample Bioassay) by all samples analysed when in co-culture. Indicating that the microalgae released either allelopathic molecules [22] or the used of communal media, hindered the production of these molecules (or a combination of both factors).

5.3.2. Solid Cultures

5.3.2.1. Metabolites detection in duo-plates

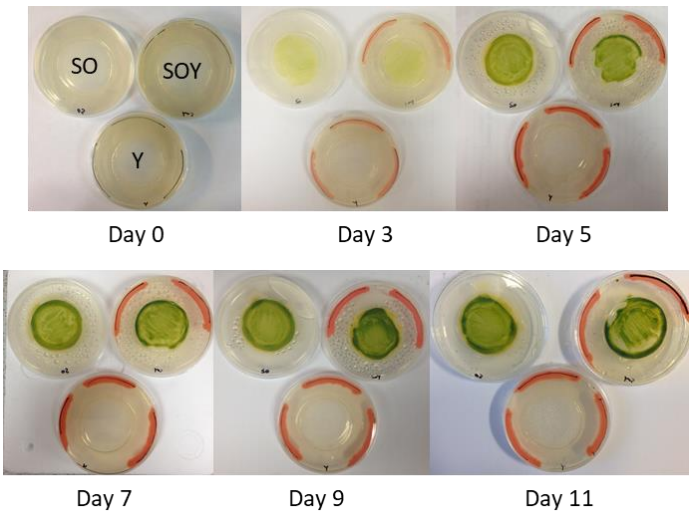

Figure 5.3.4: Pictures of the duo-plates inoculated with *S. obliquus* and *R. toruloides*.

The pictures in Figure 5.3.4 provide an overview on how the monoculture and co-culture plates developed over time. The vivid chlorophyll presence in the *S. obliquus* cells in co-culture with *R. toruloides* suggested that the cells are benefitting from the presence of the yeast. The yeast is neither hindered nor aided by the presence of the microalgae (Graph 5.3.3).

5.2.1.2.6. Growth data

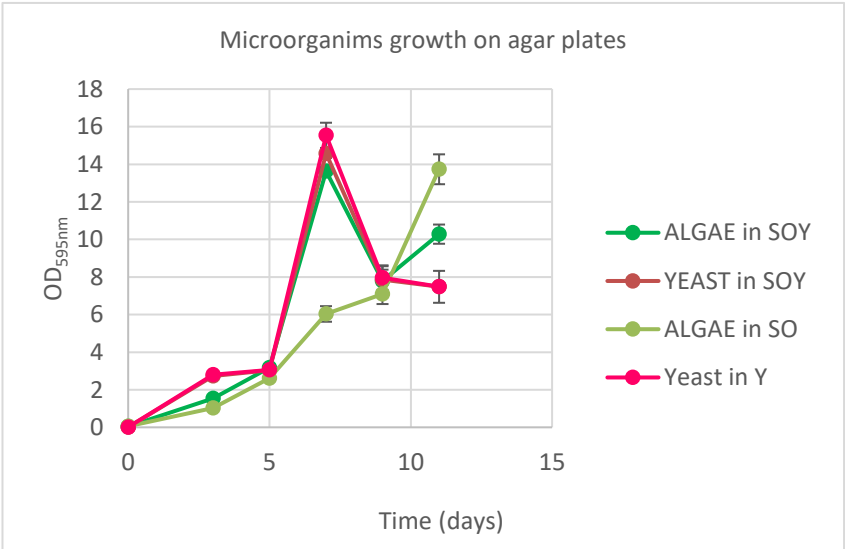

Graph 5.3.3: Growth of microorganism on agar plates. Standard error data from 3 sampling points per biological replicate. Five biological replicates for the SOY plates and three for the SO and Y plates.

The presence of bacteria would skew the results. However, the surge of microalgal cells when in co-culture with the yeast is clearly noticeable.

5.3.2.2. GC-MS

Raw chromatographs were obtained from GC-MS analysis for all metabolites analysis samples. The X-axis represents retention time in minutes, whereas Y-axis represents relative abundance. (SOY) shows yeast-yeast interaction in the presence of microalgae. (Y) Yeast-yeast interaction in yeast only plate (positive control). (YM) Yeast Mold plate with no microorganisms present (negative control). The yeast being *R. toruloides* and the microalgae *S. obliquus*.

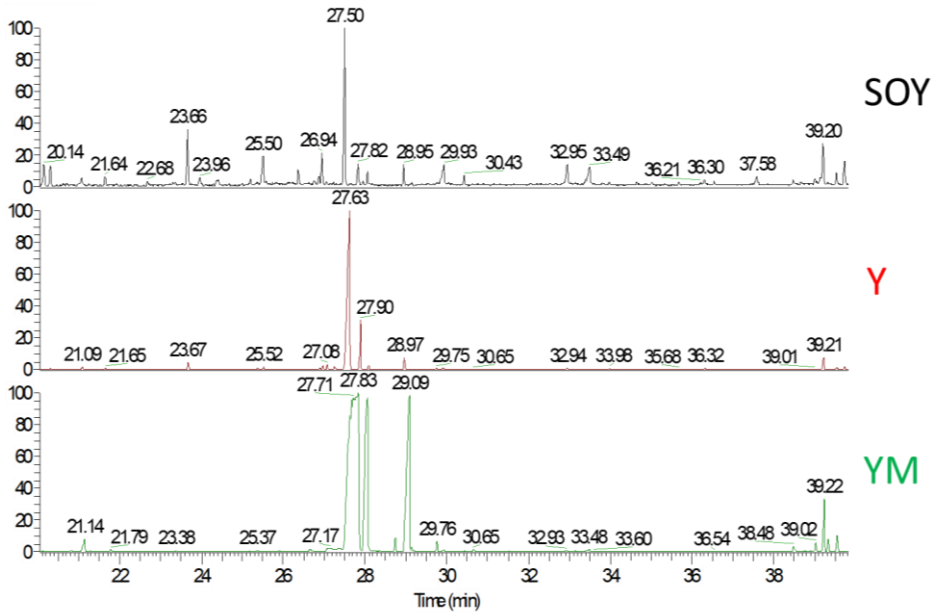

Figure 5.3.5: *GC-MS based analysis of extracellular metabolites extracted from duo-plates on the 9th day.*

The GC-MS Chromatograph obtained for yeast-yeast interactions (sampling point C in Figure 5.2.4) are shown in Figure 5.3.5. The chromatograph labelled SOY, represents the abundance of metabolites identified in yeast-yeast interaction in the presence of *S. obliquus* (SOY plates). Chromatograph Y, shows the metabolites present during yeast-yeast interaction (Y-plates) in monoculture. Chromatogram YM belongs to the 'blank' of Yeast Mold agar with no microorganisms present.

For further validation of the GC-MS data, XCMS online, was used for further analysis. This is an ideal tool to be used for complete untargeted metabolomics outputs. Up-regulated features are indicated by the green bubbles, whilst the red bubbles indicate down-regulated features. The size of the bubble corresponds to the log fold change of that feature. The shade of the bubble tallies to the magnitude of the p-value. The darker the bubble the smaller the p-value. The fold change statistical significance, as calculated

by a Welch t test with unequal variances, is conveyed by the intensity of the feature colours. The m/z ratio on the y-axis was determined by the MS. Any bubbles outlined in black were identified using METLIN database.

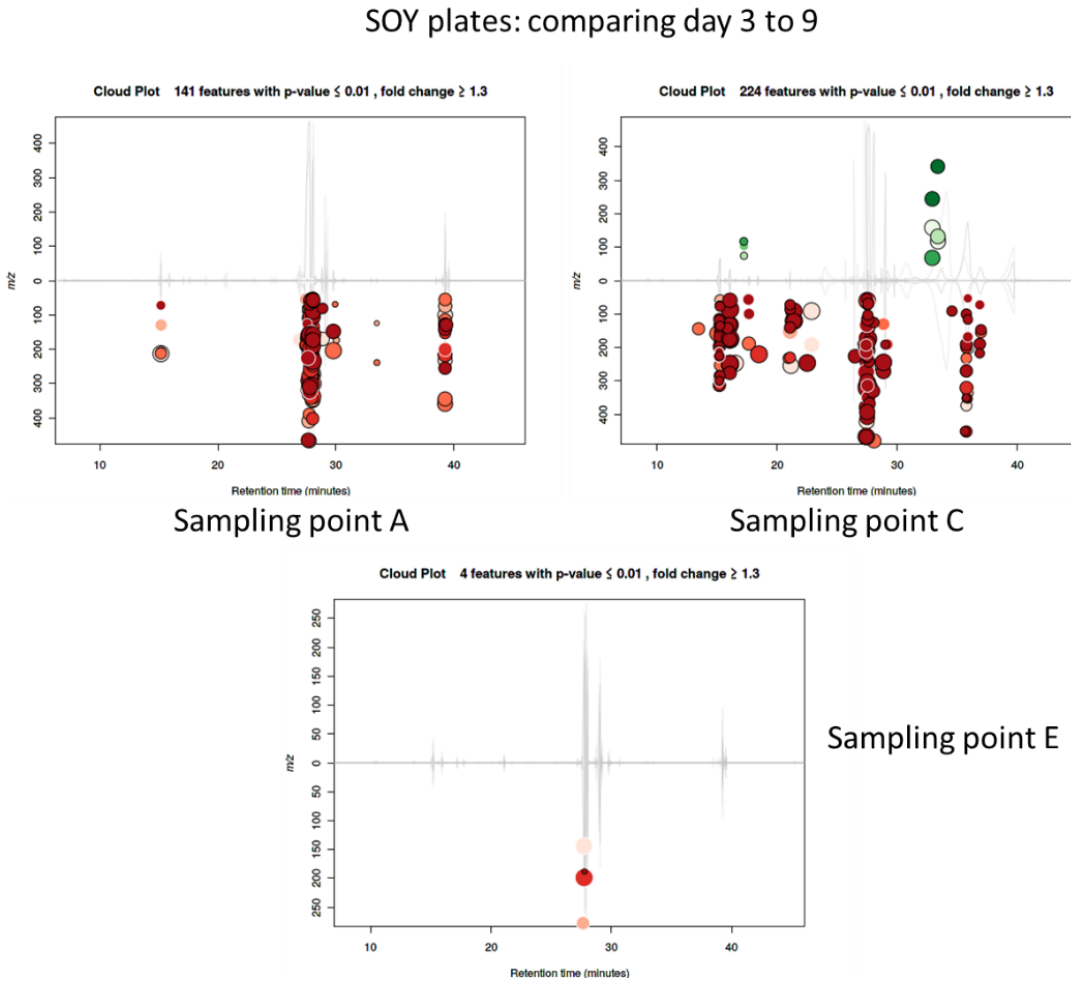

Figure 5.3.6: XCMS plots for Yeast-Agar co-culture plates (SOY) on day 3 and day 9. GC-MS results from three biological replicates per time point were analysed.

Figure 5.3.6 provides three Cloud Plots obtained from XCMS analysis. The purpose of the analysis is not to identify single metabolites but to quantify the changes that take place at each sampling point as a function of time. The SOY plates (yeast-algae co-culture) at sampling point A, C and E are indicated in Figure 5.2.4 and are compared from day 3 to day 9.

Comparison between sampling point E, A and B for all time points for Yeast-Algae plates (SOY). The 181 features belong to the yeast-algae interface (A and B). The Cloud plot on the right (Figure 5.3.7) compared all metabolite data gathered from all sampling points for all time points.

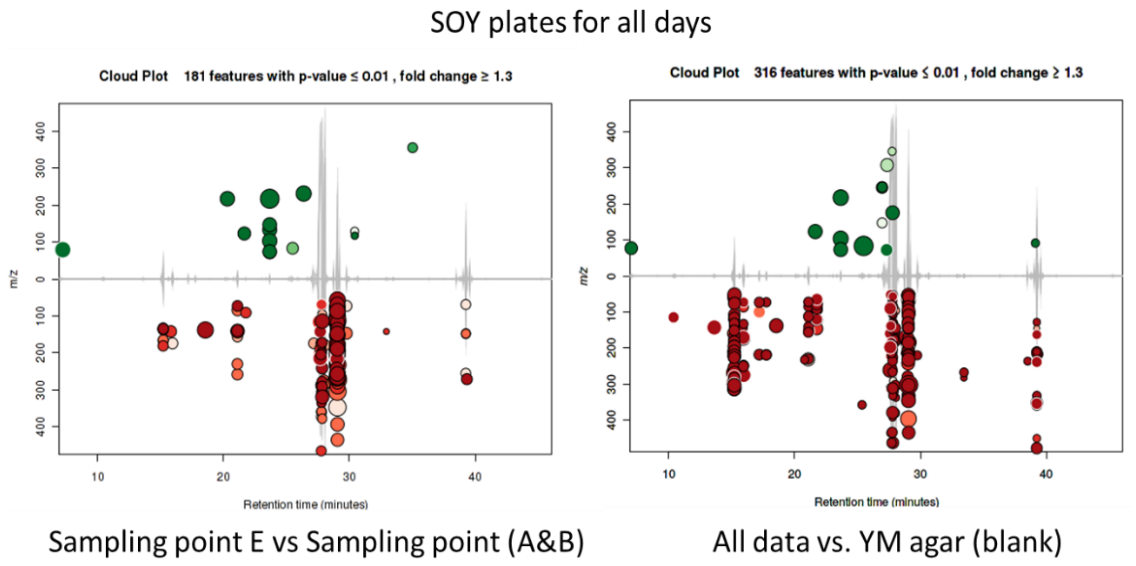

Figure 5.3.7: XCMS plots for Yeast-Agar co-culture plates (SOY) on day 3 and day 9. GC-MS results from three biological replicates per time point were analysed.

Table 5.3.1 provides a summary of all XCMS analysis conducted on the metabolite data. The highest features were seen in the samples compared within the first 9 days, No.15 in the table.

Table 5.3.1: Summary of XCMS analysis of GC-MS metabolite data

No.	Plate label		Sampling point		Downregulated features	Upregulated features	p-value	Fold-change
1	SOY	-	A	B	0	1	≤0.01	≥1.3
2	SOY	-	E	C	22	2	≤0.01	≥1.3
3	SOY	-	E	A	140	2	≤0.01	≥1.3
4	SOY	-	E	B	141	9	≤0.01	≥1.3
5	SOY	-	E	A+B	168	13	≤0.01	≥1.3
6	SOY	-	E	C	22	2	≤0.01	≥1.3
7	SO	SOY	A	A	34	2	≤0.01	≥1.3
8	SO	-	A	B	4	0	≤0.01	≥1.3
9	SO	SOY	A	C	18	7	≤0.01	≥1.3
10	Y	SOY	C	C	8	3	≤0.01	≥1.3
11	**YM**	**SOY**	**ALL**	**ALL**	**303**	**13**	≤0.01	≥1.3
12	YM	SOY	C	C	230	2	≤0.01	≥1.3
13	YM	SOY	E	E	212	8	≤0.01	≥1.3
14	SOY (DAY 3)	SOY (DAY 9)	A	A	141	0	≤0.01	≥1.3
15	**SOY (DAY 0)**	**SOY (DAY 9)**	**A**	**A**	**378**	**4**	≤0.01	≥1.3
16	SOY (DAY 3)	SOY (DAY 9)	C	C	215	9	≤0.01	≥1.3
17	SOY (DAY 3)	SOY (DAY 9)	E	E	4	0	≤0.01	≥1.3

SOY	Y	YM	**Metabolites from GC-MS**	SOY	Y	YM	**Metabolites from GC-MS**
			2-Piperidinecarboxylic acid				Phosphoric acid
			5-Hydroxymethylfurfural				Proline
			6-deoxy-Mannopyranose				Proline [+CO2]
			alpha-D-Glucopyranosyl				Psicose
			Arabinonic acid				Pyroglutamic acid
			Arabinose				Pyruvic acid
			Aspartic acid				Ribitol
			beta-D-Allose				Ribonic acid
			Cellobiose				Ribose
			D204282				Serine
			D223156				similar to Glucopyranose
			D283309				similar to NA
			Erythritol				Sorbose
			Ethanolamine				Sphingosine
			Fructose				Tagatose
			Fumaric acid				Threonine
			Galactopyranoside				Trehalose
			Galactose				Tryptophan
			Gentiobiose				UK1
			Glucose				UK2
			Glutamic acid				UK3
			Glycine				UK4
			Glycolic acid-2-phosphate				UK5
			Hexadecanoic acid				UK6
			Idose				UK7
			Inositol				UK8
			Isoleucine				Unknown#bth-pae-010
			Laminaribiose				Unknown#bth-pae-019
			Leucine				Unknown#bth-pae-020
			Maltose				Unknown#bth-pae-039
			Mannopyranoside				Unknown#bth-pae-059
			Mannose				Unknown#sst-cgl-020
			Mannose-6-phosphate				Unknown#sst-cgl-122
			NA135011				Uracil
			NA184030				Uridine
			NA192001				Valine
			Nigerose				Xylitol
			Octadecanoic acid				Xylose
			Phenylalanine				

	ALL metabolites released by Yeast when co-cultured with Algae
	ALL metabolites released by Yeast monoculture
	Metabolites ONLY detected in Yeast and Algae co-culture
	Metabolites ONLY detected in Yeast Monoculture
	Metabolites found in growth agar: Yeast Mold Agar

Figure 5.3.8: Colour map showing the distribution of metabolites across the samples belonging to *R. toruloides* in monoculture and co-culture (sampling point C), presented in the Chromatogram in Figure 5.3.5.

SO	SOY	YM	Metabolites GC-MS	SO	SOY	YM	Metabolites GC-MS
			2-Piperidinecarboxylic acid				NA201002
			5-Hydroxymethylfurfural				Nigerose
			6-deoxy-Mannopyranose				Octadecanoic acid
			Allose				Phenylalanine
			Aspartic acid				Phosphoric acid
			beta-D-Allose				Proline
			Cellobiose				Proline [+CO2]
			Cellotriose				Psicose
			D204282				Pyroglutamic acid
			D223156				Ribitol
			Erythritol				Ribose
			Galactonic acid				Serine
			Galactopyranoside				similar to Glucopyranose
			Galactose				similar to NA
			Gentiobiose				Tagatose
			Gluconic acid				Threitol
			Glucose				Threonine
			Glucuronic acid-3				Trehalose
			Glutamic acid				Tryptophan
			Glutamine [-H2O]				UK1
			Glycine				UK2
			Glycolic acid-2-phosphate				UK3
			Gulonic acid				UK4
			Hexadecanoic acid				UK6
			Idose				UK7
			Inositol				UK8
			Isoleucine				Unknown#bth-pae-010
			Lactose				Unknown#bth-pae-020
			Laminaribiose				Unknown#bth-pae-039
			Leucine				Unknown#sst-cgl-020
			Maltose				Unknown#sst-cgl-122
			Mannopyranoside				Uracil
			Mannose				Valine
			NA135011				Xylose
			NA173015				

	ALL metabolites detected in Algae monoculture
	ALL metabolites detected in Algae when in co-culture with Yeast
	Metabolites detected ONLY in Algae monoculture
	Metabolites detected ONLY in Algae and Yeast monoculture
	Metabolites found in growth agar, Yeast Mold Agar

Figure 5.3.9: Colour map showing the distribution of metabolites across the samples belonging to *S. obliquus* monoculture and in co-culture (sampling point A, day 9).

The heat maps provided in Figure 5.3.8 and 5.3.9 illustrate the metabolites identified using GC-MS harvested on the 9th day for sampling point C and A, respectively. The metabolite Figure 5.3.8 show represent the variation of these with respective to *R. toruloides* being in co-culture with *S. obliquus* (SOY and green blocks) or in monoculture. The purple blocks represented the metabolites identified to belong to the yeast only, when in co-culture with the algae, which differ from the ones detected in the yeast monoculture (pink blocks). Whilst, Figure 5.3.9 highlighted the difference in metabolites within the *S. obliquus* monoculture (SO, brown blocks) and *S. obliquus* in co-culture with *R. toruloides* (SOY, green blocks). The pale pink blocks highlight metabolites which are found in only the and light green blocks indicate the metabolites that differ from algae only (pale pink blocks) and algae in presence of yeast (pink block). With, the Yeast Mold plate (YM, yellow blocks) with the absence of microorganisms representing the negative control. The variations seen when in metabolites profiles of each microorganism (mono vs. co-culture), indicate that these communicate and changed behaviour according to the situation.

5.3.2.3. Duo-plates with gap

The interaction shown by the microalgae on duo-plates with gaps.

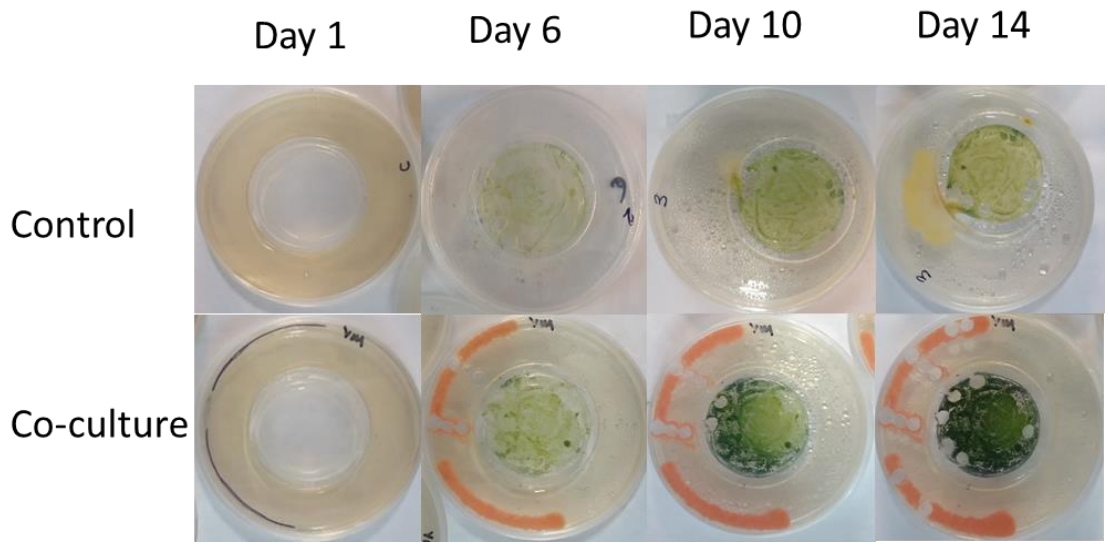

Figure 5.3.10: Duo-plates with gap for co-culture study.

The gap between the BBM agar and the YM agar tested whether the mixotrophic growth was enhancing the growth of *S. obliquus* when in co-culture. The presence of the yeast led to a significant increase in the density of algae within the co-culture flasks, as shown in Graph 5.3.4.

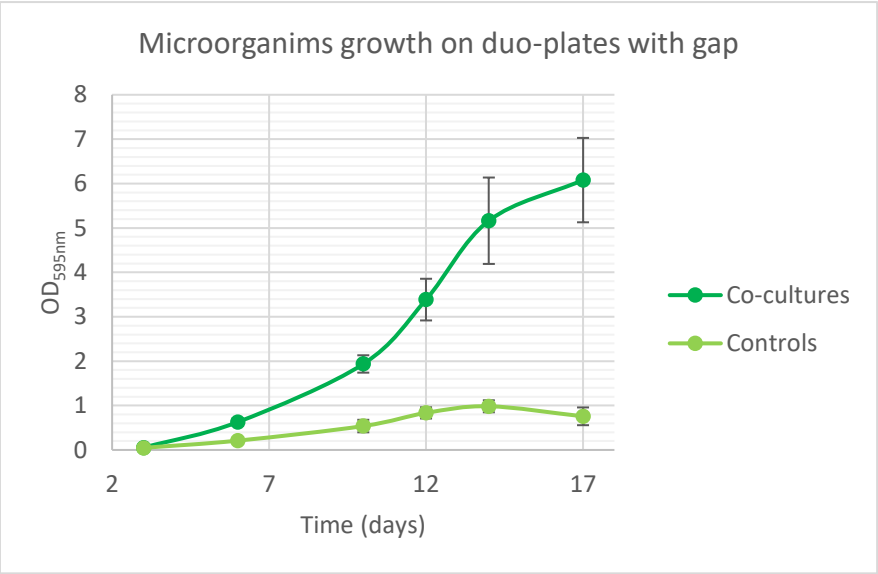

Graph 5.3.4: *S. obliquus* on duo-plates with gap. Data shown for biological triplicates.

The gap within the agar sections did not hinder the synergistic relationship between the two microorganisms, signifying that gaseous emissions also shape this co-culture.

5.4. Discussion

The work undertaken in this chapter looked at the extracellular biomolecules that characterised the two co-cultures. The first study dealt with halophilic microorganisms, *D. salina* and *Halomonas*, and *H. salinarum*. The first association showed promising results in terms of increased algae biomass, which after stressing translated into higher β-carotene production, with glycerol and other biomolecules facilitating the mutualistic relationship. The second co-culture study indicated that *S. obliquus* and *R. toruloides* established a synergisms, based carbon dioxide and oxygen exchange: leading to an increase in algae and FAMEs production.

Analysis of EPS for secreted carbohydrates and proteins, assaying for quorum sensing molecules and trapping extracellular metabolites, shed light on other factors shaping these co-cultures. The investigation will not answer all questions about why and how the co-culture behaved, but it was reasoned to provide a solid platform from which to develop more hypotheses. The analysis of the EPS revealed variation in concentration in both extracellular carbohydrate and proteins. It was assumed that the EPS collected consisted prevalently of actively secreted molecules, however, cell lysate may have contributed to some amino acids, proteins, organic acids and sugars [49].

The co-culture extracellular carbohydrates highlighted the difference in nutrient acquisition and secretion between the two microalgae species. *D. salina* is a green alga of outstanding halotolerance, with salt stress a factor known to induce the secretion of extracellular polymeric substances [50]. Mishra et al. [51] identified macromolecular polyelectrolytes with high polysaccharide content in *D. salina* EPS. Furthermore, four monosaccharides (galactose, glucose, xylose, and fructose) were identified in the *D. salina* EPS hydrolysate [16]. The high levels of carbohydrates present within the co-culture flasks of *D. salina* and *Halomonas* confirmed that the microalga not to be mixotrophic. In contrast, the drastically lower amount in the co-culture of *S. obliquus* and *R. toruloides* suggested that either the microalgae used the yeast carbohydrates as a source of nutrients or that the yeast were hindered in their production by allelochemicals release by *S. obliquus*. However, the growth data in Chapter 4 strongly suggested that *S. obliquus* cells were able to grow in mixotrophic conditions [52]. Both co-cultures show high concentrations of extracellular protein from the "aiding" partners, *Halomonas* and *R. toruloides*. The concentration of proteins within the co-culture exudate in both scenarios was between the monoculture values. This could be due to two facts: the bacteria/yeast are hindered in secreting molecules in the presence of the microalgae [53] or these are degraded by the aiding organism for consumption [54].

Quorum sensing molecules particularly AHLs were detected in *Halomonas'* extracellular supernatant [34] which agreed with the results obtained in the bioassay plate shown in Figure 5.3.3. Whereas, *R. toruloides* showed signs of sensing inhibitory (QSI) activity against AHL-based quorum sensing. So far only one study confirmed that *R. toruloides* was able to degrade AHL molecules [55]. The results from the assay indicated that the presence of the microalgae or the modified medium affected the QS abilities of the bacteria and the yeast. Further tests are required in order to attest whether either of these factors would hinder cell signalling.

Looking at the duo-plates in Figure 5.3.4, the presence of the yeast had beneficial effects on the growth of the microalgae. This was also shown in Graph 5.3.3, where the *S. obliquus* cells grew faster when compared to the monoculture plates. However, a closer look at the plates indicated that the algae at the interface with the yeast grew faster. This phenomenon can be attributed to an exchange of biomolecules and perhaps to *S.*

obliquus ability to switch to mixotrophic growth. It was also noticeable that the endogenous bacterium migrated towards the same interface for nutrient acquisition. However, this phenomenon is less prominent in the co-culture plates (SOY), where *R. toruloides*, competed for the same resources, or released inhibiting molecules, resulting in less bacterium loading.

The metabolite data indicated that certain molecules were pertinent to co-cultures. However, the plasticity of cell-cell interactions has yet to be unravelled [56]. The data obtained from the GC-MS showed variations in metabolite abundance between the cultures. An example of a GC-MS chromatograph was provided in Figure 5.3.5. The chromatogram peaks signposted the presence of a metabolite, with variation between samples apparent at first sight. The Cloud Plots provided a better understanding of which features changed during the course of the experiment. Figure 5.3.6 provided Cloud Plots, mapping the dynamics of the metabolites between day 3 and day 9, in the yeast-algae plates (SOY). Of particular interest are the changes that take place between the 3rd and 9th day on the yeast-algae plate, at sampling point A, C and E as indicated in Figure 5.2.4. Sampling point A shows that 141 dysregulated features were detected whose intensities were altered when the metabolites from day 3 were compared to day 9, with p-value ≤ 0.01 and fold change ≥ 1.3. Most of the features at the algae and yeast interface were down regulated with time.

On the other hand, the sampling point C showed 224 features with p-value ≤ 0.01 and fold change ≥ 1.3. Yeast –yeast (*R. toruloides*) interaction in the presence of algae displayed upregulated and downregulated features. In both scenarios, the darker colouring of the bubbles indicated strong statistical significance. The last plot, sampling point E (Figure 5.2.4) did not display large amounts of metabolites; with only four features detected. This showed that most of the metabolite interactions were taking place between the two co-cultured microorganisms. When looking at an overall picture of the metabolite interaction in yeast-algae plates (SOY) many features changed: 316 features, with $p<0.01$ and a variety of molecules changed during the course of the experiment (Figure 5.3.7). Many of these were down regulated, indicating that the initial response decreases with time. Some metabolites identified in the yeast-yeast in presence of algae samples (SOY sampling point C) differ from the ones present in the yeast monocultures; to name a few erythritol, ethanolamine and fumaric acid.

Ethanolamine has been shown in studies to increase the lipid production of *S. obliquus* [57]. Likewise, this could be a portion of a fatty acid secreted by the alga itself [58,59]. The yeast monoculture on the other hand showed many monosaccharides such as fructose, tagatose, sorbose and mannose, which could have been consumed by the algae species in the co-culture [52].

When looking at the data in Figure 5.3.8, again some metabolites are present only in monoculture or co-culture. Metabolites identified in *S. obliquus* monoculture on the 9th day were not seen in the co-culture plate. This could be attributed to either the *S. obliquus* being hindered by *R. toruloides* presence or by the yeast utilising those compounds. Pyroglutamic acid, Ribitol, Galactonic acid, Galactose, Glucuronic acid-3 and Lactose are amongst the metabolites that are not detected in the co-culture set-up. As mentioned previously, the analysis of the data was carried out to provide an overview of the metabolites governing the association. Further analysis is required to provide a fuller picture.

The duo-plates with gaps further demonstrated that the effect of the yeast on the microalgae should not be underestimated. The space between the two agar phases limited the exchange of molecules through the agar. However, it validated that the microalgae were sustained by the yeast without resorting to mixotrophic growth. As confirmed by the DIC results in Chapter 4, section 4.3.6, carbon dioxide release by yeast respiration was used in microalgae photosynthesis [46]. Furthermore, *R. toruloides* produced volatile organic sulphur compounds (VOSCs), methanethiol, S-methyl thioacetate, dimethyl disulfide and dimethyl trisulfide [60]. This may be the case for the yeast grown on YM agar, as the peptone used in the recipe contains methionine used in the production of VOSCs [60]. The ability to assimilate gaseous sulphur compounds, such as SO_2, has been shown in *S. obliquus* and other microalgae [61]. Hence, their mixotrophic growth may have significantly enhanced their growth compared to the control.

Improvements to the co-culturing technique are necessary, as the current Petri dish-method allowed only for the collection of agar samples. However, compared to conventional liquid co-culturing, membrane separation, transwell or bead entrapment, was easier to set-up and assess. Making it a useful tool that can be used for preliminary studies for biotechnological application.

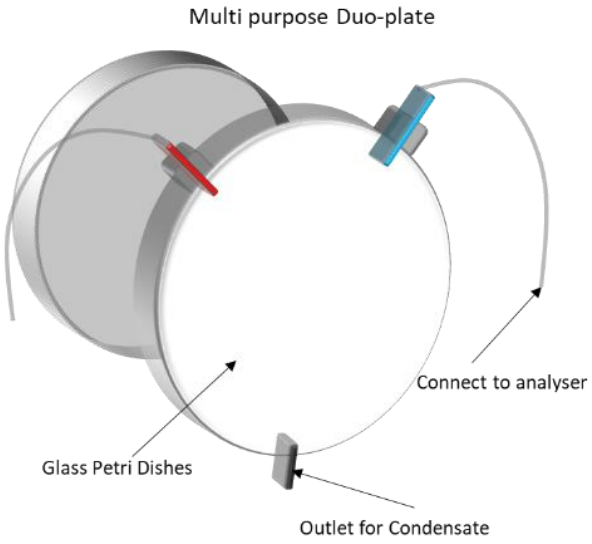

Figure 5.4.1: Proposed design for future Petri Dishes for duo-plate co-culturing.

The duo-plate design (Figure 5.4.1) would allow for gas-exchange data capture, sampling and for analysing the condensate found with the plates. Connecters are attached to the lid of the plates, allowing for in-line gas evolution. Samples can be removed at specific time points for Gas analysis to check for volatile compounds. Sampling for metabolites can be carried out as shown in Figure 5.2.4. The plates would be made of Duran glass, suitable for sterilization.

5.5. Conclusions

The aim of the investigation was to better understand the molecular cues exchanged between microalgae and their "aiding" partners when in co-culture. The two co-cultures investigated are very different. The first, *D. salina* and *Halomonas*, dealt with halophilic microorganisms whose association is found in nature. The second, *S. obliquus* and *R. toruloides* focused on the interactions of an artificially constructed system. The extracellular carbohydrates also showed the difference in nutrient acquisition by the two microalgae species. In the *D. salina* set-up, carbohydrates did not play a role in the association; however, the likelihood that *R. toruloides* extracellular carbohydrates were assimilated by *S. obliquus* as part of its mixotrophic growth is very high. Furthermore, the protein gels reveal difference in protein secretions when the cells are in co-culture. The higher expression of some proteins in co-culture was observed. The QS-bioassay

indicated that co-cultures may hinder the secretion of AHL molecules, and perhaps other quorum sensing cues, however further testing was required to validate this point.

The solid culture duo-plates have shown that aside from CO_2 other small molecules, such as monosaccharide sugars and amino acids, characterize the *S. obliquus* and *R. toruloides* co-culture. The duo-plates with gap further indicate that apart from carbon dioxide and oxygen other VOCs shaped the co-culture of microalgae and yeast. Further investigation into the metabolite data, demonstrated dynamic changes in metabolites during the course of the experimentation. This in itself is a new finding as metabolite interactions between these microorganisms had not been investigated beforehand.

5.6. References

[1] Ma Q, Zhou J, Zhang W, et al. Integrated proteomic and metabolomic analysis of an artificial microbial community for two-step production of vitamin C. PLoS One. 2011;6.

[2] Tinzl-Malang SK, Rast P, Grattepanche F, et al. Exopolysaccharides from co-cultures of Weissella confusa 11GU-1 and Propionibacterium freudenreichii JS15 act synergistically on wheat dough and bread texture. Int. J. Food Microbiol. 2015;214:91–101.

[3] Breugelmans P, Barken KB, Tolker-Nielsen T, et al. Architecture and spatial organization in a triple-species bacterial biofilm synergistically degrading the phenylurea herbicide linuron. FEMS Microbiol. Ecol. 2008;64:271–282.

[4] Koenig JE, Spor A, Scalfone N, et al. Succession of microbial consortia in the developing infant gut microbiome. Proc. Natl. Acad. Sci. U. S. A. 2011;108:4578–4585.

[5] Hays SG, Patrick WG, Ziesack M, et al. Better together : engineering and application of microbial symbiosesMicrobial Consortia Engineering for Cellular Factories: in vitro to in silico systems. Curr. Opin. Biotechnol. 2015;36:40–49.

[6] Masset J, Calusinska M, Hamilton C, et al. Fermentative hydrogen production from glucose and starch using pure strains and artificial co-cultures of Clostridium spp. ??? 2012;5:1.

[7] Brenner K, You L, Arnold FH. Engineering microbial consortia: a new frontier in synthetic biology. Trends Biotechnol. 2008;26:483–489.

[8] Ola ARB, Thomy D, Lai D, et al. Inducing Secondary Metabolite Production by the Endophytic Fungus *Fusarium tricinctum* through Coculture with *Bacillus subtilis*. J. Nat. Prod. 2013;76:2094–2099.

[9] Hofmann T, Hanlon ARM, Taylor JD, et al. Dynamics and compositional changes in extracellular carbohydrates in estuarine sediments during degradation. Mar. Ecol. Prog. Ser. 2009;379:45–58.

[10] Xiao R, Zheng Y. Overview of microalgal extracellular polymeric substances (EPS) and their applications. Biotechnol. Adv. 2016;34:1225–1244.

[11] Kightlinger W, Chen K, Pourmir A, et al. Production and characterization of algae extract from Chlamydomonas reinhardtii. Electron. J. Biotechnol. 2014;17:14–18.

[12] Kavita K, Mishra A, Jha B. Extracellular polymeric substances from two biofilm forming Vibrio species: Characterization and applications. Carbohydr. Polym. 2013;94:882–888.
[13] Mahesh M, Somashekhar R, Bagchi P, et al. Optimization for the Production of Extracellular Alkaline Phosphatase from Bacillus subtilis. Int. J. Curr. Microbiol. App. Sci. 2015;4:829–838.
[14] Garay LA, Sitepu IR, Cajka T, et al. Eighteen new oleaginous yeast species. J. Ind. Microbiol. Biotechnol. 2016;43:887–900.
[15] Stacy AR, Diggle SP, Whiteley M. Rules of engagement: defining bacterial communication. Curr. Opin. Microbiol. 2012;15:155–161.
[16] Liu L, Pohnert G, Wei D. Extracellular Metabolites from Industrial Microalgae and Their Biotechnological Potential. Mar. Drugs. 2016;14:191.
[17] Choi HP, Lee YM, Yun CW, et al. Extracellular 5-aminolevulinic acid production by Escherichia coli containing the Rhodopseudomonas palustris KUGB306 hemA gene. J. Microbiol. Biotechnol. 2008;18:1136–1140.
[18] Grant MAA, Kazamia E, Cicuta P, et al. Direct exchange of vitamin B12 is demonstrated by modelling the growth dynamics of algal–bacterial cocultures. ISME J. 2014;1–10.
[19] Helliwell KE, Pandhal J, Cooper MB, et al. Quantitative proteomics of a B_{12} -dependent alga grown in coculture with bacteria reveals metabolic tradeoffs required for mutualism. New Phytol. 2017;
[20] Kumudha A, Sarada R. Characterization of vitamin B12 in Dunaliella salina. J. Food Sci. Technol. 2016;53:888–894.
[21] Ribalet F, Intertaglia L, Lebaron P, et al. Differential effect of three polyunsaturated aldehydes on marine bacterial isolates. Aquat. Toxicol. 2008;86:249–255.
[22] Mendes B, Brantes L, Vermelho AB. Allelopathy as a potential strategy to improve microalgae cultivation. Biotechnol. Biofuels. 2013;6:152.
[23] Goulitquer S, Potin P, Tonon T. Mass spectrometry-based metabolomics to elucidate functions in marine organisms and ecosystems. Mar. Drugs. 2012.
[24] Mincer TJ, Aicher AC. Methanol production by a broad phylogenetic array of marine phytoplankton. PLoS One. 2016;11:1–17.
[25] Hard BC, Gilmour DJ. A mutant of Dunaliella parva CCAP 19/9 leaking large amounts of glycerol into the medium. J. Appl. Phycol. 1991;367–372.
[26] Mahapatra S, Banerjee D. Fungal Exopolysaccharide: Production, Composition and Applications. Microbiol. Insights. 2013;6:1–16.
[27] Flemming H, Wingender J. The biofilm matrix. Nat. Rev. Microbiol. 2010;8:623–633.
[28] Decho A. Microbial exopolymer secretions in ocean environments: their role(s) in food webs and marine processes. Ocean. Mar. Biol. Annu. Rev. 1990;28:73–153.
[29] Cordoba-Castro NM, Montenegro-Jaramillo AM, Prieto R, et al. Analysis of the effect of the interactions among three processing variables for the production of exopolysaccharides in the microalgae Scenedesmus obliquus (UTEX 393). Rev. La Fac. Química Farm. 2012;19:60–69.
[30] March JC, Bentley WE. Quorum sensing and bacterial cross-talk in biotechnology. Curr. Opin. Biotechnol. 2004;15:495–502.
[31] Williams P. Quorum sensing, communication and cross-kingdom signalling in the

bacterial world. Microbiology. 2007;153:3923–3938.
[32] Natrah FMI, Bossier P, Sorgeloos P, et al. Significance of microalgal-bacterial interactions for aquaculture. Rev. Aquac. 2014;6:48–61.
[33] Subashchandrabose SR, Ramakrishnan B, Megharaj M, et al. Consortia of cyanobacteria/microalgae and bacteria: biotechnological potential. Biotechnol. Adv. 2011;29:896–907.
[34] Llamas I, Quesada E, Martínez-Cánovas MJ, et al. Quorum sensing in halophilic bacteria: Detection of N-acyl-homoserine lactones in the exopolysaccharide-producing species of Halomonas. Extremophiles. 2005;9:333–341.
[35] González JE, Keshavan ND. Messing with bacterial quorum sensing. Microbiol. Mol. Biol. Rev. 2006;70:859–875.
[36] Lv D, Ma A, Tang X, et al. Profile of the culturable microbiome capable of producing acyl-homoserine lactone in the tobacco phyllosphere. J. Environ. Sci. (China). 2013;25:357–366.
[37] Leão PN, Pereira AR, Liu W-T, et al. Synergistic allelochemicals from a freshwater cyanobacterium. Proc. Natl. Acad. Sci. U. S. A. 2010;107:11183–11188.
[38] Gantar M, Berry JP, Thomas S, et al. Allelopathic activity among Cyanobacteria and microalgae isolated from Florida freshwater habitats. Fems Microbiol. Ecol. 2008;64:55–64.
[39] Markou G, Nerantzis E. Microalgae for high-value compounds and biofuels production: a review with focus on cultivation under stress conditions. Biotechnol. Adv. 2013;31:1532–1542.
[40] Zhao P, Yu X, Li J, et al. Enhancing lipid productivity by co-cultivation of Chlorella sp. U4341 and Monoraphidium sp. FXY-10. J. Biosci. Bioeng. 2014;118:72–77.
[41] Anbazhagan D, Mansor M, Yan GOS, et al. Detection of quorum sensing signal molecules and identification of an autoinducer synthase gene among biofilm forming clinical isolates of Acinetobacter spp. PLoS One. 2012;7.
[42] Wrede D, Taha M, Miranda AF, et al. Co-cultivation of fungal and microalgal cells as an efficient system for harvesting microalgal cells, lipid production and wastewater treatment. PLoS One. 2014;9:e113497.
[43] Covarrubias S., De-Bashan LE, Moreno M, et al. Alginate beads provide a beneficial physical barrier against native microorganisms in wastewater treated with immobilized bacteria and microalgae. Appl. Microbiol. Biotechnol. 2012;93:2669–2680.
[44] Sonnenbichler J, Guillaumin JJJ, Peipp H, et al. Secondary metabolites from dual cultures of genetically different Armillaria isolates. Eur. J. For. Pathol. 1997;27:241–249.
[45] Zhang Z, Ji H, Gong G, et al. Synergistic effects of oleaginous yeast Rhodotorula glutinis and microalga Chlorella vulgaris for enhancement of biomass and lipid yields. Bioresour. Technol. 2014;164:93–99.
[46] Santos C, Caldeira M, Lopes da Silva T, et al. Enhanced lipidic algae biomass production using gas transfer from a fermentative Rhodosporidium toruloides culture to an autotrophic Chlorella protothecoides culture. Bioresour. Technol. 2013;138:48–54.
[47] Ponomarova O, Patil KR. Metabolic interactions in microbial communities: Untangling the Gordian knot. Curr. Opin. Microbiol. 2015;27:37–44.
[48] Gobbetti M, Corsetti A, Rossi J. The sourdough microflora. Interactions between

lactic acid bacteria and yeasts: Metabolism of carbohydrates. Appl. Microbiol. Biotechnol. 1994;41:456–460.
[49] Maksimova I V., Bratkovskaya LB, Plekhanov SE. Extracellular carbohydrates and polysaccharides of the Alga Chlorella pyrenoidosa Chick S-39. Biol. Bull. 2004;31:175–181.
[50] Oren A. Microbial diversity and microbial abundance in salt-saturated brines: Why are the waters of hypersaline lakes red? Nat. Resour. Environ. Issues. 2009;15:247–255.
[51] Mishra A, Jha B. Isolation and characterization of extracellular polymeric substances from micro-algae Dunaliella salina under salt stress. Bioresour. Technol. 2009;100:3382–3386.
[52] Girard JM, Roy ML, Hafsa M Ben, et al. Mixotrophic cultivation of green microalgae Scenedesmus obliquus on cheese whey permeate for biodiesel production. Algal Res. 2014;5:241–248.
[53] Bagwell CE, Abernathy A, Barnwell R, et al. Discovery of bioactive metabolites in biofuel microalgae that offer protection against predatory bacteria. Front. Microbiol. 2016;7:1–12.
[54] Ramanan R, Kim BH, Cho DH, et al. Algae-bacteria interactions: Evolution, ecology and emerging applications. Biotechnol. Adv. 2016;34:14–29.
[55] Qiu J, ZH J, Ma H, et al. Isolation and identification of Rhodosporidium toruloides R1 degrading N-acyl homoserine lactone. Wei Sheng Wu Xue Bao. 2007;47:355–8.
[56] Hom EFY, Murray AW. Niche engineering demonstrates a latent capacity for fungal-algal mutualism. Science (80-.). 2014;345:94–98.
[57] Ashton A. Amino Alcohols—Advances in Research and Application: 2013. Q. Ashton A, editor. Scholarly Editions; 2013.
[58] Choi KJ, Nakhost Z, Krukonis VJ, et al. Supercritical fluid extraction and characterization of lipids from algae Scenedesmus obliquus. Food Biotechnol. (New York, NY, United States). 1987;1:263–281.
[59] Hu Q, Sommerfeld M, Jarvis E, et al. Microalgal triacylglycerols as feedstocks for biofuel production: perspectives and advances. Plant J. 2008;54:621–639.
[60] Buzzini P, Romano S, Turchetti B, et al. Production of volatile organic sulfur compounds (VOSCs) by basidiomycetous yeasts. FEMS Yeast Res. 2005;5:379–385.
[61] Van Den Hende S, Vervaeren H, Boon N. Flue gas compounds and microalgae: (bio-)chemical interactions leading to biotechnological opportunities. Biotechnol. Adv. 2012;30:1405–1424.

Conclusion and Future work

Discussion and Conclusion

In nature, microorganisms exist as part of organised communities, known as consortia, where through exchange of biomolecules they are able to co-habit, evolve and protect each other. Learning from nature, the application of co-cultures (only two-partners) within laboratory studies has shown that, if the these are synergistic, an increase in biomass and bioproducts can be achieved, with less nutrient supplements used (Table 1.3.1, Chapter 1). Monocultures are still the preferred route of production for biopharmaceuticals, due to stringent regulation and health and safety guidelines. With contamination being a major bottleneck [1,2], the prospect of using co-cultures or consortia in these industries is very unlikely. This technique is commonly used in bioremediation, for anaerobic digestion of spent biomass; so why not extend this concept to other industrial sectors, such the bio-nutraceutical, cosmetics and bioenergy industry.

The investigation aimed to highlight the potential of a microalgal co-culture as a biotechnological tool. The overall aim was to increase microalgal biomass and bio-product yield by co-culturing with an 'aiding' microorganism. Furthermore, the following question were addressed as part of the investigation: (a) Are microalgal co-cultures suitable for biotechnological application? (b) Can co-cultures outcompete monocultures in terms of biomass and bio-product titres? (c) Are we able to understand how the microorganisms involved interact? (d) What kind of molecules were encountered? (e) Do co-culturing methods and stress change the secretion of these molecules? (f) Was it possible to monitor each microorganism involved and understand how each contributed to the overall outcome?

The literature review presented in the first chapter highlighted the opportunities and challenges intrinsic to co-cultures. Various aspects, such as communal growth medium, inoculum ratio and timing, and reactor design, were taken into consideration when setting up the two co-cultures presented in this study [3]. Additionally, the associated trade-off derived from adaptation into new growth medium, as seen by all the aiding microorganisms, were taken into account [4,5].
The experimental designs presented in the subsequent chapters addressed the challenges pertaining to each co-culture. The goal was to design working co-cultures that allowed for increased microalgae biomass and bioproducts. The co-cultures studied in Chapters 3 and 4 demonstrated that an increase in biomass and desired product was achieved with co-cultures. The results obtained in both scenarios showed an increase in microalgae biomass, for example

in section 3.4.2.1, an increase of microalgae cells of 79.85% was achieved by co-culturing *D. salina* and *Halomonas* Similar results were seen with *S. obliquus* and *R. toruloides*, with an increase of 20% in microalgae concentration.

The *D. salina* co-culture and consortia work presented in Chapter 3 involved the co-culturing of *D. salina* with *Halomonas* and *D. salina* with *Halobacterium salinarum*. Both aiding organisms are found together with *D. salina* in nature [6]. A literature survey revealed elements of synergism that existed between these microorganisms or in association with other microalgae strains [7–9]. Associating *D. salina* with high concentrations of *Halomonas* cells resulted in an increase in microalgae cell numbers. The boost in cell numbers outweighed the low accumulation of β-carotene per cell. In fact, the co-cultured algae cells do not appear to be stressed by the high level of *Halomonas* present. The images in section 3.4.2 show bright green cells of *D. salina* when in co-culture opposed to orange/red cells in the monoculture flasks. This demonstrated that *Halomonas* was able to sustain *D. salina* growth also in adverse conditions. One assumption is that secreted algal glycerol was consumed by the *Halomonas*, which in return provided nutrients to the algae [10–12]. The other is that *Halomonas* was respiring using oxygen and nitrate in the medium whilst aiding the microalgae by producing CO_2, similarly to *Halomonas campisalis* or *Halomonas cerina sp.* [13,14].

A similar experimental procedure was used to assess whether this phenomenon would be replicated by the *D. salina* and *H. salinarum* co-culture. The results established that if one of the members were to fall or to be in dire stress, this would cause an imbalance in the matrix [15,16]. This is most likely to have happened when the *H. salinarum* consortium was subjected to stress: the stress borne by *H. salinarum* translated over to the whole system, disrupting the balance [17–19]. Overall, an increase in microalgae growth was obtained, however, not as pronounced as the levels obtained with *Halomonas,* perhaps because both heterotrophic microorganisms competed for the microalgal glycerol [20], however giving less support to the microalgae.

As outlined in Chapter 1, the timing of the inoculum and the inoculation size [4] had an effect on the co-culture of *Scenedesmus obliquus* and *Rhodosporidium toruloides* (Chapter 4). The increase microalgal cells, however, did not translate into a significant increase in lipids. By surveying the literature [21], it was clear that during co-culture studies, both the yeast and the algae were grown in rich medium. Growing an oleaginous yeast at optimal conditions in itself leads to high levels of lipids. Conversely, to these studies the communal medium here was designed to cater for the microalgae needs, and to use the yeast as an aiding partner. By

sacrificing the lipid production capabilities of the yeast, the co-culture fell short in FAMEs production. Measurements of the off-gas and dissolved organic carbon did indeed shed light into the co-culture dynamics. The exchange of carbon dioxide is indeed a major factor that if maximised, would lead to promising results.

Both co-culture studies did indeed show promising results in terms of microalgae growth. The question remained whether more details about possible communication networks could be unravelled. Work pertaining to this, was presented in Chapter 5 where the exopolymeric substance (EPS) from both co-cultures was analysed. Both the extracellular carbohydrates and proteins showed the difference in nutrient acquisition by the two microalgae species. The results suggest that in the *D. salina* set-up, carbohydrates do not play a role in the association although *Halomonas* secreted large amounts of carbohydrates and proteins into the medium. Conversely, due to the ability of *S. obliquus* to grow mixotrophically, the carbohydrates secreted by *R. toruloides* sustained its growth. The concentration of EPS within the medium, from the aiding partner, could be a response to growth in communal medium or to the presence of the microalgae. The SDS-Page gels highlighted the difference of protein expression between co-cultures and monoculture: this confirmed that the proteins belonged to the communication matrix. Concerning the quorum sensing and inhibiting molecules, the null results indicated that the communal medium might be hindering bacterial or yeast growth.

The duo-plates confirmed that gaseous exchange and large molecules shape the co-culture between *S. obliquus* and *R. toruloides*.The XCMS analysis showed that large numbers of metabolites played a part in the duo-plate co-cultures, with 382 features detected, of which 378 metabolites were downregulated and 4 were upregulated, with $p<0.01$ (day 0 vs day 9, total). Out of these metabolites, molecules such as allose, cellotriose and erythritol were only found in the metabolite exchange belonging to yeast and algae. Other molecules such as ethanolamine and fumaric acid were found only in yeast-yeast association in the presence of microalgae. These molecules acts as communication, nutrients and division of labour signals. Additionally, the parallel investigation with the duo-plates with gaps indicated that other volatile compounds may be involved in this co-culture set.

How could this be suitable for biotechnological application and larger-scale co-culturing? The results obtained from both Chapters 3 and 4, with both *D. salina* and *S. obliquus* co-cultures, suggest that a fed-batch system (Figure 6.1.1), where the 'aiding partner' is introduced into the

microalgae co-culture (STAGE 1), to later be removed before stress (STAGE 2), may lead to an overall increase in bio-product, as the biomass productivity of the microalgae would be higher.

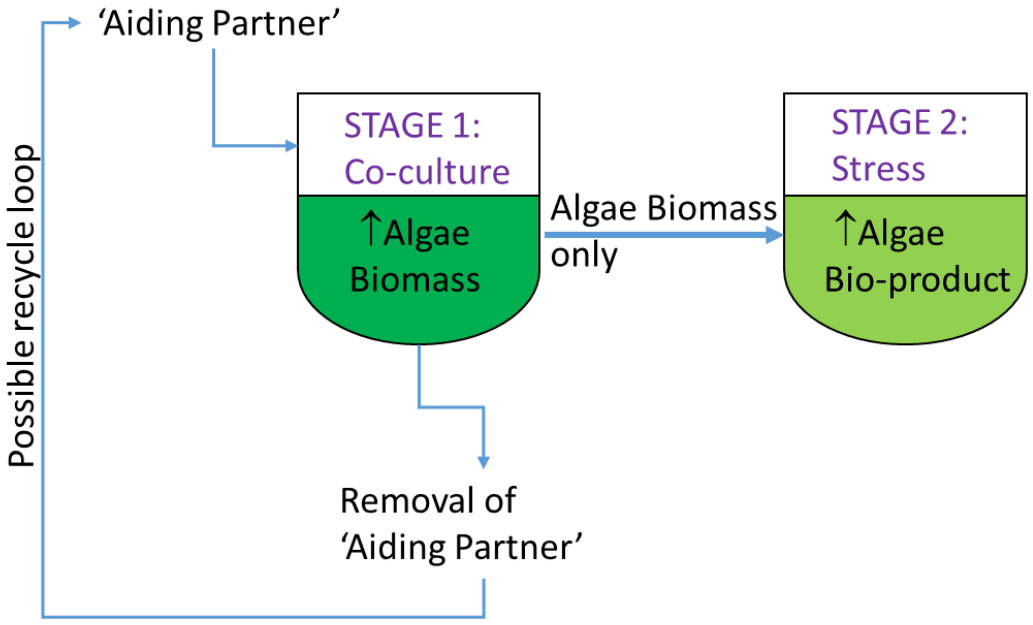

Figure 0.1: Possible set-up to for a two-stage production for artificial co-cultures.

The first reactor would focus on increasing the growth of the microalgae with the added yeast (STAGE 1). The 'aiding partner' can be trapped in beads (section 3.3.2.2.1) or be fixed on a matrix. This would allow the 'aiding partner' to release any biomolecules that would aid the growth of the microalgae. Thereafter, the microalgae, would be stressed to maximise bio-rodcut titres.

The findings in this thesis demonstrated the potential of an engineered microalgal based co-culture. A fully characterised co-culture would meet the demands for high productivity, lower the contamination risk, be self-sufficient, and decrease costs associated with nutrients. The adaptability of microalgal assemblages allow for multi-production, of high and low value compounds alike. Bioremediation can be coupled to biomass generation for the industry sector, where stringent requirements, in terms of emissions, need to be met. The application of microalgae co-cultures with their versatility can be of benefit to many industries such as the bio-nutraceutical, biomanufacturing, cosmetics, and bioenergy sector.

Future work

The benefits associated with microalgae co-cultures, such as high productivity, low contamination risk and multi-production; demonstrated potential as viable biotechnological tools. Challenges were encountered during the investigation that need to be addressed, before a robust, dynamic and fully successful system can be created. It is most likely that microalgal engineered co-cultures or consortium will be widely used for bioremediation and bioenergy generation, as these applications do not have stringent healthy and safety regulations. The increase in microalgae biomass yields in co-culture, already make this a viable route. However, to maximise the efficiency, a microorganism with the capacity of producing high value products, or high lipid contents should be added to the assemblage. The trade-off that each microorganism will experience has to be assessed, in order to maximally exploit the co-culture.

The data obtained suggested that further work is required in the area of understanding how the microorganisms communicate. For successful biotechnological application, the behaviour of the microorganisms need to be assessed also during abiotic stress. The extracellular data indicate that variations of secondary metabolites are found between microalgae in co-cultures and in monocultures. Some of these metabolites can be food for the partnering organisms, or be of industrial relevance. Therefore, to maximise the secretion of particular compounds, further understanding is required in terms of the inducing factors. The duo-plate co-cultures, for example provided a good platform from which to build models that are more complex. The current design allows for the detection of metabolites. Extrapolation of the duo-plates to systems would be possible with a better design as proposed in Figure 5.4.1. This design would enable the detection of gaseous emissions and volatile compounds, whilst also detecting metabolites and exopolymeric substances at the same time. The rising interest in this field will see the application of microalgal co-cultures for various applications in the biomanufacturing industry as a reality in the future.

References

[1] Suvarna K, Lolas A, Hughes P, et al. Case Studies of Microbial Contamination in Biologic Product Manufacturing. Am. Pharm. Rev. 2011;50–57.
[2] Ryan J. Understanding and managing cell culture contamination. Corning Tech. Bull. 2008;1–24.
[3] Padmaperuma G, Kapoore RV, Gilmour DJ, et al. Microbial consortia: a critical look at microalgae co-cultures for enhanced biomanufacturing. Crit. Rev. Biotechnol. 2017;0:1–14.
[4] Fukami T. Historical contingency in community assembly : integrating niches, species pools, and priority effects. Annu. Rev. Ecol. Evol. Syst. 2015;46:1–23.

[5] Loeuille N, Leibold M a. Evolution in metacommunities: on the relative importance of species sorting and monopolization in structuring communities. Am. Nat. 2008;171:788–799.
[6] Keerthi S, Koduru UD, Nittala SS, et al. The heterotrophic eubacterial and archaeal co-inhabitants of the halophilic Dunaliella salina in solar salterns fed by Bay of Bengal along south eastern coast of India. Saudi J. Biol. Sci. 2015;
[7] Kazamia E, Czesnick H, Nguyen TT Van, et al. Mutualistic interactions between vitamin B12 -dependent algae and heterotrophic bacteria exhibit regulation. Environ. Microbiol. 2012;14:1466–1476.
[8] Croft MT, Warren MJ, Smith AG. Algae need their vitamins. Eukaryot. Cell. 2006;5:1175–1183.
[9] Natrah FMI, Bossier P, Sorgeloos P, et al. Significance of microalgal- bacterial interactions for aquaculture. Rev. Aquac. 2014;6:48–61.
[10] Bardavid RE, Khristo P, Oren A. Interrelationships between Dunaliella and halophilic prokaryotes in saltern crystallizer ponds. Extremophiles. 2008;12:5–14.
[11] Oren A. Diversity of halophilic microorganisms: environments, phylogeny, physiology, and applications. J. Ind. Microbiol. Biotechnol. 2002;28:56–63.
[12] Oren A. Halophilic Microorganisms and their Environment. 5th ed. Dordrecht/Boston/London: Kluwer Academic Publishers; 2002.
[13] Peyton BM, Mormile MR, Petersen JN. Nitrate Reduction with Halomonas campisalis: Kinetics of Denitrification at pH 9 and 12.5% NaCl. Water Res. 2001;35:4237–4242.
[14] González-Domenech CM, Martínez-Checa F, Quesada E, et al. Halomonas cerina sp. nov., a moderately halophilic, denitrifying, exopolysaccharide-producing bacterium. Int. J. Syst. Evol. Microbiol. 2008;58:803–809.
[15] Cheirsilp B, Suwannarat W, Niyomdecha R. Mixed culture of oleaginous yeast Rhodotorula glutinis and microalga Chlorella vulgaris for lipid production from industrial wastes and its use as biodiesel feedstock. N. Biotechnol. 2011;28:362–368.
[16] Kitcha S, Cheirsilp B. Enhanced lipid production by co-cultivation and co-encapsulation of oleaginous yeast Trichosporonoides spathulata with microalgae in alginate gel beads. Appl. Biochem. Biotechnol. 2014;173:522–534.
[17] Wang E-X, Ding M-Z, Ma Q, et al. Reorganization of a synthetic microbial consortium for one-step vitamin C fermentation. Microb. Cell Fact. 2016;15:21.
[18] Brenner K, Karig DK, Weiss R, et al. Engineered bidirectional communication mediates a consensus in a microbial biofilm consortium. Proc. Natl. Acad. Sci. U. S. A. 2007;104:17300–17304.
[19] Sekar V. P.; Nandakumar, K.; Nair, K. V. K.; Rao, V. N. R. R. V. Early stages of biofilm succession in a lentic freshwater environment. Hydrobiologia. 2004;512:97–108.
[20] Oren A. Availability, uptake and turnover of glycerol in hypersaline environments. FEMS Microbiol. Ecol. 1993;12:15–23.
[21] Sitepu IR, Garay L a, Sestric R, et al. Oleaginous yeasts for biodiesel: current and future trends in biology and production. Biotechnol. Adv. 2014;32:1336–1360.

Appendix A: Isolation of species

The *Dunaliella salina* culture received was not axenic, therefore in order to be able to conduct co-culture studies, the two microorganisms had to be isolated. Furthermore, the isolating the microorganisms from one another aided during their identification process.

1. *Dunaliella salina* and *Halomonas* isolation

Dunaliella salina 19/18 culture was purchased from the Culture Collection of Algae and Protozoa (CCAP), was not axenic. Therefore, both *D. salina* and the bacterium were isolated and identified.

The *D. salina* cultures were first spread on 3M HEPES plates and isolate colonies where subcultured onto 3M HEPES plates containing 500µg/mL of cefoxamine. The algae plates where then passaged until traces of bacteria were not found under microscope observation. Finally, a few algae colonies were passaged into 30mL of medium, to get a starting liquid culture, to be later grown in 100mL and 250mL volumes.

In a similar fashion the bacteria was isolated, by spreading the 3M LB with 10µL of supernatant, with dilutions of 10^2 and 10^3. Dilution were carried out in order to separate the colony forming units (CFU) on the plate, to facilitate picking up single colonies. The 10^3 dilution plates were chosen; as the colonies were isolated form each other. A colony was chosen, to be spread on a new 3M agar plate. This procedure was carried out a few times before being satisfied that only bacteria was present. Both isolates were sent off for sequencing.

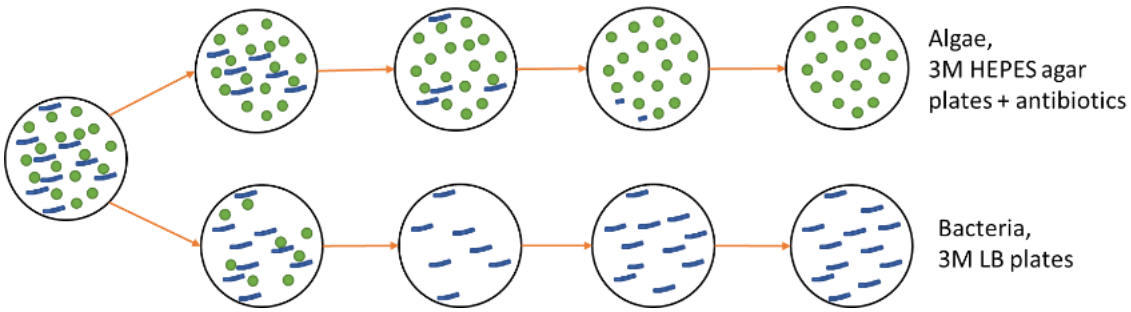

Figure 1.1: Diagram illustrating the process of isolating *D. salina* and *Halomonas* from CCAP cultures

2. Microorganisms isolation, identification and characterization

Molecular diversity analysis techniques, prevalently used to characterize bacteria, have recently gained interest in their application on algal strains [1]. The most common, 16s rRNA molecular marking technique for the identification of prokaryotes [2] and the 18s rRNA for eukaryotes, have provide data useful for the distinction of each species [3,4] However, when strains are closely linked evolutionary, the *rbcl* marker is used instead, which encodes for the carbon dioxide large fixing unit, ribulose-1, 5-busphate carboxylase/oxygenase, (RuBisCO). This subunit is conserved through evolution across all autotrophic organisms and provides greater resolution when compared to the 18S rRNA molecular marker. Furthermore, the sequences of internal transcribed spacers (ITS) within the 18S rDNA are very important in identifying strains as are the presence or absence of introns [1].

Here we want to confirm the identity of the following strains: *D. salina*, *S. obliquus,* and *Halomonas*

2.1.1. DNA Sequencing

Extraction of DNA and Polymerase Chain Reaction

Briefly, 2 x 5mL of algal cells from each strain were collected and centrifuged for 5 minutes at 2.500xg. The supernatant free pellets were then used for DNA extraction and subsequently processed through DNA amplification, using Polymerase Chain Reaction (PCR). The CTAB method [5], with modifications, and ZR Soil Microbe DNA MicroPrep™ kit were used to isolate the DNA from each species. The extraction efficiency of the CTAB method was compared to the ZR Soil Microbe DNA MicroPrep™ kit (Zymo Research, D6003) in order to attest which method should be used for future work.

CTAB Method

The cell pellets were resuspended in 500µL of CTAB solution and lysed using beat beating (3-4 minutes). The extract was then incubated for 1.5 hour at 65°C and phenol-chloroform isoamyalcohol (24:25:1) added. The colourless solution, containing the DNA, was separated from the biphasic solution and mixed with 3M sodium acetate and pre-chilled 100% ethanol to be the incubated at 4°C for 5 minutes. Through step-wise centrifuging, the supernatant was removed promptly, avoiding the pellet from to resuspend. Finally, the samples were left to air dry for no more than 5 minutes, as prolonged drying causes the DNA pellet to bind tightly to tube surface. After adding 30-

40µL of TE buffer the samples were allowed to resuspend overnight. Prior to PCR, these were incubated for 60-90minutes at 50°C.

ZR Soil Microbe DNA MicroPrepTM kit

The instructions provided on the packaging, were carried out, with a few modifications as follows. Firstly, 750 µL of the Lysis solution was added prior to bead beating. 400µL of extract was then removed into the Zymo-Spin™ IV Spin Filter, centrifuged at 7,000g for 1 minute. 1.2mL of Soil DNA Binding Buffer was added to the filtrate in the column and the mixture was then transferred into a Zymo-Spin™ IC column. The flow-through was discarded and 200µL DNA Pre-Wash Buffer was added to the Zymo-Spin™ IC column and centrifuged at 10,000g for 1 minute. Following, 500µL of Soil SBA Wash Buffer was added to the Zymo-Spin™ IC column and centrifuged at 10,000xg for 1 minute. DNA Elution Buffer was then pipetted into the Zymo-Spin™ IC column to release the DNA from the matrix.

Agarose Gel Electrophoresis

As the DNA extracted was not visible, an agarose gel was run to attest for its presence. Agarose gel electrophoresis is suitable for the separation of DNA fragments measuring from 100 bp to 25 kb. DNA fragments are loaded into a pre-made gel cast and a current is applied. The phosphate backbone of the DNA molecules, upon application on an electric filed will cause the fragments to move towards the positive electrode. Since the gel consists of a matrix comprising of varying pore sizes, it will act as a molecular sieve separating the DNA fragments according to size, where the distance travelled is inversely proportional to the log of its molecular weight. A stain has to be used in conjunction to the DNA digestate, in order to allow for the visualization of the bands under UV light. The gel was run for 60 minutes with an electric field set to 80V.

Polymerase Chain Reaction for amplification of DNA

PCR has been used as a method for the amplification of DNA sequences that encode small subunit rRNA. This technique requires on the use of two short oligonucleotides, which will act as primers for elongation [6]. PCR is a cyclic process where the original DNA strand is first denatured, by increasing the temperature, to separate the duplex strands. Following, the primers anneal and extend the strands over a period of cycles, doubling the amount of DNA per cycle [7]. Universal primers for the 18S molecular marking technique were used: the forward primer GTAGTCATATTGTCTC and the reverse

primer being CACCTACGGACGACTT. The PCR themorcycle was set as follows:94°C for 3 minutes, 94°C for 1 minute, 55°C for 1 minute, 72°C for 2 minutes, and 72°C for 5 minutes (last three cycles were repeated 30 times). Following amplification the samples were purified using Anachem PCR Clean Up kit (AM 113153). The resulting DNA was then checked nanodrop and stored at -20°C. The amplified DNA alongside the respective primers was sent to Eurofins (Germany) for sequencing.

3. Results

For the *D. salina* confirmation yielded and identity match of 99%.

Nucleotide sequence:

>2 Lim For_18S-Lim-For -- 15..520 of sequence

GTTAAAAGCTCGTAGTTGGATTTCGGGTGGGTTGTAGCGGTCAGCCTTTGGTTAGTACTGCTACGGCCTACCTTTC
TGCCGGGGACGAGCTCCTGGGCTTAACTGTCCGGGACTCGGAATCGGCGAGGTTACTTTGAGTAAATTAGAGTGT
TCAAAGCAAGCCTACGCTCTGAATACATTAGCATGGAATAACACGATAGGACTCTGGCTTATCTTGTTGGTCTGTA
AGACCGGAGTAATGATTAAGAGGGACAGTCGGGGGCATTCGTATTTCATTGTCAGAGGTGAAATTCTTGGATT
TATGAAAGACGAACTTCTGCGAAAGCATTTGCCAAGGATGTTTTCATTAATCAAGAACGAAAGTTGGGGGCTCGA
AGACGATTAGATACCGTCGTAGTCTCAACCATAAACGATGCCGACTAGGGATTGGCAGGTGTTTCGTTGATGACCC
TGCCAGCACCTTATGAGAAATCAAAGTTTTTGGGTTGCGGGGGGAAGTATGGTCA

>2 Lim Rev_18S-Lim-Rev -- 23..522 of sequence

GCAGGGTCATCAACGAAACACCTGCCAATCCCTAGTCGGCATCGTTTATGGTTGAGACTACGACGGTATCTAATCG
TCTTCGAGCCCCCAACTTTCGTTCTTGATTAATGAAAACATCCTTGGCAAATGCTTTCGCAGAAGTTCGTCTTTCATA
AATCCAAGAATTTCACCTCTGACAATGAAATACGAATGCCCCCGACTGTCCCTCTTAATCATTACTCCGGTCTTACA
GACCAACAAGATAAGCCAGAGTCCTATCGTGTTATTCCATGCTAATGTATTCAGAGCGTAGGCTTGCTTTGAACAC
TCTAATTTACTCAAAGTAACCTCGCCGATTCCGAGTCCCGGACAGTTAAGCCCAGGAGCTCGTCCCCGGCAGAAAG
GTAGGCCGTAGCAGTACTAACCAAAGGCTGACCGCTACAACCCACCCGAAATCCAACTACGAGCTTTTTAACTGCA
ACAACTTAAATATACGCTATTGGAGCTGGAAATTACCGCCA

For the *Halomonas* confirmation yielded and identity match of 100%.

Nucleotide sequence:

GCTTGTTGGTGAGGTAAAGGCTCACCAAGGCGACGATCCGTAGCTGGTCTGAGAGGATGATCAGCCACATCGGGACTG
AGACACGGCCCGAACTCCTACGGGAGGCAGCAGTGGGGAATATTGGACAATGGGCGAAAGCCTGATCCAGCCATGCCG
CGTGTGTGAAGAAGGCTTTCGGGTTGTAAAGCACTTTCAGTGAGGAAGAAGGCCTTGGGGCTAATACCCCCGAGGAAG
GACATCACTCACAGAAGAAGCACCGGCTAACTCCGTGCCAGCAGCCGCGGTAATACGGAGGGTGCGAGCGTTAATCGG
AATTACTGGGCGTAAAGCGCGCGTAGGCGGCGTGATAAGCCGGTTGTGAAAGCCCCGGGCTCAACCTGGGAACGGCAT
CCGGAACTGTCAGGCTAGAGTGCAGGAGAGGAAGGTAGAATTCCCGGTGTAGCGGTGAAATGCGTAGAGATCGGGAG
GAATACCAGTGGCGAAGGCGGCCTTCTGGACTGACACTGACGCTGAGGTGCGAAAGCGTGGGTAGCAAACAGGATTAG

ATACCCTGGTAGTCCACGCCGTAAACGATGTCGACTAGCCGTTGGGGTCCTAGAGACCTTTGTGGCGCAGTTAACGCGA
TAAGTCGACCGCCTGGGGAGTACGGCCGCAAGGTT

For the *S. obliquus* confirmation yielded and identity match of 99%, with *Acutodesmus obliquus* (a synonym for *S. obliquus*).

Nucleotide sequence:

TTAAAAGCTCGTAGTTGGATTTCGGGTGGGTTCTAGCGGTCCGCCTATGGTGAGTACTGCTATGGCCTTCCTTTCTGTCG
GGGACGGGCTTCTGGGCTTCACTGTCCGGGACTCGGAGTCGACGTGGTTACTTTGAGTAAATTAGAGTGTTCAAAGCAG
GCTTACGCCAGAATACTTTAGCATGGAATAACACGATAGGACTCTGGCCTATCTTGTTGGTCTGTAGGACCGGAGTAATG
ATTAAGAGGGACAGTCGGGGGCATTCGTATTTCATTGTCAGAGGTGAAATTCTTGGATTTATGAAAGACGAACTACTGC
GAAAGCATTTGCCAAGGATGTTTTCATTAATCAAGAACGAAAGTTGGGGGCTCGAAGACGATTAGATACCGTCGTAGTC
TCAACCATAAACGATGCCGACTAGGGATTGGCGAATGTTTTTTTAATGACTTCGCCAGCACCTTATGAGAAATCAAAGTT
TTTGGGTTGCGGGGGGGTT

4. References

[1] Ghosh S, Love NG. Application of rbcL based molecular diversity analysis to algae in wastewater treatment plants. Bioresour. Technol. 2011;102:3619–3622.

[2] Zakharova YR, Adel'shin R V., Parfenova V V., et al. Taxonomic characterization of the microorganisms associated with the cultivable diatom Synedra acus from Lake Baikal. Microbiology. 2010;79:679–687.

[3] Flechtner VR, Pietrasiak N, Lewis LA. Newly Revealed Diversity of Green Microalgae from Wilderness Areas of Joshua Tree National Park (JTNP). Monogr. West. North Am. Nat. 2013;6:43–63.

[4] Dayananda C, Kumudha A, Sarada R, et al. Isolation, characterization and outdoor cultivation of green microalgae Botryococcus sp. Sci. Res. Essays. 2012;5:2497–2505.

[5] Varela-Alvarez E, Andreakis N, Lago-Leston A, et al. Genomic DNA Isolation from Green and Brown Algae (Caulerpales and Fucales) for Microsatellite Library Construction. J. Phycol. 2006;42:741–745.

[6] Brown TA. The Polymerase Chain Reaction. Gene Cloning DNA Anal. 5th ed. Blackwell Publishing; 2001. p. 181–183.

[7] Mullis KB. The Unusual Origin of the Polymerase Chain Reaction. Sci. Am. 1990;56–65.

Appendix B: UV-Vis absorption spectroscopy to monitor individual microorganism in co-cultures

6.1. Introduction

Natural or artificial co-cultures consist of an assemblage of two organisms, which will display different traits when growing in unison, as opposed to as single species. Monitoring the growth and morphology of individual species provides an indication of how well the associates work in unison. Methods have been developed to manually or instrumentally assess population dynamics and to record their behaviour. These include haemocytometer counts, colony formation units, and viable cell counts that rely on visual inspection highly prone to human error. Other methods include spectrophotometers, Coulter counter, and fluorescence-activated cell sorting (FACS). These methods are robust and detect the light scattered by the particles within the samples, due to auto-fluorescence or added fluorescence, and in the case of FACS separation by size and morphology is possible [1,2].

Haemocytometer counts coupled with image analysis software are commonly used to estimate numbers of bacteria, algae and yeast. However, limitations occur when many counts are performed, due to user tiredness and non-homogenous pipetting. For co-culture set-ups, the species need to be easily differentiated. Furthermore, numerous counts are required, to account for all the cell types, increasing the margin of error. In addition, cells need to be a certain size and clearly distinguishable for good results. The cells need to be fixed, for example with Lugol, before counting. Lugol may cause some cells to shrivel and others to agglomerate, creating clumps that are hard to break without damaging the cells. Staining, for viability counts has been coupled with haemocytometers. However, this method does not work effectively with green/blue pigmented cells, such as microalgae.

Colony formation unit (CFU) has been widely used to estimate bacterial numbers. The method is based itself on the hypothesis that one bacterium will generate one colony. Like haemocytometer counts, CFU method becomes tiresome with a high risk of errors. Additionally, with poor sterile technique, contamination from other microorganisms is unavoidable.

Spectrophotometers, FACS and Coulter counter would provide better estimations. These instruments are able to differentiate between organisms based on size, or fluorescence. Many models are available; however, due to their high costs and maintenance hurdles, they are not present in all research labs. Looking at the options available, spectrophotometers are the most commonly available instruments within research laboratories; with many newer models equipped to measure absorption spectra and perform multi-well plate assays.

Haemocytometer microalgae counts and CFU units for bacterial, haloarchaeon coupled to spectrophotometer readings have been used in the investigations presented in chapters three, four and five of this thesis. When dealing with co-cultures, the method was quite easy to implement. However, it was not as straightforward when looking at a consortium. In this chapter, the possibility of using spectrophotometry data to distinguish between microorganisms in co-cultures is investigated. This is a method that has been applied previously to distinguish between phytoplankton cells [3,4]. The model proposed here however, allows for distinguishing microalgae populations from other microorganisms, such as bacteria, fungi, and yeast when in co-culture, and vice-versa, for the first time. With further development, the models developed can be used to estimate *in vivo* each microorganism population density in terms of cell counts or CFUs.

6.1.1. Absorbance spectrophotometry

Absorbance spectrophotometry measures the amount of incident light transmitted through a solution. It compares the amount of light that passes through the sample to the initial value. The resulting difference is the sample absorbance, expressed in optical density measurements (OD) or relative fluorescence measurements (RFM). Spectrophotometers are able to provide both chemical and turbidity absorbance measurements.

6.1.2. Chemical absorbance measurements

In chemical absorbance, the wavelength at which the optical density is measured will provide absorption value calculated from the difference between the light absorbed by the blank sample, versus the light absorbed by the analysed samples. Samples will display different absorption wavelengths that will belong to the UV-region, 200-300nm (colourless samples), or in the infrared/visible spectrum, 300nm to 800nm (coloured

samples). Through an absorption spectral scan, ranging from 200nm to 800nm it is possible to pinpoint the best wavelengths, at which the sample activity should be measured; this measurement will correspond to the highest or most pronounced peak in the scan.

6.1.3. Turbidity measurements

Furthermore, spectrophotometers are used to estimate the density of particles in suspension, usually referred to as the turbidity of the sample. Spectrophotometers are able to measure the turbidity of a sample, because a portion of the light beam is reflected by the scattering of the particles that are suspended in the sample [5]. The particles would ideally be in a colourless medium, which does not have high absorbance. Nevertheless, when a coloured medium is used, the same medium in the absence of particles is used to blank the instrument and provide a baseline for the measurements. Thus, the particles carry a different refractive index than the liquid in which they are suspended. In this case, it is assumed that all particles are similar in size, shape and that their morphology is spherical; this same principle is applied when measuring microorganisms in suspension.

6.1.4. Challenges

One of the main issues to bear in mind is that each spectrophotometer unit will have its unique combination of incident light source, detection angle, and number of detectors. These parameters, together with the natural variation from the sample, will lead to different results [1]. Therefore, it is imperative to either use the same machine throughout the investigation, or to account for the variations in reading by establishing the ‘shift factor’. The shift factor can be calculated by measuring the same samples on the different machines used; correlation graphs can be obtained from which to calculate the shifts. These shifts can also be seen when the deuterium light on the spectrophotometry is due for replacement. To circumvent this problem, researchers provide information on the type of technology used. When dealing with microorganisms, morphology changes, pH, viscosity of the media, cell lysis, and contamination are amongst some of the factors that can interfere during measurements.

6.1.5. Applications

Spectrophotometry is widely used to quantitatively monitor the growth rate of microorganisms in suspension cultures. The absorbance, also referred to as optical density, is a measurement of turbidity of the representative sample [6], which can be correlated to dry weight and cell counts. This method was initially developed to monitor bacterial growth found its application in the field of microalgae [1]. Efforts have been made to use spectrophotometry as means to differentiate phytoplankton community members. A simple method was required for real-time monitoring of harmful microalgae blooms. Spectrophotometric methods were chosen by Kirkpatrick et al. [4] to monitor *Gymnodinium breve*, a toxic dinoflagellate present in the Gulf of Mexico, whose quick detection and destruction would prevent marine and human life from adverse health. By using processing algorithms based on the absorption spectra of *G. breve* and applying similarity indexes, it could be shown that discrimination of the *G. breve* species was possible using absorption based analysis. A fourth derivative spectrum transformation allowing for the discrimination between phycobilins, non-phycobilins, fucoxathins and other spectral classes of microalgae strains was later proposed [3].

6.1.6. Absorption spectra in microorganisms

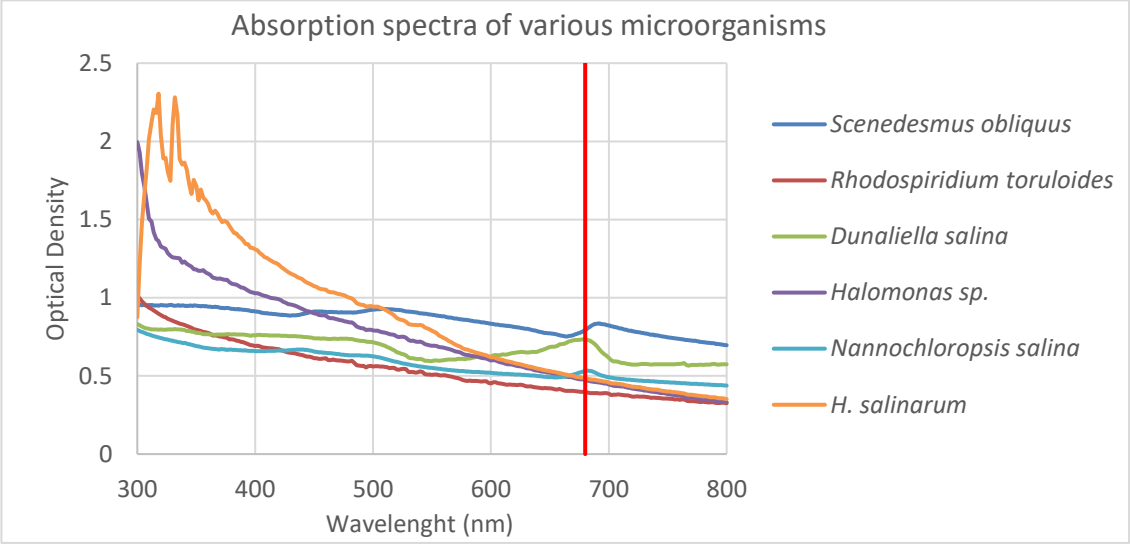

Figure 6.1.1: Absorption spectra in the visible region of the species studied in this thesis compared to a representative microalgae species.

Figure 6.1.1 depicts absorption spectra obtained for the species of algae, bacteria and yeast studied in this investigation. It is noticeable that pigmented microorganisms such

as algae, will display more than one peak, relating to the abundance of characteristic pigments [7]. In the case of the green algae, *Dunaliella salina*, *Scenedesmus obliquus*, and the Eustigmatophyte alga *Nannochloropsis salina*, peaks appear at 680nm (highlighted in red), a signature peak for microalgae, which indicates the presence of chlorophylls within the cells [8]. Other microalgae distinguishable peaks are at 450nm and 470nm attributed to the presence of various carotenoids within the microalgae cells [9,10].

In a similar fashion, pigments in yeasts and archaea, will display pigment peaks. In the case of both, *Rhodosporidium toruloides* and *Halobacterium salinarum*, this is shown when the microorganisms are under stress. As both organisms, accumulate carotenoids, respective peaks are seen in the absorption spectrum at 450-470nm regions. In the case of the non-pigmented strains, such as *E.coli* and *Halomonas*, the absorption spectrum does not show any major characteristic peak, thus measurements in the regions of 595-600nm and 750nm are chosen, as these are considered good regions for turbidity measurements. It is important to bear in mind, that the absorption spectrum of the species may display differences when subjected to stress. This can be due to nutrient limitations or when subjected to stresses, such as high light, changes in salinity, temperature, pH or medium changes.

Algorithms created based on absorption-based data would allow simultaneous detection of individual species within a consortium. Allowing, for controlled co-culturing measures to be adopted, to boost or limit the propagation of certain species. However, this method comes with its own limitations. The presence of interfering wavelength signals, as in the case of microalgae, delimits the range where the optical density can be measured. It is possible that the wavelengths chosen for measurements of turbidity may reflect the absorbance associated with pigments [11]; as in the case for 680nm, a wavelength also used to monitor the activity of PSII [8], which if used may cause interference. Within a mixed culture, distinguishing one species from another requires clear and robust models. These models are usually built on axenic cultures to be later extrapolated to mixtures [3]. By finding wavelengths or regions, of wavelengths analogous to microalgae should facilitate this task. For example, a single wavelength value (OD_{600nm}) has been stipulated for measuring optical density for *E. coli* strains grown

in LB broth at [12]. Conversely, the literature survey conducted shows that numerous wavelengths have been used to measure the optical density of microalgal samples, as shown in Table 6.1.1.

Table 6.1.1: Absorbance wavelengths used to measure microalgae

Absorbance Wavelength	Species	Reference
530nm	*Ettlia texensis*	[13]
	Monodus subterraneous	[14]
540nm	*Neochloris oleabundaus*	[15]
560nm	*Chlorella sp.*	[16]
	Dunaliella tertiolecta	
	Botrycoccus braunii	
	Scenedesmus sp.	
	Isochrysis sp.	
595nm	*Chlamydomonas reinhardtii*	[17]
600nm	*Scrippsiella trochoidea*	[18]
650nm	*Selenastrum capricornutum*	[19]
	Chlorococcum hypnosporum	
680nm	*Haemotococcus pluvialis*	[20]
	Monodus subterances	[14]
	Cyanothece sp.	[21]
	Chlorella sp.	[22]
	Chlorella vulgaris	[11]
	Nannochloropsis salina	[11]
	Spirulina platensis	[11]
	Scenedesmus sp.	[11]
	Chlorella sp.	[11]
	Dunaliella salina	[23]
	Nannochloropsis gatidana	[24]
682nm	*Chlorella sp.*	[25]
	Dunaliella salina	[23]
	Dunaliella sp.	
	Chlorella vulgaris	
700nm	*Chlorella vulgaris*	[26]
730nm	*Scenedesmus caribeanus*	[27]
	Chlorella vulgaris	
735nm	*Chlorella sokoriniana*	[28]
	Cyanothece sp.	[21]
750nm	*Microcystis aeruginosa*	[29]
	Chlorella vulgaris	[11,30]
	Nannochloropsis salina	[11,31]
	Spirulina platensis	[11]
	Scenedesmus sp.	[11]
	Dunaliella salina	[11]
	Dunaliella virdis	[11]
	Dunaliella primolecta	[11]
	Chlorella sokoriniana	[32]
	Chlorella sp.	[31]
	Tetraselmis suecica	

The values reported in Table 6.1.1 only account for some of the literature surveyed for this study. Numerous other wavelengths have been chosen depending on the author's preference. It is noticeable that most measurements have been taken in the 680-730nm region, where the presence of chlorophylls is high, and in the 500nm region, where xanthophylls and carotenes were detected.

Given this background, the question addressed here is to establish whether UV-Vis absorption spectrums can be developed to identify species in mixed cultures.

6.2. Experimental Design

Work from the early 1950s demonstrated each microorganism emits a particular spectrum, similar to a fingerprint [33]. Within this spectrum, there are regions of high intensity seen as peaks on the spectrum. These wavelengths are characteristic to organisms belonging to the same genus. However, as discussed by Hom et al. [34] the morphology and behaviours of the organisms differ with changing environment, which will translate into changes in the spectrum. These changes are not easy to factor into a model. However, efforts have been made to address them and produce a model to differentiate between *D. salina*, *Halomonas* and *H. salinarum* when present in co-culture.

6.2.1. Building the model on monocultures

6.2.1.1. Microorganism growth and data gathering

The first task was to obtain absorption spectra from axenic cultures of *D. salina*, *Halomonas* and *H. salinarum*. The microorganisms were grown as outlined in section 4.3.2.1 and 4.3.3.1 with varying salinity (NaCl concentration: 1.5M, 2M and 3M for *D. salina* and *Halomonas*, and at 3M and 4.2M for *Halobacterium salinarum*).

Biological triplicates were set-up in 250mL Erlenmeyer flasks with a working volume of 100mL. As the microorganisms entered exponential phase, 1mL of sample was pipetted into a cuvette and measured. If required, the samples were concentrated to obtain an optical density of 1, which is the upper limit of accurate detection of the spectrophotometer. Subsequent dilutions up to 1/16th for *D. salina* and *H. salinarum*, and 1/32nd for *Halomonas* of the same sample were also measured. The dilutions

allowed the building of the model to account for shifts in the peaks when low concentrations of cells were in suspension.

6.2.1.2. Second derivative

Spectral absorptions are a good way of measuring solid suspensions, and microorganisms, in liquid pigments. However, when these pigments are detected in narrow regions of the spectrum, deciphering the data becomes complicated, as absorption peaks often overlap with each other. Taking the second derivative of the data would enhance the separation of the overlapping peaks [35].

6.2.2. Univariate and Bivariate models

Using a univariate model approach, the absorption spectra data for each microorganism, at each salinity was correlated to the dilutions. The R^2 (Pearson's coefficient of determination) values was calculated for all linear models and only the 10 best models were chosen. The same wavelengths were fitted with bivariate models to check if previously obtained R^2 values could be improved.

6.2.3. PCA plots and wavelength region selection

Looking at the results obtained in method 6.2.2 a second approach was carried out. This would attempt at incorporating changes and shift in the spectra that may occur during natural growth. Principle Component Analysis (PCA) was used to correlate the second derivative data with the dilutions. The resulting factor loadings indicated the regions where the correlation coefficients between the second derivative and the dilutions were the highest. Using the summation of the regions, multivariate models were explored for the identified wavelength areas.

6.3. Results

6.3.1. Building the model on monocultures

6.3.1.1. Second derivative

The second derivate of all the absorption spectra data was taken as this allowed better visualization of the areas in which the major peaks were present.

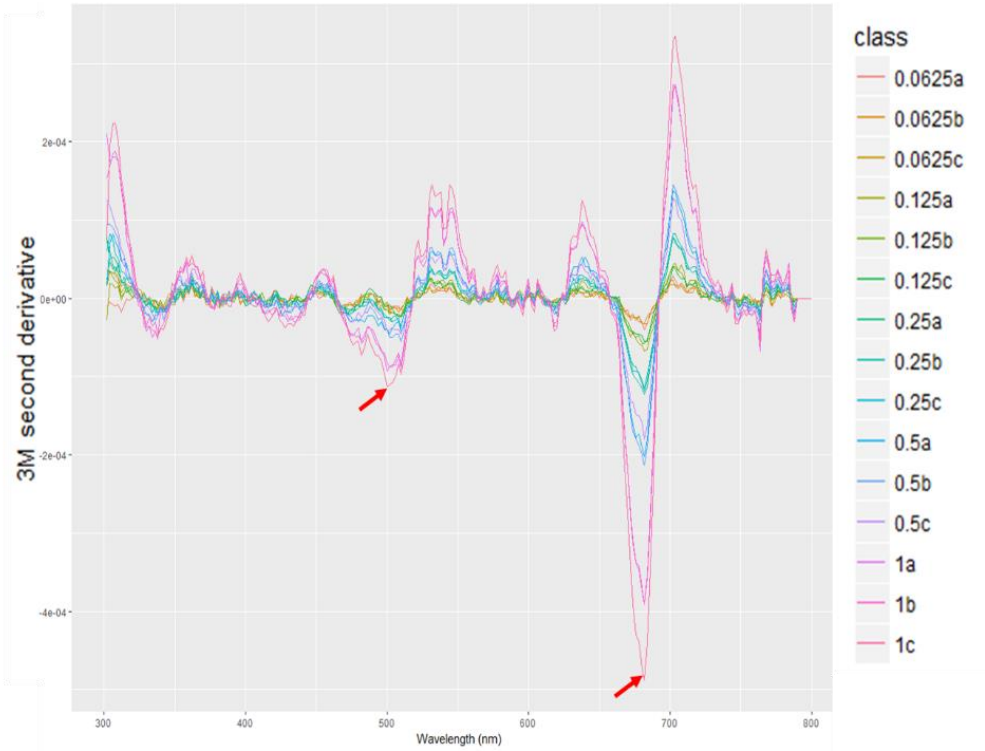

Graph 6.3.1: Second derivative data of 3M *D. salina*.

Graph 6.3.1 shows how the second derivative deconvolutes the absorption spectra. The regions selected correspond to the highest peaks (indicated by the red arrow). The same procedure was carried out for all the datasets.

6.3.2. Univariate and Bivariate models

The data presented in the table below, summarises the univariate and bivariate models found for the axenic monocultures. The data obtained shows that at particular salinities each species displays better fits for the data (high R^2 values).

Table 6.3.1: Univariate and Bivariate fittings using single wavelengths and dilutions

Microorganism	Univariate	R^2	Bivariate	R^2
3M *D. salina*	636nm	0.988	636nm+636nm	0.988
	538nm	0.979	636nm+630nm	0.987
	-	-	636nm+542nm	0.9868
	-	-	636nm+538nm	0.9864
2M *D. salina*	476nm	0.924	474nm*476nm	0.977
	548nm	0.912	-	-
1.5M *D. salina*	336nm	0.984	336nm+332nm	0.987
	694nm	0.979	363nm+363nm	0.983
4.2M *H. salinarum*	574 nm	0.998	540nm+512nm	0.998
	788nm	0.997	540nm+576nm	0.998
	576nm	0.997	540nm-576nm	0.998
3M *H. salinarum*	562nm	0.719	-	-
	422nm	0.643	-	-
1.5M *Halomonas*	304 nm	0.995	304nm + 780nm	0.995
	546nm	0.994	546nm + 304nm	0.995
2M *Halomonas*	496nm	0.995	548nm+496nm	0.997
	548nm	0.995	786nm+496nm	0.996
3M *Halomonas*	330nm	0.189	-	-

6.3.3. PCA plots and wavelength region selection

The principle component 1 (PC1) plots presented in Graphs 6.3.2 to 6.3.4, show the variance between the dilutions and the second derivative data.

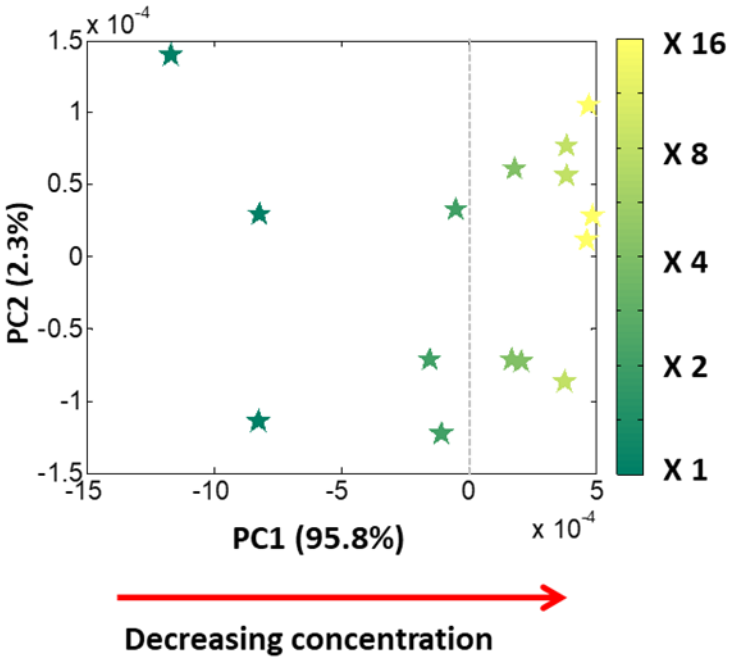

Graph 6.3.2: PCA scores plot for 3M *D.* salina data.

The *D. salina* data has a 95.8% variance in the first principal component axis, indicating that most of the variance associated with the change in concentration of *D.salina* is captured in PC1.

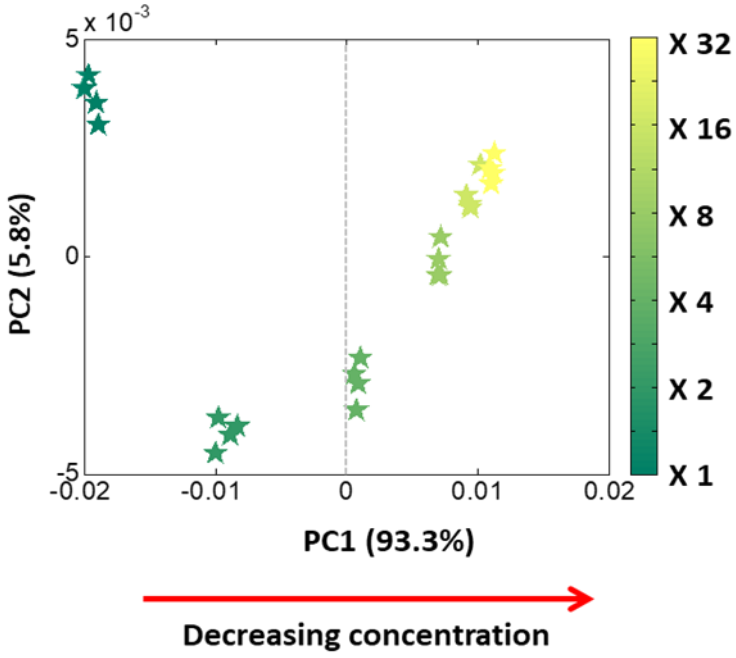

Graph 6.3.3: PCA plot for 1.5M *Halomonas*

The *Halomonas* dataset shows high degree of correlation between the second derivative and the dilution data.

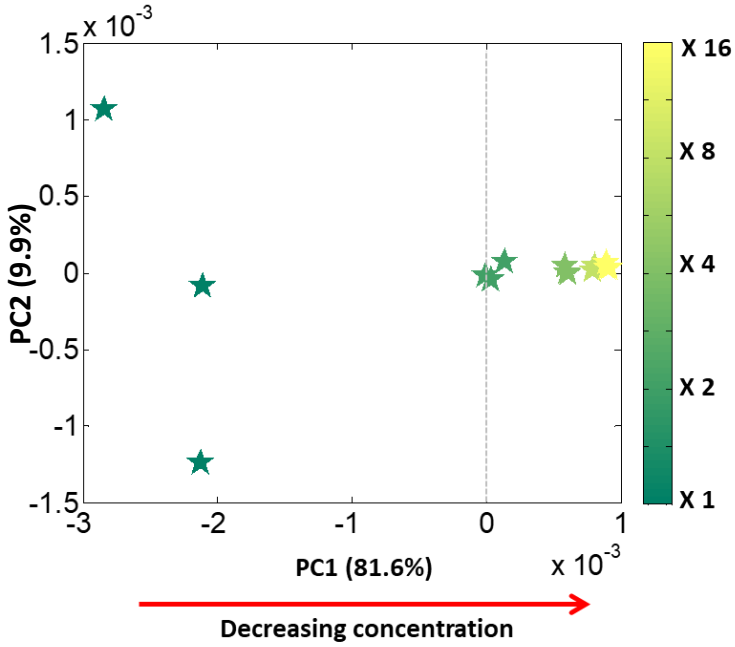

Graph 6.3.4: PCA plot for 4.2M *H. salinarum*

The *H. salinarum* dataset does not show very high correlation compared to *D. salina* or the *Halomonas* The variance of 81.6% is lower compared to the other datasets due to spectral data from the non-diluted samples.

The PCA loadings in Figure 6.3.1 indicate the regions to which the model should be applied.

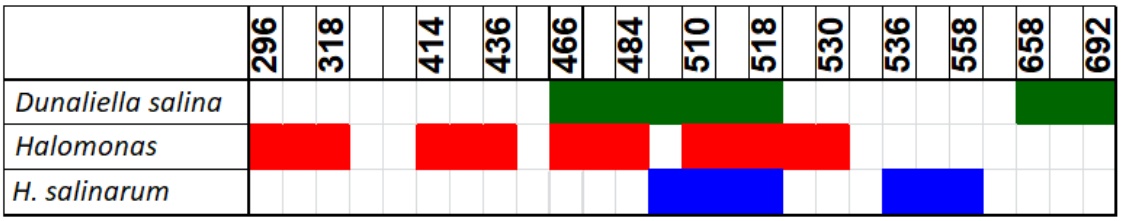

Figure 6.3.1: Wavelength regions highlighted by PCA loadings to have correlation to changes in concentration of the respective microbial species.

Graphs 6.3.5 to 6.3.7 illustrate the PCA loading results. The red squares indicate the regions indicated by in Figure 6.3.1.

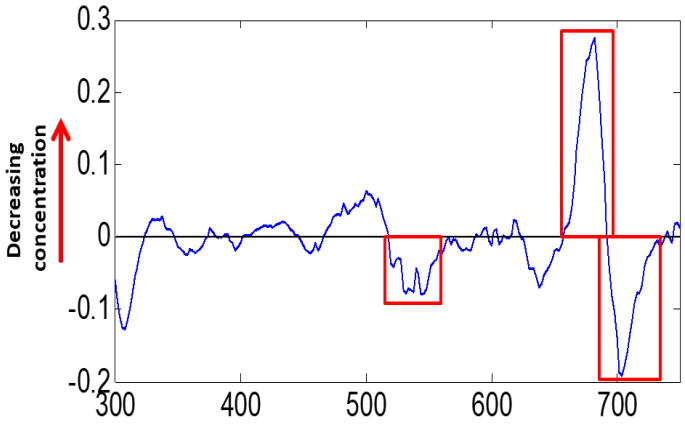

Graph 6.3.5: PCA loadings for PC1 of the 3M *D. salina* data.

An extra region was selected from the *D. salina* data. Region 694-732nm was chosen, as any effect on this region would have an impact on the 658-692nm zone.

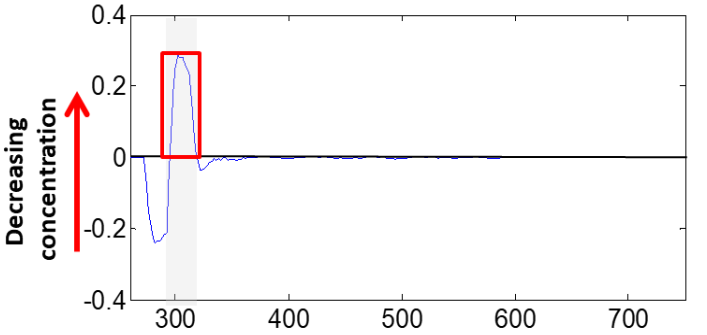

Graph 6.3.6: PCA loadings for 1.5M *Halomonas*

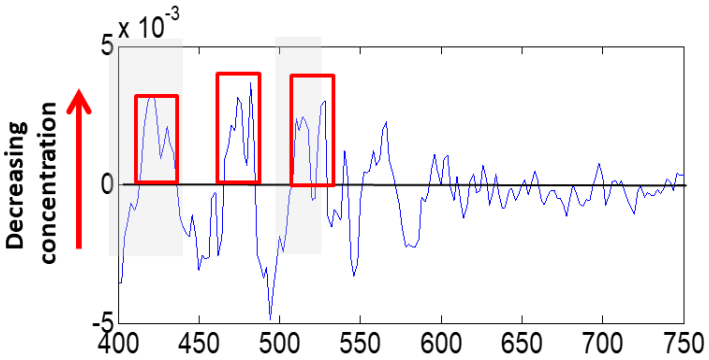

Not all the regions highlighted in the PCA loadings were chosen. Regions 466-484nm and 510-530nm, were disregarded as these regions are prominent in both *D. salina* and *H. salinarum*. Region 274-294nm was chosen, to minimise the impact of the trough near the 296nm region.

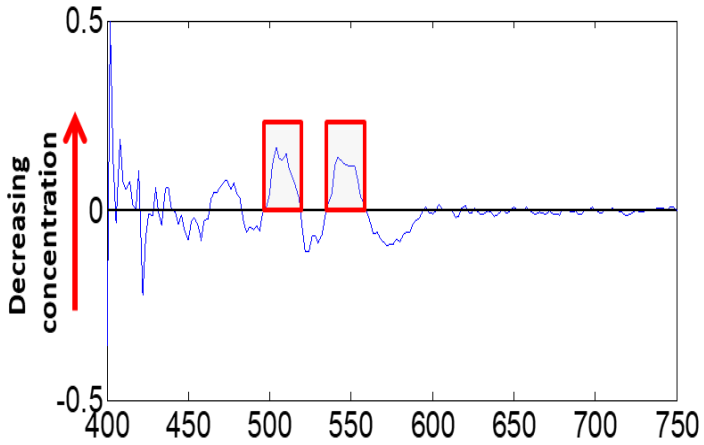

Graph 6.3.7: PCA loadings for 4.2M *H. salinarum*.

The first region, 496-518nm, falls within the regions highlighted for *D. salina*. However, the weight of the second, should allow for the detection only of *H. salinarum*.

Multivariate and bivariate models were developed according to the regions suggested by the PCA loadings. Table 6.3.2 provides an overview of the regions used for the detection of each microorganism and a summary of the nomenclature used in the graphs.

Table 6.3.2: Nomenclature used in the graphs

Label	Wavelength region	*D. salina*	*H. salinarum*	*Halomonas*
296nm	296-318nm	×	×	√
274nm	274-294nm	×	×	√
466nm	466-518nm	√	√	×
414nm	414-436nm	×	×	√

496nm	496-518nm	×	√	×
536nm	536-558nm	×	√	×
658nm	658-692nm	√	×	×
694nm	694-732nm	√	×	×

√ - indicates to which species the spectra belongs to, whilst × indicates which species are not detectable in that region.

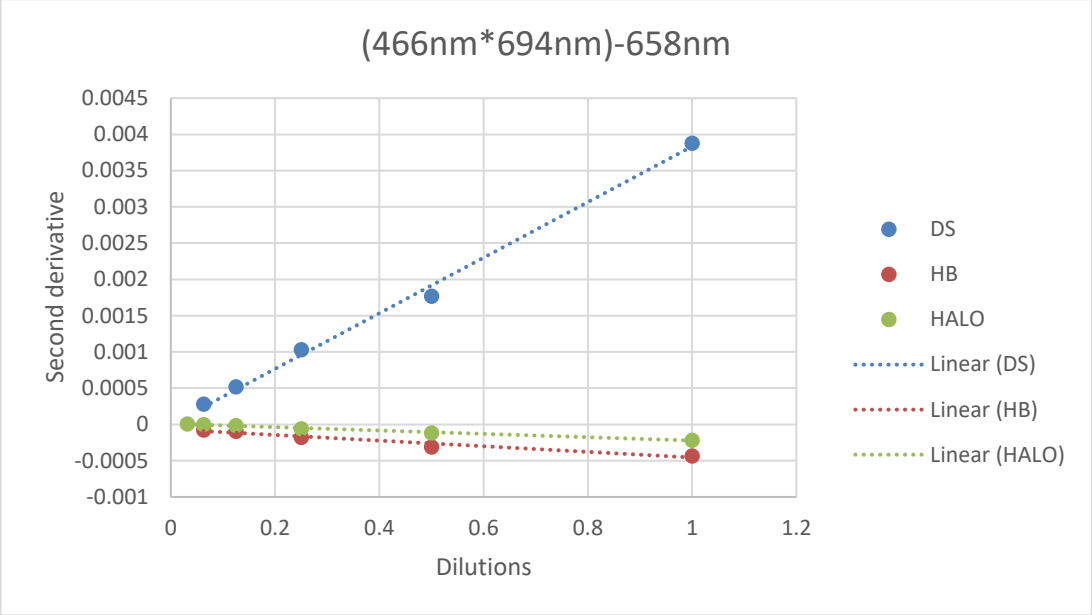

Graph 6.3.8: Multivariate model for the detection of D. salina in co-cultures.

The model proposed in Graph 6.3.8 shows how the regions selected, for the *D. salina* data at a higher magnitude compared to *Halomonas* and *H. salinarum.* Other models include 658nm-694nm and (466nm*658nm)-694nm.

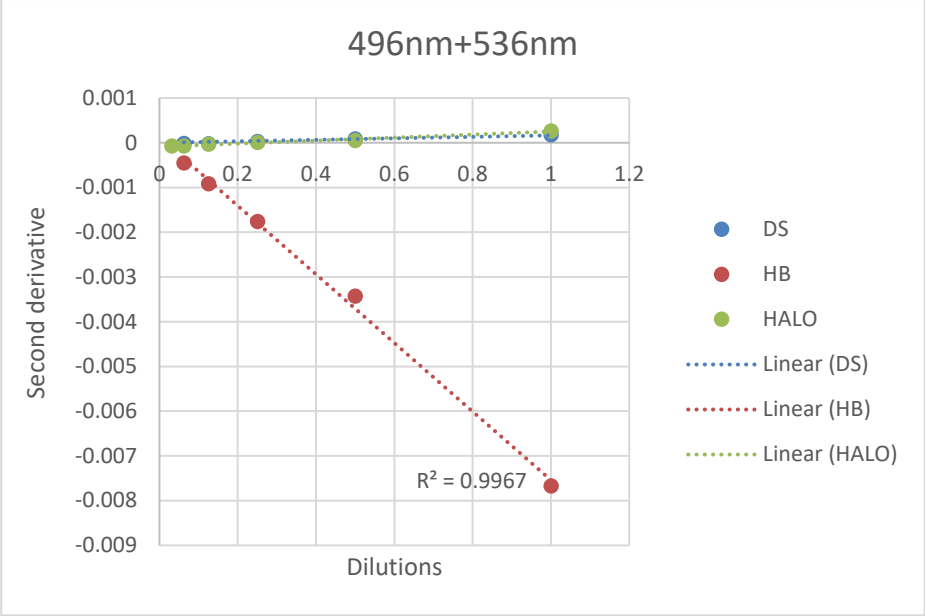

Graph 6.3.9: Bivariate model for the detection of *H. salinarum* in co-cultures.

Similarly, the model chosen for the detection of *H. salinarum* illustrates that the relationship is highly pronounced for the archaeon data compared to the other microorganisms.

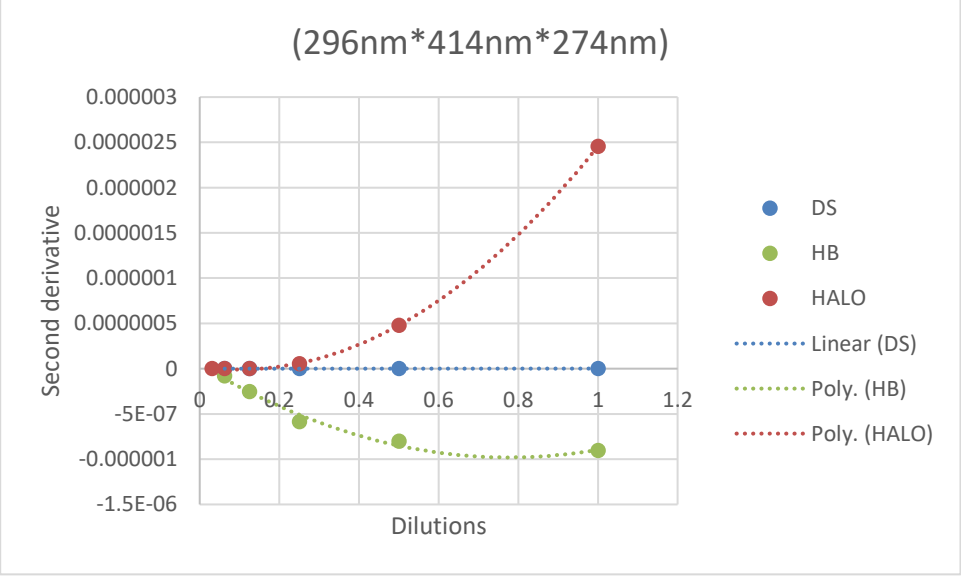

Graph 6.3.10: Multivariate model for the detection of *Halomonas*

The multivariate model for *Halomonas* is a product of the chosen regions. A polynomial plot shows how the data best fits the bacterium second derivative data. However, there may be still some interference from the *H. salinarum* presence. Another model that shows a similar trend is 296nm+414nm.

6.4. Discussion

Literature survey conducted to understand which best wavelength to use for monitoring of green microalgae cultures revealed that non-specific value have been used (Table 6.1.1). The use of a wavelength of 680nm, chlorophyll peak in green algae, is not recommended due to interference from PSII [8]. Commonly used wavelength to monitor *Dunaliella* cells are 560nm, 680nm, 682nm and 750nm, indicating that these have been chosen according to the algae strain. *Halobacterium* strains were monitored at 530nm [36] or 600nm [37] and *Halomonas* at 600nm [38], using values conventionally used for *E. coli*. As the survey provided many options but an undecided conclusion, an investigation was carried out on how to best monitor *D. salina* cells by themselves or in co-culture.

The development involved taking the second derivative of the data and correlating this to the corresponding dilutions. The correlation coefficient (R^2) or principle component analysis variances (PC1) were used to extrapolate regions of interest. These regions particular to each microorganism were used to develop the model.

The R^2 coefficient alongside the univariate and the bivariate fits for the data are provided in Table 6.3.1. The data clearly shows that at particular salinities the data fit is more accurate. This was expected, as each of the microorganism is better adapted to grow in certain conditions. The 3M data for *D. salina* for example show peaks at 636nm and 538nm, both these values are in the region close to the detection of chlorophylls and carotenoids. Similarly, data for 4.2M *H. salinarum* shows high correlation in the turbidity regions of the spectrum 788nm, and near the carotenoid region 547nm and 576nm, whereas 1.5M *Halomonas* have better fits at the beginning of the visible spectrum, and oddly in the carotenoid region. Although the single wavelength values and the bivariate analysis of these give high coefficient of determination values, the range of detection wavelengths per microorganism varies with varying salinity. This may be the case in an actively growing culture, where abiotic and biotic shocks may affect the culture. These changes need to be taken into account in the model. Therefore, a different approach was taken.

PCA analysis of the second derivative data showed regions of high correlation between the second derivative data and the spectrum. This model was built using the 3M data for *D. salina*, the 1.5M data for *Halomonas*, and the 4.2M data for *H. salinarum*. These specific salinities were chosen as these are the ideal conditions in which microorganisms are able to thrive.

Based on the PCA loadings, the second derivative of the regions was summed across the technical replicates for the dilutions. Various associations were investigated by plotting the obtained values versus the dilution data. Decision was made on which models to choose based on the R^2 correlation between the dataset and the dilution data.

The regions chosen for the detection of *D. salina* take into account the first peak seen in the carotenoids region [39], in this case 466-518nm and the chlorophyll regions (658-692nm). Adding or subtracting these two regions did actually provide a good model with R^2 fit of 0.996 (Graph 6.3.8). However, by taking into account the region soon after, 694-732nm improved the fit. Any changes to the 694-732nm region will directly affect the 658-692nm region (Graph 6.3.5) by either increase or decreasing the load in this region. When fitted with this model, both of the other microorganisms show lower gradients.

The 496nm+536nm model, shown in Graph 6.3.9, indicates how the *H. salinarum* data best fits the trend. Both *D. salina* and *Halomonas* have less affinity in these wavelength regions. Although both *D. salina* and *H. salinarum* are detected in similar regions due to the presence of bacteriorhodopsin in the haloarchaeon [40,41], the added chlorophylls wavelength in the *D. salina* region allows to differentiate between the two species. Only the regions that did not interfere with the other two microorganisms were chosen to develop the model. Graph 6.3.10 presents a model based on the regions of 296-318nm, 414-436nm and 274-294nm. The last region was taken into account, as any changes to this region would directly influence the 296nm readings. *Halomonas* usually appears white and yellow in colour, however, no distinguishable pigments are found [42]. Therefore, as for *E.coli* optical density, readings at 600nm are used. However, the spectrum obtained indicates that this region would not allow for a proper quantification of the microbe.

The models proposed demonstrated that it may be possible to differentiate between microalgae bacteria and haloarchaea in a mixed population using simple absorption spectra readings. By using the second derivative of the data and applying the model, estimates can be made. Future work is required to further develop models that would enable to differentiate between microorganisms when these are cultivated in co-cultures over time.

6.5. Conclusions

The side investigation was conducted to determine if absorption spectra data could be used to differentiate microorganisms within a mixed culture. This new look at applying absorption spectra to monitor known individual microorganisms in mixed cultures shows promising results. By taking the second derivative of the data and correlating this to dilutions, wavelength regions where each of the organisms was more prominent were selected. The models proposed that each microorganism has a specific region where the spectral intensity outweighs the others. The use of absorption spectra for differentiating between microbes in co-culture and consortium is a valuable tool. In-line monitoring would allow impromptu modifications to be made to the culturing system, be this in the lab or at industrial level. The current models require more refinements in order to be applied to large consortium studies. Factors such as variation in pigmentation and morphology changes, which will affect spectrophotometer light scattering need to be incorporated.

6.6. References

[1] Andersen RA. Algael Culturing Techniques. 1st ed. Andersen RA, editor. Conf. Res. Pract. Inf. Technol. Ser. Elsevier Academic Press; 2005.

[2] Butterwick C, Heaney SI, Talling JF. A comparison of eight methods for estimating the biomass and growth of planktonic algae. Br. Phycol. J. 1982;17:69–79.

[3] Millie D, Schofield O, Kirkpatrick G, et al. Using absorbance and fluorescence spectra to discriminate microalgae. Eur. J. Phycol. 2002;37:313–322.

[4] Kirkpatrick GJ, Millie DF, Moline MA, et al. Optical discrimination of a phytoplankton species in natural mixed populations. Limnol. Oceanogr. 2000;45:467–471.

[5] Balch RT. Measurement of Turbidity with a Spectrophotometer. Ind. Eng. Chem. Anal. Ed. 1931;3:124–127.

[6] Stein JR. Handbook of Phycological Methods: Culture Methods and Growth Measurements. 1st ed. Cambridge University Press; 1973.

[7] Pangestuti R, Kim S-K. Biological activities and health benefit effects of natural pigments

derived from marine algae. J. Funct. Foods. 2011;3:255–266.
[8] Stephenson PG, Moore CM, Terry MJ, et al. Improving photosynthesis for algal biofuels: toward a green revolution. Trends Biotechnol. 2011;29:615–623.
[9] Garbayo I, Cuaresma M, Vilchez C, et al. Effect of abiotic stress on the production of lutein and beta-carotene by Chlamydomonas acidophila. Process Biochem. 2008;43:1158–1161.
[10] Borowitzka MA, Borowitzka LJ, Kessly D. Effects of salinity increase on carotenoid accumulation in the green alga Dunaliella salina. J. Appl. Phycol. 1990;2:111–119.
[11] Griffiths MJ, Garcin C, van Hille RP, et al. Interference by pigment in the estimation of microalgal biomass concentration by optical density. J. Microbiol. Methods. 2011;85:119–123.
[12] Sezonov G, Joseleau-Petit D, D'Ari R. Escherichia coli physiology in Luria-Bertani broth. J. Bacteriol. 2007;189:8746–8749.
[13] Isleten-Hosoglu M, Ayyildiz-Tamis D, Zengin G, et al. Enhanced growth and lipid accumulation by a new Ettlia texensis isolate under optimized photoheterotrophic condition. Bioresour. Technol. 2013;131:258–265.
[14] Bosma R, Miazek K, Willemsen SM, et al. Growth Inhibition of Monodus subterraneus by Free Fatty Acids. Biotechnol. Bioeng. 2008;101:1108–1114.
[15] Gouveia L, Marques AE, da Silva TL, et al. Neochloris oleabundans UTEX #1185: a suitable renewable lipid source for biofuel production. J. Ind. Microbiol. Biotechnol. 2009;36:821–826.
[16] Yahya L, Chik MN, Pang MAMA. Biological carbon fixation: A study of Isochrysis sp. growth under actual coal-fired power plant's flue gas. 4th Int. Conf. Energy Environ. 2013 (Icee 2013). 2013;16.
[17] Choi SP, Nguyen MT, Sim SJ. Enzymatic pretreatment of Chlamydomonas reinhardtii biomass for ethanol production. Bioresour. Technol. 2010;101:5330–5336.
[18] Amin SA, Green DH, Hart MC, et al. Photolysis of iron-siderophore chelates promotes bacterial-algal mutualism. Proc. Natl. Acad. Sci. U. S. A. 2009;106:17071–17076.
[19] Chung MK, Hu R, Wong MH, et al. Comparative toxicity of hydrophobic contaminants to microalgae and higher plants. Ecotoxicology. 2007;16:393–402.
[20] Yoo JJ, Choi SP, Kim BW, et al. Optimal design of scalable photo-bioreactor for phototropic culturing of Haematococcus pluvialis. Bioprocess Biosyst. Eng. 2012;35:309–315.
[21] Nedbal L, Trtilek M, Cerveny J, et al. A photobioreactor system for precision cultivation of photoautotrophic microorganisms and for high-content analysis of suspension dynamics. Biotechnol. Bioeng. 2008;100:902–910.
[22] Shu CH, Tsai CC, Liao WH, et al. Effects of light quality on the accumulation of oil in a mixed culture of Chlorella sp and Saccharomyces cerevisiae. J. Chem. Technol. Biotechnol. 2012;87:601–607.
[23] Farooq W, Lee YC, Ryu BG, et al. Two-stage cultivation of two Chlorella sp strains by simultaneous treatment of brewery wastewater and maximizing lipid productivity. Bioresour. Technol. 2013;132:230–238.
[24] Liu JY. Optimisation of biomass and lipid production by adjusting the interspecific competition mode of Dunaliella salina and Nannochloropsis gaditana in mixed culture. J. Appl. Phycol. 2014;26:163–171.
[25] Kim W, Park JM, Gim G., et al. Optimization of culture conditions and comparison of biomass productivity of three green algae. Bioprocess Biosyst. Eng. 2012;35:19–27.
[26] Fernandes BD, Dragone GM, Teixeira JA, et al. Light Regime Characterization in an Airlift Photobioreactor for Production of Microalgae with High Starch Content. Appl. Biochem. Biotechnol. 2010;161:218–226.
[27] Westerhoff P, Hu Q, Esparza-Soto M, et al. Growth parameters of microalgae tolerant to

high levels of carbon dioxide in batch and continuous-flow photobioreactors. Environ. Technol. 2010;31:523-U80.
[28] Mattos ER, Singh M, Cabrera ML, et al. Effects of Inoculum Physiological Stage on the Growth Characteristics of Chlorella sorokiniana Cultivated Under Different CO2 Concentrations. Appl. Biochem. Biotechnol. 2012;168:519–530.
[29] Baptista MS, Stoichev T, Basto MCP, et al. Fate and effects of octylphenol in a Microcystis aeruginosa culture medium. Aquat. Toxicol. 2009;92:59–64.
[30] Beuckels A, Depraetere O, Vandamme D, et al. Influence of organic matter on flocculation of Chlorella vulgaris by calcium phosphate precipitation. Biomass Bioenergy. 2013;54:107–114.
[31] Spinden EM, Yap BHY, Hill DRA, et al. Quantitative evaluation of the ease of rupture of industrially promising microalgae by high pressure homogenization. Bioresour. Technol. 2013;140:165–171.
[32] Chi Z, Elloy F, Xie Y, et al. Selection of microalgae and cyanobacteria strains for bicarbonate-based integrated carbon capture and algae production system. Appl. Biochem. Biotechnol. 2014;172:447–457.
[33] Shibata K, Benson AA, Calvin M. THE ABSORPTION SPECTRA OF SUSPENSIONS OF LIVING MICRO-ORGANISMS*. Biochim. Biophys. Acta (BBA-Bioenergetics}. 1954;15:461–470.
[34] Hom EFY, Murray AW. Niche engineering demonstrates a latent capacity for fungal-algal mutualism. Science (80-.). 2014;345:94–98.
[35] Rieppo L, Saarakkala S, Närhi T, et al. Application of second derivative spectroscopy for increasing molecular specificity of fourier transform infrared spectroscopic imaging of articular cartilage. Osteoarthr. Cartil. 2012;20:451–459.
[36] Oren A, Stambler N, Dubinsky Z. On t h e red c o l o r a t i o n of saltern c r y s t a l l i z e r p o n d s. Int. J. Salt Lake Res. 1992;1:77–89.
[37] Yao AI, Facciotti MT. Regulatory multidimensionality of gas vesicle biogenesis in Halobacterium salinarum NRC-1. Archaea. 2011;2011.
[38] Abdelkafi S, Labat M, Casalot L, et al. Isolation and characterization of Halomonas sp. strain IMPC, a p-coumaric acid-metabolizing bacterium that decarboxylates other cinnamic acids under hypersaline conditions. FEMS Microbiol. Lett. 2006;255:108–114.
[39] Strati I, Sinanoglou V, Kora L, et al. Carotenoids from Foods of Plant, Animal and Marine Origin: An Efficient HPLC-DAD Separation Method. Foods. 2012;1:52–65.
[40] Oren A, Dubinsky Z. On the red coloration of saltern crystallizer ponds . II . Additional evidence for the contribution of halobacterial pigments. Int. J. Salt Lake Res. 1994;3:9–13.
[41] Ghasemi MF, Shodjai-Arani A, Moazami N. Optimization of bacteriorhodopsin production by Halobacterium salinarium PTCC 1685. Process Biochem. 2008;43:1077–1082.
[42] Cao J, Ma H-Y, Li H-Y, et al. Halomonas socia sp. nov., isolated from high salt culture of Dunaliella salina. Extremophiles. 2013;17:663–668.